

7.00
#8

Shorter Contributions to Stratigraphy and Structural Geology, 1979

GEOLOGICAL SURVEY PROFESSIONAL PAPER 1126-A-J



Shorter Contributions to Stratigraphy and Structural Geology, 1979

GEOLOGICAL SURVEY PROFESSIONAL PAPER 1126-A-J



UNITED STATES DEPARTMENT OF THE INTERIOR

CECIL D. ANDRUS, *Secretary*

GEOLOGICAL SURVEY

H. William Menard, *Director*

Library of Congress Catalog-card No. 80-600016

For sale by the Superintendent of Documents, U.S. Government Printing Office
Washington, D.C. 20402

Stock Number 024-001-03285-6

CONTENTS

[Letters designate the chapters]

- (A) Origin of the river anticlines, central Grand Canyon, Arizona, by Peter W. Huntoon and Donald P. Elston
- (B) Rock control and tectonism—their importance in shaping the Appalachian Highlands, by John T. Hack
- (C) The Upper Ordovician and Silurian Hanson Creek Formation of central Nevada, by Rueben J. Ross, Jr., Thomas B. Nolan, and Anita G. Harris
- (D) The Marble Hill Bed: an offshore bar-tidal channel complex in the Upper Ordovician Drakes Formation of Kentucky, by W C Swadley
- (E) Paleogene sedimentary and volcanogenic rocks from Adak Island, central Aleutian Islands, Alaska, by James R. Hein and Hugh McLean
- (F) The Livengood Dome chert, a new Ordovician formation in central Alaska, and its relevance to displacement on the Tintina fault, by Robert M. Chapman, Florence R. Weber, Michael Churkin, Jr., and Claire Carter
- (G) Intertonguing between the Star Point Sandstone and the coal-bearing Blackhawk Formation requires revision of some coal-bed correlations in the southern Wasatch Plateau, Utah, by Romeo M. Flores, Philip T. Hayes, Walter E. Marley III, and Joseph D. Sanchez
- (H) New evidence supporting Nebraskan age for origin of Ohio River in north-central Kentucky, by W C Swadley
- (I) Reconnaissance geologic study of the Vazante zinc district, Minas Gerais, Brazil, by Charles H. Thorman and Samir Nahass
- (J) Constraints on the latest movements on the Melones fault zone, Sierra Nevada foothills, California, by J. Alan Bartow

CONVERSION FACTORS

Metric unit		Inch-Pound equivalent	
Length			
millimeter (mm)	=	0.03937	inch (in)
meter (m)	=	3.28	feet (ft)
kilometer (km)	=	.62	mile (mi)
Area			
square meter (m ²)	=	10.76	square feet (ft ²)
square kilometer (km ²)	=	.386	square mile (mi ²)
hectare (ha)	=	2.47	acres
Volume			
cubic centimeter (cm ³)	=	0.061	cubic inch (in ³)
liter (L)	=	61.03	cubic inches
cubic meter (m ³)	=	35.31	cubic feet (ft ³)
cubic meter	=	.00081	acre-foot (acre-ft)
cubic hectometer (hm ³)	=	810.7	acre-feet
liter	=	2.113	pints (pt)
liter	=	1.06	quarts (qt)
liter	=	.26	gallon (gal)
cubic meter	=	.00026	million gallons (Mgal or 10 ⁶ gal)
cubic meter	=	6.290	barrels (bbl) (1 bbl=42 gal)
Weight			
gram (g)	=	0.035	ounce, avoirdupois (oz avdp)
gram	=	.0022	pound, avoirdupois (lb avdp)
metric tons (t)	=	1.102	tons, short (2,000 lb)
metric tons	=	0.9842	ton, long (2,240 lb)
Specific combinations			
kilogram per square centimeter (kg/cm ²)	=	0.96	atmosphere (atm)
kilogram per square centimeter	=	.98	bar (0.9869 atm)
cubic meter per second (m ³ /s)	=	35.3	cubic feet per second (ft ³ /s)

Metric unit		Inch-Pound equivalent	
Specific combinations—Continued			
liter per second (L/s)	=	.0353	cubic foot per second
cubic meter per second per square kilometer [(m ³ /s)/km ²]	=	91.47	cubic feet per second per square mile [(ft ³ /s)/mi ²]
meter per day (m/d)	=	3.28	feet per day (hydraulic conductivity) (ft/d)
meter per kilometer (m/km)	=	5.28	feet per mile (ft/mi)
kilometer per hour (km/h)	=	.9113	foot per second (ft/s)
meter per second (m/s)	=	3.28	feet per second
meter squared per day (m ² /d)	=	10.764	feet squared per day (ft ² /d) (transmissivity)
cubic meter per second (m ³ /s)	=	22.826	million gallons per day (Mgal/d)
cubic meter per minute (m ³ /min)	=	264.2	gallons per minute (gal/min)
liter per second (L/s)	=	15.85	gallons per minute
liter per second per meter [(L/s)/m]	=	4.83	gallons per minute per foot [(gal/min)/ft]
kilometer per hour (km/h)	=	.62	mile per hour (mi/h)
meter per second (m/s)	=	2.237	miles per hour
gram per cubic centimeter (g/cm ³)	=	62.43	pounds per cubic foot (lb/ft ³)
gram per square centimeter (g/cm ²)	=	2.048	pounds per square foot (lb/ft ²)
gram per square centimeter	=	.0142	pound per square inch (lb/in ²)
Temperature			
degree Celsius (°C)	=	1.8	degrees Fahrenheit (°F)
degrees Celsius (temperature)	=	[(1.8 × °C) + 32]	degrees Fahrenheit

Origin of the River Anticlines, Central Grand Canyon, Arizona

By PETER W. HUNTOON *and* DONALD P. ELSTON

SHORTER CONTRIBUTIONS TO STRATIGRAPHY AND
STRUCTURAL GEOLOGY, 1979

GEOLOGICAL SURVEY PROFESSIONAL PAPER 1126-A



CONTENTS

Abstract	Page A1
Introduction	1
Acknowledgments	1
Geographic and stratigraphic location	2
Structure	2
Low-angle thrust faults	4
High-angle kink bands	5
Related anticlines	5
Ancient river anticlines	5
Regional distribution	5
Origin	6
References cited	9

ILLUSTRATIONS

PLATE	1. River anticlines, central Grand Canyon, Arizona	Page In pocket
FIGURE	1. Map showing the location of the Colorado River and its principal tributary canyons in the central Grand Canyon, Ariz	A2
	2. Stratigraphic columns of Cambrian rocks in the central and eastern Grand Canyon	3
	3. Photograph of well-developed river anticlines upstream from Olo Canyon	4
	4. Photograph of a pair of low-angle echelon thrust faults	5
	5. Photograph and diagram showing kink bands in rocks along the river	6
	6. Diagram illustrating selected theories used to explain the origin of river anticlines in the central Grand Canyon	7

ORIGIN OF THE RIVER ANTICLINES, CENTRAL GRAND CANYON, ARIZONA

By PETER W. HUNTOON¹ and DONALD P. ELSTON

ABSTRACT

A system of anticlines lies along the trend of the sinuous course of the Colorado River for a distance of 97 km in the central Grand Canyon. Similar anticlines occur in some perennially wet side canyons. The anticlines are most abundant and well developed along northeast-trending reaches of the main canyon where it is floored by the Cambrian Muav Limestone. Dips of the folded strata are as great as 60°, and the folding locally extends more than 250 m from the river. Low-angle thrust faults in the limbs of the anticlines parallel the river and have formed in response to folding of the comparatively brittle carbonate strata. High-angle reverse kink bands, along which rocks are displaced up toward the river, also parallel the anticlines and have developed in response to the upward bulging of the canyon floor.

The river anticlines are an unloading phenomenon. They result from lateral squeezing toward the river of saturated shaly parts of the Muav Limestone and underlying Bright Angel Shale. The driving mechanism for the deformation is a stress gradient that results from a difference in lithostatic load between the heavily loaded rocks under the 650-m-high canyon walls and the unloaded canyon floor. Saturation appears to weaken the shaly rocks sufficiently to allow deformation to take place. River anticlines are not present in the eastern Grand Canyon, where the Cambrian rocks also occur at river level. Their absence is explained by a lack of shaly rocks that could flow when saturated.

INTRODUCTION

A series of anticlines coincides with the trend of the Colorado River in the central Grand Canyon (fig. 1). Because the anticlines follow the river around bends, they appear to have a genetic relation to the river and its canyon. The generalized axial trace of two of the folds, at and below the mouth of Matkatamiba Canyon, is shown on the geologic map of Maxson (1969). These folds have been called "river anticlines" (Ford and others, 1974).

This paper describes the river anticlines and associated faults in the Grand Canyon and relates

the origin of the anticlines to mass flowage of saturated shaly Cambrian rocks in response to horizontal stresses related to lithostatic load differences between the rocks under the high canyon walls and the unloaded canyon floor.

Fieldwork and mapping leading to this report was carried out during parts of two river trips in 1976. The existence and general characteristics of the river anticlines had been noted during seven previous research trips of Elston, the first of which was in October 1971. During a trip in May 1973, E. M. Shoemaker recognized the preferential development of river anticlines along northeast-trending stretches of the river, which led him to propose a structural origin for the river anticlines (an origin also proposed for the Meander anticline on the Colorado River, below its confluence with the Green River in Utah).

ACKNOWLEDGMENTS

We thank the U.S. National Park Service for allowing us to work and sample in Grand Canyon National Park and gratefully acknowledge the kind cooperation of David C. Ochsner and Robert Yearout.

Funds supporting work by Huntoon were provided by the Office of Water Research and Technology through the Wyoming Water Resources Research Institute under matching grant 14-34-0001-6134. The U.S. Geological Survey work of Elston was carried out under magnetostratigraphic investigations of the Cambrian strata of northern Arizona. James I. Drever, Department of Geology, University of Wyoming, conducted the X-ray analyses of clay samples collected during the course of this study. Eugene M. Shoemaker and Irving J. Witkind of the U.S. Geological Survey reviewed the manuscript and made many helpful suggestions. Shoemaker provided a sketch that led to figure 6.

¹ Department of Geology and Wyoming Water Resources Research Institute, University of Wyoming.

GEOGRAPHIC AND STRATIGRAPHIC LOCATION

We have observed river anticlines along the 97-km reach of the Colorado River between Fishtail and Parashant Canyons (fig. 1). The anticlines characteristically occur in the lower half of the Cambrian Mauv Limestone and in parts of the underlying Cambrian Bright Angel Shale where these rocks crop out at and near river level.

The combined thickness of the Bright Angel Shale and Muav Limestone in the area of the river anticlines in central Grand Canyon is about 300 m. The nomenclature and composition of these two rock units are summarized in figure 2. Member names are those of McKee (1945). His Spencer Canyon and underlying members are here reassigned to the Bright Angel Shale so as to retain the stratigraphic position of the Bright Angel Shale-Muav Limestone contact as originally defined by Noble (1914, p. 65).

In the central Grand Canyon, the Bright Angel Shale consists of interbedded shaly siltstone and sandstone and interbedded dolomite. The Muav Limestone consists of cliff-forming, in part thin bedded dolomite and limestone that contain subor-

dinate shale partings. The clay fraction diminishes in both formations toward the east, and shale is rare in the Cambrian section in the eastern Grand Canyon. Regional dip of the Cambrian rocks in the central Grand Canyon is less than 2° toward the north or northeast.

STRUCTURE

The axes of the anticlines generally follow the trend of the center of the river (fig. 1, plate 1). Between Kanab and Mohawk Canyons, there is a marked tendency for maximum dips to occur where the anticlines trend northeast. Local closures occur along the northeast-trending folds and anticlinal structures are missing or subdued along northwest-trending reaches of the river.

The anticlines are best developed along the 21-km stretch between Kanab and Havasu Canyons. Here the canyon is at its narrowest, talus is minimal, and the river level is at or above the top of the Bright Angel Shale. The steepest dips and greatest structural relief associated with the anticlines occur where McKee's (1945) Peach Springs and overlying Kanab Canyon Members of the Muav Limestone

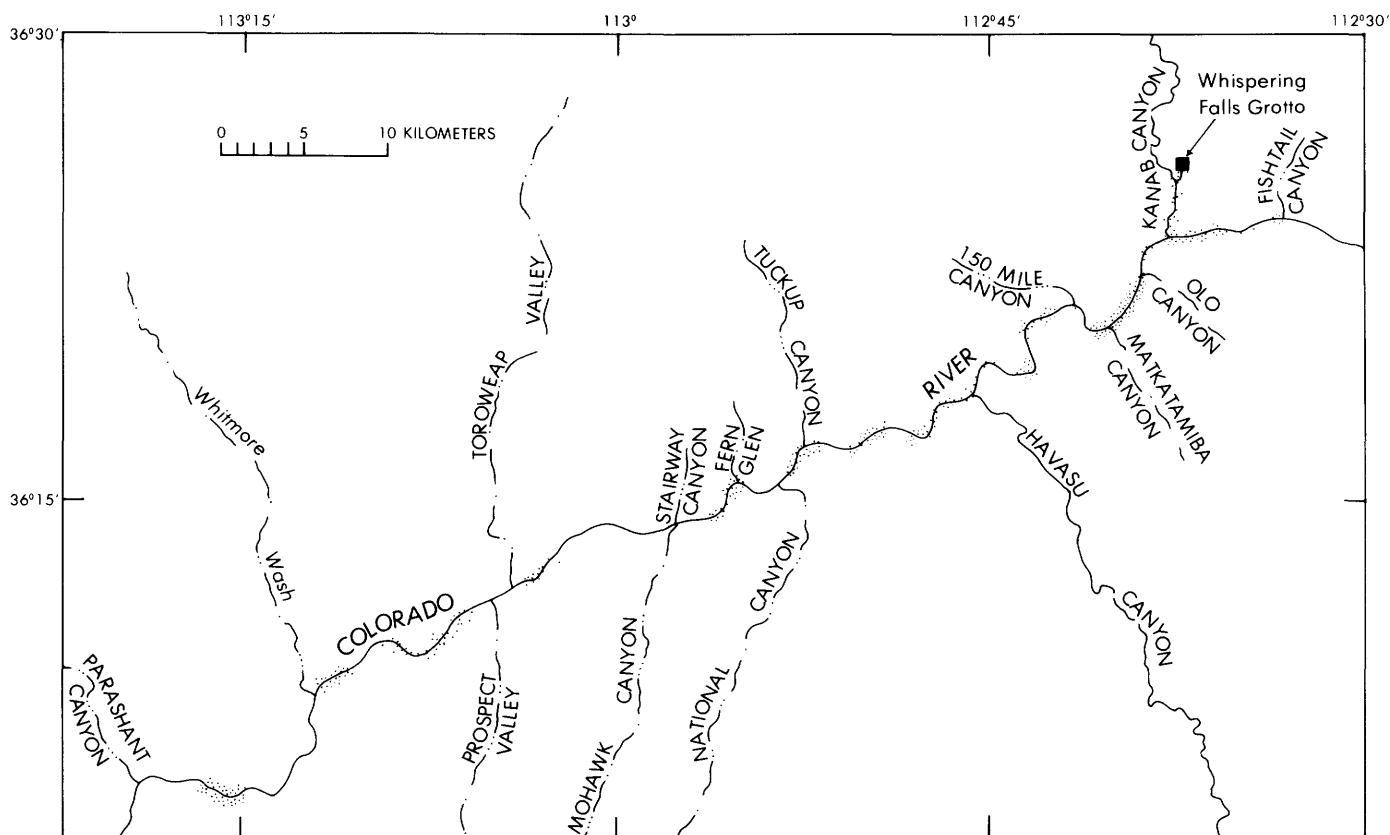


FIGURE 1.—Location of the Colorado River and its principal tributary canyons in the central Grand Canyon, Ariz. Stippled reaches contain river anticlines. Downstream is to left.

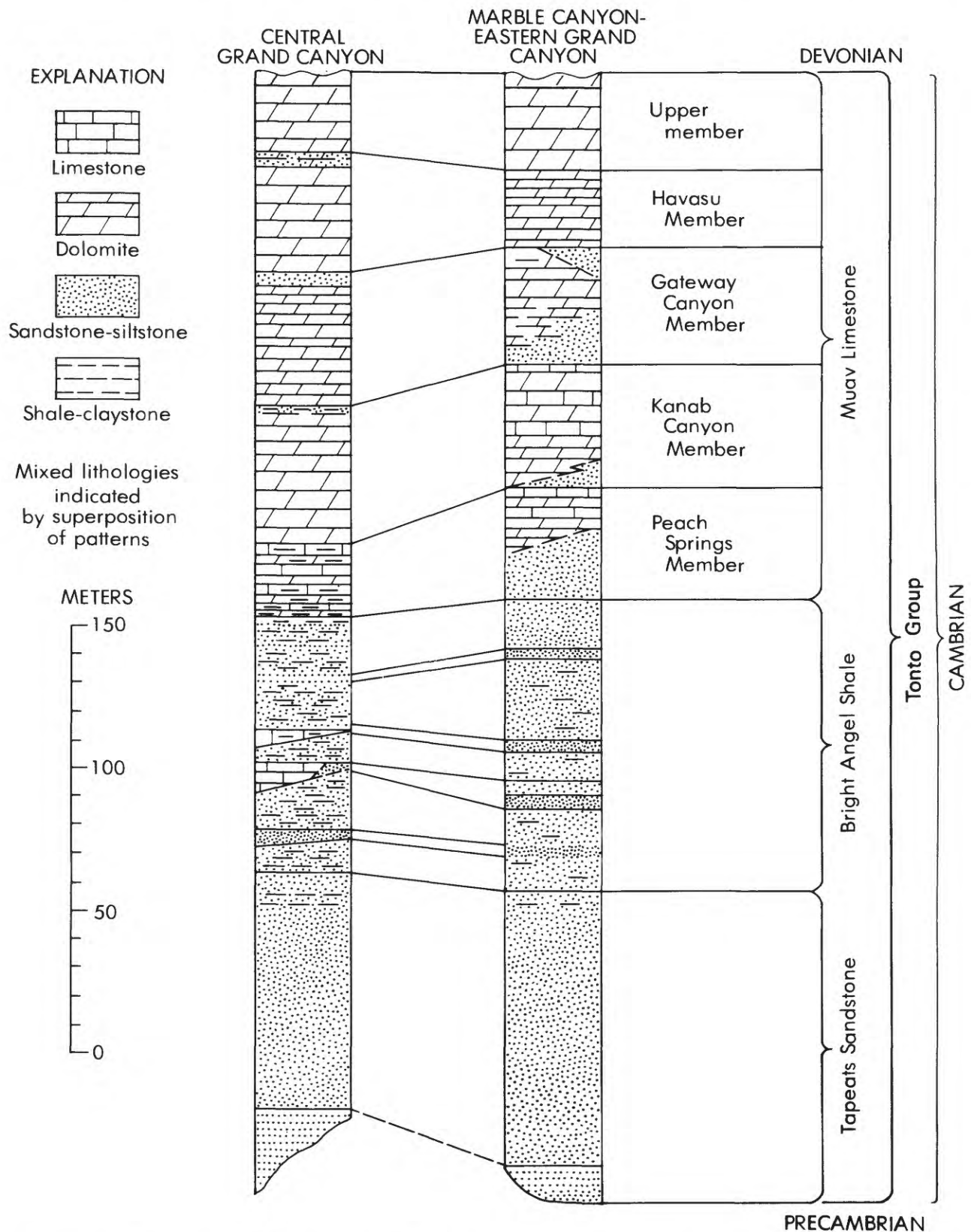


FIGURE 2.—Stratigraphic columns of Cambrian rocks in the central and eastern Grand Canyon. Note that the clay content diminishes eastward. Figure and nomenclature are slightly modified from Elston and Bressler (1977, fig. 2). Member names within Muav Limestone are those of McKee (1945).

(fig. 2) crop out at river level. Because the Muav Limestone is more resistant than adjacent strata, the canyon is narrow and the river is commonly less than 75 m wide. This constriction extends from about 0.8 km east of the Kanab Canyon to Fern Glen (fig. 1).

Between Kanab and Havasu Canyons, anticlinal dips in the Muav Limestone locally are as great as 60° , although dips are mostly less than 30° (plate 1; fig. 3). A river anticline that trends past the mouth of Matkatamiba Canyon (fig. 1) is particularly well exposed. Here dips are a maximum of 40° at the river and decrease away from the river. Folded strata extend into the canyon wall as far as 250 m from the center of the river. Below Havasu Canyon, the inner gorge widens, and dips on the flanks of the anticlines commonly are about 2° to 5° . In general, deformed strata extend no more than 25–50 m above river level. Higher on the canyon walls, the strata are undeformed. Folding is entirely restricted to the Cambrian rocks.

The maximum structural relief along the anticlines is of the order of 10 m, and most of the river anticlines have less than 5 m of structural relief. Total shortening across the structures therefore is only a few meters.

LOW-ANGLE THRUST FAULTS

Two sets of intersecting low-angle thrust faults and fractures parallel the anticlines in the Muav Limestone and dip both toward and away from the

river. The faults are particularly numerous and have greater stratigraphic offsets where the limestone is steeply folded. However, we have observed low-angle thrusts in limestone beds that dip as little as 2° .

The low-angle thrusts may occur alone but are more commonly found in parallel and echelon sets. Individual faults are discontinuous and rarely extend more than 100 m along the strike of an anticline. As shown in figure 4, the faults characteristically terminate in breccia zones. Parallel to the river, the fault planes curve in conformance with the structural relief along an anticline. The resulting curvature of the fault planes indicates that the faults encircle the up- and down-stream ends of the anticlines; however, conclusive evidence for this relationship is missing, because the critical outcrops are below river level.

Displacements along the thrust planes are dip-slip and rarely exceed a few meters. The faults that dip away from the river generally dip at angles no more than 15° greater than the beds in which they are found. The faults that dip toward the river intersect bedding planes at angles as great as 30° . In most outcrops, there has been considerably more movement along the thrusts that dip away from the river than along those that dip toward the river.

The low-angle thrusts are the result of internal shearing within the limbs of the anticlines. They are clearly a response to the folding of the brittle limestone in the section. The thrusts occur because



FIGURE 3.—Well-developed river anticlines upstream from Olo Canyon. View is downstream toward west.



FIGURE 4.—A pair of low-angle echelon thrust faults (arrows). The fault that trends from left toward lower center terminates in a breccia zone. The scene is about 7 m wide.

no differential movement is possible between the individual bedding surfaces, which are interlocked by minor irregularities. Bedding plane irregularities have as much as 2 cm of relief.

HIGH-ANGLE KINK BANDS

Discontinuous high-angle reverse kink bands locally parallel the river anticlines. As shown on figure 5, the kink bands displace the rocks up toward the river and are as wide as 2 m. The bands approximately parallel the slope of the canyon walls and are obliquely to vertically jointed in the limestone. We interpret the kink bands to result from stress buildup accompanying the upward bulging of the canyon floor during the growth of the anticlines.

RELATED ANTICLINES

Small river anticlines occur in the perennially wet reaches of Kanab Canyon and a few of its tributaries (fig. 1). The crests of these anticlines are locally exposed in the floor of Kanab Canyon and Whispering Falls Grotto and are characterized by buckled beds. The buckling demonstrates that the anticlines have formed in response to lateral compression.

ANCIENT RIVER ANTICLINES

The canyon of the Colorado River is uncommonly narrow at a few localities between Kanab and Tuck-

up Canyons. At such places, McKee's (1945) Kanab Canyon and Gateway Canyon Members of the Muav Limestone are preserved close to and several tens of meters above the present course of the river. Some of these outcrops are anticlinally folded parallel to the river. Because the rocks are deformed and the structures lie above the present generation of river level anticlines, we interpret these folded outcrops to be remnants of former river anticlines that originated before the canyon attained its present depth.

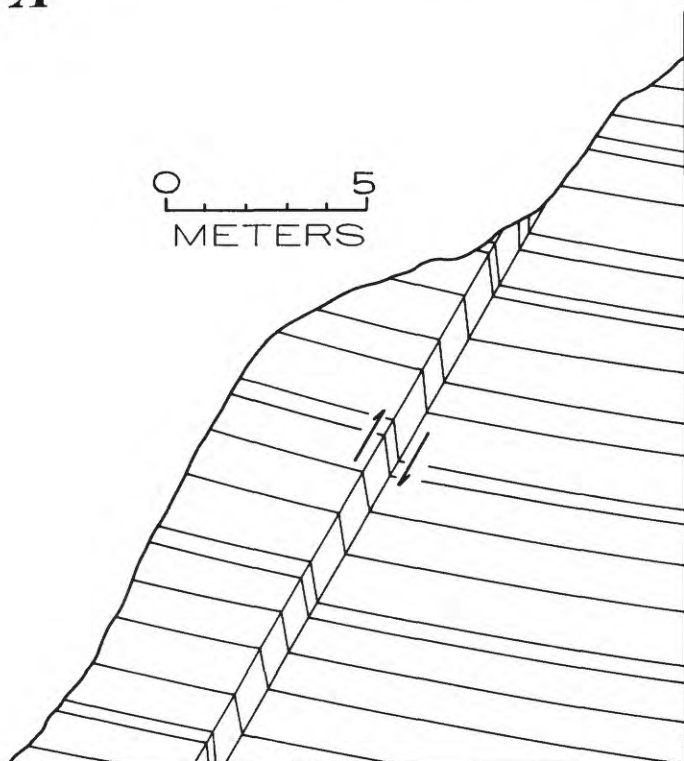
We consider these remnants to be evidence that the formation of river anticlines is a continuing process that accompanies the downward cutting of the canyon through the Muav Limestone and Bright Angel Shale. The remnants suggest that as the river cuts through and exposes the anticlines, they erode and are removed as the canyon widens. Consequently, most traces of the older generations of anticlines have been removed.

REGIONAL DISTRIBUTION

The distribution of river anticlines in the Grand Canyon is shown on figure 1 and plate 1. Significantly, river anticlines and their associated faults are not present in Marble Canyon, 60 km east of the area of figure 1, and in the contiguous eastern Grand Canyon where the canyon is also floored by the



A



B

FIGURE 5.—Kink bands in rocks along the river. A, A high-angle kink band that parallels river, exposed by spalling along the band; the length of kink band is approximately 20 m. B, A schematic diagram of a high-angle kink band on the flank of a river anticline that results from a bulging of the canyon floor; arrows indicate relative movement.

Muav Limestone and Bright Angel Shale. We attribute this fact to the absence of sufficient clay in the Cambrian section to allow plastic flowage, even when saturated. As shown diagrammatically in figure 2, the percentage of claystone in the Cambrian sec-

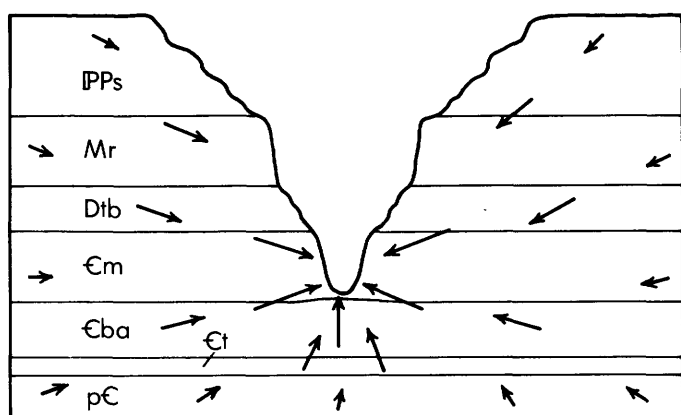
tion decreases from west to east. Where the river flows on these units in Marble Canyon and the eastern Grand Canyon, the Bright Angel Shale consists almost totally of fine-grained sandstone and siltstone, and clay represents only a few percent of the total thickness. Similarly, the shaly partings in the Muav Limestone become more silty toward the east, and the percentage of clay is correspondingly less.

ORIGIN

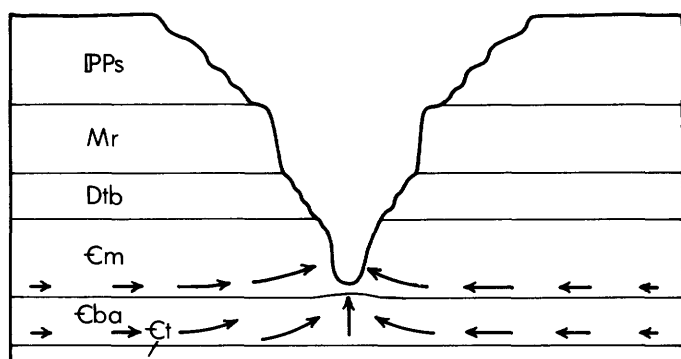
Ford and others (1974, p. 126–127) have summarized the hypotheses advanced to explain the river anticlines in the Grand Canyon. A number of explanations have been proposed, three of which are illustrated on figure 6:

1. Some workers have evoked variants on the theme of strain adjustments resulting from the removal of large volumes of overburden and the consequent realignment of stresses and deformation of the rocks near river level (McKee, *in* Ford and others, 1974, p. 126; Sturgul and Grinshpan, 1975).
2. Ford (*in* Ford and others, 1974, p. 126) considered that the Bright Angel Shale is mobile and is squeezed out from under the adjacent walls as a result of the stress gradients produced by the large lithostatic load differential between loaded rocks under the canyon walls and the unloaded canyon floors. Hamblin and Rigby (1969, p. 57 and 60) invoked a combination of these mechanisms to explain the anticlines.
3. Shoemaker (1973) proposed that the thick plate comprising the Paleozoic rocks above the Bright Angel Shale passively glides on the mobile Bright Angel Shale toward the canyon in response to a gentle northeastward dip. Shoemaker envisioned the plate as being rigid and the horizontal extension within it as being largely accommodated by tensional separations along joints.
4. Huntoon (*in* Ford and others, 1974, p. 127) thought that the anticlinal bulge along the canyon floors resulted from swelling of clay in the Muav and Bright Angel Formations.

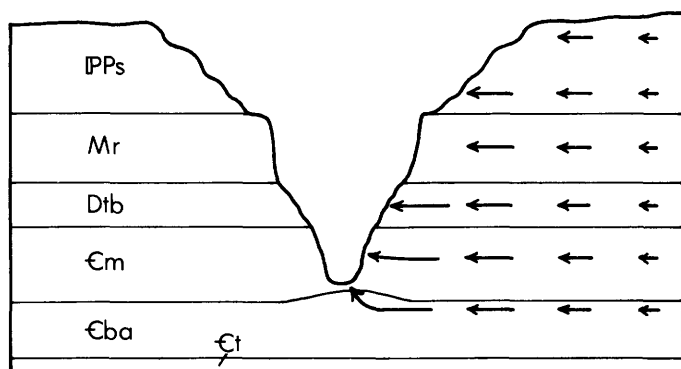
We embrace the hypothesis that the river anticlines are an unloading phenomenon. We believe that the anticlines represent strain within the shaly parts of the Muav and Bright Angel formations and that the strain results from large stress gradients that exist between the unloaded canyon floor and rocks under the heavily loaded adjacent canyon walls. In



A. Distributed flowage resulting from release of confining pressure.



B. Flowage in incompetent shale layers due to differences in lithostatic load.



C. Gliding of a plate on an incompetent layer.

FIGURE 6.—Selected theories used to explain the origin of river anticlines in the central Grand Canyon, Ariz. A, This report. B, Ford and others (1974) and Sturgul and Grinshpan (1975). C, Shoemaker (1973). Combination of figures A and B, Hamblin and Rigby (1969). Arrows indicate movement caused by stress. pC, Precambrian igneous and metamorphic rocks. Ct, Tapeats Sandstone. Cba, Bright Angel Shale. Cm, Muav Limestone. Dtb, Temple Butte Limestone. Mr, Redwall Limestone. IPPs, Supai Group, capped by Esplanade Sandstone.

our model, flowage is initiated in the shaly parts of the Bright Angel and Muav formations close to the river as they become exhumed.

The model in part devolves from the observation that fossil river anticlines are preserved stratigraphically high in the Muav Limestone, well above present river level (pl. 1). The fossil anticlines are found where the central gorge of the canyon is very narrow. They do not appear to be physically connected to underlying river anticlines found at present river level. We consider this evidence that formation of the river anticlines has been a continuing process and that older river anticlines once existed but have been removed by erosion during widening of the canyon.

The primary differences between our hypothesis and that of Ford (Ford and others, 1974, p. 126) are that we recognize that saturation of the shale in the section is necessary for the rocks to become plastic enough to deform under the imposed stress gradients and that the river anticlines are not necessarily related to the presence of a closely underlying Bright Angel Shale. Without saturation and without shale, these same rocks do not deform.

The various hypotheses proposed by others and the one we favor can be examined in light of the structure of the anticlines and of other data collected during the course of our investigation. One fact is clear from field observations: The strain observed in the river anticlines is a combination of plastic flowage and brittle failure within the Muav Limestone and of mostly plastic flowage within the Bright Angel Shale. A concept that implies elastic rebound, such as that proposed by Sturgul and Grinshpan (1975), is negated by the observed non-elastic strain.

Huntoon's swelling-clay hypothesis was based on observations in which clay partings between individual limestone beds appear to be expanded under the floor of Whispering Falls Grotto. The grotto is eroded beneath a waterfall in beds near the middle of the Muav Limestone. Exposures of the grotto floor indicate a slight but measurable increase in the thickness of the shale partings toward the axis of the fold. To test for the presence of swelling clay, we collected claystone and siltstone samples from shaly and thin-bedded parts of the Muav Limestone and Bright Angel Shale in the central and eastern Grand Canyon, in areas with and without river anticlines. X-ray analyses revealed that the clay in all samples is composed of illite and kaolinite or chlorite. Montmorillonite, if present, occurs only in trace amounts. Because of the virtual lack of

swelling clays in all samples, we believe that the swelling-shale hypothesis can be rejected. The expanded beds observed at Whispering Falls Grotto thus are undoubtedly the result of physical separations between limestone beds caused by buckling of the strata along the crests of the anticlines.

The hypothesis of Shoemaker involves a plate that glides toward the river on the incompetent Bright Angel Shale and is detached from the northeast-trending Sinyala fault that parallels the general trace of the river on the south (pl. 1). In this model, the plate moves northwestward toward the river on a dipping surface that slopes less than 2° throughout the central Grand Canyon. As envisioned by Shoemaker, the top part of the Bright Angel Shale deforms plastically or by shearing. As long as the upper contact of the Bright Angel Shale is near or below river level, the Muav Limestone and upper part of the Bright Angel Shale would bulge upward along the axis of the river. Deformation would be confined to the northeast-trending segments perpendicular to the direction of plate movement.

Shoemaker's hypothesis would explain the tendency for the anticlines to align along the northeast-trending segments of the river. However, we find difficulties with the theory. First, we have been unable to document tensional separations along joints parallel to the river in the cross sections along tributary canyons south of the river. Moreover, there are no faults or grabens aligned parallel to the river that exhibit tensional separations (Ford and others, 1974, p. 127). (The northeast-trending Sinyala fault is a deep-seated fault.) Tensional separation should be evident in the brittle and erosionally resistant Permian Esplanade Sandstone that caps the benches surrounding the inner gorge. Secondly, no tear faults, which would be required to accommodate the northwestward motion of the moving plate, have been observed along or parallel to the northwest-trending segments of the river. Thirdly, anticlines that we have observed near the upstream and downstream ends of the river anticline belt (fig. 1, pl. 1) occur in competent limestone beds in the lower and middle parts of the Bright Angel Shale (fig. 2). This demonstrates that anticlinal deformation has occurred through the full thickness of the Bright Angel Shale and is not necessarily restricted to the upper part of the formation, as would be required by the model depicted in figure 6C. We thus conclude that there is no field evidence for appreciable lateral movement of the Paleozoic section toward the Colorado River.

From field relations, then, flowage of saturated shaly strata involves only small volumes of rock in close proximity to the river. These rocks are folded at places where there is a large stress between heavily loaded zones under canyon walls that are as high as 650 m and an unloaded canyon floor. Shaly strata appear to have been squeezed laterally toward the river, and local lateral flowage, which has amounted to no more than a few meters at the river, has occurred in response to the compressive stress to create the river anticlines. In this model, the thrust faults result from the folding of the strata in the anticlines and they are not primary shears related directly to differential lateral flowage of the rocks under the canyon walls.

Saturation of the shale is essential for the deformation. The lack of flowage features in shaly outcrops high in the walls of the Grand Canyon or away from perennial streams supports this conclusion. Hundreds of kilometers of such dry outcrops exist in the Grand Canyon under load conditions identical to those near the river anticlines, yet anticlinal deformation has only occurred where the shaly rocks have been or are in nearly constant contact with water.

Our hypothesis accounts for the formation of river anticlines but not for a preferred orientation where they might tend to parallel a deep-seated fault and not follow the stream course in detail. West of Fern Glen, the anticlinal trends vary, and some minor river anticlines trend northwest as well as northeast. However, east of Fern Glen, very well developed anticlines trend northeast along northeast-trending stretches of the river and disappear along the short segments of the river that trend northwest (fig. 1, pl. 1). In this area the river is paralleled on the south by the northeast-trending Sinyala fault, which lies about 3–6 km to the southeast. The possibility exists that some small component of northwestward, down-dip translation of the Paleozoic section has occurred between the Sinyala fault and the Colorado River, employing the model of Shoemaker in a restricted sense. Such creep would produce a differential stress that presumably would enhance development of river anticlines along the northeast-trending stretches of the river and suppress their formation along the northwest-trending stretches. The differential stress would augment stresses produced as a consequence of unloading along the river, which in turn suggests that a preferred orientation of stream or river anticlines might be a comparatively sensitive indicator of differential stresses of tectonic origin.

REFERENCES CITED

- Elston, D. P., and Bressler, S. L., 1977, Paleomagnetic poles and polarity zonation from Cambrian and Devonian strata of Arizona: *Earth and Planetary Science Letters*, v. 36, no. 3, p. 423-433.
- Ford, T. D., Huntoon, P. W., Billingsley, G. H., Jr., and Breed, W. J., 1974, Rock movement and mass wastage in the Grand Canyon, in Breed, W. J., and Roat, E. C., eds., *Geology of the Grand Canyon: Flagstaff, Museum of Northern Arizona and Grand Canyon Natural History Association*, p. 116-128.
- Hamblin, W. K., and Rigby, J. K., 1969, Guidebook to the Colorado River, pt. 2, Phantom Ranch in Grand Canyon National Park to Lake Mead, Arizona-Nevada: Provo, Utah, Brigham Young University Geological Studies, v. 15, pt. 2, 126 p.
- McKee, E. D., 1945, Stratigraphy and ecology of the Grand Canyon Cambrian, pt. 1 of *Cambrian history of the Grand Canyon region: Carnegie Institute of Washington Publication 563*, p. 3-168.
- Maxon, J. H., 1969, Preliminary geologic map of the Grand Canyon and vicinity, Arizona (western and central sections): Grand Canyon Natural History Association (P.O. Box 219, Grand Canyon, Ariz.)
- Shoemaker, E. M., 1973, River anticlines of the Colorado: Paper presented at Symposium on Northern Arizona Geology, Museum of Northern Arizona, August 31, 1973 (unpublished).
- Sturgul, J. R., and Grinshpan, Z., 1975, Finite-element model for possible isostatic rebound in the Grand Canyon: *Geology*, v. 3, p. 169-171.

Rock Control and Tectonism— Their Importance in Shaping the Appalachian Highlands

By JOHN T. HACK

SHORTER CONTRIBUTIONS TO STRATIGRAPHY AND
STRUCTURAL GEOLOGY, 1979

GEOLOGICAL SURVEY PROFESSIONAL PAPER 1126-B



CONTENTS

	Page
Abstract	B1
Introduction	1
Major topographic features and drainage systems	2
Relation of the highland form to bedrock geology	2
The belt of Cambrian and Ordovician rocks	6
Duration of erosion	8
Evidence for late tectonic activity	9
Rates of erosion and uplift	12
Development of the Appalachian Highlands in late geologic time	14
Conclusion	15
References cited	16

ILLUSTRATIONS

	Page
FIGURE 1. Generalized topographic map of the Appalachian Highlands, showing the divide between the drainage to the Atlantic and to the Gulfs of Mexico and St. Lawrence	B3
2. Subenvelope map showing contours drawn on altitudes along the major stream channels	4
3. Generalized map of major rock units based on their resistance to erosion	5
4. Profile and outline map of the Cambrian and Ordovician belt from Coosa River to Lake Champlain	7
5. Generalized relief map of Piedmont and Blue Ridge provinces	10
6. Map of Eastern United States showing Bouguer gravity anomalies	14

TABLES

	Page
TABLE 1. Thickness of sediments penetrated in COST No. B-2 and estimated deposition rate	B9
2. Estimates of erosion rates	12
3. Estimates of tilt rates	12

ROCK CONTROL AND TECTONISM—THEIR IMPORTANCE IN SHAPING THE APPALACHIAN HIGHLANDS

By JOHN T. HACK

ABSTRACT

The current interest in contemporary tectonic processes in the Eastern United States is turning up abundant evidence of crustal movements in late geologic time. Topographic analysis of the highland areas from the southern Blue Ridge to the Adirondack Mountains indicates that most of the landforms owe their origin to erosion of rocks of different resistance rather than to tectonic processes. Most areas of high relief and high altitude have been formed on resistant rocks. The Cambrian and Ordovician belt, containing mostly shale and carbonate rock, on the other hand, forms an extensive lowland from Alabama to the Canadian border and girdles the Adirondack Mountains. Differences in altitude can be explained by the presence of resistant rocks outside the belt; these resistant rocks form local base levels on the streams that drain the belt. A few areas may have undergone local uplift at a higher rate than areas nearby—for example, the Piedmont region northwest of Chesapeake Bay. Most estimates of erosion rates, based on the load transported by streams, and of uplift rates, based on removal of the known or inferred amount of overburden during a known period of time, are of the same order of magnitude, averaging about 4×10^{-2} millimeters per year. Rates of uplift, based on study of tilted Pleistocene beaches and repeated geodetic traverses, are at least an order of magnitude higher for comparable areas. Tectonic uplift of the highlands has been slow and involves mostly warping or tilting on a large scale. Erosion rates keep up with or exceed the rate of uplift and have been sufficient to mask evidence of faulting or other differential movements. The high rates of uplift that are inferred on tilted water planes in the glaciated regions or that are measured by differences in repeated geodetic traverses cannot have been sustained for long periods of time.

INTRODUCTION

Differential erosion of rocks of varying resistance has long been considered a major factor in shaping the landscape of the Eastern United States. Theories to explain the erosional history have been concerned mainly with cyclical landform development, relict surfaces such as peneplains, and the evolution of the drainage pattern (Thornbury, 1965, p. 72–87). Although most geologists agree that uplift did take place in the Eastern United States during late geologic time (since the middle Mesozoic), few have thought that local topographic forms are of tectonic origin. Faults active in late geologic time have been discovered (York

and Oliver, 1976; Mixon and Newell, 1977), but it has not been proved that any modern topographic features owe their origin to contemporary faulting.

Recent studies of precise leveling data along geodetic traverses that have been rerun one or more times indicate that many of the monuments have changed in elevation during the intervals between the traverses. Some of these changes may be due to errors in leveling or to disturbances of the monuments, but it is generally agreed that many of the changes are related to actual motion of the ground or of the Earth's crust. The differences between traverses expressed as velocities of vertical motion are commonly quite large (see Brown and Oliver, 1976, for discussion of the method of analysis). The interpretation of the repeated traverses poses many problems. The rates of uplift, or depression are commonly so high that they could not be long sustained without resulting in much larger topographic features than are observed.

In spite of the difficulties involved in interpreting evidence for recent crustal movements, there is little doubt that rates obtained from precise leveling data as well as from study of ancient strand lines indicate rapid contemporary crustal movements. Analysis of topography of the Appalachian Highlands shows, however, that differential erosion of rocks of different resistance is the major factor that controlled the development of today's topographic forms, including even large features. A few major topographic discontinuities apparently unrelated to rock type do exist, however, and can be identified. The picture that emerges from topographic analysis is that the major drainage system of the area has, over a long period of time, become closely adjusted to rock type. In places, it still deviates from lithologic controls. Some of the deviations occur in response to competing major drainage systems that have different base levels, lengths, and gradients, which are basically caused by rock control within the different systems. Some may be due to tectonic influence, and others may be inherited from the past.

The rate of topographic adjustment because of erosion is so rapid that detection of the details of tectonic control is difficult or impossible, even in areas where it is reasonable to expect that such control exists. On the other hand, the sedimentary record preserved in the Coastal Plain and Continental Shelf as well as the grossest topographic relationships are clear evidence of tectonism. The intent of this paper is to describe the major drainage systems and topographic forms of the Appalachian Highlands between Alabama and northern New York and to discuss their adjustment to bedrock. Some topographic anomalies that may be caused by differential movement of separate tectonic blocks are also considered.

I wish to thank C. S. Denny, Richard Goldsmith, Sheldon Judson, and Wayne Newell for their thoughtful criticism.

MAJOR TOPOGRAPHIC FEATURES AND DRAINAGE SYSTEMS

The general outlines of the topography and drainage of the Appalachian Highlands are shown in figures 1 and 2. In figure 1, an envelope map originally defined by Stearns (1967), contours are drawn across the ridge crests and drainage divides. Essentially, figure 1 is a map of the high parts of the topography. In this paper, the envelope map is used as a reference map showing the major streams and the continental divide separating the drainage to the Atlantic Ocean from that to the Gulf of Mexico and St. Lawrence River. Figure 2, a subenvelope map (Stearns, 1967; Hack, 1973), is another way to generalize the topography. In this map, the contours are drawn on altitudes along the major streams. It shows the position of the major drainage divides as well as the general configuration of the topography. The degree of generalization is controlled by the spacing of the streams used in the generalization. The streams chosen can be selected precisely, simply by eliminating the upper reaches of a certain length of all the streams. The length of reach chosen for elimination determines the degree of generalization. The subenvelope map is useful for the present purpose because the larger streams are flowing on bedrock, and their channel gradients are adjusted to the bedrock.

In preparing figure 2, the contours were drawn on the streams shown on the U.S. Geological Survey's base map of the United States at 1:2 500 000 scale. Contours were plotted only on streams more than 32 km long. The resulting map shows the altitudes to which the major streams have eroded. The true altitudes of the divide areas, of course, are higher than the contours shown. Narrow ranges of mountains that

do not correspond to the major divide areas do not have topographic expression on the map. For example, the Blue Ridge of northern Virginia north of Roanoke (fig. 1, BR) contains peaks higher than 1220 m, but, as the entire range averages less than 32 km in width, it does not shown in figure 2.

The highland area (fig. 2) from Georgia to northern New York is about 1600 km long and averages about 240 km in width. It is broken by several large reentrants. The Tennessee River valley at T in the south divides it into two prongs. The New River valley forms a prominent reentrant at N and is the only river system that crosses the highland from southeast to northwest. Large reentrants occur at the Potomac River basin (P) and Susquehanna River basin (S). The Mohawk Valley at M separates the Adirondack Mountains from the main highland area.

Many of the forms are closely related to the kinds of bedrock directly beneath them. This relationship probably accounts in large part for the features just mentioned, thus obscuring the evidence for the interpretation of the Appalachian and Adirondack Mountains as uplifted features. The problem, then, is the extent to which the present topography has been formed by differential erosion as opposed to tectonism.

In a general way, the highlands owe their existence to uplift, for the rocks of the highlands pass under the Coastal Plain at the southern end. On the other hand, local topographic features such as the individual ridges in the Valley and Ridge province owe their height to differential erosion. The local importance of differential erosion is evident even in the southern Blue Ridge, an area of complex geology in which it is more difficult to identify resistant or nonresistant rock (Hack, 1973, 1976). Were the highlands, including the Adirondack Mountains and the Blue Ridge, uplifted as a single tectonic unit or are they composed of a group of separate tectonic blocks? If the highland is a single unit, has the uplift been differential, and at what scale or wavelength?

RELATION OF THE HIGHLAND FORM TO BEDROCK GEOLOGY

Figure 3 is a generalized geologic map of the Appalachian Highlands that has selected contours from the subenvelope map superimposed on it. The rock units are grouped according to broad lithologic types having different resistance to erosion. Units 1 and 4 contain extensive outcrop areas of resistant rock that tend to form highlands or high relief. Unit 2 contains alternating sequences of resistant and nonresistant rocks, which, where folded, produce the elongate ridges and valleys of the Valley and Ridge

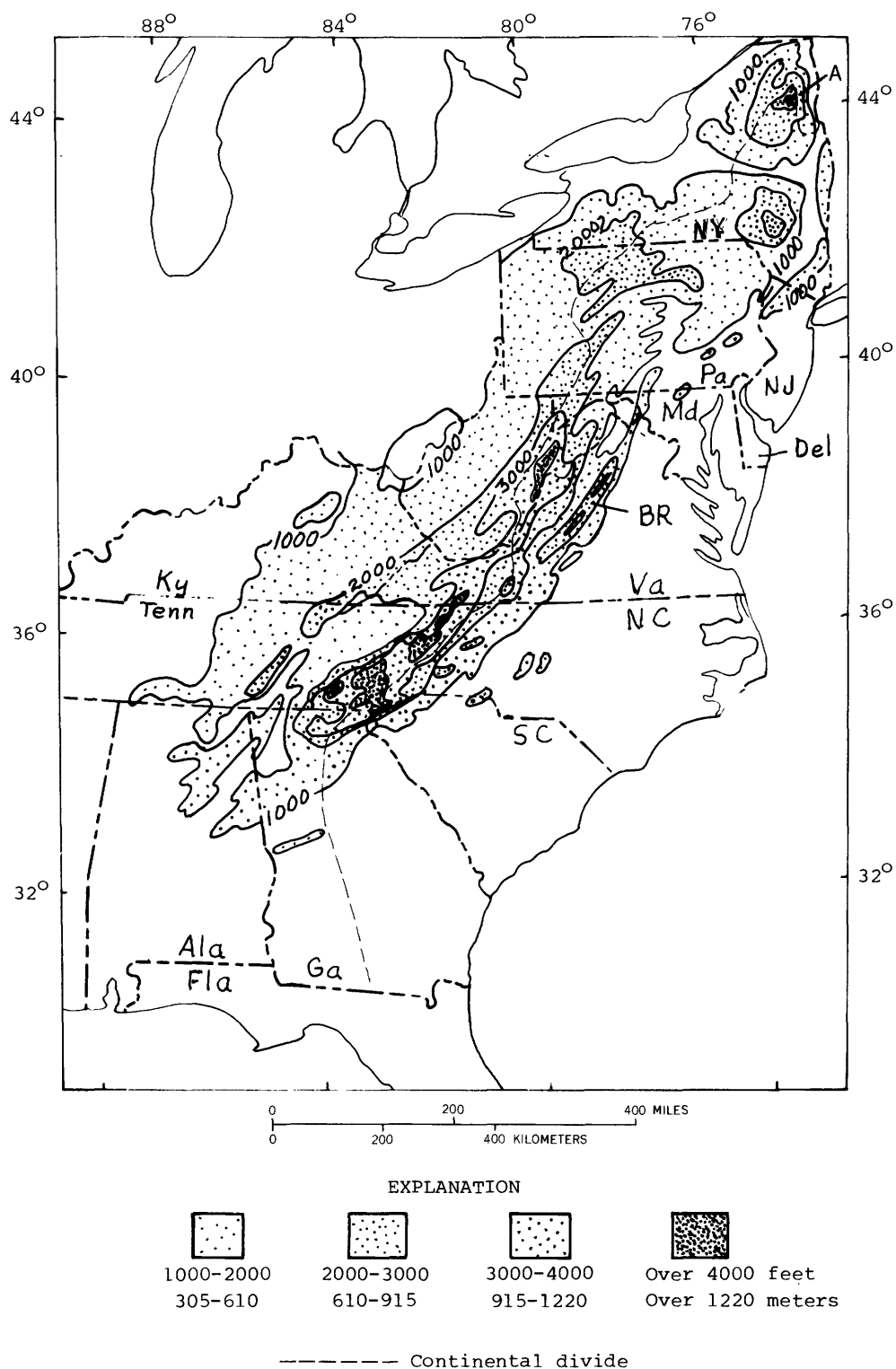


FIGURE 1.—Generalized topographic map (envelope map) of the Appalachian Highlands, showing the divide between the drainage to the Atlantic and to the Gulfs

of Mexico and St. Lawrence. Localities referred to in text include: A, Adirondack Mountains; BR, Blue Ridge of northern Virginia.

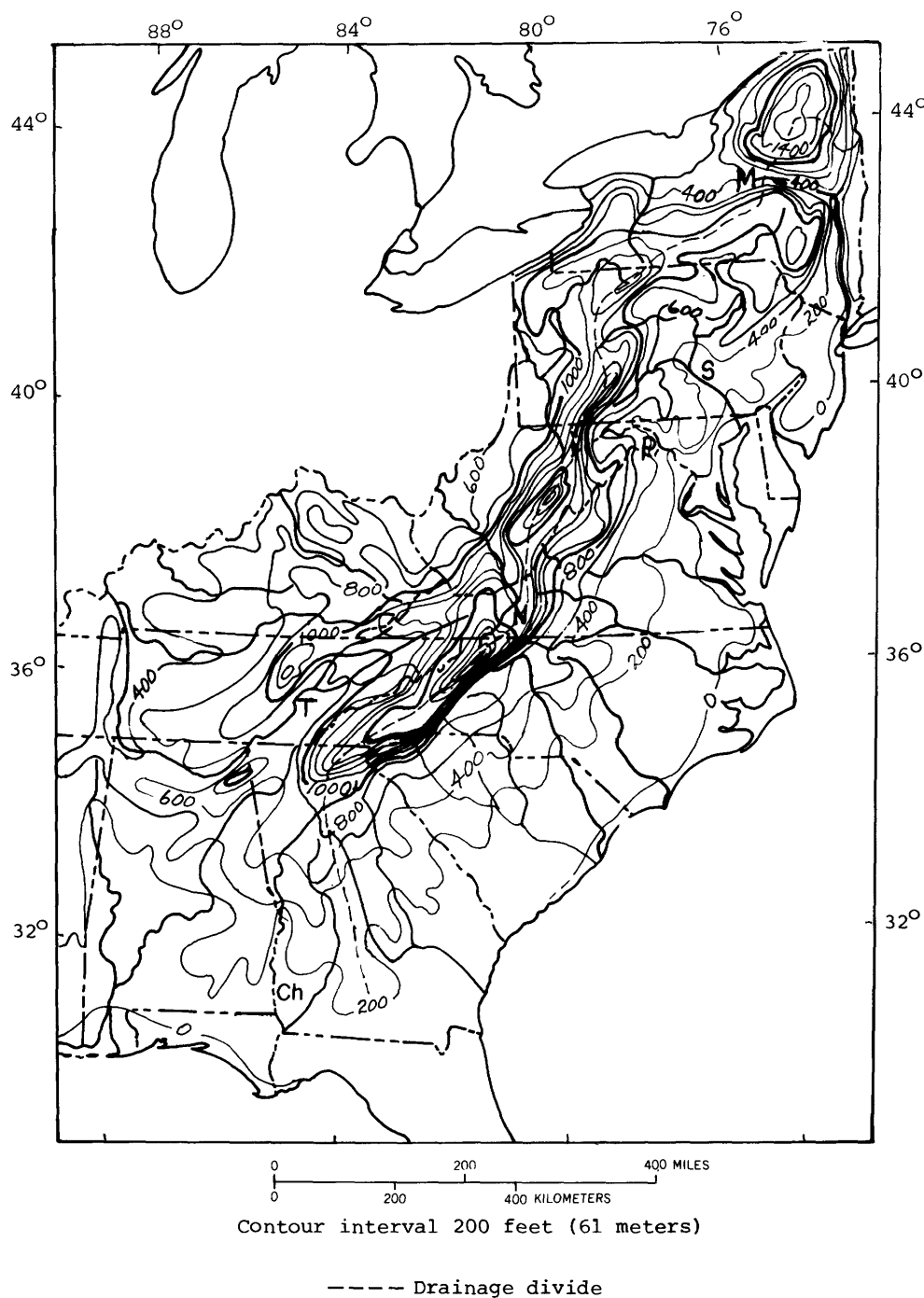


FIGURE 2.—Subenvelope map showing contours drawn on altitudes along the major stream channels. Altitudes on streams less than 32 km long as measured from the

source are not included. Ch, Chattahoochee River; T, Tennessee River; N, New River; P, Potomac River; S, Susquehanna River; M, Mohawk River.

province. Unit 3 contains mostly nonresistant shale and carbonate sequences. The four units are defined as follows largely on the basis of summary by Colton, 1970):

Unit 1: Includes the entire sequence of rocks of Pennsylvanian age as well as the Upper Devonian of

New York and Pennsylvania and the Permian of West Virginia. The rocks of Pennsylvanian age are clastic sequences, both marine and continental, and contain coal beds. They include thick sandstone, especially in the lower part of the section. These more resistant rocks crop out near the eastern edge of the Appala-

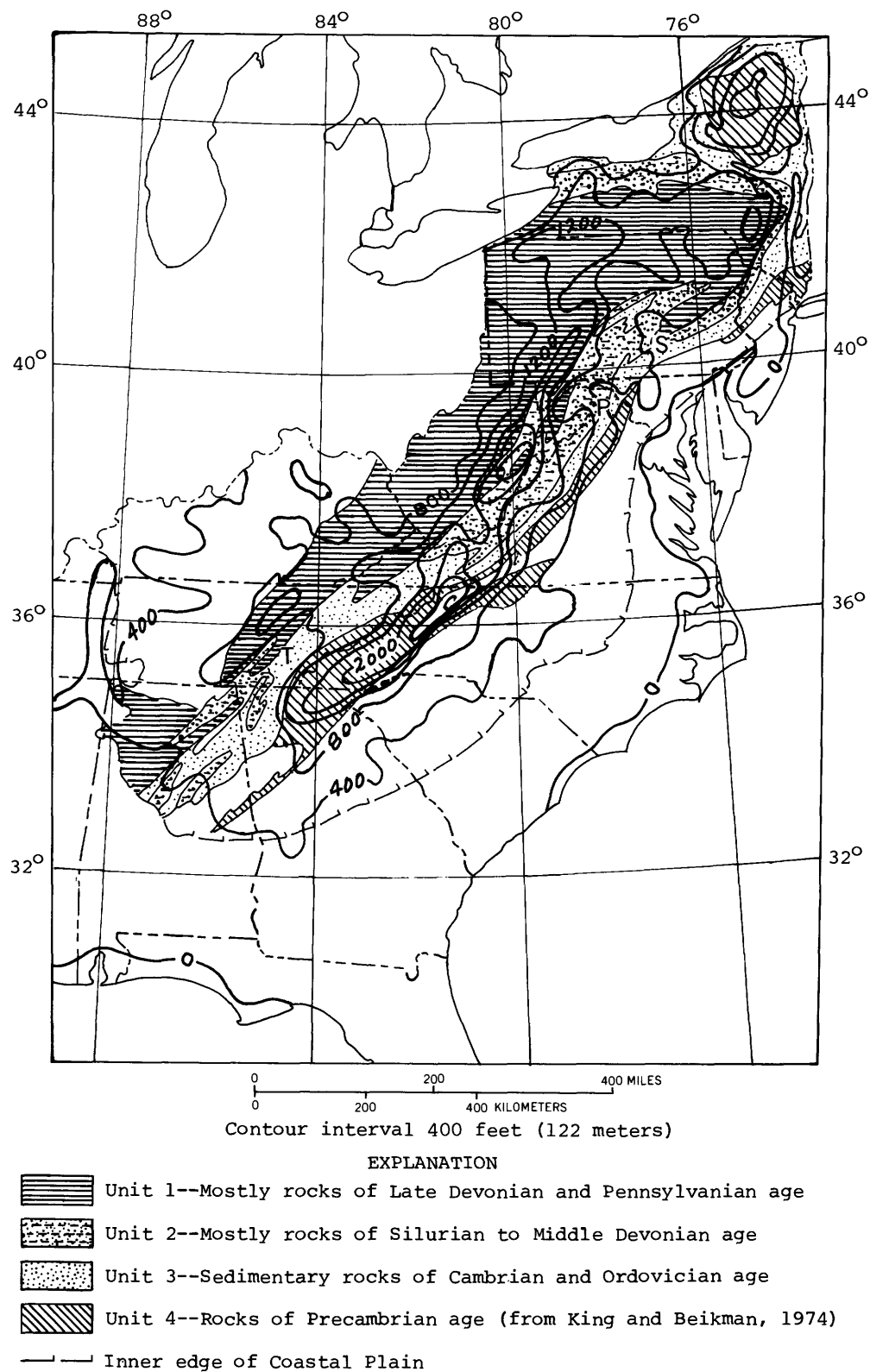


FIGURE 3.—Generalized map of major rock units based on their resistance to erosion. Selected contours from the subenvelope map are superimposed.

chian Plateau and in the area east of the Susquehanna River basin. The higher areas of the plateau of northern Pennsylvania as well as the Catskill Mountains are underlain by continental clastic rocks of Devonian age. They include coarse conglomerate and sandstone in the units designated as Upper Devonian by King and Beikman (1974).

Unit 2: Includes virtually all kinds of rock typical of platform deposits ranging from limestone and shale to sandstone and conglomerate. This unit includes the following chronostratigraphic map units of King and Beikman (1974): Silurian, Lower and Middle Devonian, Devonian, undivided, and Silurian and Devonian, undivided. The Upper Devonian of King and Beikman (1974) is not included. South of Pennsylvania, the unit also includes Mississippian sequences.

Unit 3: Includes the sedimentary rock of Cambrian and Ordovician age, mostly carbonate rocks and shale. The carbonate rocks increase in thickness from 180 m in New York to more than 3000 m in Tennessee. Shale, siltstone, and mudstone make up most of the remainder; they increase in thickness to the north. The unit omits the basal quartzite south of Pennsylvania but includes it to the north.

Unit 4: Includes the rocks designated Precambrian by King and Beikman (1974). These rocks vary widely in their degree of resistance, but they do contain resistant sequences of great thickness, especially in the south. The Ocoee Supergroup, for example, which underlies the Great Smoky Mountains and the Black Mountains, including Mount Mitchell, contains 5200 m of metamorphic quartz-rich sandstone and siltstone. The narrow Blue Ridge of Virginia is underlain by quartzite, metavolcanic rocks, and coarse-grained granitic rocks.

The subenvelope map superimposed on the geologic units (fig. 3) indicates that, except near the southern edge of the Appalachians, the high areas are on the most resistant rocks. The Lower Pennsylvanian sequence (unit 1), the Devonian clastic sequence (unit 2), and the Precambrian rocks (unit 4) form the highest areas. The bifurcation of the southern highland occurs where the main highland shifts southeastward to correspond with the large outcrop area of unit 4. The highland on the Pennsylvanian sequence continues to the southwest, forming the western prong.

In southern Pennsylvania, sandstone of Pennsylvanian age holds up large plateaulike areas. In the northern part, the Devonian and Mississippian clastic rocks underlie the present erosion surface and form the northern glaciated section of the Allegheny Plateau. The Catskill Mountains of New York locally include peaks as high as 1220 m. The Adirondack

Mountains form a separate dome underlain by rocks of Precambrian age.

In contrast, the large areas of nonresistant rocks found mostly in units 2 and 3 are responsible for the large reentrants in the Appalachian highlands at T, P, and S in figure 2. The large valley at T is drained by the Tennessee River and its tributaries and corresponds to a broad outcrop area of carbonate rocks (unit 4). At P, the principal tributaries of the Potomac are subsequent streams flowing in valleys in carbonate and shale (unit 2). The same is true of the Susquehanna basin at S.

THE BELT OF CAMBRIAN AND ORDOVICIAN ROCKS

At the crossover of the subenvelope crest from the Precambrian area to the plateau in southwest Virginia, the altitude of the subenvelope (fig. 3) appears to be unrelated to the bedrock. It crosses the nonresistant Cambrian and Ordovician sequence at an altitude of more than 730 m comparable with or higher than, altitudes at many other places along the crest. At the Hudson River, for comparison, the Cambrian and Ordovician belt is almost at sea level. Study of this belt of rocks shows that the altitudes within it can be explained at least in part by adjustments of the major streams that cross the belt to bedrock downstream from the belt. These adjustments, in effect, form local base levels at various altitudes that control the profiles upstream.

Figure 4A, which illustrates the argument for this hypothesis, is a profile along a series of stream reaches that flow along the strike in the Cambrian and Ordovician rocks. The profile is drawn along the streams as the crow flies and does not include bends or meanders. The altitudes are on the valley floors or flood plains adjacent to the streams. Except for small parts of the Coosa River, the streams are entirely within the Cambrian and Ordovician rocks. However, all have tributaries or upper reaches that head in more resistant rocks, and they depart from the belt to cross terrains having a great variety of rock types. The divides between the streams within the belt are narrow everywhere, so that a continuous longitudinal profile is formed.

The profile along the strike of the Cambrian and Ordovician rocks (fig. 4A) is divided into concave-upward segments, each of which is part of the drainage basin of a large stream that exits the Cambrian and Ordovician belt. The high point is near Rural Retreat south of the continental divide, between headwaters of the Tennessee and New Rivers. This place is close to where the Cambrian and Ordovician belt

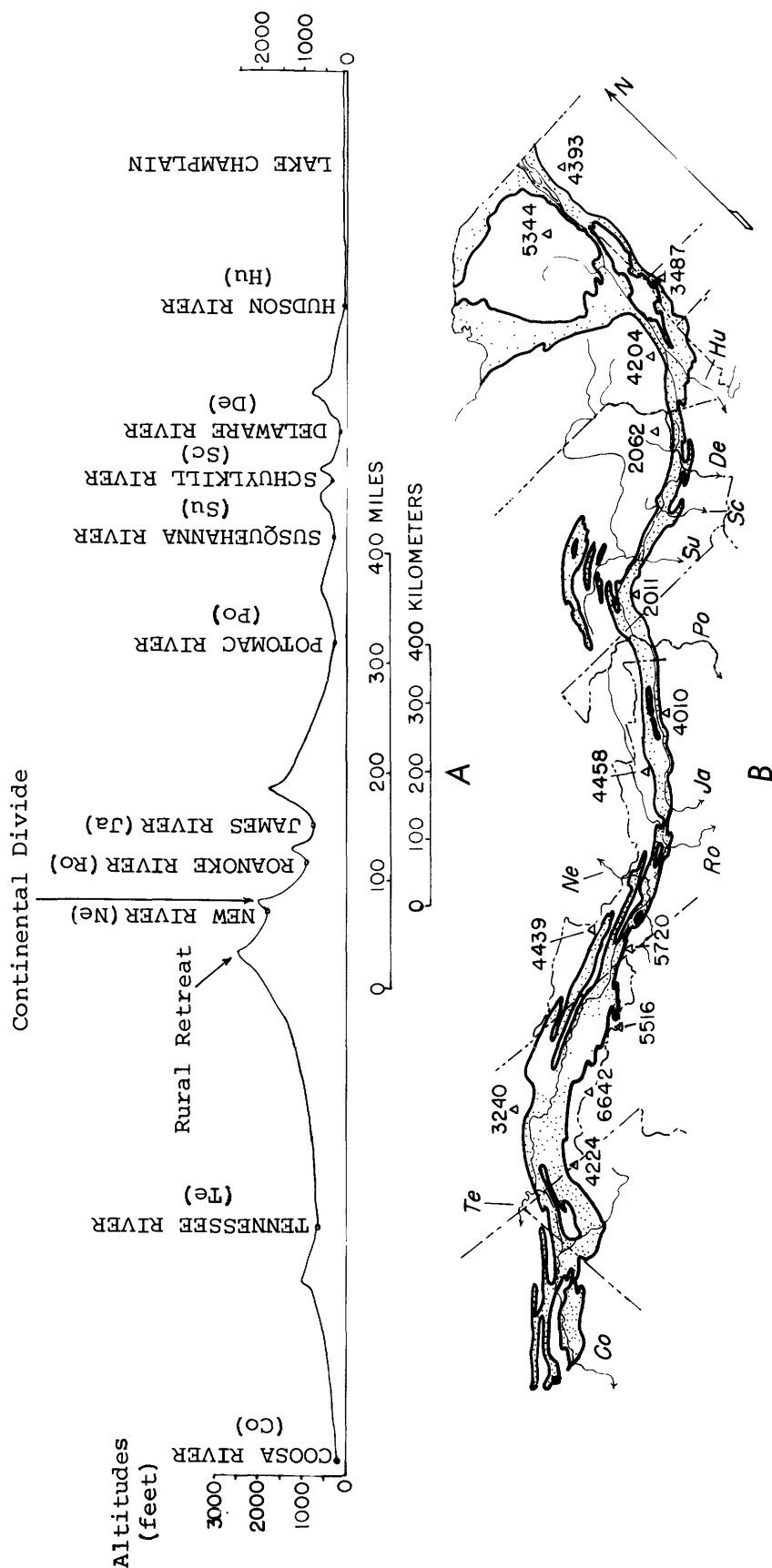


FIGURE 4.—Profile (A) and outline map (B) of the Cambrian and Ordovician belt from Coosa River to Lake Champlain. Numbers represent altitudes of selected high peaks.

narrows and is broken up by ridges of more resistant rocks younger than Ordovician. Profiles of streams of small and intermediate size such as those in the belt are generally shaped by the amount of discharge and various factors related to flow resistance of the channel, the most important of which are probably load and size of bed material. The channel slopes of streams are normally inversely proportional to the discharge, and, as discharge and length are directly related quantities, channel slopes are generally inversely proportional to a function of length. This explains the concave-form characteristics of most longitudinal valley profiles. As channel slope tends to be directly proportional to a function of size of bed load, the concave profile is modified in steepness and in the details of its form by the resistance of the rocks in its drainage basin. The high point at Rural Retreat on the divide between the Tennessee River drainage and the New River drainage is a striking feature of the composite profile (fig. 4A). It can be explained by differences in the geology of the Tennessee River drainage basin and the New River basin (Hack, 1973). The Tennessee system descends from Rural Retreat via the Holston River as far as Chattanooga through a broad valley in shale and carbonate rocks. The altitude at Chattanooga, where the river system exits the Cambrian and Ordovician belt, is only about 210 m. Below this point, it crosses resistant sandstone beds in a short reach below Chattanooga. It crosses northern Alabama through an area underlain mostly by Ordovician and Mississippian limestone. Thus, almost its entire course is in nonresistant rocks.

The New River, on the other hand, heads in the Blue Ridge and crosses the Cambrian and Ordovician belt at a narrow point. It then flows northward toward the Ohio River, crossing thick sandstone sequences of Pennsylvanian age. Its gradient is actually steepened in these reaches in spite of the increased discharge. Its steep descent ceases above Charleston where it joins the Gauley River at an altitude of about 200 m.

Northeast of the New River, the regional drainage is to the southeast into the Atlantic by streams that head along the resistant rocks of the plateau and flow more directly across the Cambrian and Ordovician belt. Only in the Potomac and Susquehanna basins are there major streams parallel to the regional strike. The Roanoke and James River cross resistant Precambrian rock before reaching the Piedmont lowlands, but the outcrop widths are narrow compared with those of the resistant rocks crossed by the New River. The Potomac exits the belt at a place where the resistant rocks are unusually thin (Hack, 1965, p. 28). The Susquehanna and Schuylkill Rivers flow directly

across the nonresistant beds of the Newark Group in the Triassic and Jurassic basin. The Delaware crosses only a narrow band of rocks of Precambrian age in the Reading Prong. The absence of a high resistant barrier between the Cambrian-Ordovician rocks and the Piedmont lowlands in Pennsylvania permits even small streams like the Schuylkill to survive without capture by subsequent drainage from the Susquehanna or Delaware. In New York State, the Cambrian and Ordovician belt forms a narrow lowland separating the Appalachian Plateaus province on the west from the New England province on the east. The altitudes are low; the Hudson River is at tide level as far north as Albany. The belt intersects tidewater again at the St. Lawrence River. Adjustments to resistant and nonresistant rocks do not explain why the Hudson River cuts through the Precambrian rocks of the Hudson Highlands in a preglacial gorge southeast of the Cambrian and Ordovician belt. Many explanations have been offered (Thornbury, 1965, p. 165).

The relationships cited above show that the general topography of the belt can be explained without involving the hypothesis of differential uplift, except, of course, the obvious condition that the entire Appalachian system formed as a result of one or more periods of uplift at some time in the past. The height of the divide at the New River crossing is explained by the necessity for that river to cross many miles of resistant rocks downstream exposed on the Appalachian Plateau. North of the New River, the lower areas are explained by the fact that the drainage out of the Cambrian and Ordovician belt crosses lesser barriers to reach the lowlands.

The altitudes marginal to the Cambrian and Ordovician belt can be judged by the spot altitudes of peaks shown on figure 4B. These altitudes are generally high all along the belt except locally in Pennsylvania, where the belt is bordered on the south by weak rocks and on the north by narrow ridges underlain by thin resistant beds.

DURATION OF EROSION

The general evidence for a close adjustment of the surface forms to the rocks, especially obvious in the Cambrian and Ordovician belt, is an indication that the region must have been exposed to subaerial erosion for a long time; however, more positive evidence does exist. A narrow zone of deposits containing lignite, wood, leaf fragments, and other organic material was called the Brandon Formation by Clark (1891), who regarded these occurrences as of Eocene age. The deposits are now known to range in age from Cretaceous

through Tertiary. They extend down the southeastern margin of the Appalachian basin from Vermont as far south as Alabama. These deposits are small and are generally in residuum overlying the Lower and Middle Cambrian carbonate rocks of the Shady and Tomstown Dolomites and their equivalents. The surface topography in the zone of these deposits is in many places pitted by modern sag ponds that commonly contain peat and other organic matter of Pleistocene to Holocene age. The close association suggests a common origin for the organic deposits. They have evidently been formed by solution in the underlying carbonate rocks as part of a continuous process operative since the Cretaceous. The literature on the occurrences is scattered, but a discussion of the implications of a Cretaceous locality in Pennsylvania has been presented by Pierce (1965). Some modern sag ponds have been described by Craig (1969). Additional references have been cited by Mathews (1975). As the fossil deposits could have slumped downward several thousands of meters since they formed because of solution of the underlying carbonate rocks, they do not necessarily inform us about the past nature of the relief, but their occurrence and the lack of marine fossils indicate that the Cambrian and Ordovician belt has been exposed to erosion for a long time.

EVIDENCE OF LATE TECTONIC ACTIVITY

Abundant evidence indicates that tectonism has taken place in late geologic time, that is, during the late Mesozoic and Cenozoic. The evidence includes changes in the rates and kinds of deposition through time on the Continental Shelf, late faults, tilting or warping of features of the coastal zone, differences in height of land, and areas of anomalous relief. The sedimentary record in the Coastal Plain and Continental Shelf has, of course, been used by many to interpret the history of the hinterlands, and this record will surely become increasingly useful as exploration of the shelf continues. Analysis of the Coastal Plain and shelf deposits, however, is outside the scope of this paper, though the use of sedimentary volumes to interpret erosion rates on the land should be mentioned. Mathews (1975) estimated, by analysis of a series of sections off the Atlantic coast, that at least 2,000 m has been eroded during the Cenozoic on the adjacent land, an average rate of 0.027 mm/yr. The data also suggest that erosion was greatly accelerated during the Miocene.

Data (table 1) from the COST No. B-2 well on the outer shelf off New Jersey (Scholle, 1977) permit an estimate of sedimentation rates since the beginning of the Cretaceous, though density, compaction, and other

factors are not taken into account. As this well seems to penetrate a typical sequence of major units, the sedimentation rates probably are roughly indicative of relative erosion rates in the source area. The data support the idea that rates were high in Early Cretaceous and Miocene time.

Judging by the quick response of the crust by uplift to the removal of the continental glacier of Pleistocene age, changes in erosion rates probably have been balanced closely by changes in uplift rates; the reverse was probably also true. Thus, high uplift rates probably prevailed in the Early Cretaceous and Miocene, and lower rates, from Late Cretaceous to Eocene time. Nevertheless, uplift was probably continuous throughout post-Jurassic time.

That faulting took place in late geologic time in the Eastern United States is not easy to demonstrate. Nevertheless, actual faults cutting beds of late geologic age have been observed at more than 30 places in eastern North America (York and Oliver, 1976). Probably many more late faults will be discovered. Most of them are along the Fall Zone where thin sedimentary strata overlap the basement. Two of these faults have been studied in some detail. The Stafford fault zone, west of the Potomac River (Mixon and Newell, 1977), consists of an echelon faults and a parallel monocline 56 km long. The displacements are small, not exceeding 60 m. They involve sediments as young as middle Tertiary, but some movement in the late Tertiary is possible. The sense of motion is reverse. A somewhat similar group of faults that had small displacements in late geologic time has been found near Augusta, Ga. These faults are also reverse and involve Cretaceous and younger sediments, possibly as young as Miocene (David Prowell, oral commun. 1977).

The displacements observed are too small to account for the rate of uplift of the area inland from the Coastal Plain as determined by the sedimentary record. Other faults farther inland would be difficult to de-

TABLE 1.—*Thickness of sediments penetrated in COST No. B-2 (Scholle, 1977) and estimated deposition rate*

Period or epoch	Duration (millions of years)	Thickness of sediment (m)	Rate (mm/yr)
Pliocene and Pleistocene.	12	130	0.011
Miocene -----	14	860	.061
Oligocene -----	12	150	.012
Eocene -----	16	220	.014
Paleocene -----	11	60	.005
Late Cretaceous ----	35	980	.028
Early Cretaceous ---	36	2470	.068
Total -----	136	4870	
Average -----			.036

tect because of the sparse sedimentary cover younger than the basement.

Another tectonic process of late geologic age is the general downward tilt of the coastal zone to the northeast. This tilt can be seen on figure 3, which shows the Fall Zone or inner margin of the Coastal Plain. In Georgia, the Fall Zone is crossed by streams at an altitude of 120 m. At the northern end of Chesapeake Bay, the zone is at sea level, and, in New England it is below sea level. The tilt of the Fall Zone is matched by the tilt of the Continental Shelf. These features imply a broad tilt of the continent down to the northeast. The head of tidewater extends inland different distances in different rivers, as shown by the 0 contour in figure 3, but this phenomenon is not necessarily related to the tilt of the coastal zone. Eardley (1964) explained the tilt of the Coastal Plain and the Continental Shelf as part of a worldwide process of poleward rise of sea level related to a long-term decrease in period of the Earth's rotation, beginning in the

Cretaceous. The fact that some river valleys appear to be drowned more deeply toward the north, however, suggests that a process acting more rapidly may be involved.

Differences in relief or sharp changes in altitude may be evidence for unequal uplift in the past, provided that relief differences are in rocks of similar resistance to erosion. Figure 5 is a simplified relief map of the Piedmont and Blue Ridge provinces south of the glacial border. The two provinces have extreme differences in relief. The Piedmont relief is comparatively low over extensive areas, and the map is intended to emphasize differences in relief within the Piedmont. Most of the areas of moderate relief on the outer Piedmont are directly related to resistant bedrock. For example, the Pine Mountain belt containing quartzite beds forms a moderate relief area at A. Cataclastic rocks of the Brevard zone occur at B. Resistant beds of the Kings Mountain belt are found at C. At area D, moderate relief is caused primarily by fel-

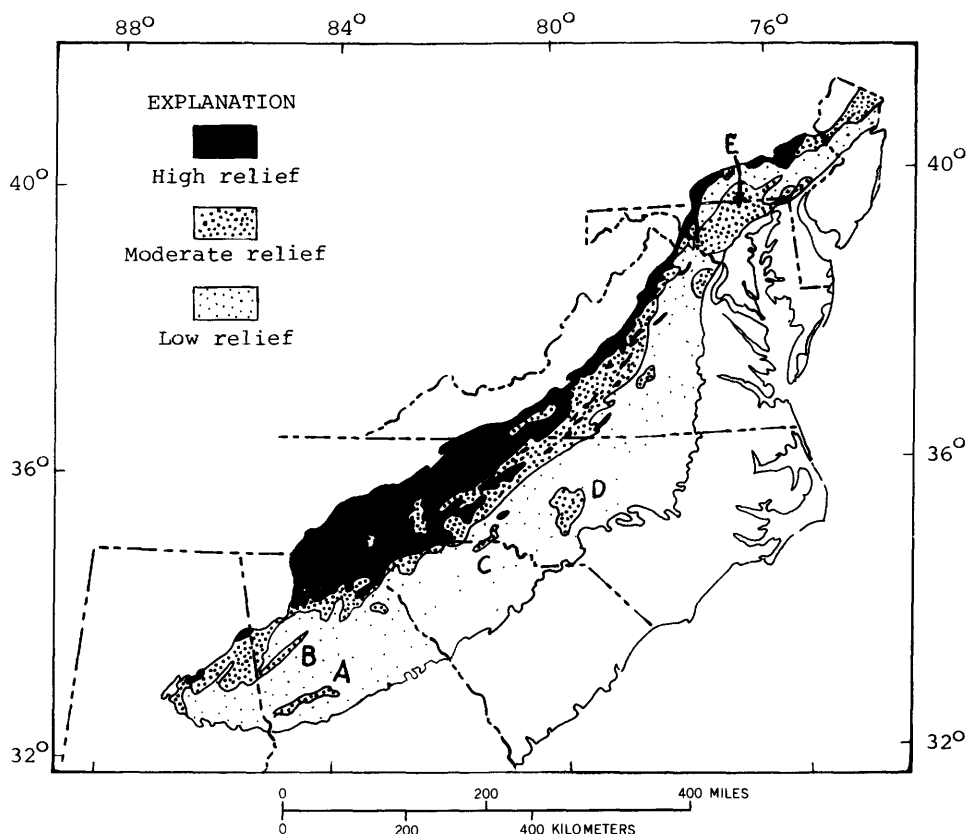


FIGURE 5.—Generalized relief map of Piedmont and Blue Ridge provinces. The relief classes are based on the number of contours within square areas 10 km on a side, as indicated on the 1:250 000-scale series of topographic maps by the U.S. Geological Survey. Less than 90-

120 m in low-relief areas and 120–240 m in moderate-relief areas. High-relief areas are generally more rugged and have relief of more than 240 m and as much as 1200 m. Letters indicate areas discussed in the text.

sitic rocks of the slate belt. A large area of moderate relief (E) lies between the Coastal Plain and the Culpeper and Gettysburg Triassic and Jurassic basins. Its highest point exceeds 305 m above sea level near Westminster, Md. This area was referred to as the Westminster anticline by Campbell (1929, 1933), who believed that it represented an upwarped peneplain of Miocene age on the basis of warped stream terraces along the Potomac, Susquehanna, and Schuylkill Rivers. Although the existence of a peneplain of lower relief in Miocene time cannot be proved, the higher relief that exists there now is probably the result of upwarping of the area at a higher rate than other parts of the Piedmont farther south.

Several arguments support this idea. The rocks in the area of the Westminster anticline, or uplift, to use a less specific term, are both igneous and sedimentary, similar to rocks of the Virginia Piedmont farther south where relief is lower. They include gabbro, granite, gneiss, diamictite gneiss, quartzose schist, volcanic rock, phyllite, and marble.

The altitude of the highest parts of the Westminster uplift exceeds 305 m. Total relief within 100-km² areas was measured on 1:24 000-scale maps of the following quadrangles: Downingtown, Pa. (162 m), and Mt. Airy (125 m), Winfield (125 m), and Rockville (105 m), Md. In low-relief areas shown on figure 5, total relief is generally less than 90 m in areas 10 km on a side.

On its west side, most of the uplifted area is bounded by a low escarpment that overlooks Triassic and Jurassic basins to the west. As these basins are underlain mostly by shale and mudstone, the relatively low altitude and low relief are perhaps related to rock control. On the east, the Piedmont margin is overlapped by a sequence of sedimentary deposits ranging in age from Early Cretaceous to late Tertiary (Darton, 1951). The surface of basement and base of the Cretaceous has a slope of about 0.02 in Washington, D.C., whereas the slope of the Miocene in Washington is only 0.005. A river gravel deposit resting on the Miocene, believed to be of late Tertiary age, has an even lower slope, averaging about 0.0025 at the same cross section. Although the slope of the surface on which these sediments were laid down is not known, the Lower Cretaceous gravel is similar in size composition to the upper Tertiary gravel. Thus, the difference between the two slopes (approximately 0.0175) may reasonably be taken as a measure of the tilt that has taken place. Assuming an age difference of 100 million years between the two gravels, the rate of tilt would average about 1.75×10^{-4} (mm/km)/yr. If the present slope tangent of the basement were projected 50 km inland from the Fall Zone to a point

near the center of the highest altitude near Westminster, Md., assuming no erosion and no bending, the altitude of this point would be about 1000 m above sea level or 700 m above the present surface. The average rate of lowering at this point since middle Cretaceous time would have been 7×10^{-3} mm/yr. As will be shown in the next section, these rates of uplift and erosion are somewhat lower than average rates calculated for other places and other time spans using a variety of methods (tables 2 and 3).

It should be noted that the present slope of the basement beneath the Coastal Plain in the Washington area, as indicated on the "Tectonic Map of the United States" (U.S. Geol. Survey and Am. Assoc. Petroleum Geologists, 1962), is greater in the northern Piedmont near Washington east of the Westminster uplift than it is farther south. At the Virginia-North Carolina boundary, the slope tangent of the basement near the inner edge of the Coastal Plain is about 0.005 as compared with 0.02 in the Washington area. In the northern Piedmont, the increased relief is also related to the general depression of the Coastal Plain in the Salisbury embayment, which brings the edge of the Piedmont to sea level in the larger river valleys like the Potomac. The Pleistocene lowering of sea level lowered the base level still more and probably affected the relief inland, at least close to the larger streams (Hack, 1975, p. 96).

The most dramatic difference in relief unaccounted for by geology is along the Blue Ridge escarpment. As shown by figure 3, a steep escarpment in Georgia and North Carolina crosses the boundary between the Precambrian terrane and the generally younger metamorphic rocks of the Piedmont. The same escarpment also crosses the Cambrian and Ordovician belt, and its crest forms the continental divide between the Gulf of Mexico and Atlantic drainages. The relief and altitudes of the terrain on either side are strikingly different. Within areas 10 km wide, the relief averages less than 90 m in the Piedmont. In areas of comparable size in the Blue Ridge, the relief ranges from about 180 m to more than 1000 m, and altitudes rise to more than 2000 m.

Davis (1903) explained the escarpment by the differences in lengths of the rivers on either side in their descent to the sea. White (1950) thought the escarpment was essentially a fault scarp. Hack (1973) thought that the escarpment was due to differences in the geology crossed by the streams on either side. In other words, the westward-flowing streams cross a series of local base levels formed on resistant rocks, thus, in effect, maintaining the high altitude of the continental divide. The faulting hypothesis remains a

possibility, though clear evidence for a fault or faults has not been found. Nevertheless, over long distances, the rocks forming the present escarpment are not more resistant than those on the adjacent Piedmont at the toe of the scarp. If no faulting is involved, tilting must have taken place on the southeast side of the Blue Ridge.

RATES OF EROSION AND UPLIFT

Many estimates have been made of erosion and uplift rates based on a variety of methods. In addition, contemporary uplift or tilting of the land has been measured in the field by repeated geodetic traverses. Some of these estimates that relate to the Appalachian Highlands are summarized in tables 2 and 3. Table 2 deals with erosion and uplift rates measured at a single locality within an area. These rates are absolute values

related to a constant but unspecified data base expressed as erosion in millimeters per year or as velocities of uplift in millimeters per year.

The estimates in table 3, on the other hand, are differences between rates at points along a linear feature or traverse. In other words, they are relative rates or angular tilt rates rather than uplift or subsidence. They are expressed in millimeters per kilometer per year (compare with Brown and Oliver, 1976, p. 17).

The first five items in table 2 are based on amounts of material being carried out of one or more drainage basins over a period of at least a year. Item 1 in the table is from a general paper by Judson and Ritter (1964), which contains a review of earlier literature as well as newer data. The first three estimates deal with fairly large drainage basins. Items 4 and 5 are small watersheds that may not be typical, though the

TABLE 2.—*Estimates of erosion rates*

Item no.	Process	Rate (mm/yr)	Sources of data
1	Modern erosion, North Atlantic drainage basins---	4.8×10^{-2}	Judson and Ritter, 1964.
2	Modern erosion, South Atlantic and Gulf basins----	4.1×10^{-2}	Judson and Ritter, 1964.
3	Modern erosion, South Fork of Shenandoah River watershed.	4.3×10^{-2}	Hack, 1965.
4	Modern erosion, small watershed, Coweta, N.C. ----	9×10^{-3}	Berry, 1977.
5	Modern erosion, small watershed, Maryland Piedmont.	4.6×10^{-3}	Cleaves and others, 1970 ¹
6	Cenozoic erosion rate based on sediment volumes on Continental Shelf (Atlantic drainage).	2.7×10^{-2}	Mathews, 1975.
7	Phanerozoic erosion rate for U.S. based on sedimentary volumes. (Figure given is minimum; estimated by authors as up to six times too low).	1×10^{-2}	Gilluly and others, 1970.
8	Uplift and erosion (some possibly tectonic) based on depth of intrusion of Stone Mountain Granite, Georgia.	4.1×10^{-2}	Whitney and others, 1976 ¹
9	Uplift and erosion (some possibly tectonic) based on thickness of Paleozoic sequence in eastern Pennsylvania.	5.3×10^{-2}	This paper, data from Colton, 1970.
10	Removal of overburden from Middle Devonian rocks and conodont color in Appalachian basin—rate calculated since Permian.	$4.8 \text{ to } 8.8 \times 10^{-2}$	This paper, data from Epstein and others, 1977.

¹ The rates reported here were calculated by Hack from data in references cited.

TABLE 3.—*Estimates of tilt rates*

Item no.	Tilted feature	Rate [(m/km)/yr]	Source of estimate
1	Modern tilt rate in Potomac basin if balanced by average erosion rate of 4×10^{-2} mm/y.	3.5×10^{-4}	This paper.
2	Tilt rate of basement rocks from the Cretaceous to late Miocene, Washington, D.C.	1.75×10^{-4}	This paper.
3	Domal uplift of Canadian Shield since 7000 B.P. (average tilt of southeast part of dome).	2.2×10^{-2}	Walcott, 1972, fig. 16. ¹
4	Downwarp to south of beach of high stand of Champlain Sea since 10 000 B.P.	9.3×10^{-2}	Denny, 1974, p. 42. ¹
5	Upwarp to south of level line west of Lake Champlain, Rouses Point to Ticonderoga after 18 years.	3×10^{-2}	Isachsen, 1975. ¹
6	Downwarp of rerun level line 100 km long between Atlanta and Columbus, Ga.	5.5×10^{-2}	Brown and Oliver, 1976, fig. 11.

¹ The tilt rates reported here were calculated by Hack from data in the references cited.

methods of analysis used in these two cases are rigorous. Items 6 and 7 are estimates based on the volume of sedimentary sequences that have been redeposited after erosion from the land. These estimates are the same order of magnitude as rates in items 1–3. Item 8 (Whitney and others, 1976) is an entirely different kind of analysis based on depth of emplacement of a granite body in metamorphic rocks. By using isotope ratios, the age and the temperature and, hence, by inference, the depth of emplacement can be estimated. The rate of removal of overburden can, of course, be determined from these data, though whether all the removal was due to subaerial erosion is not certain. It is interesting that item 8 is comparable in magnitude with items 1, 2, 3, and 6.

Items 9 and 10 are similar in concept to item 8 in that uplift rates are estimated by inferences about age and depth in the Earth before the time of uplift. It is assumed that because the rocks are now at the surface, the average uplift rate and erosion rate have been the same. Item 10 is taken from a study of conodonts (Epstein and others, 1977), which shows that conodont colors in the Appalachian basin consistently indicate depth of burial. These data give results similar in magnitude to the others. The two modern erosion rates from small watersheds (items 4 and 5, table 2) are significantly different, but it should be noted that the rates in these two places are lower rates rather than higher.

The results obtained from direct measurements of tilt cannot be compared with the uplift velocities or erosion rates given in table 2 without making some sort of conversion that involves assumptions about the distribution of the uplift or erosion rates within an area. To do so, the absolute rates must be converted to tilt rates. Item 1 in table 3 is such a conversion. It is based on the assumption that the Potomac Basin is now being tilted upward at its western headwaters near the continental divide relative to the mouth at sea level and that uplift is balanced by an erosion rate of 0.04 mm/y (from table 2). As the erosion rate varies throughout the basin, the average rate is assumed to be centered at a point about halfway (112 km) from the river mouth to the continental divide. On this basis, the tilt-rate estimate in the basin is 3.5×10^{-4} , expressed as millimeters per kilometer per year. This rate can be compared with tilt rates measured along level lines (items 5 and 6, table 3) or along water planes whose age is known (items 3 and 4, table 3). The data show that the measured modern and post-Pleistocene tilt rates are at least an order of magnitude higher than rate number 1, on the basis of the erosion rates estimated in table 2. The same conclusion is

reached by comparing erosion estimates with absolute uplift rates of domal features that have been measured. One example is the Canadian Shield, which near its center at Hudson Bay is estimated by Walcott (1972) to be rising at a rate of 20 mm per year, a rate much higher than any of the absolute rates of table 1. In this example, the uplift area has a radius of about 1000 km, and this rapid rate is, of course, compatible with the calculated tilt rate for this area (item 3, table 3).

Another example of a high absolute rate is the Adirondack dome, studied by Isachsen (1976). On the basis of differences between two geodetic traverses, assuming 0 base at the south edge of the rising area at Utica, 240 km from the center, the Adirondacks are rising at a rate of 3.7 mm/y. This translates to a tilt rate of 2.4×10^{-2} mm/yr, approximately the tilt rate of the southern margin of the Canadian Shield. The northern flank of the Adirondack domal uplift also shows on a geodetic traverse along the shore of Lake Champlain (item 5, table 3), but the direction of tilt is the reverse of the postglacial tilt of the water planes parallel to it (item 4, table 3). Therefore, if the tilt is real, it has only recently reversed its direction.

A brief consideration of the rate of change of landforms in postglacial time is useful. Glacial deposits of Wisconsinan age in the Central United States, as much as 55 000 yr old (Flint, 1971, p. 559), have a constructional topography that has undergone little change in form since deposition. On the other hand, glaciated terrain of Illinoian age, more than 100 000 yr old, has been considerably modified, though the deposits themselves are mostly preserved. Nebraskan glacial deposits, which are more than 400 000 yr old, have been eroded extensively, and none of the original topographic form survives. These general conditions are consistent with an average erosion rate of 0.04 mm/yr or 4 m/100 000 yr.

The data indicate that erosion rates in the Eastern United States, both modern and Cenozoic in age, are, on the average, low. For large areas, they average as much as about 4×10^{-2} mm/yr. Judging by two anomalously low rates estimated by more detailed analysis of very small watersheds, the true rates may be even lower. All these rates are much lower than uplift rates at the center of large areas like the Canadian Shield, where the rate at the center is 20 mm/yr. However, uplift rates depend on the size of the area being deformed, so it is more reasonable to compare tilt rates than absolute uplift rates. If erosion rates are converted to or are considered the inverse of tilt rates, then a large discrepancy remains, amount-

ing to at least one order of magnitude. It thus appears that the rates of deformation now observed cannot have been sustained for long periods. The rates of rebound after the removal of the ice are consistent, however, with measured tilt rates. Rebound can take place rapidly, with only a short lag time between removal of a load and compensation by uplift. Much of the data contained in repeated geodetic traverses, however, is not readily explained. For example, if the tilt downward south of Atlanta, Ga., involving a 100-km traverse (item 5, table 3), were sustained for 100 000 yr, it would result in a depression 550 m deep. No depression exists at this locality, and the topography is a normal erosional topography resembling its surroundings.

DEVELOPMENT OF THE APPALACHIAN HIGHLANDS IN LATE GEOLOGIC TIME

The present topography of the Appalachian Highlands is closely adjusted to the rocks. However, the available evidence shows that the highlands have undergone warping and minor faulting in late geologic time. No positive evidence has yet been found that the bedrock at the surface has been broken by differential movements of any great magnitude since at least Cretaceous time. Though uplift took place, it must have involved broad warping of the crust. Data from the Coastal Plain and Continental Shelf indicate that though the tilting of this area has probably been continuous, it was particularly rapid in early Cretaceous and Miocene to Pliocene time. Assuming these conditions, the present topography could have been derived by normal erosional processes.

The outlines of the present landscape began to form some time in the middle Mesozoic after the breakup of the continent and the establishment of a drainage system toward the opening Atlantic. The first coarse clastic sediments deposited on the Coastal Plain and Continental Shelf are Early Cretaceous in age. The outlines of the hinterlands from which this material came are not known except by inference. The material deposited on the Coastal Plain contains elements from both the Piedmont and the Coastal Plain (Glaser, 1969). Because the coarser gravel contains a high proportion of quartzite and finer gravel contains a significant amount, at least some of the material probably came from the Appalachians west of the Blue Ridge. On the other hand, the heavy minerals and the paucity of chert indicate that, in general, the greatest proportion of material probably came from the Piedmont, perhaps indicating that the relief on the Piedmont was high at the time.

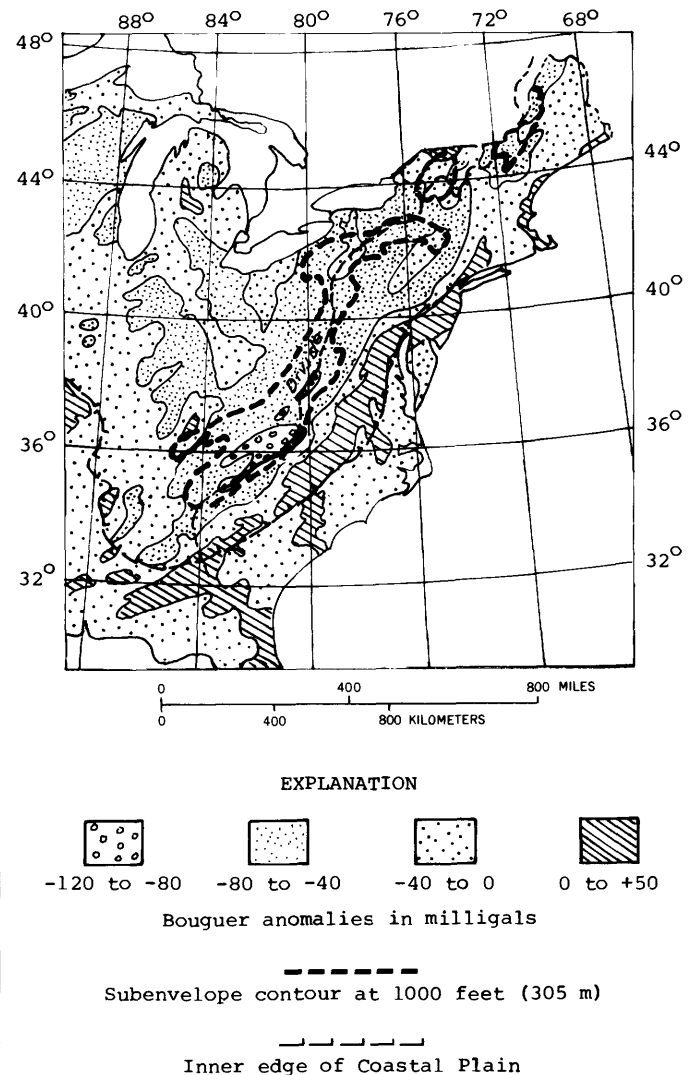


FIGURE 6.—Map of Eastern United States showing Bouguer gravity anomalies. Data from Defense Mapping Agency, Aerospace Center, St. Louis, Mo.

Geomorphic evidence concerning the limits of the initial drainage system and the position of the divide has been controversial, and much has been written on the subject (Thornbury, 1965, p. 82). Judson (1975) noted that the continental drainage divide corresponds to a gravity low in the central and southern Appalachians (fig. 6). The meaning of the gravity low is not understood, but the low may relate either to a thick crust or to the thick sequence of low-density rocks in the eastern part of the Appalachian basin. In any case, the correspondence of the low to the drainage divide is consistent with the idea that the divide has had a stable position for a long time. The correspondence of the divide to the low is lost north of lat 40°. In a general way, low anomalies do tend to correspond

to high topographic areas, though, in detail, this correspondence breaks down in the Adirondacks and New England (fig. 6).

During the Cretaceous, base level of erosion was established at about its present position or higher; it could have varied little more than 300 m in altitude since then. During the Early Cretaceous, when large amounts of coarse sediments were poured onto the Continental Shelf, derived largely from crystalline terrane, base level was lower than it is at present. By Late Cretaceous time, the rate of sedimentation had slowed, and base level rose so that the sea probably covered some of what is now the Piedmont. In Oligocene time, at least in the north, sea level again was lowered. In Miocene time, base level was generally lowered, though in some areas the sea was higher than now. The positions of base level were never parallel to those at present, as certain areas like the Cape Fear and South Jersey uplifts tended to be higher than others (Owens, 1970), and there has been a general down tilt of the shelf to the northeast.

It is assumed that continuing uplift as well as erosion inland were responsible for the high rate of sedimentation on the Continental Shelf. As the absolute rate of uplift relative to base level must have increased inland, the uplift was in the form of a broad arch, its axis centered somewhere near the present continental divide. Thus, topographic relief that formed as a result of uplift would have been higher inland near the crest of the arch, especially in areas of resistant rocks. West of the Blue Ridge, where streams were eroding sedimentary rocks arranged in distinct and contrasting layers, the drainage system became adjusted to differences in the bedrock by multiple piracy, and local differences in relief were marked. This condition was especially true along the Cambrian and Ordovician belt in which solution was a factor in the erosion mechanism. In the crystalline rock areas of the Blue Ridge and Piedmont, some rocks, such as the Ocoee Supergroup, felsitic volcanic rocks, or the quartz kyanite rocks of the Kings Mountain belt, had great resistance to erosion. As Flint (1963) showed in southern Connecticut, rocks having high quartz content tend to form high relief. Massive, coarsely crystalline rocks tend to be more resistant than sheared or foliated rocks. When erosion was rapid, differences in relief related to rock type would have been large. Under conditions of slower erosion in the crystalline-rock areas, because of the polyminerally nature of most of the rocks, a residue of saprolite would collect at the surface. When the residual mantle became generally thick, differences in relief were largely eliminated over broad areas.

At present in the Piedmont and Blue Ridge, saprolite underlies most areas that have low relief. It may be more than 90 m thick though it averages about 18 m (Hack, 1976). In areas of high relief, it is thin, lacking, or is found mostly in valley bottoms.

The shape of the domal uplift that produced the highlands is a significant problem. The steep gravity gradient that parallels the Blue Ridge front is suggestive of different crustal blocks that may separate areas having two rates of uplift. On the other hand, as shown by figure 5, the gradient loses its character in New England north of lat 40°, yet great contrasts in topographic relief are found in New England. An analysis by Best and others (1973) based on modeling of various assumed crustal conditions indicates that in North Carolina, at about lat 35°45', the steep gradient is related to high-density rocks in the Carolina slate belt at high levels in the crust.

Although the argument for a tectonic break near the east foot of the Blue Ridge is strong, the present topography could have resulted from a warping over the axis of the Appalachian Highlands. According to this hypothesis, the Blue Ridge escarpment south of Roanoke was tilted eastward (on the southeast side of the upwarp), and the escarpment reached its present position by retreat.

The gentle gradient and presumed rate of tilt of the basement just east of the Fall Zone may provide a clue. At the North Carolina-Virginia boundary, the gradient of the basement is only about 0.005. If projected inland as far as the Blue Ridge, the top of the basement would reach an altitude of only about 1200 m, almost equal to the crest of the present mountain range. We have reason to believe, however, from estimated erosion and uplift rates, that the middle Cretaceous crest of the range would have been at about 4000 m relative to present sea level. Therefore, if faulting is ruled out, the warping of the Piedmont must have taken place at a higher rate inland toward the Blue Ridge than at the Fall Zone. Farther north in the Washington area where the Piedmont narrows, the warping of the basement at the Fall Zone is steeper and may account for much of the uplift.

CONCLUSION

Analysis of the landscape, the major concern of this study, indicates that the topography is quite varied in altitude and relief, but this variation is in general related to differential erosion of the bedrock rather than to differential uplift. Even the Adirondack Mountains, which have the form of an uplift, are girdled by a wide belt of nonresistant rock. Much of the Ap-

palachian Highlands region, however, can be interpreted as an upwarp of large proportions, but the entire highland cannot be explained that simply. For example, differential uplift, or warping, must be invoked to explain the sharp break between the Blue Ridge and the Piedmont. This is attested to by the gentle slope of the Piedmont at its margin along the Fall Zone and by the lack of large-scale faulting along that zone. The Blue Ridge escarpment, at least in the south, cannot be explained by differential erosion alone. Thus, the up-arching of the Appalachian Highlands must have been differential, and it could have been accompanied by small-scale movements along fault zones parallel to the structural grain.

Data from a variety of sources indicate that the Earth's crust probably responds quickly to loading or unloading and that erosion rates and uplift rates are probably mutually dependent. The effect of a high rate of uplift is to increase erosion rates gradually, eventually producing topography of greater relief. The converse would also be true, that decreased erosion rates would be correlated with lower relief. Local variations in the relief, even of great magnitude, are related to rock control and, in places, to differences in uplift rates as well, thus obscuring the outlines of tectonic blocks that may exist.

Data obtained from repeated geodetic traverses indicate rapid rates of tilt in many areas. These rapid rates are matched by similar rates along ancient water planes in deglaciated regions. Clearly, rapid changes in elevation or rates of tilt can and do occur locally. Nevertheless, many of those observed cannot have been sustained for long periods of time. The erosion rates that have been estimated are an order of magnitude or more lower, and, if the high rates of tilt or uplift were long sustained, they would result in much larger topographic features than are observed.

REFERENCES CITED

- Berry, J. L., 1977, Chemical weathering and geomorphological processes at Coweeta, North Carolina [abs.]: *Geol. Soc. America Abs. with Programs*, v. 9, no. 2, p. 120.
- Best, D. M., Geddes, W. H., and Watkins, J. S., 1973, Gravity investigation of the depth of source of the Piedmont gravity gradient in Davidson County, North Carolina: *Geol. Soc. America Bull.*, v. 84, no. 4, 1213-1216.
- Brown, L. D., and Oliver, J. E., 1976, Vertical crustal movements from levelling data and their relation to geologic structure in the eastern United States: *Rev. Geophysics and Space Physics*, v. 14, no. 1, p. 13-35.
- Campbell, M. R., 1929, Late geologic deformation of the Appalachian Piedmont as determined by river gravels: *Natl. Acad. Sci. Proc.*, v. 15, p. 156-161.
- 1933, Chambersburg (Harrisburg) peneplain in the Piedmont of Maryland and Pennsylvania: *Geol. Soc. America Bull.*, v. 44, no. 3, p. 553-573.
- Clark, W. B., 1891, Correlation papers—Eocene: *U.S. Geol. Survey Bull.* 83, 173 p.
- Cleaves, E. T., Godfrey, A. E., and Bricker, O. P., 1970, Geochemical balance of a small watershed and its geomorphic implications: *Geol. Soc. America Bull.*, v. 81, no. 10, p. 3015-3032.
- Colton, G. W., 1970, The Appalachian Basin—its depositional sequences and their geologic relationships, in Fisher, G. W., and others, eds., *Studies of Appalachian geology—central and southern*: New York, Interscience Publishers, p. 5-48.
- Craig, A. J., 1969, Vegetational history of the Shenandoah Valley, Virginia, in Schumm, S. A., and Bradley, W. C., eds., *United States contributions to Quaternary research*: *Geol. Soc. America Spec. Paper* 123, p. 283-296.
- Darton, N. H., 1951, Structural relations of Cretaceous and Tertiary formations in part of Maryland and Virginia: *Geol. Soc. America Bull.*, v. 62, no. 7, p. 745-780.
- Davis, W. M., 1903, The stream contest along the Blue Ridge: *Geog. Soc. Philadelphia Bull.*, v. 3, p. 213-244.
- Denny, C. S., 1974, Pleistocene geology of the northeast Adirondack region, New York: *U.S. Geol. Survey Prof. Paper* 786, 50 p.
- Eardley, A. J., 1964, Polar rise and equatorial fall of sea level since the Cretaceous: *Jour. Geol. Education*, v. 12, no. 1, p. 1-11; *Am. Scientist*, v. 52, p. 488-497.
- Epstein, A. G., Epstein, J. B., and Harris, L. D., 1977, Conodont color alteration—an index, to organic metamorphism: *U.S. Geol. Survey Prof. Paper* 995 27 p.
- Flint, R. F., 1963, Altitude, lithology, and the Fall Zone in Connecticut: *Jour. Geology*, v. 71, no. 6, p. 683-697.
- 1971, *Glacial and Quaternary geology*: New York, John Wiley & Sons, 892 p.
- Gilluly, James, Reed, J. C., Jr., and Cady, W. M., 1970, Sedimentary volumes and their significance: *Geol. Soc. America Bull.*, v. 81, no. 2, p. 353-376.
- Glaser, J. D., 1969, Petrology and origin of Potomac and Magothy (Cretaceous) sediments, Middle Atlantic Coastal Plain: *Maryland Geol. Survey Rept. Inv.* 11, 102 p.
- Hack, J. T., 1965, Geomorphology of the Shenandoah Valley, Virginia and West Virginia, and origin of the residual ore deposits: *U.S. Geol. Survey Prof. Paper* 484, 84 p.
- 1973, Drainage adjustment in the Appalachians, in Morisawa, Marie, ed., *Fluvial geomorphology*: Binghamton, N. Y., State Univ. New York, Pubs. Geomorphology, p. 51-69.
- 1975, Dynamic equilibrium and landscape evolution, in Melhorn, W. N., and Flemal, R. C., eds., *Theories of landform development*: Binghamton, N. Y., State Univ. New York, Pubs. Geomorphology, p. 87-102.
- 1976, Geomorphic framework of the Piedmont and Blue Ridge [abs.]: *Geol. Soc. America Abs. with Programs*, v. 8, no. 6, p. 897-898.
- Isachsen, Y. W., 1975, Possible evidence for contemporary doming of the Adirondack Mountains, New York, and suggested implications for regional tectonics and seismicity: *Tectonophysics*, v. 29, p. 169-181.
- 1976, Contemporary doming of the Adirondack, Mountains, New York: *EOS (Am. Geophys. Union, Trans.)*, v. 57, p. 325.

- Judson, Sheldon, 1975, Evolution of Appalachian topography, in Melhorn, W. N., and Flemal, R. C., eds., *Theories of landform development*: Binghamton, N. Y., State Univ. New York, Pubs. Geomorphology, p. 29-44.
- Judson, Sheldon, and Ritter, D. F., 1964, Rates of regional denudation in the United States: *Jour. Geophys. Research*, v. 69, no. 16, p. 3395-3402.
- King, P. B., and Belkman, H. M., compilers, 1974, *Geologic map of the United States (exclusive of Alaska and Hawaii)*: Reston, Va., U.S. Geol. Survey, 3 sheets, 1:2 500 000.
- Mathews, W. H., 1975, Cenozoic erosion and erosion surfaces of eastern North America: *Am. Jour. Sci.*, v. 275, no. 7, p. 818-824.
- Mixon, R. B., and Newell, W. L., 1977, Stafford fault system—Structures documenting Cretaceous and Tertiary deformation along the Fall Line in northeastern Virginia: *Geology*, v. 5, no. 7, p. 437-440.
- Owens, J. P., 1970, Post-Triassic tectonic movements in the central and southern Appalachians as recorded by sediments of the Atlantic Coastal Plain, in Fisher, G. W., and others, eds., *Studies of Appalachian geology—central and southern*: New York, Interscience Publishers, p. 417-427.
- Pierce, K. L., 1965, Geomorphic significance of a Cretaceous deposit in the Great Valley of southern Pennsylvania: U.S. Geol. Survey Prof. Paper 525-C, p. C152-C156.
- Scholle, P. A., ed., 1977, Geological studies on the COST No. B-2 well, U.S. Mid-Atlantic Outer Continental Shelf area: U.S. Geol. Survey Circ. 750, 71 p.
- Stearns, R. G., 1967, Warping of the western Highland Rim peneplain in Tennessee by ground-water sapping: *Geol. Soc. America Bull.*, v. 78, no. 9, p. 1111-1124.
- Thornbury, W. D., 1965, *Regional geomorphology of the United States*: New York, John Wiley & Sons, 609 p.
- U.S. Geological Survey and American Association of Petroleum Geologists, 1962, *Tectonic map of the United States, exclusive of Alaska and Hawaii*: Washington, D.C., 2 sheets, scale 1:2 500 000.
- Walcott, R. I., 1972, Late Quaternary vertical movements in eastern North America—quantitative evidence of glacial-isostatic rebound: *Rev. Geophysics and Space Physics*, v. 10, no. 4, p. 849-884.
- White, W. A., 1950, Blue Ridge Front—a fault scarp: *Geol. Soc. America Bull.*, v. 61, no. 12, pt. 1, p. 1309-1346.
- Whitney, J. A., Jones, L. M., and Walker, R. L., 1976, Age and origin of the Stone Mountain Granite, Lithonia district, Georgia: *Geol. Soc. America Bull.*, v. 87, no. 7, p. 1067-1077.
- York, J. E., and Oliver, J. E., 1976, Cretaceous and Cenozoic faulting in eastern North America: *Geol. Soc. America Bull.*, v. 87, no. 8, p. 1105-1114.

The Upper Ordovician and Silurian Hanson Creek Formation of Central Nevada

By REUBEN J. ROSS, JR., THOMAS B. NOLAN, *and* ANITA G. HARRIS

SHORTER CONTRIBUTIONS TO STRATIGRAPHY AND
STRUCTURAL GEOLOGY, 1979

GEOLOGICAL SURVEY PROFESSIONAL PAPER 1126-C

*Detailed geologic mapping and
collection of fossils has led
to revision of lithostratigraphy
and dating of the formation in
the Bellevue Peak Quadrangle*



CONTENTS

	Page
Abstract	C1
Introduction	1
The Hanson Creek Formation near Eureka, Nevada	1
Distribution of fossils and their ages	5
Age of the Hanson Creek Formation	8
Evidence of the corals	8
Evidence of the bryozoans	8
Evidence of the brachiopods	8
Evidence of the trilobites	8
Combined evidence of the megafossils	10
Evidence of the microfauna: conodonts	11
Conclusions	15
References cited	15

ILLUSTRATIONS

	Page
FIGURE 1. Map showing outcrop areas of the Hanson Creek Formation and numbered fossil localities in the Bellevue Peak Quadrangle and elsewhere in central Nevada	C3
2. Preliminary geologic map and sections of the Wood Cone Peak area, Bellevue Peak Quadrangle, Eureka County, Nev	4
3. Lithostratigraphic section of the Hanson Creek Formation, measured on the west side of the Mountain Boy Range, Nev	7
4. Trilobites from the Hanson Creek Formation	13
5. Trilobites from the Kimmswick Limestone, in Missouri, and the Hanson Creek Formation	15
6. Late Ordovician conodonts from the lower dark dolomite member and the middle limestone and dolomite member of the Hanson Creek Formation, Mountain Boy Range, and from the graptolite-bearing platy limestone facies of the Hanson Creek Formation, Monitor Range, Eureka County, Nev	17
7. Latest Ordovician and (or) earliest Silurian conodonts from the middle limestone and dolomite member of the Hanson Creek Formation, Mountain Boy Range, Eureka County, Nev	20

TABLES

	Page
TABLE 1. Trilobites of the Hanson Creek Formation in the Bellevue Peak Quadrangle, Nevada	C9
2. Distribution of conodonts in collections from the Hanson Creek Formation, Mountain Boy Range, and Wood Cone Peak area, Bellevue Peak 15-minute Quadrangle, Eureka County, Nev	19

THE UPPER ORDOVICIAN AND SILURIAN HANSON CREEK FORMATION OF CENTRAL NEVADA

By REUBEN J. ROSS, JR., THOMAS B. NOLAN, and ANITA G. HARRIS

ABSTRACT

The Hanson Creek Formation southwest of Eureka, Nev., in the Bellevue Peak Quadrangle is composed of three lithostratigraphic members: (1) a basal dark-gray dolomite, (2) a middle silty thin- to thick-bedded, locally nodular, dark-gray, light-yellow-mottled limestone topped by light-gray dolomite, and (3) an upper dark-gray dolomite, which is herein named the Combs Canyon Dolomite Member. Detailed geologic mapping and accompanying fossil collecting prove that the same lithostratigraphic and biostratigraphic sequence is present in the Mountain Boy Range and 11 km to the south near Wood Cone Peak. Minor differences in lithology and fossil preservation are attributed to intrusion of quartz monzonite and complex structural disruption near Wood Cone Peak. *Bighornia* sp., *Lobocorallium major*, *Sceptropora facula*, *Thaerodonta* sp., *Lepidocyclus capax*, *Ceraurinus icarus*, and a new species of *Hypodiceranotus* favor a Maysvillian, preferably a Richmondian, age for the middle member. The presence of the conodonts *Amorphognathus ordovicicus* and *Protopanderodus insculptus* supports this preference, as does the occurrence near the top of the member of latest Ordovician and (or) earliest Silurian conodonts, including distomodids, *Exochognathus keislognathoides* s.f., and *Aphelognathus*? n. sp. Conodonts also indicate that the lower member is not older than Edenian.

INTRODUCTION

Mapping of the Bellevue Peak Quadrangle by Nolan has included the outcroppings from which Hague (1892, 1883 atlas) originally reported Ordovician fossils in carbonate rocks above the Eureka Quartzite southwest of the Eureka mining district, Nevada. The combined mapping and paleontological effort has shown these historically important outcroppings to be far more complex structurally than might be supposed from Hague's (1883) reconnaissance maps, has demonstrated a stratigraphic sequence that crosses the Ordovician and Silurian boundary within a single formation, and has re-

vealed the association of Late Ordovician corals, brachiopods, trilobites, and conodonts that have at times been considered to be of differing ages.

THE HANSON CREEK FORMATION NEAR EUREKA, NEVADA

The Hanson Creek Formation in the central basin ranges is composed of limestone and dolomite, the lateral equivalents of which are widely distributed in Utah and Nevada and have been given other formation names—Fish Haven Dolomite to the northeast and Ely Springs Formation to the east and south.

The fauna that characterizes these beds was first found by Arnold Hague, assisted by C. D. Walcott, in the course of their survey of the Eureka mining district in Nevada (Hague, 1892, p. 57–59). They assigned the fauna to the lower beds of their Lone Mountain Limestone and considered it to be of Trentonian, or Early Silurian, age. (At the time of their work, the Ordovician System had not been generally recognized.) Their fossil collections were made near Wood Cone Peak, about 19 km southwest of Eureka, and half of the fossil collections discussed in this report were taken from the same localities. The fauna was not found at the type locality of the Lone Mountain Dolomite on Lone Mountain.

The fossils listed by Hague (1892, p. 59) were unfortunately believed to represent a "Trenton" fauna on the basis of misconceptions dating back to the work of James Hall. "*Orthis subquadrata*" and "*Orthis plicatella*," for instances, were stated by Hall (1847, p. 122, 126) to be common in the "Trenton Limestone" at Maysville, Ky., and at Cincinnati and Oxford, Ohio. Today, these two brachiopods would be recognized as *Plaesiomys subquadrata* (Hall) of Richmondian age and *Plectorthis plicatella* (Hall) of

Maysvillian age. When Hague's faunal list is updated to reflect modern taxonomy, it agrees with a Maysvillian-Richmondian correlation as much as or more than with a Trentonian-Edenian correlation.

The fossils listed by Hague (1892, p. 59), with modern designations, are as follows:

<i>Leptaena sericea</i>	= <i>Sowerbyella</i> or <i>Thaerodonta</i> , several possible species
<i>Orthis subquadrata</i>	= <i>Plaesiomys</i> or <i>Pionorthis</i> , species not determined
<i>Orthis</i> (like <i>O. plicatella</i>)	= <i>Plectorthis plicatella</i> (Hall) (we have not identified this species in our Hanson Creek collections to date)
<i>Trinucleus concentricus</i>	= <i>Cryptolithoides</i> sp.
<i>Asaphus platycephalus</i>	= <i>Isotelus</i> ; might be <i>Anataphrus</i>
<i>Streptelasma</i>	= <i>Bighornia</i> , <i>Lobocorallium</i> , or one of several other genera
<i>Rhynchonella</i>	= <i>Lepidocyclus</i> , possibly <i>Rhynchotrema</i>
<i>Ceraurus</i>	= <i>Ceraurus</i> or <i>Ceraurinus</i>
<i>Dalmanites</i>	= <i>Calyptraulax</i>
<i>Illaenus</i>	= <i>Illaenus</i> (we have not identified any <i>Illaenid</i> trilobite in our collections from the Hanson Creek)

Mapping in the Bellevue Peak Quadrangle has disclosed additional occurrences of fossiliferous beds in the Hanson Creek Formation, particularly in the Mountain Boy Range about 4 km due east of Dry Lake Well (fig. 1).

As originally defined by Merriam (1940, p. 10-11, table 1), the Hanson Creek Formation was that part of the Lone Mountain Limestone of Hague (1892) that overlay the Eureka Quartzite and underlay a conspicuous chert interval at the base of the Silurian Roberts Mountains Formation. Merriam (1940) considered the Hanson Creek Formation at the type section above Pete Hanson Creek in the Roberts Mountains (fig. 1) to be Middle and Late Ordovician in age; he measured a total thickness of 545 ft and described five units, in descending order, as follows:

	Feet
Limestone, massive, dark-gray, fine-grained ¹ -----	180
Limestone, poorly stratified ² -----	140
Limestone, slabby and shaly, dark-bluish-gray; weathers very light gray; very fossiliferous ³ -----	140
Limestone, poorly bedded, noncrinoidal; small black chert nodules common ³ -----	45
Limestone, dolomitic, dark-gray; flecked with crinoidal columnals ³ -----	40
Total -----	545

¹ Probably Combs Canyon Dolomite Member of this report.

² Probably middle limestone member of this report.

³ Probably lower dark dolomite member of this report.

Merriam (1940, p. 19, fig. 3) extended the name Hanson Creek southward to Lone Mountain, although the lithology was considerably different; at Lone Mountain the entire interval between the Eureka Quartzite and the basal chert of the Roberts Mountains is dolomite. The fossiliferous limestone of the middle of the type section was not recognized. In 1942 Merriam and Anderson (p. 1686) included as the Hanson Creek still a third lithology—a laminated, thin-bedded graptolite-bearing limestone—on the basis of exposures on Martin Ridge, in the Monitor Range (fig. 1). This graptolite-bearing lithology is present as far south as Dobbin Summit and is also present near the crest of the Antelope Range not far from the head of Ninemile Canyon.

Nolan, Merriam, and Williams (1956, p. 32-34) followed the practice of Merriam and Anderson (1942) but also noted localities in the Eureka district where the formation is represented by dark dolomite.

The Hanson Creek Formation was modified in 1972 by Mullens and Poole, who recognized a sandy zone within the rocks mapped as Hanson Creek; they reported finding a Silurian fauna above the zone. A Silurian age for an upper member of the Ely Springs and Fish Haven Dolomites has been accepted also. In most if not all of these occurrences, the Silurian fauna is found in an upper dark dolomite. Similarly, the uppermost member of the Hanson Creek Formation in the Bellevue Peak Quadrangle and in all other outcrop areas shown in figure 2 contains Silurian fossils. Indeed, conodonts collected during this study show that even the upper part of the underlying middle limestone and dolomite unit in the Bellevue Peak Quadrangle is of latest Ordovician and (or) earliest Silurian age.

Outcrops of the Hanson Creek Formation are widely distributed in the Bellevue Peak Quadrangle and are in all places tectonically disturbed. They constitute a relatively easily deformed sequence of thinly and moderately thick bedded limestones and dolomites between two resistant and massively bedded sequences. The Eureka Quartzite underlies the formation, in most places with a tectonic rather than a sedimentary contact.

Similarly, the overlying Lone Mountain Dolomite of probable Silurian age constitutes an extensive thrust plate that not only rests on different units of the Hanson Creek but also locally has cut through both the Hanson Creek and the Eureka Quartzite and directly overlies Limestones of the Pogonip Group of Early and Middle Ordovician age.

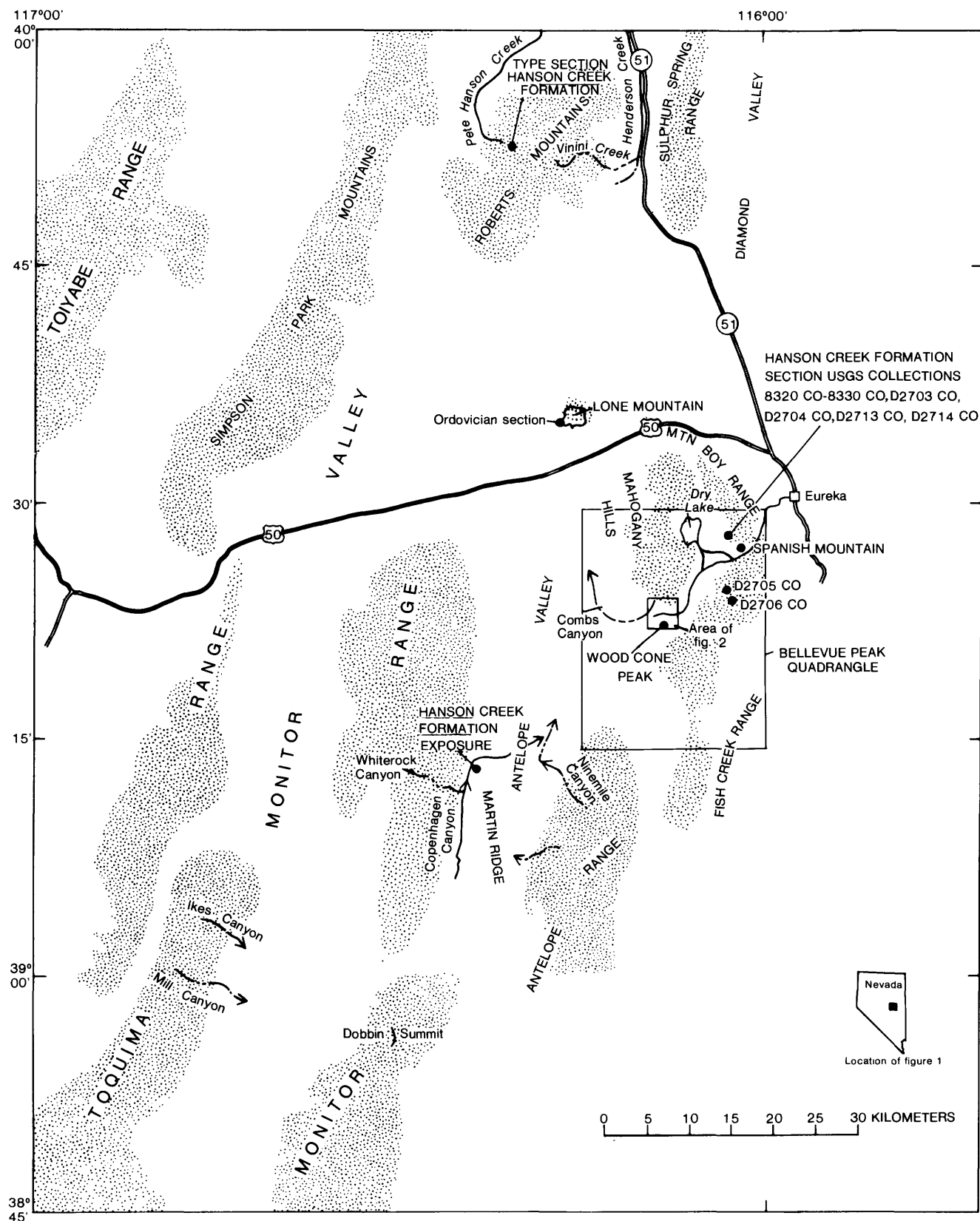


FIGURE 1.—Outcrop areas of the Hanson Creek Formation and numbered fossil localities (dots) in the Bellevue Peak Quadrangle and elsewhere in central Nevada.

As a result there is no single continuous exposure of the Hanson Creek Formation, and the exposed sequences normally exhibit one or more minor thrust faults that may bring different units into juxtaposition. In addition, conglomeratic layers have been recognized in all three of the members and may represent sedimentary breccia flows, erosional breaks, or intraclasts.

The two most extensive exposures of the Hanson Creek Formation in the quadrangle are near Wood Cone Peak and in the Mountain Boy Range east of Dry Lake. In the Wood Cone Peak area particularly, the beds are cut by at least three minor thrust faults. The fault planes are folded together with the sedimentary rocks; the thinner bedded limestone units are in many places rather intensely folded (fig. 2). A quartz monzonite intrusion on the southwest side of the area of outcrop has heated and slightly recrystallized the limestone. As a result, the silty limestone at the bottom of the middle member does not weather to form the same rubbly nodular slope that is found in the Mountain Boy Range, although clearly the limestone in both areas was originally identical.

Three lithologic units can be recognized in the more extensive exposures. The lowest is a massive dark (nearly black) dolomite; the only recognizable megafossils are tiny (1 mm diameter) white crinoid columnals. At several places in the higher part of the southern Mountain Boy Range appear local intraclastic conglomerate bands in the dolomite; here too, small masses of black chert are included. In the most nearly complete exposure of the member, north and northeast of Wood Cone Peak summit, the unit lies above a thrust fault that separates the member from the light-gray dolomites and thin-bedded limestones that normally are conformably above it. At some places in the Mountain Boy Range, the brecciated contact between the Eureka Quartzite and the lower dolomite member exhibits nearly isoclinal folding.

Above the basal dark dolomite, a sequence of thin- and medium-bedded silty limestone and thin-bedded light-gray dolomite is found at all the more extensive exposures. In most places limestone directly overlies the basal dolomite, but both north of Wood Cone Peak and in the Mountain Boy Range, one or two meters of the light-gray dolomite occur below

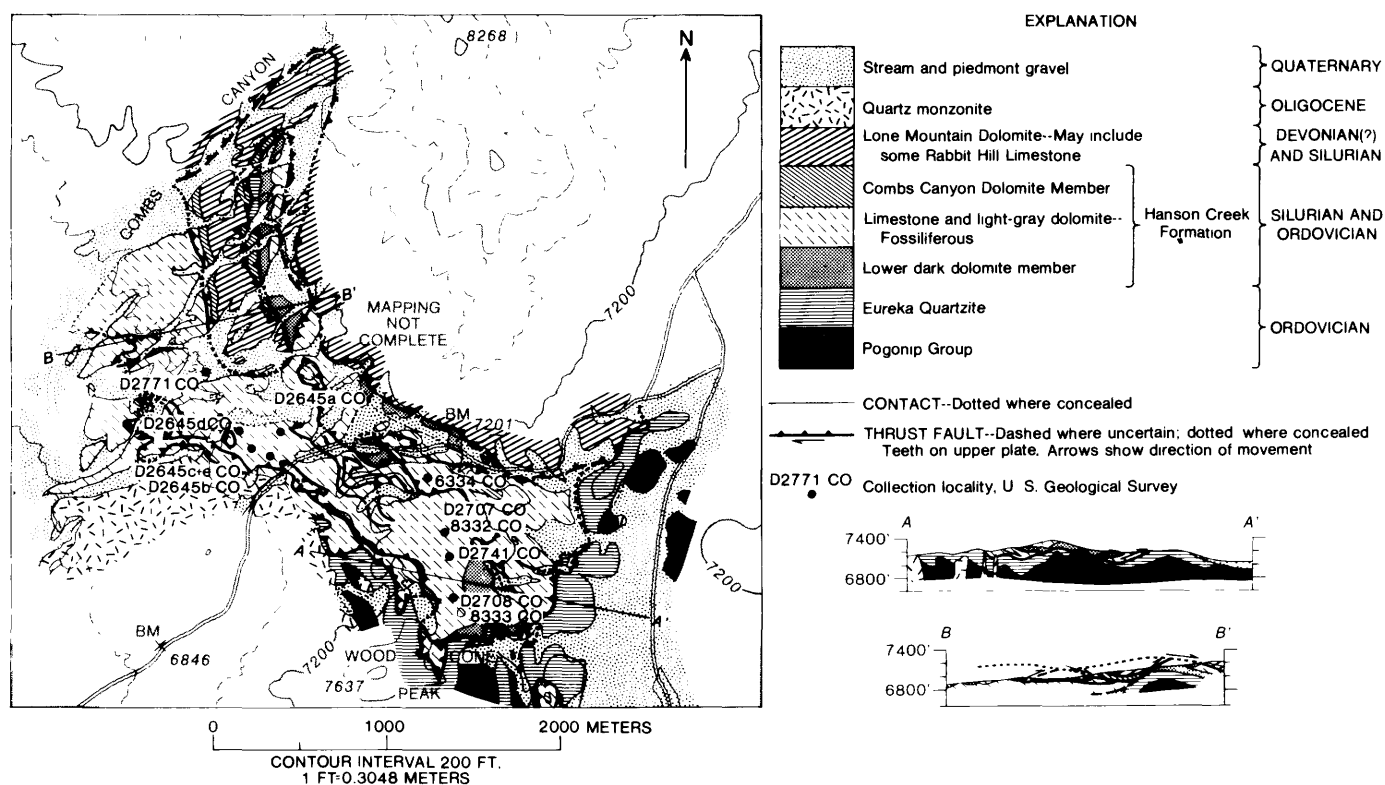


FIGURE 2.—Preliminary geologic map and sections of the Wood Cone Peak area, Bellevue Peak Quadrangle, Eureka County, Nevada. Geology by T. B. Nolan, R. J. Ross, Jr., and L. A. Wilson. Base from U.S. Geological Survey 1:62,500 Bellevue Peak (1956).

the limestone. Locally the limestone is abundantly fossiliferous; localities where fossil collections have been made are indicated on figures 1 and 2. Higher in the sequence, thin- to medium-bedded light-gray dolomite is interbedded with limestone. In the higher units, the limestone beds contain nodules of black chert that are abundant and distinctive. In the higher limestone beds are also a few local intraclastic conglomeratic zones. Fragments as large as 5-cm across were found in an isolated fossiliferous limestone outcrop 1 km southwest of Spanish Mountain at the south end of the Mountain Boy Range (fig. 1).

Limestone of the middle member is thicker bedded in what is apparently the upper part of the sequence. Most of the more massive limestone, however, is part of a minor thrust plate that rests in places on both the thinner bedded limestones and the light-gray dolomite, as well as on the basal dark dolomite. Fossils have been found in the massive limestone in only one place, about 1.6 km northwest of BM 7201 at the divide north of Wood Cone Peak.

At what appears to be the very top of the middle member, both at Wood Cone Peak and in the Mountain Boy Range, is a sequence of as much as 30 m of very light gray dense dolomite.

The uppermost unit of the more inclusive Hanson Creek dolomite of Mullens and Poole (1972) is a second dark dolomite, which occurs in most if not all areas in which fossiliferous Hanson Creek crops out. In most exposures, this upper unit is characterized by beds in which sections of brachiopods are abundant. In some places, the brachiopods are sufficiently well preserved to be recognized as pentamerids. In other places, halysitid corals have been preserved. Intraclastic conglomeratic beds and horizons with black chert are present in this member also.

North of Wood Cone Peak on the south side of Combs Canyon, the dark dolomite member, which contains pentamerid brachiopods and halysitid corals, apparently conformably overlies the uppermost light-gray dense dolomite of the middle member. The sandy horizon described by Mullens and Poole (1972) was not recognized here, however.

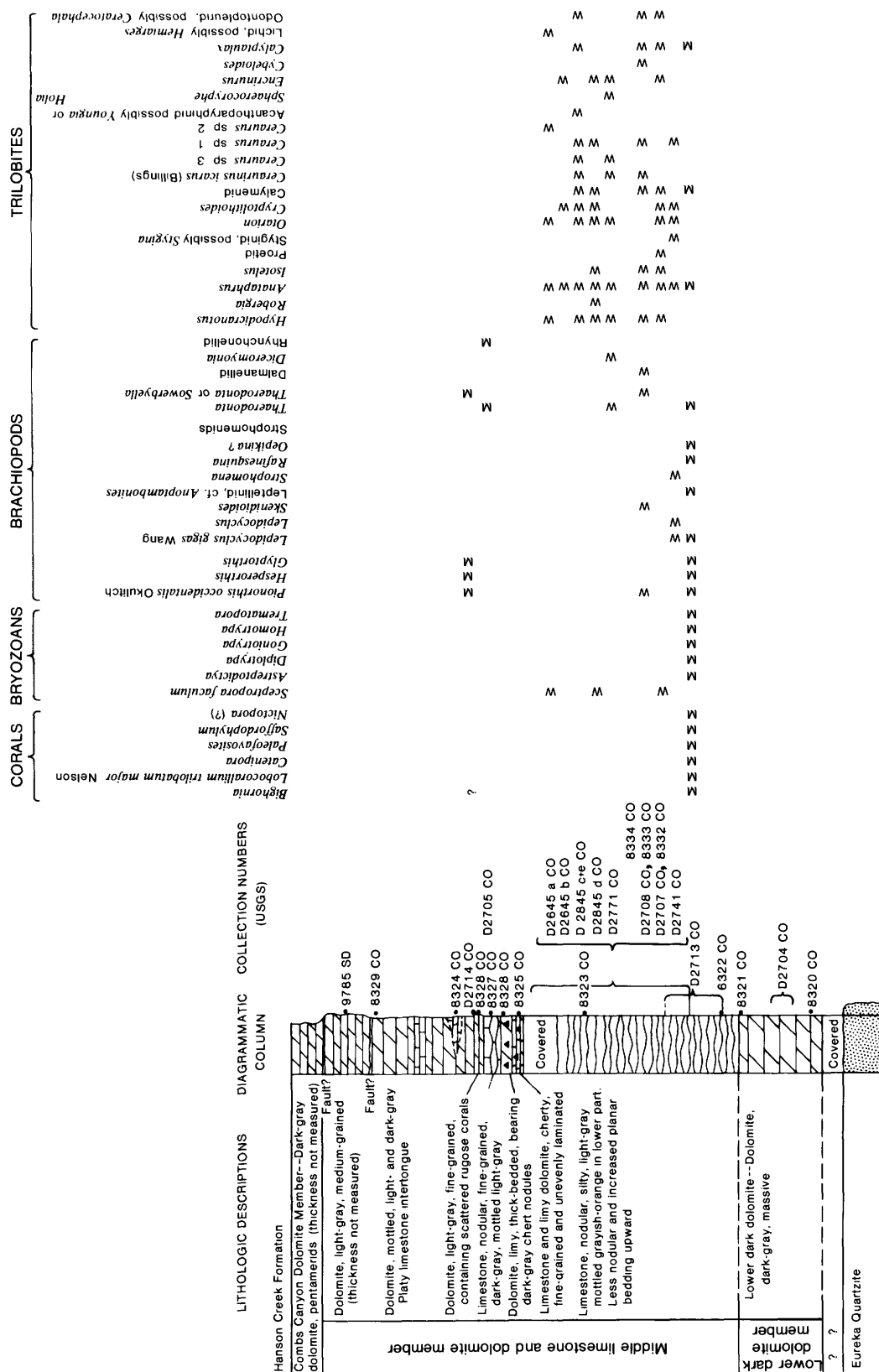
The redefinition of the Hanson Creek Formation by Mullens and Poole (1972) includes this third, or upper, member within the formation. Since it is an easily recognized and mappable unit, we suggest that it be given the name of the Combs Canyon Dolomite Member of the Hanson Creek Formation; its type locality is on the south side of Combs Canyon in the NE cor. sec. 31, T. 18 N., R. 52 E.

(unsurveyed). Here the member overlies the upper very light gray dolomite of the Hanson Creek Formation and appears to be conformable beneath the typical massive, vuggy, coarsely crystalline Lone Mountain Dolomite.

DISTRIBUTION OF FOSSILS AND THEIR AGES

The larger collections of fossils have been made from two areas in the Bellevue Peak Quadrangle. One of these areas contains exposures of dark-gray locally thick or thin bedded locally silty beds of the middle limestone member of the Hanson Creek and is north of and within 2 km of Wood Cone Peak (figs. 1, 2). This is the area mentioned by Hague (1892, p. 58-59; 1883, Atlas, Sheet IX). Many of the trilobites reported in this paper come from the same outcrops. Collections made from strata in three small conical hills aligned approximately north to south and located east and north of Wood Cone Peak are from the lower part of the middle limestone member of the Hanson Creek Formation. There we have found silicified brachiopods and corals, several genera of which are common to the Maquoketa Shale (Iowa) and the Stony Mountain Formation (Manitoba; Wyoming) (fig. 3; USGS collns. D2707-CO, D2708-CO, D2741-CO).

The second area is on the west side of the Mountain Boy Range and is exposed mainly on the north side of a dry wash draining westward into Dry Lake playa (fig. 1) (200 m east of C, sec. 31, T. 19 N., R. 53 E.; UTM grid, zone 11: E. 581,775 m, N. 4,369,500 m) (See fig. 3.) This second area is the site of the most nearly complete section of the Hanson Creek Formation we have found in the Bellevue Peak Quadrangle, although it is poorly exposed at the base; the underlying Eureka Quartzite crops out south of the wash and dips northerly, but its contact with the Hanson Creek is covered by sand and gravel. The light-gray dolomite that overlies the main body of the middle limestone member north of the wash may be above a thrust fault; it contains latest Ordovician and (or) earliest Silurian conodonts. The dark-gray Combs Canyon Dolomite Member (Silurian) is exposed about 150 m southeast of the main section (UTM Grid, zone 11: E. 581,880 m, N. 4,369,500 m). Despite its limitations, this section is the basis for the lithostratigraphic sequence found to be usable throughout our mapping (fig. 3). In the lower part of the middle limestone member, corals, bryozoans, brachiopods, and a few trilobites closely resemble genera found in the Maquoketa Shale of Iowa, the Stony Mountain Formation of Wyoming (Ross, 1957, p. 446-488, pls. 37-41), and



- COLLECTION DESCRIPTIONS
- D2645a-C0. Hanson Creek Formation. Altitude 2158 m. 1372 m N. 33° W. from Wood Cone Peak. UTM Grid, zone 11: E. 573 810 m, N. 4 360 130 m, Bellevue Peak quadrangle, Nevada.
- D2645-C0. Hanson Creek Formation. Altitude 2160 m. 1372 m N. 33° W. from Wood Cone Peak. UTM Grid, zone 11: E. 573 710 m, N. 4 359 940 m, Bellevue Peak quadrangle, Nevada.
- D2645c-C0. Hanson Creek Formation. Altitude 2161 m. 1524 m N. 33° W. from Wood Cone Peak. UTM Grid, zone 11: E. 573 590 m, N. 4 360 000 m, Bellevue Peak quadrangle, Nevada.
- D2645d-C0. Hanson Creek Formation. Altitude 2134 m. 1676 m N. 33° W. from Wood Cone Peak. UTM Grid, zone 11: E. 573 450 m, N. 4 360 160 m, Bellevue Peak quadrangle, Nevada.
- D2645e-C0. Hanson Creek Formation. Approximately the same locality as D2645c-C0. Collection made by D. Budge and P. Sheehan.
- D2704-C0. Hanson Creek Formation, lower dark dolomite member; exposed on south side of dry wash. Altitude 2298 m. UTM Grid, zone 11: E. 581 700 m, N. 4 369 350 m, Bellevue Peak quadrangle, Nevada.
- D2705-C0. Hanson Creek Formation, middle limestone dolomite member. Near head of Lamoreux Canyon, north side. Altitude 2420 m. UTM Grid, zone 11: E. 581 675 m, N. 4 363 180 m, Bellevue Peak quadrangle, Nevada.
- D2706-C0. Hanson Creek Formation, middle limestone and dolomite member. East side of Lamoreux Canyon. Altitude 2397 m. UTM Grid, zone 11: E. 582 340 m, N. 4 362 050 m, Bellevue Peak quadrangle, Nevada.
- D2707-C0. Hanson Creek Formation, one of Walcott's original localities of 1880. Approximately 915 m north-northeast from Wood Cone Peak. Altitude 2292 m. UTM Grid, zone 11: E. 574 750 m, N. 4 359 550 m, Bellevue Peak quadrangle, Nevada.
- D2708-C0. Hanson Creek Formation, on a small hill 610 m northeast of Wood Cone Peak. UTM Grid, zone 11: E. 574 800 m, N. 4 359 125 m, Bellevue Peak quadrangle, Nevada.
- D2713-C0. Hanson Creek Formation, light-gray, silty, nodular limestone, above basal dark-gray dolomite. West side of Mountain Boy Range, on north side of wash draining westward into Dry Lake Playa. UTM Grid, zone 11: E. 581 750 m, N. 4 369 500 m, Bellevue Peak quadrangle, Nevada.
- D2714-C0. Hanson Creek Formation, light-gray dolomite above nodular limestone. West side of Mountain Boy Range, north of wash draining westward into Dry Lake Playa. UTM Grid, zone 11: E. 581 750 m, N. 4 369 500 m, Bellevue Peak quadrangle, Nevada.
- D2714-C0. Hanson Creek Formation, middle limestone and dolomite member. On SW. side of crest of small hilllock 800 m NNE of Wood Cone Peak. UTM Grid, zone 11: E. 357 760 m, N. 4 359 425 m, Bellevue Peak quadrangle, Nevada.
- D2771-C0. Hanson Creek Formation, middle limestone and dolomite member. 0.9 km southeast of Combs Canyon. Altitude 2130 m. UTM Grid, zone 11: E. 573 325 m, N. 4 360 360 m, Bellevue Peak quadrangle, Nevada.

FIGURE 3.—Lithostratigraphic section of the Hanson Creek Formation, measured on the west side of the Mountain Boy Range (UTM Grid, zone 11: E. 581,775 m, N. 4,369,500 m). Stratigraphic positions of fossil collections shown by braces. Distribution of corals, bryozoans, brachiopods, and trilobites are indicated by collection numbers; for distribution of conodonts, see table 2. M, occurs in Mountain Boy Range; W, occurs near Wood Cone Peak.

the Ely Springs Dolomite in the New York Butte Quadrangle, Inyo Mountains, Calif. (Merriam, 1963b, p. 10–11).

The stratigraphic positions of our collections are shown accurately in figure 3 for the Mountain Boy Range section. Because of structural complexity (fig. 2), the stratigraphic position of the collections made 11 km to the south near Wood Cone Peak cannot be precisely determined; nonetheless, we have indicated the position in a general way on figure 3.

Merriam and Anderson (1942, p. 1686) assigned the entire Hanson Creek a Late Ordovician age on the basis of graptolites from the Monitor Range locality but not on the basis of shelly fossils from the type section or the Wood Cone Peak area. That assignment was continued by Nolan and others (1956) and by Merriam (1963a, p. 31–33). The correlation presented by the latest of these references was based largely on the resemblance of brachiopods, including collections from the Inyo Mountains, to those of the Maquoketa Shale of Iowa, which were compared with Richmondian faunas of Ohio.

AGE OF THE HANSON CREEK FORMATION

Our collections, made from 1975 to 1977, include not only the expectable megafossils, such as corals, bryozoans, brachiopods, and trilobites, but also a very representative conodont microfauna. The evidence that each of these kinds of fossils provides for determining the age of the Hanson Creek Formation is reviewed in the paragraphs that follow, as well as in figure 3 and tables 1 and 2.

EVIDENCE OF THE CORALS

The corals of the Hanson Creek Formation (fig. 3) were identified by W. A. Oliver (written commun., March 15, 1976); they include a generic assemblage reviewed by Duncan (1956, p. 218–220), who concluded that they are of Late Ordovician age. Nelson (1963) also found this assemblage in the Hudson Bay Lowland; the questionably identified *Nyctopora*(?) and *Saffordophyllum*(?) are in the Bad Cache Rapids Group, which Nelson (1963, p. 24–25) correlated with the Red River Group of Manitoba but for which he favored a Richmondian age rather than Edenian or Trentonian. *Bighornia* is restricted to the younger Churchill River Group, as is *Lobocorallium trilobatum major* Nelson; according to Nelson, that group is of Richmondian or Gamachian age.

Oliver (written commun., Jan. 4, 1978) commented on the distinctive *Lobocorallium* found in USGS colln. D2713-CO:

1. If the *Lobocorallium* is either of Nelson's species it is the younger one, i.e. *L. trilobatum major*. The similarity is close.
2. If Nelson's trend to increasing distinctness of lobation (Nelson, 1963, p. 34) with time is real, then your specimens may be even younger than Nelson's *L. major*, as yours is one of the most distinctly trilobate group of specimens that I have seen.

Duncan (1957, p. 611) reviewed the stratigraphic range of *Bighornia*, concluding that it was of Richmondian age and noting that the genus had never been found in Trentonian (in the old sense) strata. As noted by Nelson (1963, p. 28, 39–43), *Bighornia* is represented by several species in the Churchill River Group but by none in the underlying Bad Cache Rapids Group.

EVIDENCE OF THE BRYOZOANS

Five of the six genera of bryozoans were identified by O. L. Karklins (written commun., March 3, 1976), who stated that preservation was too poor to permit determination of species and that no conclusion as to age within the Ordovician was therefore possible. On the other hand *Sceptropora facula* Ulrich is readily identified (Ross, 1957, pl. 37, figs. 10, 11). Originally identified from Richmondian strata of Minnesota (Ulrich, 1888, p. 228–229), this species is present in shale of the Stony Mountain Formation of the upper part of the Bighorn Group in Wyoming (Ross, 1957, p. 459) and in the English Head Formation and lower part of the Vaureal Formation of Anticosti Island (Twenhofel, 1927, p. 86–87). It is known from no older formations.

EVIDENCE OF THE BRACHIOPODS

Most of the brachiopods listed in figure 3 are fragmentary. Several genera are of little use in differentiating rocks of Middle and Late Ordovician age. *Pionorthis* is present in the Stony Mountain beds of Manitoba and Wyoming (Ross, 1957; Macomber, 1970). *Lepidocyclus gigas* occurs in the Maquoketa Shale of Iowa as well as in the shale of the Stony Mountain Formation of Wyoming. *Thaerodonta* is another form found in Maquoketa and younger rocks. Leptellinids like *Anoptambonites* are found in very late Ordovician strata of eastern Alaska (Ross and Dutro, 1966, p. 10–13) and in the Craighead Limestone of Ayrshire of late Caradocian age (probably early Cincinnati equivalent) (Williams, 1962, p. 170–172).

EVIDENCE OF THE TRILOBITES

The ranges of the 18 Hanson Creek trilobite genera are shown in table 1. (See also figs. 4, 5.) The

TABLE 1.—*Trilobites of the Hanson Creek Formation in the Bellevue Peak Quadrangle, Nevada*

[Trilobites identified to family, genus, or species where possible. List of previously reported occurrences may not be all inclusive but is intended to show the known range of each family, genus, or species. Leaders, ---, no data]

Trilobites and collection no. (USGS)	Selected previously reported occurrences	Age range previously assigned	Reference and remarks
<i>Hypodiceranotus</i> n. sp. --- D2645a, c, d, e-CO D2707-CO D2708-CO D2771-CO	Genus reported in Trenton Limestone (New York); Prosser Limestone (Minnesota); Viola Limestone (Oklahoma); uppermost Copenhagen Formation (Nevada); Silliman's Mount (Baffin Island); Whittaker Formation (Dist. of MacKenzie); Albany and Stinchar beds (Ayrshire); Tipliski horizon (central Urals).	Middle to late Caradocian.	Whittington, 1952; Tripp, 1965, 1967; Ross and Shaw, 1972; Ancigin, 1973; Ludvigsen, 1975. Middle body of hypostome differs markedly from those of <i>H. striatulus</i> (Walcott) and <i>H. missouriensis</i> (Foerste). Roy, 1941.
<i>Robergia</i> sp. ----- D2645d-CO	Road River Formation (Yukon); Ogygiocaris Shale (Sweden).	Llandelian to Ashgillian.	Whittington, 1950; Lenz and Churkin, 1966.
<i>Isotelus</i> sp. ----- D2645d-CO D2707-CO D2708-CO	Chazy Group (New York); Lexington Limestone (Kentucky); Ellis Bay Formation (Anticosti Island). Numerous other occurrences.	Chazy to Richmondian. Llandeilian to Ashgillian.	Twenhofel, 1927; Ross, 1967; Shaw, 1968, 1974.
<i>Anataphrus</i> sp. ----- D2645a-e-CO D2707-CO D2708-CO D2741-CO D2771-CO	Silliman's Mount (Baffin Island); Cape Calhoun Formation (Greenland); Maquoketa Shale (Iowa); uppermost Copenhagen Formation (Nevada).	Late Mohawkian to Richmondian.	Whittington, 1954; Troedsson, 1928; Ross and Shaw, 1972.
Styginid, possibly <i>Stygina</i> . D2741-CO	Chair of Kildare Limestone (Eire); Upper Ordovician (Poland); Boda Limestone (Sweden); Killey Bridge (North Ireland).	Ashgillian -----	Dean, 1974, p. 67; Kielan, 1960, p. 82, pl. 8, figs. 1, 2; Warburg, 1925, p. 96, pl. 3, fig. 1; Whittington, 1950, p. 547-549.
Proetid ----- D2707-CO	Numerous localities; widespread in world.	Middle Ordovician to Mississippian.	Owens, 1973.
<i>Otarion</i> sp. ----- D2645a, c-e-CO D2707-CO D2741-CO D2771-CO	Many species in United Kingdom, Estonia, Sweden, Poland, Quebec, MacKenzie, New York, Oklahoma, Iowa, New Jersey, Virginia, Anticosti Island.	Llanvirnian to Middle Devonian (Chazy through Richmondian).	Lamont, 1935; Öpik, 1937; Twenhofel, 1927 (listed as <i>Cyphasphus</i>); Begg, 1939; Weller, 1903; Tripp, 1954, 1967; Ingham, 1970; Warburg, 1925; Whittington, 1966; Kielan, 1960; Schuchert and Cooper, 1930; Shaw, 1968, 1974; Raymond, 1925; Hu, 1975; Ludvigsen, 1975, 1976a.
<i>Cryptolithoides</i> sp. ----- D2645b-e-CO D2707-CO D2741-CO	Viola Limestone (Oklahoma); Copenhagen Formation (Nevada); Road River Formation (Yukon).	Mid-Caradocian to Ashgillian.	Whittington, 1941; Ross and Shaw, 1972; Lenz and Churkin, 1966.
Calymenid (possibly <i>Gravicalymene</i> or <i>Calymene</i>). D2645d, e-CO D2707-CO D2708-CO	Numerous localities in North America and Europe.	Llanvirnian to Middle Devonian.	Shirley, 1936; Twenhofel, 1927; Dean, 1962; Ross, 1967.
<i>Ceraurinus</i> cf. <i>C. icarus</i> (Billings). D2645e-CO	Richmond Gp. (Indiana and Ohio); English Head Formation and Vaureal Formation (Anticosti Island).	Richmondian Maysvillian?	Ludvigsen, 1977; Twenhofel, 1927.
<i>Ceraurus</i> sp. 1 ----- D2645d, e-CO D2741-CO	Whittaker Fm. (Dist. MacKenzie).	"Black River-Trenton".	Ludvigsen, 1975, pl. 5, figs. 8, 9.
<i>Ceraurus</i> , sp. 2 (radial ornament)-n. sp.? D2645a-CO D2741-CO	Not known previously (?) -----	Arenigian to Ashgillian.	For generic range see Lane, 1971, text fig. 2.
<i>Ceraurus</i> sp. 3 (fine ornament). D2645e-CO	Not known previously (?) -----	-----	-----
Acanthoparyphid, possibly <i>Holia</i> or <i>Youngia</i> . D2645e-CO	Kimmswick Ls. (Missouri and Illinois); Lincolnshire and Edinburgh Formations (Virginia); Esbatattaotine and Whittaker Formations (Dist. of MacKenzie).	Chazy to Edenian. Llandeilian to Llandoveryan.	Schmidt, 1881; Warburg, 1925; Bradley, 1930; Whittington and Evitt, 1954; Ludvigsen, 1975, 1976a; Lane, 1971.

TABLE 1.—*Trilobites of the Hanson Creek Formation in the Bellevue Peak Quadrangle, Nevada—Continued*

Trilobites and collection no. (USGS)	Selected previously reported occurrences	Age range previously assigned	Reference and remarks
<i>Sphaerocoryphe</i> sp. ----- D2771-CO	Uppermost Copenhagen Fm. (Nevada); Ellis Bay Formation (Anticosti Island); Chair of Kildare Limestone (Eire); Boda Limestone (Sweden); Rhiwlas Limestone (North Wales); Chazy Group (New York); Ashgill (Cumbria); Balclatchie beds, Drummuck beds (Ayrshire).	Chazy to Gamachian. (Llandeilian to Ashgillian).	Ross and Shaw, 1972; Shaw, 1968; Lane, 1971; Warburg, 1925; Ingham, 1974; Twenhofel, 1927. Also in middle limestone member of Hanson Creek type section.
<i>Encrinurus</i> sp. (may be 2 sps.) D2645b, d-CO D2707-CO D2771-CO	Ellis Bay Formation to Jupiter Formation (Anticosti Island); Stile End beds (United Kingdom); Ashgill (Cumbria).	Caradocian? Ashgillian to Silurian.	Twenhofel, 1927; Dean, 1963; Ingham, 1974.
<i>Cybeloides</i> sp. ----- D2708-CO	Maquoketa Shale (Iowa); Edinburgh Formation and Effna Limestone (Virginia); Lincolnshire Limestone (Tennessee); Rhiwlas Limestone (Wales).	Chazy to Richmondian.	Slocum, 1913; Cooper 1953; Shaw, 1968; Whittington, 1964.
<i>Calyptaulax</i> sp. ----- D2645c, e-CO D2707-CO D2708-CO D2713-CO	Whitehead Formation, Perce (Quebec); Tyrone Limestone (Kentucky); Galena Dolomite and Platteville Limestone (of Mississippi Valley); Middle Ordovician of Appalachians (Virginia); Copenhagen Formation (Nevada).	Chazy to Richmondian.	Delo, 1940; Shaw, 1968; Cooper, 1953; Schuchert and Cooper, 1930; Ross and Shaw, 1972.
Lichid, possibly <i>Hemiarges</i> . D2645a-CO	-----	Family range Ordovician to Devonian.	-----
Odontopleurid, possibly <i>Ceratocephala</i> . D2645e-CO D2708-CO	-----	Middle Ordovician Late Devonian.	-----

silicified trilobites are almost all immature and therefore either difficult or impossible to identify as to species. Six taxa can be given only family designation.

Late Ordovician trilobites from the Cordilleran and Rocky Mountain regions are poorly known. As a result, many if not most taxonomic comparisons must be made with the Middle Ordovician forms that have been much better monographed.

In this case the importance of modern taxonomic assessment of a genus is illustrated by the recent work of Ludvigsen (1977) on *Ceraurinus*; his work leaves no doubt that *C. icarus* (Billings) or a very closely related variety is present in the Hanson Creek (fig. 4, s, z) and that its age is Richmondian, possibly as old as Maysvillian.

Only *Hypodiceranotus* would seem to contradict the evidence of *C. icarus*. That genus has previously been considered an indicator of an age equivalent to that of the Trenton Limestone of New York and the Kimmswick of Missouri. (See table 1.) The nearly equally tripartite subcircular middle body of the hypostome of *H. missouriensis* (Foerste) (fig. 5a) differs markedly from the elongate middle body of

the Hanson Creek hypostome (fig. 5h-k). The Trenton species *H. striatulus* (Walcott), as shown by Whittington (1952), bears the same middle body as *H. missouriensis*. The species of *Hypodiceranotus* from the Hanson Creek beds clearly differs from these two late Mohawkian (or early Cincinnati) species and may prove to be an index to upper Cincinnati strata.

No other trilobite taxon provides more definitive evidence as to whether the Hanson Creek is of Richmondian or an older age. If future collecting should prove that the styginid is really Ashgillian *Stygina*, rather than an older form like *Raymondaspis*, or that the acanthoparyphid (fig. 4, aa-ac) *Youngia*, rather than an older form like *Holia*, little question could remain about the Richmondian or Gamachian age of the trilobites.

COMBINED EVIDENCE OF THE MEGAFOSSILS

When the evidence of *Bighornia* and particularly of *Lobocorallium major* Nelson among the corals, of *Sceptropora facula* Ulrich among the bryozoans, and of *Thaerodonta* and *Lepidocyclus capax* among the brachiopods is joined to that of the trilobites

Ceraurinus icarus (Billings) and a new species of *Hypodiceranotus*, a Richmondian (possibly a Late Maysvillian) age for the middle limestone member of the Hanson Creek is reasonable and agrees with the late Caradocian to Ashgillian age indicated by the graptolites (Ross and Berry, 1963, p. 65–67).

EVIDENCE OF THE MICROFAUNA: CONODONTS

The microfauna from the measured section in the Mountain Boy Range consists of conodonts. Nearly 2,300 identifiable elements (table 2) were recovered from the section by using dilute acetic- and formic-acid treatment of limestone and dolomite samples, respectively. Insoluble residues were washed through a 20-mesh sieve nested in a 200-mesh sieve; a heavy-liquid (tetrabromethane) separation of the residue retained on the 200-mesh sieve was then made. The heavy-mineral concentrate was picked for conodonts at about $\times 50$ magnification.

Amorphognathus ordovicicus Branson and Mehl (fig. 6, a–f) occurs in the basal 5.2 m of the section. This index species of the latest Ordovician North Atlantic conodont zone has a range that begins a little above the base of the Ashgillian (a little above the base of the Maysvillian through the Richmondian; see Sweet and Bergström, 1976, fig. 4). Another indicator of slightly younger Maysvillian through Richmondian age, *Protopanderodus insculptus* (Branson and Mehl) s.f., occurs 20.7 m above the base of the section. Other elements of less restrictive but definitely Late Ordovician age that co-occur with or above *A. ordovicicus* in the section are *Belodina* sp. D of Shatzer (1976) (fig. 6, r, s), *Oulodus ulrichi* (Stone and Furnish) (fig. 6, m–p), and *Plegagnathus nelsoni* Ethington and Furnish s.f. (fig. 6, q). These elements along with many other Ordovician conodonts of less biostratigraphic value (fig. 6) were found within the lower 22.9 m of the measured section.

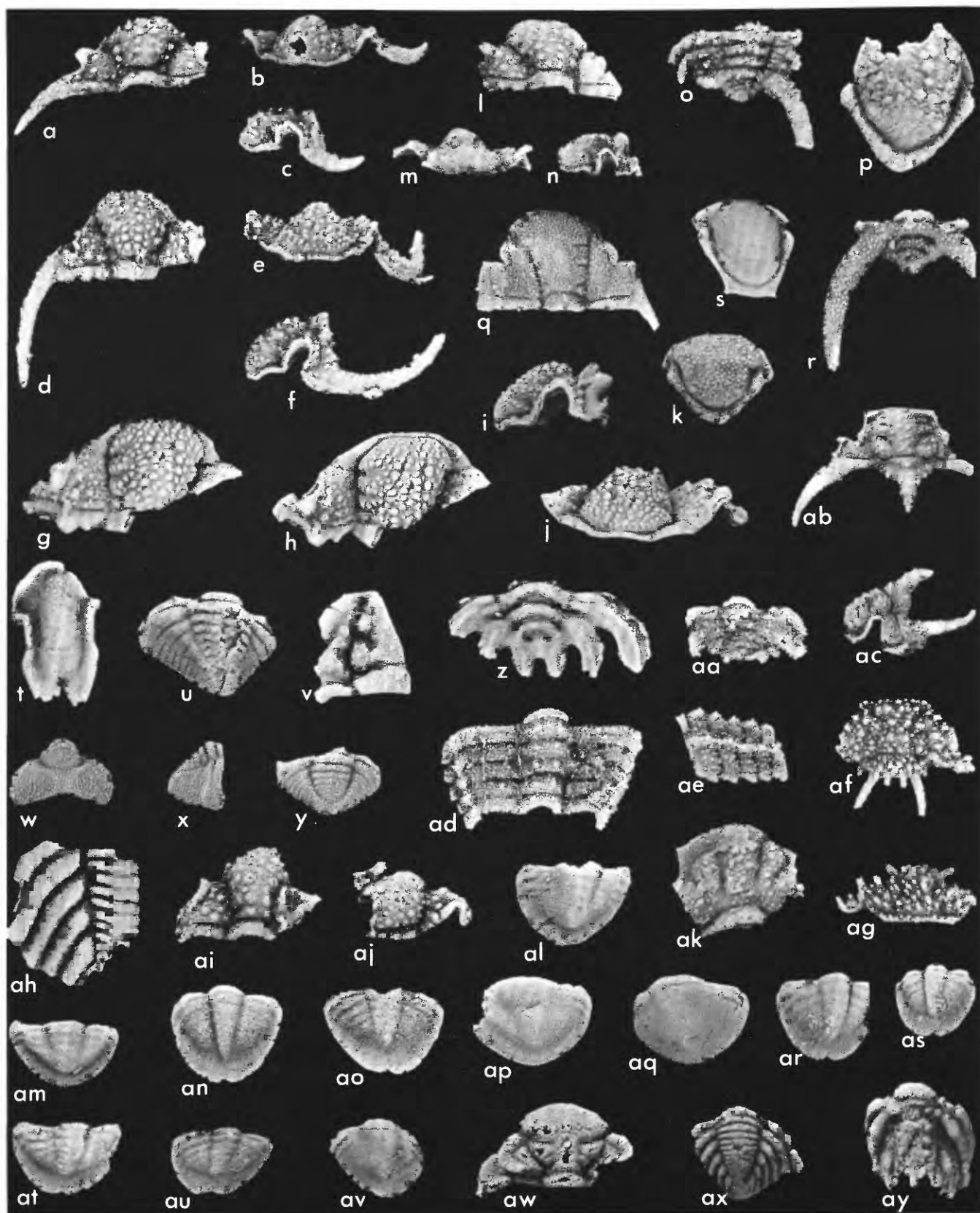
An outcrop of dark-gray thick-bedded limestone 200 m west of the measured section (table 2; USGS colln. 8292–CO) also contains elements of *Amorphognathus ordovicicus* and therefore lies within the same age range as collections 8320–CO to 8328–CO of the measured section. Although we have yet to verify the relationship, this outcrop seems to overlie the middle limestone of the measured section but to underlie the light-gray dolomite. Lithologically, it strongly resembles the limestone near Wood Cone Peak.

The uppermost collection (table 2; USGS colln. 8329–CO) within the measured part of the section

contains conodonts of Late Ordovician (zygognathiform elements) and Silurian aspect (plectospathodiform elements). A possible fault separates the measured part of the section from overlying beds. Conodonts from light-gray dense dolomite above this fault (table 2; USGS colln. 9785–SD) but still within the middle limestone and dolomite member of the Hanson Creek are of latest Ordovician and (or) earliest Silurian age (fig. 7). These include spathognathodiform and plectospathodiform elements that are probably part of the same *Ozarkodina* apparatus (fig. 7, j, k) and *Exochognathus keislognathoides* Pollock, Rexroad, and Nicoll (fig. 7, l) and distomodids (fig. 7, h, i) that probably belong with other elements assigned to *Aphelognathus*? n. sp. (fig. 7a–g). Significantly, *A.*? n. sp. elements are abundant and co-occur with latest Ordovician and earliest Silurian species in the basal beds of the upper part of the Ely Springs Dolomite in the Funeral Mountains, Calif. (A. G. Harris and J. F. McAllister, USGS collns., unpub. data).¹

Conodont data from the measured section demonstrate that (1) the lower 22.9 m of the Hanson Creek are of Late Ordovician (Ashgillian) age and no older than early Maysvillian; (2) beds immediately below the possible fault are of latest Ordovician and (or) earliest Silurian age; and (3) the light-gray dense dolomite above the fault(?) is of latest Ordovician and (or) earliest Silurian age. Moreover, data about conodonts from this section in conjunction with those about other Hanson Creek conodonts from central Nevada provide new information on the age of the Hanson Creek. The base of the measured section includes the uppermost beds of the lower dark dolomite member. No complete section of this member has been found thus far in the

¹ Since this report was originally prepared (1977), abundant and very well preserved conodont faunas have been recovered from the Vauréal and overlying Ellis Bay Formations of Anticosti Island, Québec (Nowlan and Barnes, 1979; McCracken and Barnes, 1979). Representatives of what we have assigned to *Aphelognathus*? n. sp., distomodids, and *Exochognathus keislognathoides* are among the most abundant elements in the Vauréal and Ellis Bay conodont faunas. McCracken and Barnes (1979) placed these elements in a new genus and species, *Gamachignathus ensifer*. This species is restricted to the Upper Ordovician Vauréal Formation and the Ordovician part of the overlying Ellis Bay Formation, where it co-occurs with other typical Late Ordovician conodonts. According to McCracken and Barnes, however, *Gamachignathus* co-occurs with *Ozarkodina* of Silurian aspect in the upper 1 to 2 m of its occurrence. McCracken and Barnes used the upper limit of *Gamachignathus* and the succeeding prevalence of *Ozarkodina* without *Gamachignathus* to mark the Ordovician/Silurian boundary on Anticosti Island. It would appear from their data that USGS coll. 9785–SD, which contains representatives of both genera (table 2), is equivalent to the interval of overlap of *Gamachignathus* and typical Silurian *Ozarkodina* on Anticosti Island and therefore lies immediately below the Ordovician/Silurian boundary as determined by McCracken and Barnes. Because no international Ordovician/Silurian boundary stratotype has yet been established, this part of the Hanson Creek Formation is assigned a latest Ordovician and (or) earliest Silurian age.



area of this report, although mapping indicates the member is about 46–61 m thick.

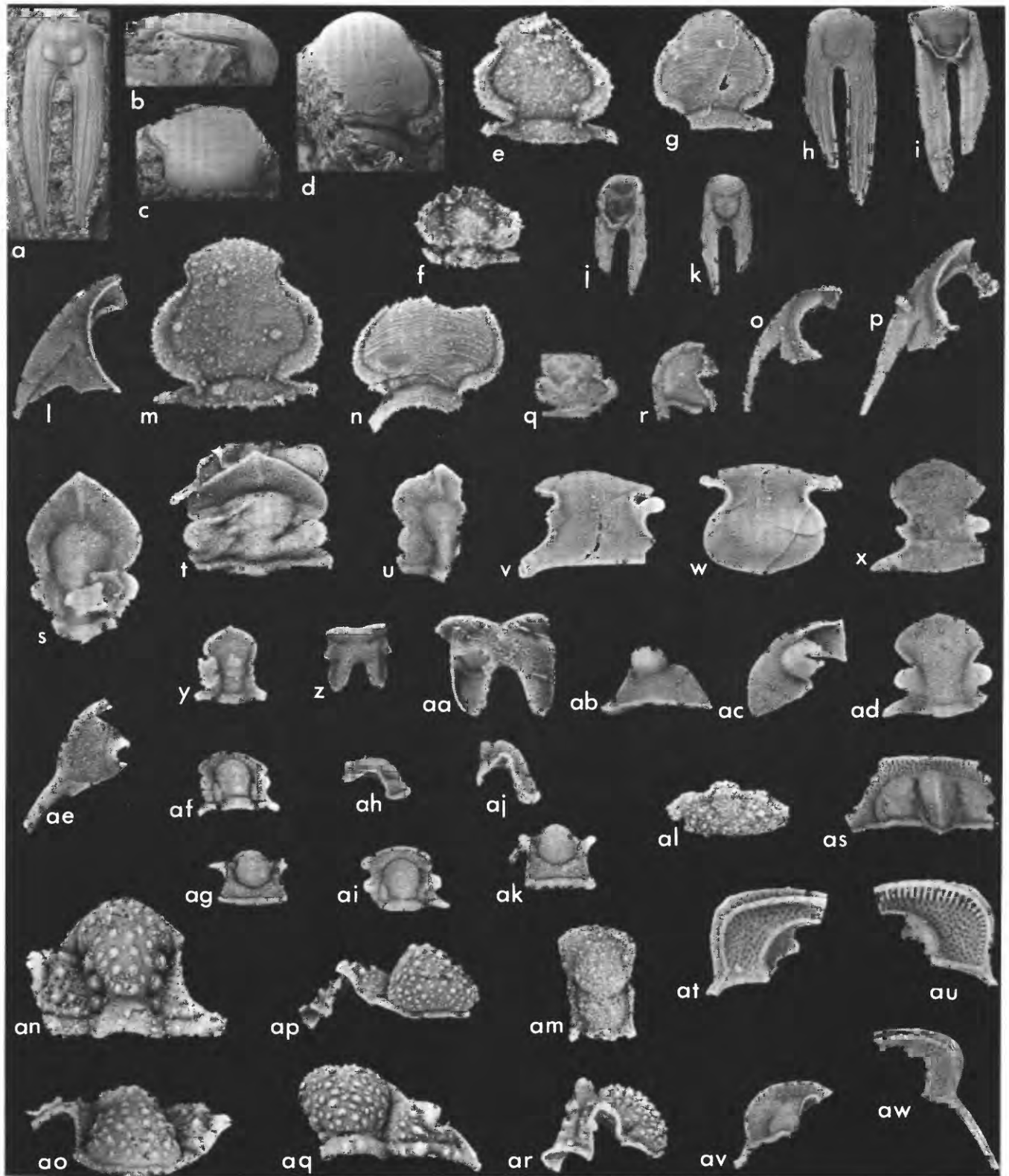
The Eureka–Hanson Creek contact, however, is exposed in the Mountain Boy Range at Spanish Mountain, 2.4 km southwest of the measured section (fig. 1). There, a single adenticulate detortiform element of *Belodina* sp. A of Sweet, Ethington, and Barnes (1971) was recovered from 2 m above the base of the Hanson Creek (fig. 6,g). Elements of this same species, moreover, occur 10 m above the base of the Hanson Creek Formation at its type locality in the Roberts Mountains (about 53 km northwest). According to W. C. Sweet (oral commun., 1977), *Belodina* sp. A has a known range of middle Edenian to middle Maysvillian in his undescribed conodont collections from the western United States, although he suspects that the range of this species may extend to at least the base of the Edenian (base of the Upper Ordovician). Thus, the base of the Hanson Creek in the Mountain Boy Range and Roberts Mountains appears to be no younger than middle Maysvillian and no older than Edenian.

In the course of our studies, conodonts were also collected from the lower part of the graptolite-bearing platy limestone facies of the Hanson Creek Formation in the Monitor Range, on Martin Ridge, about 2.5 km south of its north end (Horse Heaven Mountain 15-minute quadrangle) and 35 km southwest of the Mountain Boy Range locality. Collections from 6.1, 16.8, and 24.4 m above the base of the formation all contain *Protopanderodus insculptus* (Branson and Mehl) (fig. 6,ac) and only a few other conodonts of little biostratigraphic value. Some of the *P. insculptus* elements have part of a second denticle posterior to the cusp preserved—the diagnostic characteristic of this middle Maysvillian through Richmondian North American species. In this same vicinity on Martin Ridge (although not the same locality), Ross and Berry (1963, p. 65–67) made several float collections of graptolites from about the lower 9.1 m of the Hanson Creek. At that time, they believed that a fault separated the Hanson Creek from the underlying Eureka Quartzite. They have since decided that no fault exists and the sec-

FIGURE 4.—Trilobites from the Hanson Creek Formation.

[a–j, q–s, z, aa–ag, from USGS colln. D2645e–CO; k, t–y, ah–aj, from USGS colln. D2645d–CO; l–p, ak, from USGS colln. D2645a–CO; ax, from USGS colln. D2707–CO]

- a–k. *Ceraurus* sp. 1. a–c, cranium, dorsal, anterior, and lateral views, $\times 7$, USNM 252215. d–f, cranium, dorsal, anterior, and lateral views, $\times 6$, USNM 252216. g, h, i, j, cranium, dorsal, antero-dorsal, lateral, and anterior views, $\times 3$, USNM 252217. k, hypostome, ventral view, $\times 8$, USNM 252218.
- l–p. *Ceraurus* sp. 2. l, m, n, cranium, dorsal, lateral, and anterior views, $\times 5$, USNM 252219; note radial ornament around each tubercle. o, partial thorax and pygidium, dorsal view, $\times 10$, USNM 252220; lacks radial ornament of associated cranium. p, hypostome, fragmentary, ventral view, $\times 10$, USNM 252221; lacks radial ornament.
- q, r. *Ceraurus* ? sp. 3. Cranium and pygidium, dorsal views, $\times 7$, USNM 252222, 252223.
- s, z. *Ceraurus icarus* (Billings). s, hypostome, ventral view, $\times 3$, USNM 252224. z, pygidium, dorsal view, $\times 3$, USNM 252225.
- t–y. Calymenid, possibly *Gravicalymene*. t, hypostome, ventral view, $\times 7$, USNM 252226. u, pygidium, dorsal view, $\times 6$, USNM 252227. v, cranium, fragmentary, dorsal view, $\times 5$, USNM 252228. w, x, y, pygidium, posterior, lateral, and dorsal views, $\times 9$, USNM 252229.
- aa–ac. Acanthoparyphid, possibly *Youngia* or *Holia*. aa, pygidium plus one thoracic segment, dorsal view, $\times 7$, USNM 252230. ab, ac, cranium, dorsal and lateral views, $\times 4$, USNM 252231.
- ad–ag. Odontopleurid, possibly *Ceratocephala*. ad, ae, partial thorax, probably assignable to this genus, dorsal and lateral views, $\times 7$, USNM 252232. af, ag, cranium, dorsal and anterior views, $\times 7$, USNM 252233.
- ah–aj, ax. *Encrinurus* sp. ah, pygidium, fragmentary, dorsal view, $\times 5$, of a small part of the pleura and axis, USNM 252234. ai, aj, cranium, fragmentary, dorsal and anterior views, $\times 9$, USNM 252235. ax, pygidium, dorsal view, $\times 8$, USNM 252236.
- ak. Lichid, possibly *Hemiarges*. Cranium, dorsal view, $\times 10$, USNM 252237.
- al–au. *Anataphrus* sp. and *Isotelus* sp. Because complete ontogenetic series are lacking distinction is uncertain. Every specimen bears at least one transitory thoracic segment at the front of the pygidium. al, am, pygidia, dorsal views, $\times 7$, USNM 252238, 252239. an, ao, ar, as, at, au, pygidia, dorsal views, $\times 10$, USNM 252240, 252241, 252244, 252245, 252246, 252247 respectively. ap, pygidium, dorsal view, $\times 6$, USNM 252242. aq, av, pygidia, dorsal views, $\times 5$, USNM 252243, 252248.
- aw. *Calyptaulax* sp. Cranium, immature, dorsal view, $\times 7$, USNM 252249.
- ay. *Cybeloides* sp. Pygidium, fragmentary, dorsal view, $\times 8$, USNM 252250.



tion is probably continuous. Ross and Berry (1963) concluded that the Hanson Creek graptolites were chiefly late Caradocian forms but had some Ashgillian components. This conclusion would be in reasonable accord with the conodont data, which indicate an Ashgillian age for beds 6–24 m above the base of the formation.

CONCLUSIONS

We find that the Hanson Creek Formation in the Bellevue Peak Quadrangle is of Late Ordovician and Silurian age, confirming the previous conclusion of Mullens and Poole (1972) based on other areas. We suspect that continuous deposition took place in this area from latest Ordovician into Early Silurian time.

The combined macro- and micro-faunas indicate that the base of the formation is not older than Edenian and that the lower part of the middle limestone and dolomite member is at least as young as Maysvillian and is more likely to be Richmondian. The latest Ordovician and (or) earliest Silurian age of the top of this member, evidenced by conodonts, agrees with such a likelihood.

Any apparent uncertainty or discrepancy in dating of these beds is caused largely by ignorance of both stratigraphic and paleogeographic ranges of many of the taxa. The Ordovician paleoenvironments of Ohio, type area of the Cincinnati Series, and of Nevada were very different (Ross, 1976, 1977). As a result the two areas have little in common paleontologically, even in strata deposited at the same time.

REFERENCES CITED

- Aldridge, R. J., 1972, Llandovery conodonts from the Welsh Borderland: London, British Museum (Natural History) Bulletin, Geology, v. 22, no. 2, p. 127–231.
- Ancigin, N. I., 1973, Trilobita, in Ordovician Stratigraphy and fauna of the central Urals: Ministry of Geology SSSR, Ural. Terr. Geol. Uprav., Nedra, Moskva, 166 p., 30 pls.
- Barnes, C. R., 1974, Ordovician conodont biostratigraphy of the Canadian Arctic, in Aitken, J. D., and Glass, D. J., eds., Symposium on the geology of the Canadian Arctic, Proceedings: Calgary, Geological Association and Canadian Society of Petroleum Geology Special Volume, p. 221–240.
- Barnes, C. R., and Fahraeus, L. E., 1975, Provinces, communities, and the proposed nektobenthic habit of Ordovician conodontophorids: Lethaia, v. 8, no. 2, p. 133–149.

[References continued on p. C18]

FIGURE 5.—Tribolites from the Kimmswick Limestone, of Missouri, and the Hanson Creek Formation.

[a–d, from Kimmswick Limestone, from quarry 1.6 km south of Elsberry, Mo.; lowest bed quarried; USGS colln. 258g–CO. e–g, l–p, Hanson Creek Formation, USGS colln. D2645a–CO. an–ar, Hanson Creek Formation, USGS colln. D2645e–CO. All others, from USGS colln. D2645d–CO]

- a–d. *Hypodicranotus missouriensis* (Foerste). All $\times 3$. a, hypostome, ventral view; note almost circular middle body divided almost equally into three parts; USNM 252181. b, c, d, cranidium, lateral, anterior, and dorsal views, USNM 252182.
- e–p. *Hypodicranotus* n. sp. e, cranidium, dorsal view, $\times 20$, USNM 252183. f, cranidium, smallest specimen recovered, $\times 20$, USNM 252184. g, m, n, cranidia, dorsal views, respectively, $\times 10$, $\times 20$, $\times 10$, USNM 252185, 252189, 252190. h, i, hypostome, ventral and dorsal views, $\times 3$, USNM 252186; note that middle body has transversely wide anterior lobe and narrowly elongate posterior lobe and that median furrow (sag.) is distinguished more clearly on interior than on exterior. j, k, hypostome, dorsal and ventral views, $\times 8$, USNM 252187. l, o, p, free cheeks, left, dorsal views, respectively $\times 6$, $\times 10$, $\times 10$, USNM 252188, 252191, 252192.
- q,r. *Roborgia* sp. Fragmentary cranidium and free cheek, dorsal views, $\times 10$, USNM 252193, 252194.
- s–u. *Isotelus* sp. Immature cranidia, deformed tectonically, all dorsal views, $\times 10$. USNM 252195, 252196, 252197, respectively.
- v–ad. *Anataphrus* sp. v, w, cranidium, dorsal and anterior views, $\times 5$, USNM 252198. x, y, ad, cranidia, dorsal views, respectively $\times 7$, $\times 10$, $\times 10$, USNM 252199, 252200, 252204. z, aa, hypostomes, ventral views, $\times 10$, USNM 252201, 252202. ab, ac, free cheek, anterior and dorsal views, $\times 7$, USNM 252203.
- ae–am. *Otarion* sp. ae, free cheek, dorsal view, $\times 7$, USNM 252205. af, ag, ah, cranidium, dorsal, anterior, and lateral views, $\times 7$, USNM 252206. ai, aj, ak, cranidium, lateral, dorsal, and anterior views, $\times 6$, USNM 252207. al, pygidium, dorsal view, $\times 20$, USNM 252208. am, associated hypostome, ventral view, $\times 20$, USNM 252209.
- an–ar. *Ceraurus* sp. 1. an, ao, cranidium, fragmentary, dorsal and anterior views, $\times 6$. USNM 252210. ap, aq, ar, cranidium, fragmentary, anterior, dorsal, and lateral views, $\times 5$, USNM 252211.
- as–aw. *Cryptolithoides* sp. as, cranidium, dorsal view, $\times 7$, of immature specimen; note that eye tubercles are still present. USNM 252212. at, au, ventral and dorsal views, $\times 5$, of right side of fragmentary cranidia with free cheek in place, USNM 252213. aw, free cheek, fragmentary, ventral view, $\times 7$, USNM 252214.

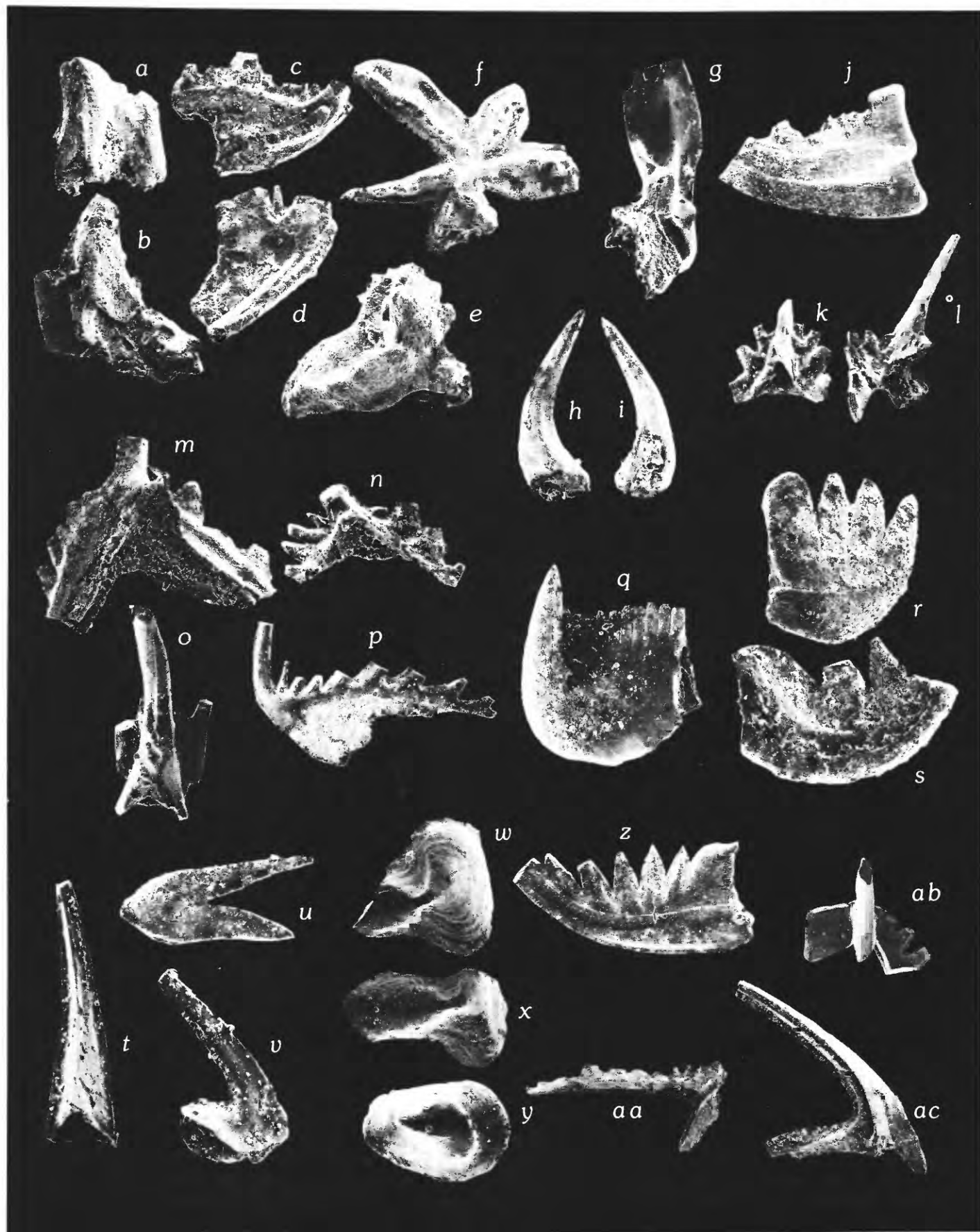


FIGURE 6.—Late Ordovician conodonts from the lower dark dolomite member (a–j) and the middle limestone and dolomite member (k–ab) of the Hanson Creek Formation, Mountain Boy Range, and from the graptolite-bearing platy limestone facies of the Hanson Creek Formation (ac), Monitor Range, Eureka County, Nevada. All specimens illustrated on figures 6 and 7, except 6g, are repositied in the U.S. National Museum of Natural History, Washington, D.C. (USNM). Susann Braden assisted in the SEM photography.

- a–f. *Amorphognathus ordovicicus* Branson and Mehl, from USGS colln. 8320–CO. a–e, $\times 100$; f, $\times 50$. This is the zonal index for the latest Ordovician North Atlantic A. *ordovicicus* Zone (=upper third of Fauna 11 and Fauna 12 of the midcontinent faunas of Sweet, Ethington, and Barnes, 1971); Maysvillian through Richmondian (Ashgillian).
- a, b. Outer lateral views of two holodontiform elements, USNM 248444 and USNM 248445.
- c. Lateral view of trichonodelliform element, USNM 248446.
- d. Inner lateral view of eoligonodiniform element, USNM 248448.
- e. Upper view of ambalodiform element, USNM 248447.
- f. Upper view of amorphognathiform element, USNM 248449.
- g. *Belodina* sp. A of Sweet, Ethington, and Barnes (1971) (=a new species of *Belodina* described by Craig (1968) from the lower half of the Fernvale Limestone of northern Arkansas). Postero-lateral inner view of adenticulate detortiform element, OSU 33382 (Orton Museum of Geology, The Ohio State University, Columbus, Ohio), $\times 50$. From 2 m above base of Hanson Creek Formation, Spanish Mountain, Mountain Boy Range, Bellevue Peak 15-minute Quadrangle (UTM grid, zone 11, E. 583,400 m, N. 4,368,250 m). Specimen courtesy of S. M. Bergström. This species is characteristic of middle Edenian (but may extend to the base of the Edenian according to W. C. Sweet, oral. commun., 1977) through middle Maysvillian of the central and western United States (Sweet and Bergström, 1976; Shatzter, 1976) and the Canadian Arctic (Barnes, 1974). It appears to be a component of the "Arctic-Red River" fauna of earlier workers.
- h, i. *Panderodus gracilis* (Branson and Mehl) element, from USGS colln. 8321–CO. Inner and outer lateral views, USNM 248450, $\times 25$. Elements of this species comprise 71 percent of all conodonts in the definitely Ordovician collections from the Hanson Creek Formation in the Mountain Boy Range and Wood Cone Peak area.
- j. *Belodina dispansa* (Glenister) s.f., from USGS colln. 8321–CO. Outer lateral view, USNM 248451, $\times 100$.
- k, l. Zygognathiform element, posterior and oblique lateral views of two specimens, USNM 248456 and USNM 248460, $\times 50$; USGS colln. 8323–CO. Several different zygognathiform elements occur in our collections without other associated ramiform elements. Accordingly these were not referred to a discrete or multielement taxon.
- m–p. *Oulodus ulrichi* (Stone and Furnish), $\times 50$.
- m. Posterior view of oulodiform element, USNM 248452; USGS colln. 8321–CO.
- n. Inner lateral view of prioniodiniform element, USNM 248454; USGS colln. 8326–CO.
- o. Oblique posterior view of trichonodelliform element, USNM 248455; USGS colln. 8323–CO.
- p. Lateral view of cordylodiform element, USNM 248453; USGS colln. 8323–CO.
- q. *Plegagnathus nelsoni* Ethington and Furnish s.f. Inner lateral view, USNM 248459, $\times 50$; USGS colln. 8322–CO. *P. nelsoni*, *P. dartoni* Ethington and Furnish s.f., and *Cordylodus robustus* Ethington and Furnish s.f. form one apparatus that is a diagnostic component of post-early Edenian Ordovician "Arctic-Red River" conodont faunas. *P. dartoni* and *C. robustus* elements have not been identified in our collections.
- r, s. *Belodina* n. sp. D of Shatzter (1976), $\times 100$; USGS colln. 8325–CO. Outer and inner lateral views of two different belodiniform elements, USNM 248457 and USNM 248458. This apparatus includes *Belodina profunda* (Branson and Mehl) of most previously described Late Ordovician conodont faunas. This species is a Maysvillian-Richmondian component of the "Arctic-Red River" fauna.
- t. *Coelocerodontus trigonius* Ethington s.f. Posterior view, USNM 248469, $\times 100$, USGS colln. 8323–CO.
- u. *Oistodus venustus* Stauffer s.f. Outer lateral view, USNM 248464, $\times 100$; USGS colln. 8322–CO.
- v. *Drepanoiostodus suberectus* (Branson and Mehl). Inner lateral view of oistodiform element, USNM 248463, $\times 100$; USGS colln. 8325–CO. Elements of this species comprise nearly 10 percent of the conodonts in Ordovician collections from the Hanson Creek Formation in the Mountain Boy Range and Wood Cone Peak area.
- w, x. *Pseudoneotodus mitratus* (Moskalenko). (= *Oistodus* (?) sp. of Branson and Mehl (1933, pl. 9, fig. 3). Upper views of two specimens, USNM 248466 and USNM 248465, $\times 50$; USGS colln. 8322–CO. This is a sporadic element in Middle and Late Ordovician conodont faunas in the western United States.
- y. *Pseudoneotodus beckmanni* (Bischoff and Sanne-mann) s.f. Upper view, USNM 248467, $\times 100$; USGS colln. 8323–CO. *P. beckmanni* ranges from the Late Ordovician through Early Devonian and appears to be the only morphotype in its apparatus.
- z. *Belodina compressa* (Branson and Mehl). Inner lateral view of belodiniform element, USNM 248461, $\times 100$; USGS colln. 8322–CO.
- aa. Prioniodiniform element. Oblique anterior view, USNM 248470, $\times 50$; USGS colln. 8327–CO.
- ab. Zygognathiform element, posterior view, USNM 248462, $\times 50$; USGS colln. 8327–CO. This distinctive element with a greatly laterally compressed cusp bearing a posterior costa and short but high lateral processes appears to be rather common in

FIGURE 6.—Continued.

Late Ordovician conodont faunas of the western United States.

- ac. *Protopanderodus insculptus* (Branson and Mehl) s.f. Outer lateral view, USNM 248468, $\times 50$; from 6.1 m above the base of the Hanson Creek Formation (graptolite-bearing platy limestone facies), about 2.5 km south of the north end of Martin Ridge, Horse Heaven Mountain 15-minute Quadrangle. The extremely elongate posterior process is typical of true North American *P. insculptus* (middle Maysvillian-Richmondian).

This is the most common element in the meager conodont fauna recovered from three 5-kg samples from the lower part of the graptolite-bearing platy limestone facies on Martin Ridge. In contrast, only one specimen of *P. insculptus* was found among the nearly 2,500 conodonts from the Hanson Creek of the Mountain Boy Range and Wood Cone Peak area. Clearly, *P. insculptus* is a component of deeper and (or) cooler water conodont biofacies.

References Cited—Continued

- Begg, J. L., 1939, Some new species of Proetidae and Otarionidae from the Ashgillian of Girvan: The Geological Magazine, v. 76, p. 372–382, pl. VI.
- Bradley, J. H., Jr., 1930, Fauna of the Kimmswick Limestone of Missouri and Illinois: Chicago University, Walker Museum of Paleontology Contributions, v. 2, no. 6, p. 219–290, pls. 23–30.
- Branson, E. B., and Mehl, M. G., 1933, Conodonts from the Plattin (Middle Ordovician) of Missouri: Missouri University Studies, v. 8, p. 101–119.
- Cooper, B. N., 1953, Trilobites from the lower Champlainian formations of the Appalachian Valley: Geological Society of America Memoir 55, 69 p., 19 pls.
- Craig, W. W., 1968, The stratigraphy and conodont paleontology of Ordovician and Silurian strata, Batesville District, Independence and Izard Counties, Arkansas: Austin, University of Texas Ph.D. thesis, 393 p.
- Dean, W. T., 1962, The trilobites of the Caradoc Series in the Cross Fall Inlier of northern England: London, British Museum (Natural History) Bulletin, v. 7, no. 3, p. 65–134, pls. 6–18, 5 text figs.
- 1963, The Stile End Beds and Drygill Shales (Ordovician) in the east and north of the English Lake District: London, British Museum (Natural History) Bulletin, v. 9, no. 3, p. 47–65, pls. 1–5.
- 1974, The trilobites of the Chair of Kildare limestone (upper Ordovician) of eastern Ireland, part 2: Palaeontographical Society Monograph, p. 61–98, pl. 26–44.
- Delo, D. M., 1940, Phacopid trilobites of North America: Geological Society of America Special Paper 29, 135 p., 13 pls.
- Duncan, Helen, 1956, Ordovician and Silurian coral faunas of western United States: U.S. Geological Survey Bulletin 1021-F, p. 209–236.
- 1957, *Bighornia*, a new Ordovician coral genus: Journal of Paleontology, v. 31, no. 3, p. 607–615.
- Hague, Arnold, 1892, Geology of the Eureka district, Nevada: U.S. Geological Survey Monograph 20, 419 p., and atlas of geologic maps [1883].
- Hall, James, 1847, Paleontology of New York, containing descriptions of the organic remains of the lower division of the New York System, in Natural history of New York: Albany, C. van Benthuysen, v. 1, 338 p.
- Hu, Chung-Hung, 1975, Ontogenies of four species of silicified Middle Ordovician trilobites from Virginia: Proceedings of the Geological Society of China, no. 18, p. 115–127, 4 figs., 2 pls.
- Ingham, J. K., 1970, The Upper Ordovician trilobites from the Cautley and Dent Districts of Westmoreland and Yorkshire: Palaeontographical Society Monograph, pt. 1, p. 1–58, pls. 1–9. [Published as part of v. 124.]
- 1974, The Upper Ordovician trilobites from the Cautley and Dent districts of Westmoreland and Yorkshire: Palaeontographical Society Monograph, pt. 2, p. 59–87, pls. 10–18. [Published as part of v. 128.]
- Kielan, Z., 1960 (1959), Upper Ordovician trilobites from Poland and some related forms from Bohemia and Scandinavia: Palaeontologia Polonica, no. 11, i–vi, 198 p., 36 pls.
- Kirk, Edwin, 1933, The Eureka quartzite of the Great Basin region: American Journal of Science, 5th ser., v. 26, p. 27–44.
- Lamont, A., 1935, The Drummuck group, Girvan; a stratigraphical revision, with descriptions of new fossils from the lower part of the group: Geological Society of Glasgow Transactions, v. 19, p. 288–332, pls. 7–9.
- Lane, P. D., 1971, British Cheiruridae (Trilobita): Palaeontographical Society Monograph, 95 p., 16 pls. [published as part of v. 125.]
- Le Fevre, Jean, Barnes, C. R., and Tixier, Michel, 1976, Paleocology of Late Ordovician and Early Silurian conodontophorids, Hudson Bay Basin, in Barnes, C. R., ed., Conodont paleocology: Canada Geological Association Special Paper 15, p. 69–89.
- Lenz, A. C., and Churkin, Michael, Jr., 1966, Upper Ordovician trilobites from northern Yukon: Palaeontology, v. 9, pt. 1, p. 39–47, pls. 4–5.
- Ludvigsen, Rolf, 1975, Ordovician formations and faunas, southern MacKenzie Mountains: Canadian Journal of Earth Sciences, v. 12, no. 4, p. 663–697, 5 pls.
- 1976a, Middle Ordovician trilobite biofacies, southern MacKenzie Mountains: Canada Geological Association Annual Meeting, P. S. Warren Biostratigraphy Symposium, Program with Abstracts, v. 1, p. 39.
- 1976b, New cheirurid trilobites from the lower Whitaker Formation (Ordovician), southern MacKenzie Mountains: Canadian Journal of Earth Sciences, v. 13, no. 7, p. 947–959, 2 pls.
- 1977, The Ordovician trilobite *Ceraurinus* Barton in North America: Journal of Paleontology, v. 51, no. 5, p. 959–972, pls. 1, 2.
- McCracken, A. D., and Barnes, C. R., 1979, Conodonts and the Ordovician-Silurian boundary from the Ellis Bay Formation, Anticosti Island: Canada Geological Survey Bulletin [in press].

TABLE 2.—Distribution of conodonts in collections from the Hanson Creek Formation, Mountain Boy Range, and Wood Cone Peak area, Bellevue Peak 15-minute Quadrangle, Eureka County, Nev.

[Collections 8320-8329-CO and 9785-SD from measured section 200 m east of center sec. 31, T. 19 N., R. 53 E., described in text. Collection 8292-CO from dark-gray thick-bedded limestone about 200 m west of measured section (UTM Grid, zone 11, E. 581 450 m, N. 4 369 600 m); mapping indicates this outcrop may overlie the middle limestone of the measured section. Collections 8332-8334-CO from Wood Cone Peak area. Leaders, --, not present]

Distance (meters) above base of section -----	0 to 0.6	5.2	6.1	14.9	18.6	19.8	20.7	21.3	22.9	27.4 to 28						
Collection No. (USGS) -----	8320-CO	8321-CO	8322-CO	8323-CO	8325-CO	8326-CO	8327-CO	8328-CO	8324-CO	8329-CO	9785-SD	8292-CO	8332-CO ¹	8333-CO ²	8334-CO ³	
Sample weight ----- kilograms--	4.9	4.5	3.6	4.3	4.6	5	5.2	3.8	3.5	4.2	4.3	2	3.6	4.2	3.8	
<i>Amorphognathus ordovicicus</i> Branson and Mehl:																
Ambalodiform element -----	7	2	---	---	---	---	---	---	---	---	---	2	---	---	---	
Amorphognathiform element -----	43	13	---	---	---	---	---	---	---	---	---	7	---	---	---	
Eoligonodiniiform element -----	5	1	---	---	---	---	---	---	---	---	---	---	---	---	---	
Holodontiform element -----	6	3	---	---	---	---	---	---	---	---	---	---	---	---	---	
Tetraprioniodiform element -----	1	---	---	---	---	---	---	---	---	---	---	---	---	---	---	
Trichonodelliform element -----	8	2	---	---	---	---	---	---	---	---	---	---	---	---	---	
<i>Aphelognathus?</i> n. sp.:																
Eoligonodiniiform element -----	---	---	---	---	---	---	---	---	---	---	8	---	---	---	---	
Prioniodiform element -----	---	---	---	---	---	---	---	---	---	---	4	---	---	---	---	
Spathognathodiform element -----	---	---	---	---	---	---	---	---	---	---	6	---	---	---	---	
Trichonodelliform element -----	---	---	---	---	---	---	---	---	---	---	4	---	---	---	---	
Zygognathiform element -----	---	---	---	---	---	---	---	---	---	---	3	---	---	---	---	
<i>Belodina compressa</i> (Branson and Mehl):																
Eobelodiniiform element -----	5	1	6	3	5	---	---	---	---	---	---	---	---	---	---	
Belodiniiform element -----	1	---	2	1	---	---	---	---	---	---	---	---	---	---	---	
<i>B. dispansa</i> (Glenister) s.f. -----	---	26	12	13	33	14	---	1	---	---	---	---	---	3	1	
<i>B. n. sp.</i> D elements of Shatzer (1976) -----	---	---	---	---	11	2	---	---	---	---	---	1	---	---	---	
<i>Coelocerodontus trigonius</i> Ethington s.f. -----	---	---	---	2	---	---	---	---	---	---	1	---	---	---	---	
<i>Drepanoistodus suberectus</i> (Branson and Mehl) elements -----	23	34	32	27	30	22	2	---	3	---	---	2	26	22	4	
<i>Exochognathus keislogathoides</i> Pollock, Rexroad, and Nicoll s.f. -----	---	---	---	---	---	---	---	---	---	---	6	---	---	---	---	
<i>Oistodus venustus</i> Stauffer s.f. -----	---	2	---	---	1	---	---	---	---	---	---	---	---	---	---	
<i>Pseudoneotodus beckmanni</i> (Bischoff and Sannemann) s.f. -----	---	---	---	3	---	---	---	---	---	---	---	---	---	---	---	
<i>Pseudoneotodus mitratus</i> (Moskalenko) -----	---	---	3	3	1	---	---	---	---	---	---	---	---	---	---	
<i>Oulodus ulrichi</i> (Stone and Furnish):																
Cordylodiform element ⁴ -----	---	---	---	8	14	3	---	1	1	---	---	---	---	---	---	
Cyrtoniodiform element -----	1	3	8	6	---	6	3	1	---	---	---	---	2	1	---	
Eoligonodiniiform element ⁴ -----	1	---	---	7	---	5	2	---	---	---	---	---	1	---	---	
Oulodiform element -----	---	5	4	5	6	4	6	1	1	---	---	---	3	1	---	
Prioniodiniiform element -----	---	1	---	6	3	5	9	1	2	---	---	---	---	1	---	
Trichonodelliform element -----	---	---	3	1	---	---	---	---	1	---	---	---	---	---	---	
Zygognathiform element -----	---	1	1	3	---	1	2	1	---	---	---	---	---	---	---	
<i>Panderodus gracilis</i> (Branson and Mehl) elements -----	169	405	252	288	197	150	16	9	11	10	---	12	54	122	26	
<i>Panderodus</i> sp. elements -----	---	---	---	---	---	---	---	---	---	---	9	---	---	---	---	
<i>Plegagnathus nelsoni</i> Ethington and Furnish s.f. -----	2	1	1	4	---	---	---	---	1	---	---	---	1	---	---	
<i>Protopanderodus insculptus</i> (Branson and Mehl) s.f. -----	---	---	---	---	---	---	1	---	---	---	---	---	---	---	---	
Cyrtoniodiform elements -----	---	---	---	---	---	---	4	---	---	---	---	---	---	---	---	
Distomodiform elements -----	---	---	---	---	---	---	---	---	---	16	---	---	---	---	---	
Eoligonodiniiform elements -----	---	---	---	---	---	---	---	---	---	1	---	---	---	---	---	
Plectospathodiform elements -----	---	---	---	---	---	---	---	---	---	1	1	---	---	---	---	
Prioniodiform elements -----	---	---	---	---	---	---	1	---	---	---	---	---	---	---	---	
Prioniodiniiform elements -----	---	---	---	---	---	---	---	---	---	1	---	---	---	---	---	
Spathognathodiform elements -----	---	---	---	---	---	---	---	---	---	2	---	---	---	---	---	
Trichonodelliform elements with very laterally compressed cusp -----	---	---	1	---	1	---	---	---	---	---	---	---	---	---	---	
Zygognathiform elements with very laterally compressed cusp -----	---	4	6	---	3	---	7	---	---	2	---	---	---	---	2	

¹ Dark-gray platy limestone. UTM Grid, zone 11, E. 574 750 m, N. 4 359 550 m (=D2707-CO).² Dark-gray flaggy skeletal limestone. UTM Grid zone 11, E. 574 800 m, N. 4 359 125 m (=D2708-CO).³ Dark gray fine-grained limestone. UTM Grid, zone 11, E. 574 630 m, N. 4 359 840 m.⁴ Cordylodiform and eoligonodiniiform elements both appear to occupy the Sc position (apparatus nomenclature of Sweet and Schonlaub, 1975) in this species of *Oulodus*. These collections contain no other apparatus in which an eoligonodiniiform or cordylodiform element can be accommodated.

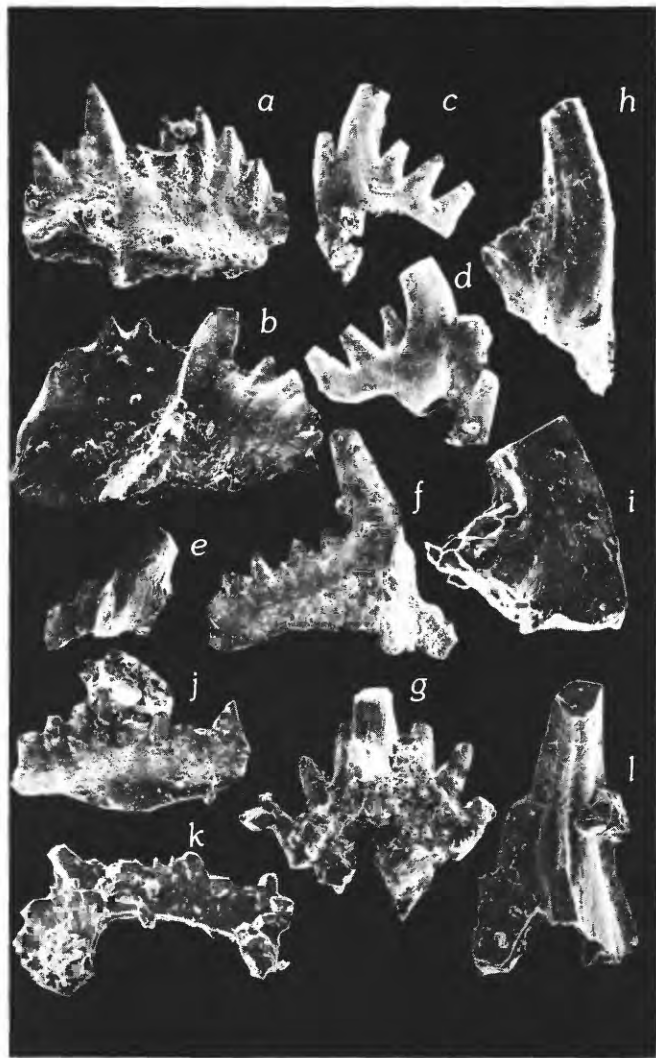


FIGURE 7.—Latest Ordovician and (or) earliest Silurian conodonts from the middle limestone and dolomite member of the Hanson Creek Formation, USGS colln. 9785-SD, Mountain Boy Range, Eureka County, Nev. (except *f*).

a-g. *Aphelognathus*? n. sp. The generic assignment is queried because Sweet, Thompson, and Satterfield (1975) diagnosed the apparatus of *Aphelognathus* as containing a dichognathiform or prioniodiniform element in the O_1 position. In this species, a prioniodiniform element occupies the O_1 position. In addition, the denticle pattern and profile designated by Sweet, Thompson and Satterfield (1975, p. 29) as characteristic of the genus does not fit elements of this species. The apparatus of *A.?* n. sp. was partly determined from conodont collections from near the base of the upper part of the Ely Springs Dolomite, Funeral Mountains, Inyo County, Calif. In these collections, *A.?* n. sp. elements are abundant, well preserved, and are nearly the only conodont elements aside from distomodids, keislognathodids, *Oulodus* sp., and panderodids. *Aphelognathus* is sup-

FIGURE 7.—Continued.

posedly a Middle and Late Ordovician genus. Pollock, Rexroad, and Nicoll (1970), however, designated a *p* element from Lower Silurian beds in northern Michigan and Ontario, *Aphelognathus siluricus*. Moreover, the same form occurs in the B and lower C divisions of the Llandovery in the Welsh Borderland (Aldridge, 1972). The *p* element of our species closely resembles *A. siluricus* s.f., but *A.?* n. sp. has only one adenticulate lateral process, whereas *A. siluricus* s.f. has an outer and inner adenticulate process. *A.?* n.sp. may well be ancestral to *A. siluricus*.

a, b. Spathognathodiform (*p*) element, inner and outer lateral views of two specimens, USNM 248472 and USNM 248473, $\times 50$. Note the adenticulate outer lateral process extending from the anterior edge of the main cusp. This feature demonstrates the consanguinity of this and the prioniodiniform element.

c, d. Eoligonodiniform element, outer and inner lateral views of two specimens, USNM 248474 and USNM 248475, $\times 75$.

e, f. Prioniodiniform element, oblique anterior views of two specimens, $\times 50$.

e. USNM 248476. Thus far, all prioniodiniform elements recovered from the Hanson Creek Formation are fragmentary and only the adenticulate upper part of the anterior process is preserved. If we had not had complete specimens of this element available to us from the Ely Springs Dolomite of the Funeral Mountains (fig. *f*), we would have assumed this element to be dichognathiform.

f. USNM 248477, from USGS colln. 9628-SD (about 1.5 m above the base of the upper part of the Ely Springs Dolomite, northwest base of spur 4298, southeast end of Funeral Mountains, SW $\frac{1}{4}$ sec. 33, T. 26 N., R. 4 E., Ryan 15-minute quadrangle, Inyo County, Calif.). Note the denticulate anterior process.

g. Trichonodelliform element, posterior view, USNM 248478, $\times 75$.

h, i. Distomodiform elements, outer and inner lateral views of denticulate and adenticulate elements, USNM 248472 and USNM 248471, $\times 100$. These are characteristic Early Silurian morphotypes.

j. Spathognathodiform element, outer(?) lateral view, USNM 248481, $\times 100$.

k. Plectospathodiform element, inner lateral view, USNM 248480, $\times 100$. This is a typical post-Ordovician morphotype. It probably belongs in the same apparatus as the element shown in *j*.

l. *Exochognathus keislognathoides* Pollock, Rexroad, Nicoll s.f. Posterior view, USNM 248479, $\times 100$. Better preserved specimens have denticulate outer lateral and posterior processes and an adenticulate inner lateral process. This is a common element in Early Silurian conodont faunas.

References Cited—Continued

- Macomber, R. W., 1970, Articulate brachiopods from the upper Bighorn Formation (Late Ordovician) of Wyoming: *Journal of Paleontology*, v. 44, no. 3, p. 416-450, pls. 77-80.
- Merriam, C. W., 1940, Devonian Stratigraphy and Paleontology of the Roberts Mountains Region, Nevada: Geological Society of America Special Paper 25, 114 p.
- 1963a, Paleozoic rocks of Antelope Valley, Eureka and Nye Counties, Nevada: U.S. Geological Survey Professional Paper 423, 67 p.
- 1963b, Geology of the Cerro Gordo mining district, Inyo County, California: U.S. Geological Survey Professional Paper 408, 83 p.
- Merriam, C. W., and Anderson, C. A., 1942, Reconnaissance survey of the Roberts Mountains, Nevada: Geological Society of America Bulletin, v. 53, no. 12, p. 1675-1727.
- Moskalenko, T. Z., 1973, Conodonts of the Middle and Upper Ordovician on the Siberian Platform: Academy of Sciences of the USSR, Siberian Branch, Transactions of the Institute of Geology and Geophysics, v. 137, 143 p. [in Russian].
- Mullens, T. E., and Poole, F. G., 1972, Quartz-sand-bearing zone and Early Silurian age of upper part of the Hanson Creek Formation in Eureka County, Nevada: U.S. Geological Survey Professional Paper 800-B, p. B21-B24.
- Nelson, S. J., 1963, Ordovician paleontology of the northern Hudson Bay Lowland: Geological Society of America Memoir 90, 152 p., 37 pls.
- Nolan, T. B., Merriam, C. W., and Williams, J. S., 1956, The stratigraphic section in the vicinity of Eureka, Nevada: U.S. Geological Survey Professional Paper 276, 77 p.
- Nowland, G. S., and Barnes, C. R., 1979, Late Ordovician conodonts from the Vauréal Formation, Anticosti Island, Québec: Canada Geological Survey Bulletin [in press].
- Õpik, A., 1937, Trilobiten aus Estland: Tartu University Geological Institution, Publications No. 52, 163 p., 26 pls.
- Owens, R. M., 1973, British Ordovician and Silurian Proetidae (Trilobita): Paleontographical Society Monograph, p. 1-98, pls. 1-15. [Published as part of v. 127.]
- Pollock, C. A., Rexroad, C. B., and Nicoll, R. S., 1970, Lower Silurian conodonts from northern Michigan and Ontario: *Journal of Paleontology*, v. 44, no. 4, p. 743-764.
- Raymond, P. E., 1925, Some trilobites of the lower middle Ordovician of eastern North America: Harvard College Museum of Comparative Zoology Bulletin, v. 67, no. 1, 180 p., 10 pls.
- Ross, R. J., Jr., 1957, Ordovician Fossils from wells in the Williston Basin, eastern Montana: U.S. Geological Survey Bulletin 1021-M, p. 439-510, pls. 37-43.
- 1967, Calymenid and other Ordovician trilobites from Kentucky and Ohio: U.S. Geological Survey Professional Paper 583-B, p. B1-B18, 5 pls.
- 1976, Ordovician sedimentation in the western United States, in Bassett, M. G., ed., The Ordovician System—Proceedings of a Palaeontological Association Symposium, Birmingham, 1974: Cardiff, University of Wales Press and National Museum of Wales, p. 73-105.
- 1977, Ordovician paleogeography of western United States, in Stewart, J. H., Stevens, C. H., and Fritsche, A. E., eds., Paleozoic Paleogeography of the Western United States, Pacific Coast Paleogeography, Symposium 1, Pacific Section: Society of Economic Paleontologists and Mineralogists, p. 19-38.
- Ross, R. J., Jr., and Berry, W. B. N., 1963, Ordovician graptolites of the Basin Ranges in California, Nevada, Utah, and Idaho: U.S. Geological Survey Bulletin 1134, 177 p., 13 pls.
- Ross, R. J., Jr., and Dutro, J. T., Jr., 1966, Silicified Ordovician brachiopods from east-central Alaska: Smithsonian Miscellaneous Collections, v. 149, no. 7, 22 p., 3 pls.
- Ross, R. J., Jr., and Shaw, F. C., 1972, Distribution of the Middle Ordovician Copenhagen Formation and its trilobites in Nevada: U.S. Geological Survey Professional Paper 749, 33 p. 8 pls.
- Roy, S. K., 1941, The Upper Ordovician fauna of Frobisher Bay, Baffin Land: Field Museum of Natural History Publications, Geology Memoirs, v. 2, 212 p., 146 figs.
- Schmidt, F., 1881, Revision der Ostbaltischen Silurischen Trilobiten, Abteilung 1, Phacopiden, Cheiruriden, und Encrinuriden: Memoires de l'Académie Impériale des Sciences de St. Petersburg, VII^e Série, Tome XXX, N^o 1, 237 p., 16 pls.
- Schuchert, Charles, and Cooper, G. A., 1930, Upper Ordovician and Lower Devonian stratigraphy and paleontology of Percé, Quebec: American Journal of Science, 5th series, v. 20, p. 161-176, 265-288, 365-392.
- Shatzer, D. C., 1976, Conodont biostratigraphy of the Fremont and Priest Canyon Formations (Upper Ordovician) at Kerber Creek, Saguache County, Colorado: Columbus, The Ohio State University M. S. thesis, 141 p.
- Shaw, F. C., 1968, Early Middle Ordovician Chazy trilobites of New York: New York State Museum and Science Service Memoir 17, 163 p., 24 pls.
- 1974, Simpson Group (Middle Ordovician) trilobites of Oklahoma: *Journal of Paleontology*, v. 48, no. 5, supp. II, Paleontological Society Memoir 6, 54 p., 12 pls.
- Shirley, Jack, 1936, The British trilobites of the family Calymenidae: Geological Society of London Quarterly Journal, v. 92, pt. 4, p. 384-422, pls. 29-31.
- Slocum, A. W., 1913, New trilobites from the Maquoketa beds of Fayette County, Iowa: Field Museum of Natural History, Publications in Geology, ser. 4, p. 43-83.
- Sweet, W. C., and Bergström, S. M., 1976, Conodont biostratigraphy of the Middle and Upper Ordovician of the United States Midcontinent, in Bassett, M. G., ed., The Ordovician System—Proceedings of a Palaeontological Association Symposium, Birmingham, 1974: Cardiff, University of Wales Press and National Museum of Wales, p. 121-151.
- Sweet, W. C., Ethington, R. L., and Barnes, C. R., 1971, North American Middle and Upper Ordovician conodont faunas, in Sweet, W. C., and Bergström, S. M., eds., Conodont biostratigraphy: Geological Society of America Memoir 127, p. 163-193.
- Sweet, W. C., and Schönlaub, H. P., 1975, Conodonts of the genus *Oulodus* Branson & Mehl, 1933: *Geologica et Palaeontologica*, v. 9, p. 41-59.
- Sweet, W. C., Thompson, T. L., and Satterfield, I. R., 1975, Conodont stratigraphy of the Cape Limestone (Maysvillian) of eastern Missouri, in Missouri Geological Survey, Studies in Stratigraphy: Missouri Geological Survey Department of Natural Resources, Report Investigations 57, pt. 1, p. 1-59.

- Tripp, R. P., 1954, Caradocian trilobites from mudstones at Craighhead Quarry, near Girvan Ayrshire: Royal Society of Edinburgh Transactions, v. 62, pt. 3, p. 655-693, pls. 1-4.
- 1965, Trilobites from the Albany division (Ordovician) of the Girvan district, Ayrshire: Palaeontology, v. 8, pt. 4, p. 577-603, pls. 80-83.
- 1967, Trilobites of the Upper Stinchar limestone (Ordovician) of the Girvan District, Ayrshire: Royal Society of Edinburgh Transactions, v. 67, no. 3, p. 43-93, pls. I-VI.
- Troedsson, G. T., 1928, On the Middle and Upper Ordovician faunas of northern Greenland—Part II: Meddelelser om Grönland, Bd. 72, p. 1-197, pls. 1-56.
- Twenhofel, W. H., 1927, Geology of Anticosti Island: Canada Geological Survey Memoir 154, 480 p., 60 pls.
- Ulrich, E. O., 1888, On *Sceptropora*, a new genus of Bryozoa, with remarks on *Helopora* Hall, and other genera of that type: American Geologist, v. 1, p. 228-234.
- Warburg, Elsa, 1925, Trilobites of the Leptaena Limestone in Dalarne with a discussion of the zoological position and the classification of the Trilobita: Bulletin of the Geological Institutions of the University of Uppsala, v. 17, p. 1-446, 11 pls.
- Weller, S., 1903, The Paleozoic Faunas: New Jersey Geological Survey, Report on Paleontology, v. 3, 462 p., 52 pls.
- Whittington, H. B., 1941, The Trinucleidae, with special reference to North American genera and species: Journal of Paleontology, v. 15, no. 1, p. 21-41, pls. 5, 6.
- 1950, Sixteen Ordovician genotype trilobites: Journal of Paleontology, v. 24, no. 5, p. 531-565, pls. 68-75, 9 text figs.
- 1952, A unique remopleurid trilobite: Breviora, Harvard University Museum of Comparative Zoology, no. 4, 9 p., 1 pl.
- 1954, Ordovician trilobites from Silliman's Fossil Mount: Geological Society of America Memoir 62, p. 119-149, pls. 59-63.
- 1959, Silicified Middle Ordovician trilobites—Remopleurididae, Trinucleidae, Raphiophoridae, Endymioniidae [Va.]: Harvard College Museum of Comparative Zoology Bulletin, v. 121, no. 8, p. 373-496, 36 pls.
- 1963-1968, Monograph of the Ordovician Trilobites of the Bala Area, Merioneth, 138 p., 32 pls.: London, Palaeontographical Society, published in parts, as follows: 1962, v. 116, Part I, p. 1-32, pls. I-VIII; 1964, v. 118, Part II, p. 33-62, pls. IX-XVIII; 1966, v. 120, Part III, p. 63-93, pls. XIX-XXVIII; 1968, v. 122, Part IV, p. 93-138, pls. XXIX-XXXII.
- Whittington, H. B., and Evitt, W. R., II, 1954, Silicified Middle Ordovician trilobites [Va.]: Geological Society of America Memoir 59, 137 p., 33 pls.
- Williams, Alwyn, 1962, The Barr and Lower Ardmillan Series (Caradoc) of the Girvan District, south-west Ayrshire, with descriptions of the Brachiopods: Geological Society of London Memoir 3, 267 p., 25 pls.

The Marble Hill Bed: An Offshore Bar-Tidal Channel Complex in the Upper Ordovician Drakes Formation of Kentucky

By W C SWADLEY

SHORTER CONTRIBUTIONS TO STRATIGRAPHY AND
STRUCTURAL GEOLOGY, 1979

GEOLOGICAL SURVEY PROFESSIONAL PAPER 1126-D

*Prepared in cooperation with
the Kentucky Geological Survey*



CONTENTS

	Page
Abstract	D1
Introduction	1
Previous nomenclature	1
Stratigraphy	1
Extent and thickness	3
Lithology	4
Environments of deposition	5
Depositional history	6
Summary	8
References cited	8

ILLUSTRATIONS

	Page
FIGURE 1. Map showing location of study area and areas of exposure of the Rowland Member of the Drakes Formation and the Bull Fork Formation in north-central Kentucky	D2
2. Diagrammatic cross section showing relation of the main elements of the Marble Hill Bed to the enclosing stratigraphic units within the study area	3
3. Map showing thickness and stratigraphic position of the Marble Hill Bed within the Rowland Member	4
4. Cross sections showing position of Marble Hill Bed within Rowland Member	5
5. Sketch map of study area showing interpretation of depositional environments	7

THE MARBLE HILL BED: AN OFFSHORE BAR-TIDAL CHANNEL COMPLEX IN THE UPPER ORDOVICIAN DRAKES FORMATION OF KENTUCKY

By W C SWADLEY

ABSTRACT

The Marble Hill Bed of the Rowland Member of the Drakes Formation consists of a group of linear bodies of biosparudite and biosparite that occur near the northern edge of the Rowland Member in north-central Kentucky and southeastern Indiana. The Rowland Member, a unit of interbedded micritic limestone and mudstone, abruptly thins and pinches out into interbedded fossiliferous limestone and shale of the Bull Fork Formation. The Marble Hill was deposited as an offshore bar and tidal channel complex along the seaward northern edge of the shallow marine platform on which the Rowland was deposited. Deposition was probably initiated by uplift that resulted in a northward transgression of the platform environment over the southern edge of the open shelf on which the Bull Fork was deposited. Later subsidence of the area resulted in a southward regression of the platform environment and ended Marble Hill deposition.

INTRODUCTION

The Marble Hill Bed is a unit of bioclastic limestone in the Rowland Member of the Drakes Formation in north-central Kentucky and southeastern Indiana (fig. 1). It consists of several related limestone bodies along or near the abrupt northern pinchout of the Rowland Member into the Bull Fork Formation. Recent mapping in the area as part of the statewide U.S. Geological Survey-Kentucky Geological Survey cooperative mapping program has for the first time determined the extent and shape of the Marble Hill Bed and its stratigraphic relations. The depositional environments and history are herein analyzed on the basis of lithology, field relationships, and faunal content.

This report is based largely on field data obtained during the mapping of six 7½-minute quadrangles in north-central Kentucky and reconnaissance mapping in southeastern Indiana. Field descriptions of the rock units were supplemented by the study of thin sections. Thin-section preparation and part of the petrographic analysis were done by Brandon C.

Nuttall, a graduate student at the University of Cincinnati.

PREVIOUS NOMENCLATURE

The Marble Hill was first described by Owen (1859), who named it for exposures in a building-stone quarry at Marble Hill, Ind. The name was used in several reports in the early 1900's and then apparently fell into disuse (Weiss and Norman, 1960). Much of the later literature on the area assigns the part of the stratigraphic section that includes the Marble Hill to the Waynesville Shale. In a summary of stratigraphic nomenclature of Indiana, Shaver and others (1970) included the Marble Hill Bed in the Dillsboro Formation. Recent work in north-central Kentucky by Swadley and Gibbons (1976) reassigned the unit as the Marble Hill Bed of the Rowland Member of the Drakes Formation. The name Drakes Formation is herein extended to a small area in southeastern Indiana where the Marble Hill Bed is exposed.

STRATIGRAPHY

Upper Ordovician strata of the study area consist largely of limestone interbedded with shale and mudstone. The Marble Hill Bed comprises two clastic limestone bodies within and near the north edge of the Rowland Member of the Drakes Formation (fig. 2). The Rowland consists of interbedded limestone and mudstone. It overlies fossiliferous limestone and shale of the Bull Fork Formation and is overlain by fossiliferous limestone and shale of the Bardstown Member of the Drakes Formation. The Bardstown is overlain by the Saluda Dolomite Member of the Drakes.

The Bull Fork Formation is a unit of interbedded limestone and shale that is exposed along two north-

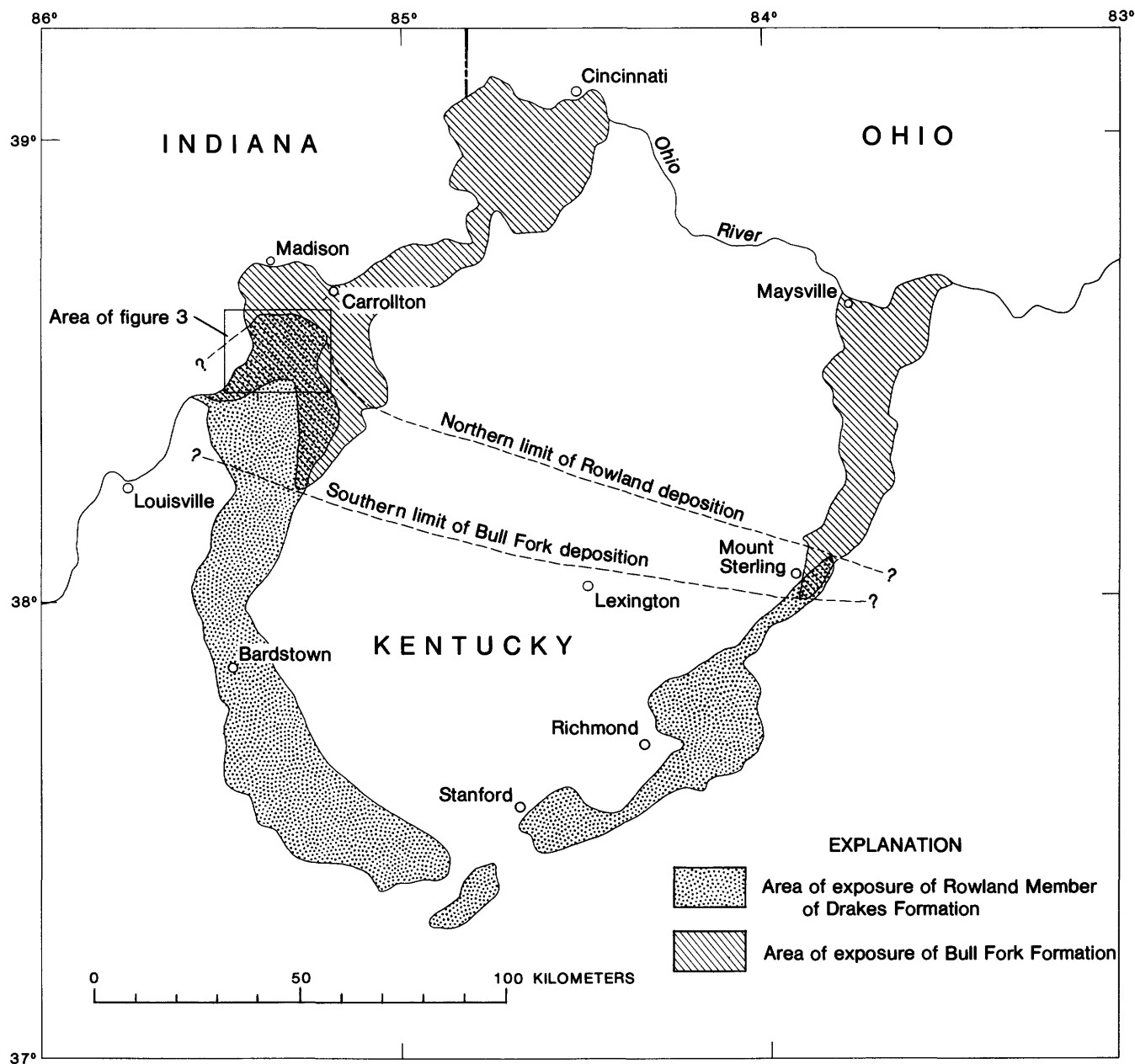


FIGURE 1.—Map showing location of study area and areas of exposure of the Rowland Member of the Drakes Formation and the Bull Fork Formation in north-central Kentucky

trending bands of outcrop flanking the inner part of the central Kentucky region (fig. 1). Along the eastern band, the formation thins from about 60 m at the type section near Maysville, Ky. (Peck, 1966), to a pinchout about 75 km to the south. In the west, the Bull Fork is about 65 m thick near Carrollton, Ky., and thins southward, pinching out 50 km to the south. The formation consists of medium-gray poorly sorted biomicrudite in thin, even to irregular beds that are interlayered with gray calcareous shale. Well-sorted, fine-grained biosparite in thin even

beds and even-bedded calcareous siltstone are minor components. Overall, the limestone and shale contents are nearly equal, but limestone is generally more abundant near the base of the unit, and shale is more abundant toward the top. Fossil brachiopods and bryozoans are abundant in the Bull Fork; echinoderms, trilobites, and gastropods are common; and solitary corals occur sporadically.

The Rowland Member of the Drakes Formation is a sparsely fossiliferous, thin-bedded, dolomitic to limy mudstone named by Weir and others (1965) in

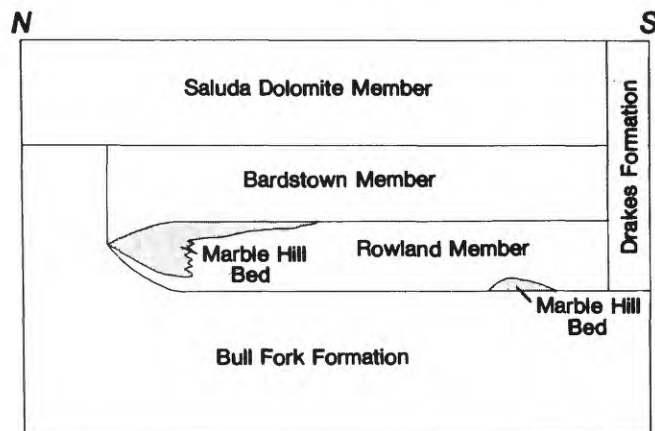


FIGURE 2.—Diagrammatic cross section showing relation of the main elements of the Marble Hill Bed to the enclosing stratigraphic units within the study area.

southeastern central Kentucky. It crops out in an arcuate belt along the south and west side of the inner part of the central Kentucky region (fig. 1). Northwestward from the type area it becomes more limy and more fossiliferous. Near the northwest end of its outcrop belt, in the study area, the Rowland consists of about 12 m of light-gray clayey micrite interbedded with medium-gray to greenish-gray calcareous mudstone. The limestone is commonly in nodular to even beds as much as 1 m thick but locally is in thin laminae. Many beds have been extensively burrowed and weather to a knobby surface with numerous vertical finger-size holes. Mudstone is dominant in the lower half of the member and commonly forms a 1- to 2-m-thick bed at the base. Fossils include common to abundant colonial corals as much as 0.6 m in diameter, common ostracodes, and sparse brachiopods and bryozoans. At its northern limit, the Rowland thins abruptly and pinches out into the Bull Fork Formation (fig. 2).

The Marble Hill Bed occurs as a thin linear body at the base of the Rowland and as a thicker, more complex unit along the northern edge, where it locally makes up almost the entire thickness of the member. The Marble Hill is described in more detail in following paragraphs.

Overlying the Rowland Member is the Bardstown Member of the Drakes, a unit of fossiliferous limestone and interbedded shale named by Peterson (1970) in southwestern central Kentucky. It occurs along a belt of outcrop similar to the western part of the Rowland outcrop (fig. 1). In the study area, it consists of 12 to 18 m of medium-gray limestone interbedded with an equal amount of medium-gray calcareous shale. The Bardstown is lithologically and

faunally so much like the Bull Fork Formation that it cannot be differentiated from the Bull Fork north of the pinchout of the Rowland Member (fig. 2).

The Saluda Dolomite Member is the upper member of the Drakes and consists of 20 m of dolomite and dolomitic to limy mudstone. It overlies the Bardstown Member and the laterally equivalent part of the Bull Fork.

EXTENT AND THICKNESS

The Marble Hill Bed is exposed in a small area of north-central Kentucky and southeastern Indiana south of Madison, Ind. (fig. 1). It consists of two clastic limestone bodies: a narrow, elongate unit at the base of the Rowland Member about 11 km south of the Rowland pinchout and a wider, more complex body that occurs mostly along the northern pinchout of the member (fig. 3).

The basal unit is about 1 km wide and is discontinuously exposed for 29 km along an east-northeast trending outcrop. Near the east end it breaks into a line of discontinuous pods or lenses. In cross section, the body is flat bottomed, convex, and asymmetrical and has the steeper face to the northwest (fig. 4, section *B-B'*). The basal contact appears conformable. The thickness averages about 1.2 m; the maximum observed thickness is 4 m. The body goes into the subsurface at the west end. Its subsurface extent is unknown.

The larger unit of Marble Hill limestone occurs along the northern edge of the Rowland Member as an elongate body that parallels the basal unit and extends a short distance into Indiana before descending into the subsurface (fig. 3). It is as much as 9 m thick, thinning abruptly to the northwest and more gradually to the southeast (fig. 4, sections *A-A'* and *B-B'*). The unit appears to rest conformably on the basal mudstone of the Rowland. Near the west end of the exposed body, the southward-thinning edge occurs as an irregular tongue of Marble Hill strata that extends for 3 km into the main body of the Rowland Member. It is overlain by a northward-thinning tongue that has Rowland lithology (fig. 4, section *A-A'*). From 1 to 5 km east of the Ohio River, the southward extension occurs at the top of the member (fig. 4, section *B-B'*). There is a small area about 1.5 km east of the Ohio River (fig. 3) where both tongues are present.

At the east end the larger body of the Marble Hill Bed is joined by three subunits. The first subunit joins at the eastern tip and extends for nearly 10 km to the east-southeast. For about half that distance,

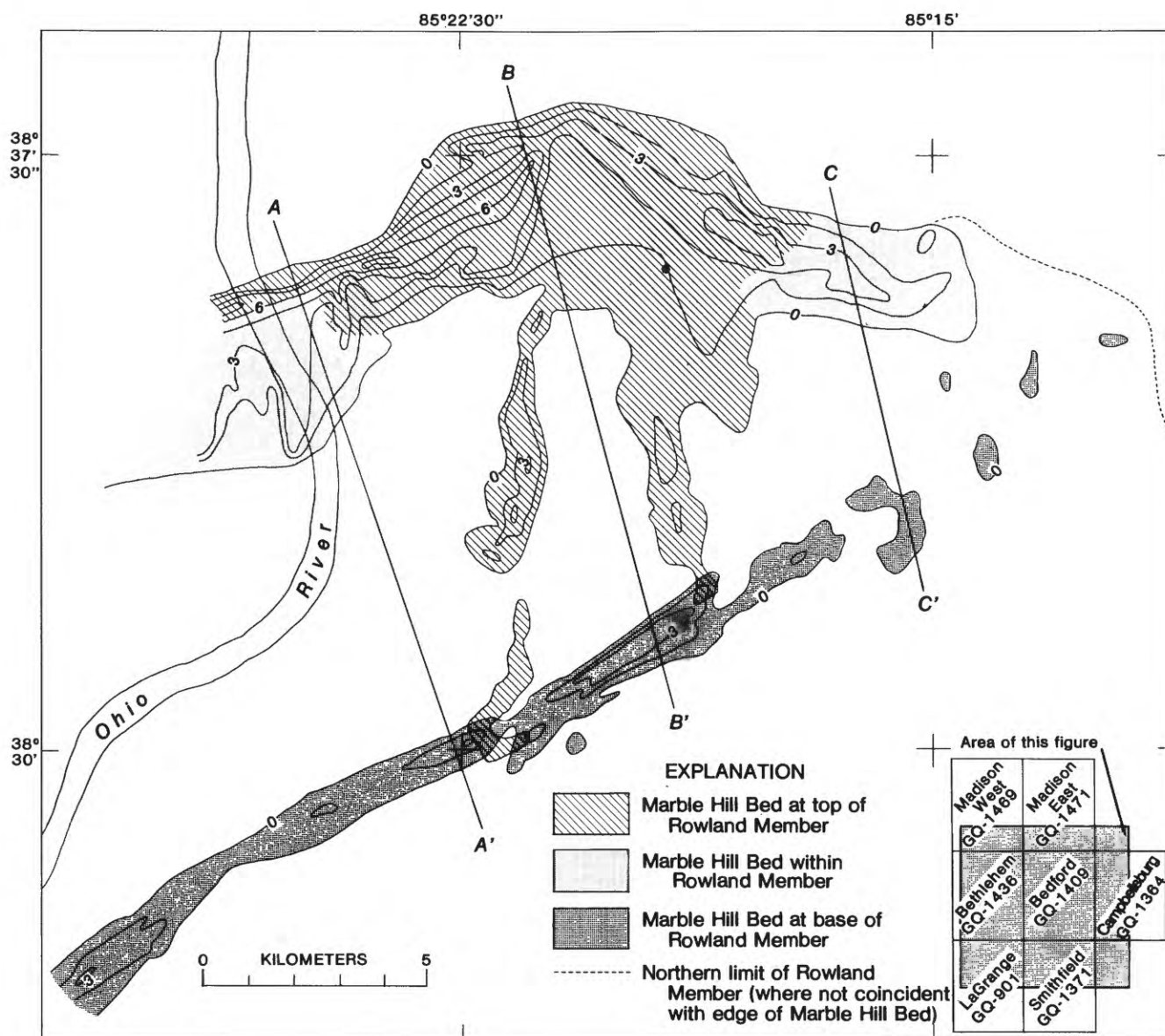


FIGURE 3.—Map showing thickness and stratigraphic position of the Marble Hill Bed within the Rowland Member. Contour interval 1.5 m. Cross sections A-A', B-B', and C-C' are shown in figure 4. Inset map gives numbers of U.S. Geological Survey 7½-minute geologic quadrangles within which the Marble Hill Bed occurs.

this subunit occurs at the top of the Rowland Member; then the upper contact drops gradually in the section as the subunit thins to a feathered edge near the middle of the Rowland (fig. 4, section C-C'). The basal contact is sharp and locally disconformable. Farther west, two other subunits join the larger body of the Marble Hill near its east end. These are south-trending linear bodies as much as 3 m thick and about 0.8 km wide that extend for as much as 13 km to the south (fig. 3). In cross section each of these two bodies is convex downward and

has a flat upper surface coincident with the upper contact of the Rowland Member. The basal contact seems to be conformable; these units grade laterally into and intertongue with poorly bedded to thinly laminated Rowland micrite over a distance of 1 to 2 m.

LITHOLOGY

The Marble Hill Bed typically consists of gastropod biosparrodite and echinoderm biosparite. Biomicrudite locally is an important component. The

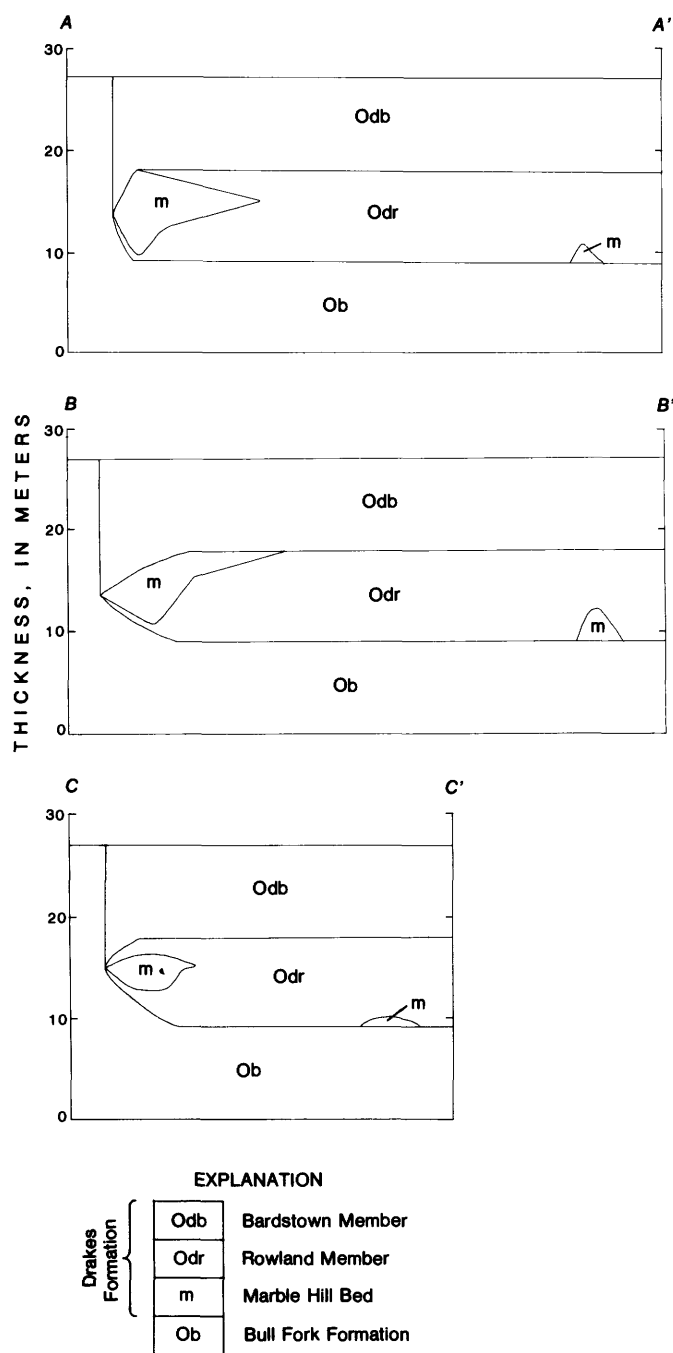


FIGURE 4.—Cross sections showing position of Marble Hill Bed within Rowland Member. Location of sections shown on figure 3.

bioparrudite is very light gray and weathers very pale orange. It occurs commonly in even beds as much as 1 m thick and is locally thinly crossbedded in sets 0.5 to 1.0 m thick. The major components are abundant whole and broken high-spined gastropods as much as 50 mm long, common bryozoan and brachiopod fragments, common to sparse echinoderm

fragments, and sparse trilobite fragments. Fossil fragments are abraded, and sorting is poor. The cement is commonly medium to coarse sparry calcite with minor amounts of microspar. Small amounts of colophane occur as fillings in fossil cavities. The bioparrudite is resistant and weathers to bold rounded ledges. The sparry calcite that fills the abundant gastropod shells weathers readily, yielding a pitted surface.

Biosparite is light olive gray to very light gray and weathers yellowish gray. It consists of abundant broken and rounded echinoderm plates, common trilobite fragments, and sparse bryozoan and brachiopod fragments. Grains are fine to medium, and sorting is generally good. The cement is medium- to coarse-grained sparry calcite, much of which occurs as overgrowths on echinoderm fragments. The rock is slightly phosphatic. Biosparite is commonly thinly crossbedded in sets 0.3 to 0.6 m thick. It is less resistant than the bioparrudite but forms conspicuous ledges.

Biomicrodite is light to medium gray and weathers light gray to grayish orange. It consists of abundant whole and broken gastropods, abundant coarse to fine brachiopod and bryozoan fragments, and abundant to common echinoderm plates. Sorting is very poor. The cement varies from micrite to sparry calcite. Beds are even to slightly irregular and generally 0.3 to 0.6 m thick.

A common exposure of the Marble Hill Bed consists of a basal unit of crossbedded biosparite overlain by an equal or greater thickness of thick-bedded gastropod bioparrudite. At some exposures, the two lithologies are interbedded, and infrequently the biosparite is dominant. Where the unit is 1 to 2 m thick, the biosparite is commonly absent. Biomicrodite is present in areas where the Marble Hill is less than about 1 m thick, and it is commonly the dominant lithology where the unit is less than 0.5 m. At a few exposures, the Marble Hill includes thin tongues of micritic limestone and calcareous mudstone of characteristic Rowland lithology.

ENVIRONMENTS OF DEPOSITION

The study area prior to the development of the Marble Hill Bed was a shallow marine shelf. The abundant and diverse fauna of the underlying Bull Fork Formation indicates an area of shallow, well-aerated water of normal salinity. The jumble of whole and coarsely broken fossils in a micritic matrix probably resulted from current action sufficient to produce some breaking and sorting of the fossils but too weak to winnow out lime mud. Thus, most of

the Bull Fork was probably deposited below normal wave base but within the zone affected by storm waves. This environment is the shelf facies or deep undathem of Wilson (1975, p. 355), who describes the water depth as "tens of meters or even a hundred meters." The shelf environment existed for tens of kilometers south of the study area before Rowland time and north of the study area before, during, and after Rowland deposition. The greatest southern extent of the pre-Rowland shelf is indicated by the southern limit of Bull Fork deposition, shown in figure 1.

The dolomitic to limy mudstone of the type Rowland Member in southern central Kentucky was deposited in very shallow areas along the landward (south) side of a marine platform. The great sparsity of the marine fauna there indicates restricted circulation, and the dolomitic character of the sedimentary rocks suggests intermittent hypersaline conditions. Deposition occurred partly in intertidal areas, as evidenced by mudcracks (Weir and others, 1965, p. D17). The Rowland of the study area was deposited seaward (north) of the type Rowland, in deeper water; it represents a lagoonal area in which argillaceous micrite and calcareous mudstone were deposited. The common corals and ostracodes and sparse brachiopods and byozoans indicate an area of more normal salinity but one with only moderate circulation and limited food supply. The area supported an abundant infauna, as evidenced by numerous burrows in the limestone. There was little wave action and very little winnowing of lime mud. Wilson (1975, p. 358) describes this type of environment as an open marine platform having a water depth from a few meters to a few tens of meters. The open marine platform on which the Rowland was deposited covered central Kentucky and extended northward. As shown by the superposition of the Rowland on the Bull Fork Formation (fig. 1), the platform overlapped the southern part of the shelf on which the Bull Fork was deposited.

The Marble Hill Bed was deposited along a narrow band at the northern limit of the shallow Rowland platform. Immediately to the north lay the deeper water of the open marine shelf on which the Bull Fork was being deposited. The well-sorted biosparite and the abraded biosparrudite of the Marble Hill indicate deposition in a high-energy environment capable of extensive reworking. The abundance of sparry calcite cement in an area bounded on the north and south by micritic limestone indicates a narrow zone of high energy levels needed for thorough winnowing of carbonate sands.

The Marble Hill formed as a platform-edge sand where the open shelf, at depths below wave base, shoaled to the shallow depth of the Rowland platform. The impingement of the wave base on this shoal, probably at depths of 5 to 10 m, produced a zone of turbulence in which skeletal material generated by the abundant fauna of the shelf was broken, abraded, and sorted. The environment was one of well-oxygenated water of normal salinity and good circulation, but it probably did not support a plentiful fauna because of the shifting substrate. Gastropods, a major component of the biosparrudite, are typical of organisms indigenous to this environment (Wilson, 1975, p. 358).

The Bardstown Member overlying the Rowland in the study area consists of the same rock types and fauna as the underlying Bull Fork Formation. The Bardstown represents a recurrence of the marine shelf environment that preceded the deposition of the Rowland.

DEPOSITIONAL HISTORY

Prior to the deposition of the Marble Hill Bed, north-central Kentucky was part of a open marine shelf on which the Bull Fork Formation was being deposited. This shelf extended for more than 20 km south of the study area, where it was bordered by a shallower marine platform. The deposition of the Marble Hill was initiated by a shoaling that probably affected all of central Kentucky. As a result of the shoaling, the shallow, restricted-circulation environment of south-central Kentucky extended northward; thus the lagoonal sediments of the basal part of the Rowland were deposited on the southern part of the Bull Fork shelf. The shoaling seems to have been more pronounced in the study area than it was farther east, as is indicated by the extent to which the Rowland overlies the Bull Fork (fig. 1).

Where the wave base impinged on the rising sea floor, an offshore bar formed along a northeast-southwest line and deposited the basal unit of the Marble Hill (fig. 5). The bar commonly rests directly on the Bull Fork and marks the seaward edge of early Rowland deposition. The orientation of the bar suggests a prevailing wave direction from the northwest. Toward the eastern end of the area, the water may have been somewhat deeper, as the bar thinned and formed a line of isolated patches of carbonate sand. No evidence has been found to indicate that the bar followed the margin of the Rowland environment where it swings southeast (fig. 3). No corresponding bar deposits have been reported in the area of Rowland-Bull Fork overlap along the east-

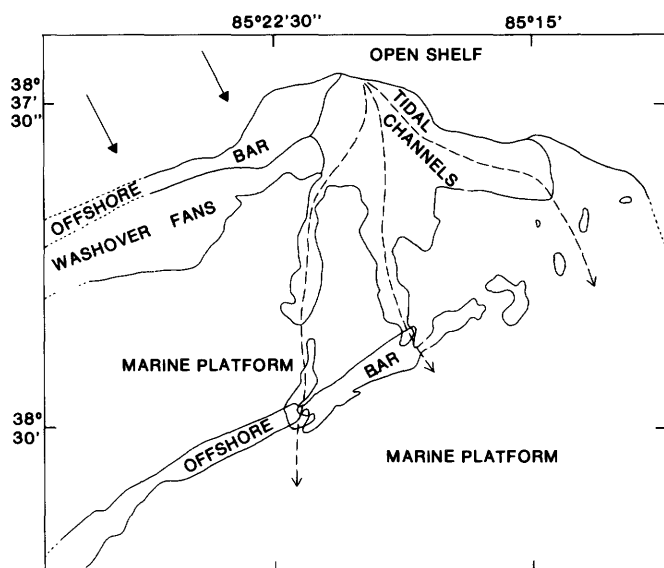


FIGURE 5.—Sketch map of study area showing interpretation of depositional environments. Solid arrows indicate prevailing wave direction on the open shelf. Dashed arrows show inferred path of tidal currents onto the platform. Border between depositional areas dotted where inferred. Area same as figure 3.

ern belt of outcrop (Weir and McDowell, 1976; Weir, 1976).

The deposition of the bar that forms the basal unit of the Marble Hill Bed was followed by an influx of terrigenous clastic sediments that formed a 1- to 2-m mudstone unit on both sides of the bar. This mudstone occurs at the base of the Rowland Member throughout the study area, except at the northern edge and where the basal unit of the Marble Hill is present. Further shallowing accompanying this influx caused the first bar to be abandoned and shifted bar deposition about 10 km seaward. A second bar formed on the basal mudstone unit, parallel to the first bar and flanked by open shelf to the north (fig. 5). This second bar persisted through the remainder of Rowland deposition and formed the main body of the Marble Hill at the north edge of the Rowland Member. Skeletal material carried onto the second bar by incoming waves was reworked in the turbulent zone along the bar and deposited as biosparite and biosparrudite. Gastropods living on the bar contributed large amounts of coarse skeletal material to the biosparrudite. The width of the main bar (fig. 3) indicates that deposition was confined to a narrow zone at the seaward edge of the platform. Deposition of this bar and the laterally equivalent lagoonal sediments generally kept pace with subsidence of the area. A rapid build-up of sediments would have caused the Rowland to

prograde onto the shelf. Conversely, a too slow rate of sedimentation relative to the rate of subsidence would have resulted in an advance of the deeper shelf environment over the outer part of the lagoon.

North of the second bar, interbedded biomicrudite and shale of the Bull Fork Formation were deposited on the shelf. On the shallower platform to the south, partly protected from wave action by this bar, Rowland micrite and interbedded mudstone were deposited in a lagoonal environment. The fine-grained calcite deposited on the platform was probably derived from the disintegration of organisms living in the lagoon and from the fine debris produced by abrasion of skeletal grains on the bar.

Two southward extensions of the main Marble Hill bar occur along its south edge, one along and near the Ohio River within the Rowland Member and the other 1 to 5 km east of the Ohio at the top of the Rowland (fig. 3). These tongues, which consist largely of biosparrudite, may be washover fan deposits formed of material swept over the bar onto the platform during periods of storm (fig. 5).

After the second bar was established, a body of carbonate sand at the east end was spread, probably by tidal currents, to the southeast along the seaward edge of the platform. The presence of corals, brachiopods, and bryozoans in the lagoonal sediment of the Rowland indicates some exchange of water with the open shelf, but the sparseness of the fauna suggests only weak currents that brought in small amounts of food for bottom-dwelling forms. The bar restricted flow from the open shelf to the northwest, so that tidal exchange was concentrated in a channel around the east end of the bar. The southeastward direction of the tidal channel from the end of the bar may have been influenced by the first Marble Hill bar. The abandoned bar probably remained a topographic high that had enough relief to divert the main tidal flow to the east (fig. 5).

Deposition of carbonate sand continued along the tidal channel until the deposit was locally as much as 5 m thick, then this channel was abandoned in favor of channels to the west. The eastern half of the old channel returned to a normal platform environment, and a tongue of Rowland micrite and mudstone was laid down across the channel deposits (fig. 3).

The new path of the tidal flow was still around the east end of the main bar, but there it split into two south-trending channels (fig. 5). Carbonate sand deposited in these channels formed two linear bodies that eventually extended as much as 13 km south of the northern edge of the Marble Hill Bed.

Both these channels are aligned with low spots in the lower Marble Hill bar (fig. 3). These low spots may be the result of scouring by tidal currents, or low spots in the older bar may have controlled the path of the later tidal channels. Tidal channels persisted in this position through the remainder of Rowland deposition. The filling of the channels with biosparite and biosparrudite kept pace with the buildup of lagoonal sediments, as evidenced by the intertonguing and gradational nature of the contacts along the edges of the channels.

In the final stages of deposition of the Rowland Member in the study area, the amount of terrigenous clastic sediments supplied to the seaward part of the platform was reduced. As a result, the upper 1 to 2 m of the Rowland consists of micrite and only minor mudstone interbeds. Deposition of the Rowland and Marble Hill ended with the subsidence of the area that brought a return of the shelf environment and the beginning of the deposition of the Bardstown Member. The sharp basal contact of the Bardstown (Swadley, 1977) suggests that subsidence was rapid. Scattered lenses of carbonate sand occur at the base of the Bardstown south of the study area (Kepferle, 1977; Luft, 1977), but there is no evidence indicating a uniform southward migration of a bar ahead of the advancing shelf.

SUMMARY

The Marble Bed of the Rowland Member of the Drakes Formation is made up of poorly sorted gastropod biosparrudite and well-sorted echinoderm biosparite. It was deposited as a complex of offshore bars, washover fans, and related tidal-channel deposits in a narrow zone at the seaward edge of the shallow marine platform on which interbedded micrite and mudstone of the Rowland Member were deposited. The Bull Fork Formation, which underlies the Rowland and is its lateral equivalent to the north, and the Bardstown Member of the Drakes Formation, which overlies the Rowland, were deposited on an open marine shelf that bordered the Rowland platform. The Marble Hill developed in a high-energy environment, where the wave base impinged on the sea floor between the open shelf and

the shallower surface of the platform. Deposition of the Marble Hill was initiated by an uplift of the area that caused the platform environment of central Kentucky to migrate northward over the southern edge of the open shelf. Deposition was ended by subsidence that brought about a return of the shelf environment.

REFERENCES CITED

- Kepferle, R. C., 1977, Geologic map of the Ballardsville quadrangle, north-central Kentucky: U.S. Geological Survey Geologic Quadrangle Map GQ-1389, scale 1:24,000.
- Luft, S. J., 1977, Geologic map of the Smithfield quadrangle, north-central Kentucky: U.S. Geological Survey Geologic Quadrangle Map GQ-1371, scale 1:24,000.
- Owen, D. D., 1859, Report of a geological reconnaissance of the State of Indiana made in the year 1837, pt. 1: Indianapolis, John C. Walker, 63 p.
- Peck, J. H., 1966, Upper Ordovician formations in the Maysville area: U.S. Geological Survey Bulletin 1244-B, 30 p.
- Peterson, W. L., 1970, Bardstown Member of the Drakes Formation in central Kentucky: U.S. Geological Survey Bulletin 1294-A, p. A36-A41.
- Shaver, R. H., and others, 1970, Compendium of rock-unit stratigraphy in Indiana: Indiana Geological Survey Bulletin 43, 229 p.
- Swadley, W. C., 1977, Geologic map of the Bedford quadrangle, north-central Kentucky: U.S. Geological Survey Geologic Quadrangle Map GQ-1409, scale 1:24,000.
- Swadley, W. C., and Gibbons, A. B., 1976, Geologic map of the Campbellsburg quadrangle, north-central Kentucky: U.S. Geological Survey Geologic Quadrangle Map GQ-1364, scale 1:24,000.
- Weir, G. W., 1976, Geologic map of the Mount Sterling quadrangle, Montgomery County, Kentucky: U.S. Geological Survey Geologic Quadrangle Map GQ-1335, scale 1:24,000.
- Weir, G. W., Greene, R. C., and Simmons, G. C., 1965, Calloway Creek Limestone and Ashlock and Drakes Formations (Upper Ordovician) in south-central Kentucky: U.S. Geological Survey Bulletin 1224-D, 36 p.
- Weir, G. W., and McDowell, R. C., 1976, Geologic map of the Preston quadrangle, Bath and Montgomery Counties, Kentucky: U.S. Geological Survey Geologic Quadrangle Map GQ-1334, scale 1:24,000.
- Weiss, M. P., and Norman, C. E., 1960, The American Upper Ordovician standard II, Development of stratigraphic classification of Ordovician rocks in the Cincinnati region: Ohio Division of Geological Survey, Information Circular no. 26, 14 p.
- Wilson, J. L., 1975, Carbonate facies in geologic history: New York, Springer-Verlag, 471 p.

Paleogene Sedimentary and Volcanogenic Rocks from Adak Island, Central Aleutian Islands, Alaska

By JAMES R. HEIN *and* HUGH McLEAN

SHORTER CONTRIBUTIONS TO STRATIGRAPHY AND
STRUCTURAL GEOLOGY, 1979

GEOLOGICAL SURVEY PROFESSIONAL PAPER 1126-E



CONTENTS

	Page
Abstract	E1
Introduction	1
Acknowledgments	2
Analytical procedures	3
Andrew Lake Formation	3
Stratigraphy and depositional environment	3
Secondary minerals	7
Age	8
Hydrocarbon potential	9
Yakak Peninsula strata (Wedge Point area)	9
Stratigraphy and depositional environment	9
Secondary minerals	10
Age	11
Hydrocarbon potential	11
Finger Bay Volcanics	11
Metamorphism	11
Age	12
Discussion	12
Paleogene sedimentation	12
Source of sediment	12
Depositional basin	13
Alteration of sedimentary rocks	13
Regional tectonics	14
Concluding remarks	14
References cited	15

ILLUSTRATIONS

	Page
FIGURE 1. Map showing location of outcrops of granodiorite plutons on Adak and Kagalaska Islands in the central Aleutian Islands, Alaska	E2
2. Map showing sample locations and topography of Andrew Lake area, northern Adak Island	3
3. Map showing sample locations and topography near Wedge Point, Yakak Peninsula, southwest Adak Island	4
4. Composite stratigraphic sections of Andrew Lake Formation and two sections near Wedge Point	5

TABLES

	Page
TABLE 1. Description of rock samples from the Andrew Lake Formation, Finger Bay Volcanics, and Yakak Peninsula, Adak Island, Alaska	E6
2. Foraminifers from the Andrew Lake Formation	8
3. K-Ar data and age for an andesite sill, Andrew Lake Formation	9
4. Organic geochemistry of Tertiary sedimentary rocks from Adak Island	9

PALEOGENE SEDIMENTARY AND VOLCANOGENIC ROCKS FROM ADAK ISLAND, CENTRAL ALEUTIAN ISLANDS, ALASKA

By JAMES R. HEIN and HUGH McLEAN

ABSTRACT

The Andrew Lake Formation on northern Adak Island, here redefined, consists of conglomerate, sandstone, chert, shale, and pyroclastic ejecta of late Eocene age. These strata were deposited in a marine basin no deeper than 500 meters. Nonmarine to shallow marine volcanoclastic rocks, probably correlative in age with the Andrew Lake Formation, crop out in the Wedge Point area of southwestern Adak Island. The sedimentary rocks contain secondary minerals including chlorite, vermiculite, smectite, analcime, laumontite, clinoptilolite, wairakite, and the rare zeolite yugawaralite. These minerals reflect a complex history of alteration involving burial diagenesis, migration of hydrothermal solutions associated with intrusion of granodiorite plutons, and local thermal metamorphism caused by intrusion of dikes and sills. The late Eocene strata both at Andrew Lake and near Wedge Point overlie the Finger Bay Volcanics, which consists of highly altered interbedded flows and pyroclastic rocks that contain secondary minerals (chlorite, albite, actinolite, muscovite, epidote) characteristic of greenschist-facies metamorphism. The age of the Finger Bay Volcanics is unknown, but because of the contrast in degree of alteration and metamorphism between it and the overlying Andrew Lake Formation, it is believed to be late Paleocene or early Eocene. The late Eocene strata are low in total organic carbon and are therefore not considered a potential source rock for petroleum.

Other workers suggest that subduction of the Kula ridge spreading center beneath the Aleutian arc, 30 million years ago, resulted in an episode of regional greenschist-facies metamorphism throughout the arc. However, absence of metamorphism in the Andrew Lake Formation indicates either that the Kula ridge was subducted at an earlier time (about 50 m.y. ago) or that low-grade regional metamorphism did not accompany the subduction of the spreading center.

INTRODUCTION

Adak Island, part of the Andreanof group of central Aleutian Islands, consists of late Cenozoic stratovolcanoes that overlie uplifted Tertiary volcanic, sedimentary, and plutonic rocks (fig. 1). In general, most of the larger Aleutian islands are characterized by a Late Cretaceous(?) and early Tertiary mafic

volcanic basement overlain by Paleocene volcanic and sedimentary rocks. Commonly, as on Adak Island, lower Tertiary rocks of the Aleutians are intruded by middle Miocene plutonic bodies, mostly granodiorite (Fraser and Snyder, 1959; Marlow and others, 1973; DeLong and others, 1978).

Marine volcanoclastic strata that crop out between Andrew Lake and Clam Lagoon on northern Adak Island (figs. 1 and 2) were mapped by Coats (1956) as part of the Finger Bay Volcanics and were tentatively dated as Paleozoic on the basis of leaflike impressions identified as *Annularia stellata*. Because rocks of unequivocal Paleozoic age were not known from other Aleutian islands, Scholl, Green, and Marlow (1970) re-examined these strata and found that the "*Annularia*" beds are in fact of middle or late Eocene age on the basis of foraminifers, dinoflagellates, and pelecypods. They named the fossiliferous strata the Andrew Lake Formation and reported that it rests depositionally on the Finger Bay Volcanics, which they assumed to be of slightly older Tertiary age.

The Finger Bay Volcanics, defined by Coats (1947), occurs widely on Adak Island and is especially well exposed on southern Adak (Fraser and Snyder, 1959). Fraser and Snyder (1959) found that, in general, the Finger Bay Volcanics consists of pervasively altered pyroclastic deposits and basaltic and andesitic flows. They deduced from dated rocks exposed on nearby Kanaga Island that the volcanic rocks of southern Adak are probably of Tertiary age. They also included bedded pyroclastic rocks, volcanic wacke, and argillite as part of the Finger Bay Volcanics. One of these sedimentary rocks sections is well exposed at Wedge Point on the Yakak Peninsula (figs. 1 and 3).

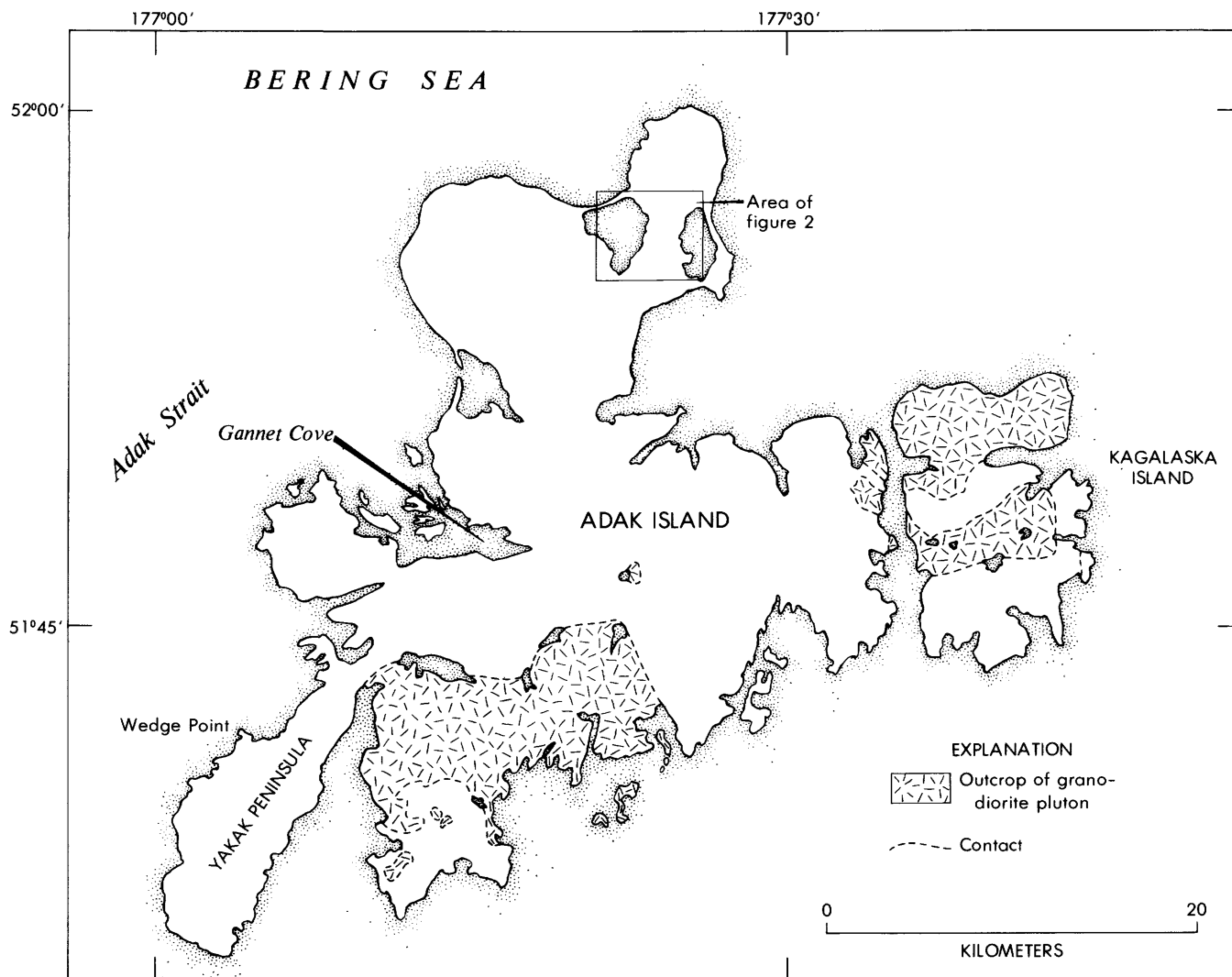


FIGURE 1.—Location of outcrops of granodiorite plutons on Adak and Kagalaska Islands in the central Aleutian Islands. Area of figure 2 is indicated by rectangle, Wedge Point area is shown in figure 3.

Here we present information on the petrology, mineralogy, stratigraphy, and depositional environments of the Andrew Lake Formation and the sedimentary and pyroclastic rocks at and near Wedge Point. We also assess the potential of these rocks as sources of hydrocarbons. We define mineral assemblages formed by hydrothermal processes as distinguished from assemblages developed by regional low-grade metamorphism. We speculate on the significance of the Paleocene history of Adak Island in the regional development of the Aleutian island arc and the early Tertiary plate-tectonic interaction of the Kula ridge with the Aleutian subduction zone.

ACKNOWLEDGMENTS

We thank Capt. T. P. Driver, commanding officer of U.S. Naval Station, Adak, for permission to work on the Naval Station and Comdr. Elton Himes for

providing transportation and logistic support for fieldwork. The U.S. Naval Special Service Corps provided logistic support for our works on Yakak Peninsula. H. N. Meeks of the National Oceanographic and Atmospheric Administration Observatory, Adak, provided a vehicle during part of our work. Paul T. Fuller was our able field assistant. C. E. Gutmacher provided X-ray diffractograms and processed a sample for K-Ar dating; G. B. Dalrymple made the K-Ar age determination. John Barron, Kristin MacDougall, Richard Poore, William Sliter, Fred May, and Louie Marincovich searched, often fruitlessly, for fossils. Kam Leong determined the Fe content of three samples by atomic absorption techniques. A. J. Koch, of Mobil Oil Corp., and George Claypool, U.S. Geological Survey, provided organic geochemical analyses and interpretation. We benefited from review

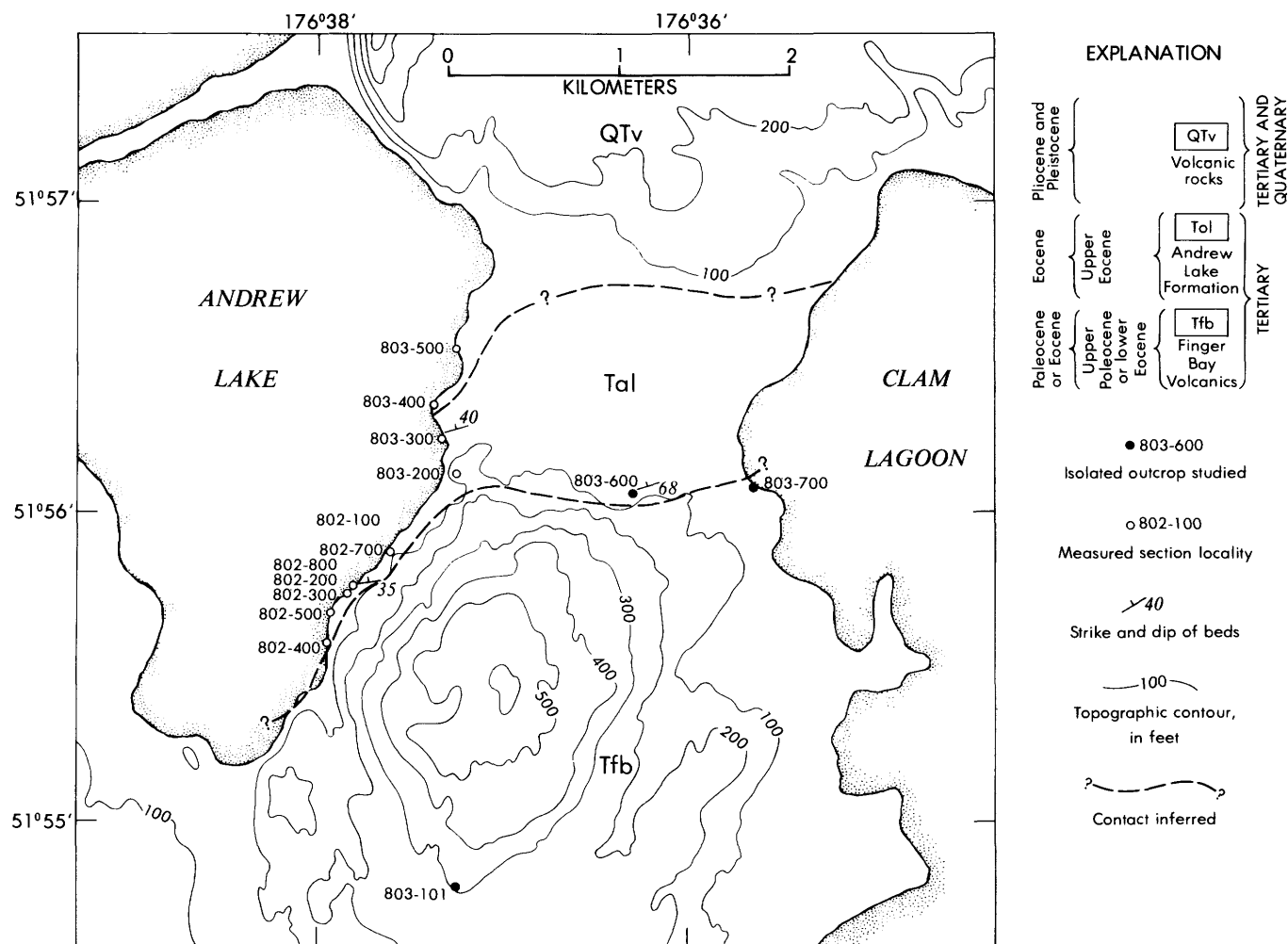


FIGURE 2.—Sample locations and topography of Andrew Lake area, northern Adak Island. (Note that No. 803-600, for example, includes all samples from 600 through 699.) Measured sections are keyed to figure 4. Base from Coats (1956).

by and helpful comments of R. R. Coats, D. W. Scholl, D. A. Swanson, M. S. Marlow, and A. K. Cooper, U.S. Geological Survey; Yotaro Seki, Saitama University, Japan; and A. C. Waters, University of California at Santa Cruz.

ANALYTICAL PROCEDURES

Bulk rock samples and mineral separates were powdered and examined with a Norelco¹ X-ray diffractometer. Most rock samples were cut into thin sections for textural and mineralogical study. Three samples were analyzed for iron content with an atomic absorption spectrophotometer.

ANDREW LAKE FORMATION

Scholl and others (1970) defined and briefly described the Andrew Lake Formation. They suggested

that it is more than 850 m thick, although only about 40 m of section is actually exposed in quarries and low cliffs along the east shore of Andrew Lake (figs. 2 and 4). An additional 30 m of sedimentary and pyroclastic rocks crops out south of the south limit of the Andrew Lake Formation as described by Scholl and others (1970). Although this lower section is only sparsely fossiliferous and its age is a matter of conjecture, we include it as part of the Andrew Lake Formation. Even with the addition of this section, the total thickness of the formation may not be greater than 800 m (fig. 4).

STRATIGRAPHY AND DEPOSITIONAL ENVIRONMENT

A composite stratigraphic section of the Andrew Lake Formation (fig. 4) compiled from outcrops located on figure 2 shows that the lower half of the section consists mainly of volcanoclastic sedimentary rocks. Volcanic sandstone and silty sandstone are most common, but they range from unsorted sandy

¹ Any use of trade names in this publication is for descriptive purposes only and does not constitute endorsement by the U.S. Geological Survey.

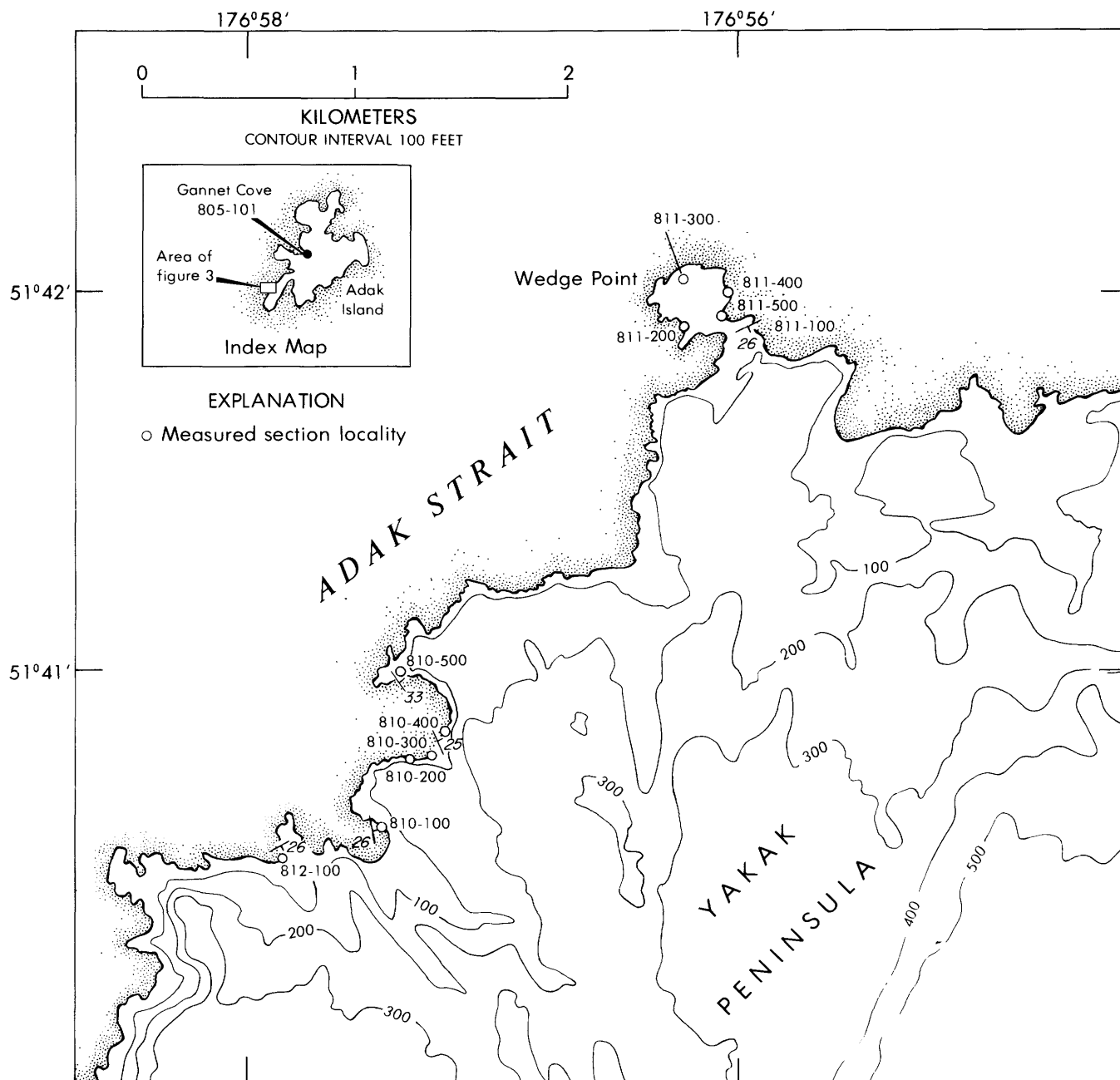


FIGURE 3.—Sample locations and topography near Wedge Point, Yakak Pensinsula, southwest Adak Island. Measured sections are keyed to figure 4. Note location of station 805-101 at Gannet Cove, western Adak Island (inset). Base from Fraser and Snyder (1959).

conglomerate to tuffaceous mudstone. Diatoms are rare in these rocks. Intercalated devitrified ash-fall tuff attests to coeval volcanism. Numerous dikes and sills cut this part of the Andrew Lake Formation. Descriptions of the samples studied are given in table 1, in stratigraphic order.

Overlying this relatively coarse grained clastic section are the only richly fossiliferous lower Tertiary strata known on Adak Island (fig. 4). These

strata mark the lower contact of the Andrew Lake Formation as defined by Scholl and others (1970). In this section are thin devitrified ash-fall tuff beds interbedded with quartz chert, laminated quartz porcelanite, siliceous shale, laminated pyritic shale, calcareous chert, and the first recognized occurrence known to us of bedded quartz chert that contains abundant diatoms.

The stratigraphically highest beds in the Andrew

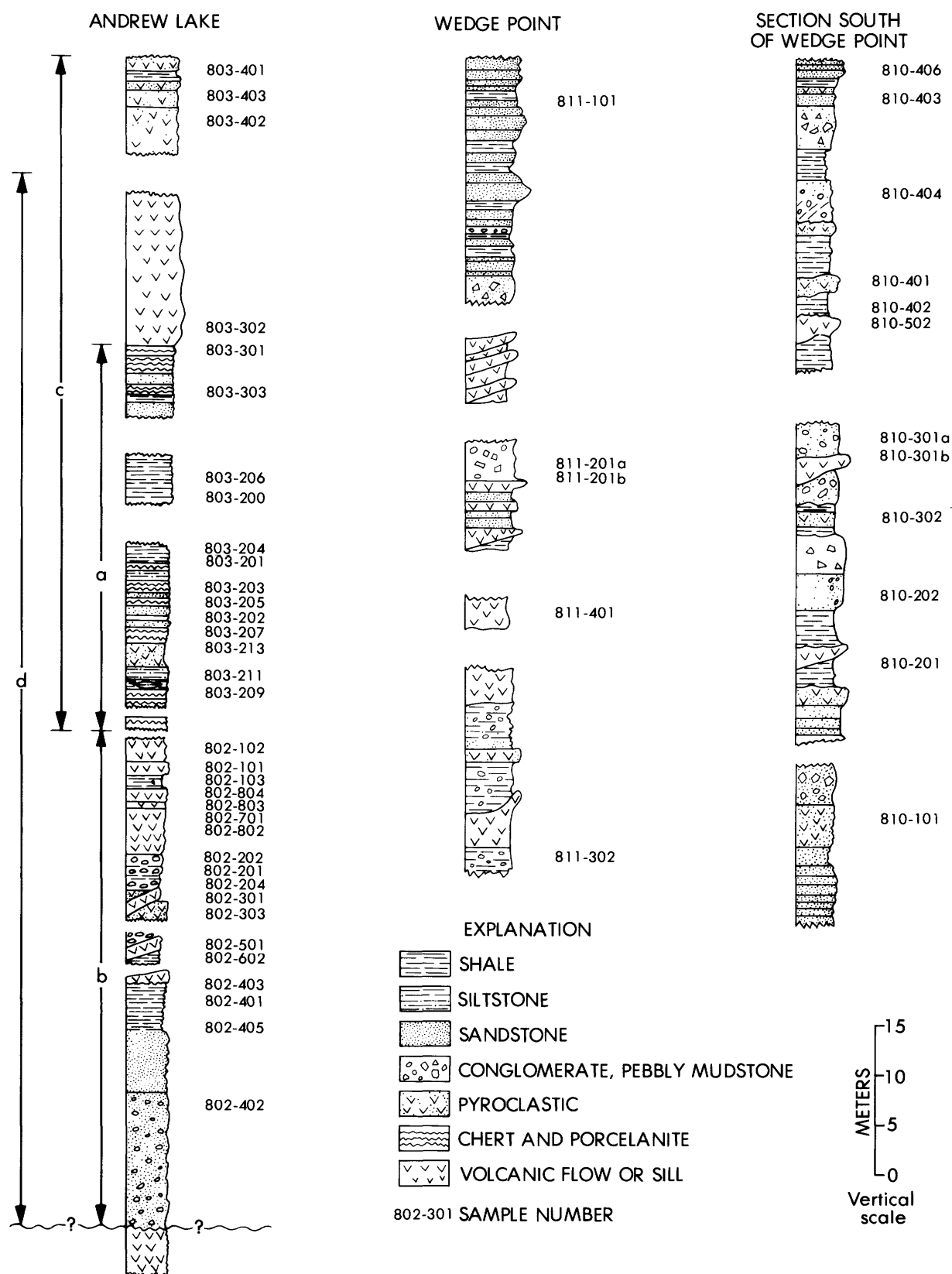


FIGURE 4.—Composite stratigraphic sections of Andrew Lake Formation and two sections near Wedge Point. Sections and sample localities are keyed to figures 2 and 3. Thickness of covered areas (breaks in sections) is unknown. Top part of Andrew Lake section and upper 7 m of Wedge Point section were measured. Queried line marks contact of Andrew Lake Formation with underlying Finger Bay Volcanics. (a) Chert-porcelanite section, (b) section rich with volcanic detritus, (c) Andrew Lake Formation as defined by Scholl and others (1970), and (d) Andrew Lake Formation as redefined.

TABLE 1.—Description of rock samples from the Andrew Lake Formation, Finger Bay Volcanics, and Yakak Peninsula, Adak Island, Alaska

[Locations and formations are keyed to figures 1, 2, and 3. Samples are listed in stratigraphic order starting at the base of the section. A, analcime; Ac, actinolite; Al, albite; Am, amphibole; Au, augite; B, biotite; C, calcite; Ca, chalcidony; Ce, celadonite; Ch, chlorite; Cl, clinoptilolite; Cr, chert; Cz, clinzoisite; E, epidote; F, fossil debris; Fe, iron oxides; H, hypersthene; He, heulandite; Ho, hornblende; I, illite; L, laumontite; M, magnetite; Mn, Mn-dendrites; Mu, muscovite; P, plagioclase; Ph, prehnite; Pr, piemontite; Py, pyroxene; Q, quartz; S, stilpnomelane; Sm, smectite; Sp, sphene; St, stilbite; T, tremolite; V, vermiculite; Vg, altered volcanic glass; VRF, volcanic rock fragments; W, wairakite; Y, yugawaralite; Z, undifferentiated zeolites. Tr., trace. He and St occur only in sample 803 — 701]

Sample No.	Location	Rock type	Major primary constituents	Secondary minerals	Fossils	Comments
802 - 402	Andrew Lake area..	Sandy pebble conglomerate.	VRF, Pr, P, Q, Vg	Al, V, Ch, Q, Fe, L	Diatoms -----	Poorly sorted up to 9 mm.
802 - 405	---do -----	Silty mudstone and fine-grained sandstone.	Q, P, VRF, Pr, Vg	Al, V, Ch, Q, Fe	---do -----	Burrowed, lenses, contorted bedding.
802 - 401	---do -----	Lithic sandstone -----	VRF, P, Vg, Q, I	Q, V-Ch, Ce, Cl, Ch, Fe, Al	Barren -----	
802 - 403	---do -----	Lithic sandstone and siltstone.	VRF, Vg, I, P, Q	Ch, L, Q, Fe, V-Ch, Cl, S	Rare fragments..	Pods of vitric ash, lenses, contorted bedding.
802 - 602	---do -----	Porphyritic dike -----	P, Pr, Q	V-Ch, L, Q, Fe, Al	Not looked for --	
802 - 501	---do -----	Lithic sandstone and sandy and silty mudstone.	VRF, Vg, Pr, Q, P	Q, V-Ch, Ch, L, Al, Fe	Barren -----	Lenses of organic matter, burrowed.
802 - 303	---do -----	Pebble conglomerate and silty mudstone and sandstone.	Vg, VRF, Q, I, Pr	L, V-Ch, Q, Fe	---do -----	Grains compact-penetrated. Conglomerate is well graded. Clasts to 12 mm.
802 - 301	---do -----	Pumiceous ash-fall tuff?.	Vg, P, Pr	L, Q, V, Fe	---do -----	Nearly totally replaced by laumontite.
802 - 204	---do -----	Pebbly sandstone -----	VRF, P, Au, Q, Vg	Q, V, Ch, L, Al, Ph, S, Fe	---do -----	Very poorly sorted clasts to 13 mm.
802 - 201	---do -----	Fine-grained sandstone and silty mudstone.	VRF, P, Q, Pr, Ac, E, C, Ph	Q, V-Sm, L, Al, Fe	---do -----	Sandy layers are poorly sorted and crudely graded.
802 - 202	---do -----	Fine-grained lithic sandstone.	P, VRF, Au, Ac, E, C, Mu	Q, Al, V, Ch, Fe, L	---do -----	
802 - 802	---do -----	Volcanic sill -----	P, Q, Au, H, B	Ch, V	Not looked for --	K-Ar date 14 m.y.
802 - 701	---do -----	Volcanic flow? or sill --	P, Pr, Q, B	Q, V, Ch	---do -----	Pillowlike structures.
802 - 803	---do -----	Altered vitric tuff -----	P, Vg, Q	V, Sm, Q	Barren -----	
802 - 804	---do -----	Volcanic siltstone -----	Q, P, Vg	Q, Z, Ch, V, C, Fe	Fragments -----	Pods of tuff.
802 - 103	---do -----	Tuffaceous mudstone --	Q, P, Vg, Pr, B	Q, C, Ch	Diatoms and radiolarians.	
802 - 101	---do -----	Tuff? -----	P, Vg, Pr, Q	V-Ch, Fe, Al, Q, Ch	Benthic foraminifers.	Completely altered, 14 cm below dike.
802 - 102	---do -----	Volcanic dike -----	P, Pr, Q	V, Ch, Q	Not looked for --	
803 - 209	---do -----	Black chert -----	Q	Q, Tr, Z	Dinoflagellate ---	Much organic debris.
803 - 211	---do -----	Vitric tuff -----	Vg, P	Sm, Cl	Barren -----	Friable.
803 - 213	---do -----	---do -----	Vg, P, Pr	Sm-V, Ce, Fe, Q	---do -----	Do.
803 - 207	---do -----	Chert and porcelanite --	Q, P, I, F	Q, Fe, Ch	See table 2 -----	Late Eocene, upper bathyal.
803 - 202	---do -----	Calcareous chert -----	Q, P, F	Q, C	Diatoms, radiolarians.	
803 - 205	---do -----	Chert and porcelanite --	Q, P, F	Q, Py, Mn	Microfossil molds.	Burrowed, laminated.
803 - 203	---do -----	---do -----	Q, P, F	Q, Py, Mn	---do -----	Laminated.
803 - 201	---do -----	---do -----	Q, P, F	Q, Py, Mn	---do -----	
803 - 204	---do -----	Siliceous shale -----	?	?	Benthic foraminifers.	Cretaceous through Oligocene.
803 - 200	---do -----	Pyritic silty shale -----	Q, P, I, F	Q, C, Py, Ce, V	See table 2 -----	Laminated, late Eocene, upper bathyal.
803 - 206	---do -----	Black silty shale -----	?	?	Barren -----	
803 - 303	---do -----	Diatom chert and siliceous shale with chert nodules.	Q, P, F, Am, VRF	Q, V-Ch, C, Fe	Diatoms, radiolarians, foraminifers.	Vermiculite clay nodules, shale is laminated.
803 - 301	---do -----	---do -----	Q, P, F, VRF	Q, C, V-Ch, Fe	Diatoms, radiolarians, foraminifers, and fish.	Laminated shale, hematite pseudomorphs after pyrite.

Lake Formation described by Scholl and others (1970) include aquagene tuff, ash-fall tuff and possibly ash-flow tuff, and volcanic dikes (fig. 4). These pyroclastic rocks differ texturally and mineralogically (table 1) from strata in the lower part of the formation. Mild alteration of framework grains and traces of sideromelane(?) that has not devitrified contrast with the greater alteration shown by underlying rocks and suggest that this uppermost section

may be younger than the underlying, more altered part of the section. Therefore, both the lower and upper contacts of this formation as originally proposed by Scholl and others (1970) are redefined here.

We redefine the base of the Andrew Lake Formation exposed along the southeast shore of Andrew Lake (fig. 2) to include the conglomerate at locality 802-400 (figs. 2 and 4); the underlying silicified

TABLE 1.—Description of rock samples from the Andrew Lake Formation, Finger Bay Volcanics, and Yakak Peninsula, Adak Island, Alaska—Continued

Sample No.	Location	Rock type	Major primary constituents	Secondary minerals	Fossils	Comments
803 - 302	Andrew Lake area	Volcanic dike	P, Pr	Al, Ch, V	Not looked for	
803 - 403	do	Aquagene tuff	Vg, P, VRF, Pr	Q, W, V, Ce, rare C	do	Unaltered minerals and some glass (?).
803 - 403	do	Ash-flow tuff	Vg, VRF, P, B, Au, Cz	Q, W, Sm, Cl, Ch, C, V	do	Unaltered minerals.
803 - 401	do	Ash-fall tuff	Vg, P, B, Am	Q, Cl, W, V, Sm	Barren	Unaltered minerals and some glass (?).
803 - 601	do	Clayey siltstone	Q, P, F	Ch, V-Ch, Fe, Q	Foraminifers, echinoid.	
803 - 602	do	Lithic sandstone	P, Q, VRF	V-Ch, C, Q, Ch, Al	Barren	Baked by nearby dike.
803 - 604	do	do	P, VRF, Q	V-Ch, C, Q, Ch, Al, Fe	do	Do.
810 - 101	South of Wedge Point.	Welded tuff	Vg, P, Pr	Y, Ch, Ce, Fe, I-Mu, L	do	Purple with green mottling.
810 - 201	do	Volcanic dike	P, Pr, Vg	Vesicles: Q, S-Ce-Ch, L or C; Matrix: Fe, C, Q	Not looked for	
810 - 202	do	Lithic sandstone	VRF, P, Pr	Y, Q, Al, Ch, Fe	Barren	Poorly sorted, compact, grains penetrate.
810 - 302	do	Tuff	?	?	do	
810 - 301a	do	Pebbly mudstone	Vg, P, Au, VRF	Y, Q, Fe, Ch, V, Tr, L, Al	do	Lahar.
810 - 301b	do	Volcanic flow	P, Au	Vesicles: W, S, L; Matrix: Al, Fe, I	Not looked for	
810 - 502	do	Sandy shale	?	?	Barren	
810 - 402	do	do	?	?	do	
810 - 401	do	Ash-flow tuff	Vg, Au, P	I, Ch, V, Ce, C, Fe, Tr, Y, L	Not looked for	Slightly welded.
810 - 404	do	Pebbly mudstone	Vg, P, W	An, Q, Ch, Ce, Y (?)	Barren	Pumiceous lahar.
810 - 403	do	Lithic sandstone	VRF, P, Pr	An, Fe, clays	do	Banded, well sorted, crudely graded.
810 - 406	do	do	VRF, P, Pr, Q	Z, Q, Ch, Fe	do	Poorly sorted, graded.
812 - 104	do	Silicified ash	Vg, P	Q, Ch, Fe, C	Spicules?	
811 - 302	Wedge Point	Pebbly mudstone	?	?	Barren	
811 - 401	do	Volcanic dike	Au, P, Sp, M	Vesicles: Q, Ch+S+Ce, L, Q, Tr, Pr, E; Matrix: Q, L, Al, E, Fe, Ch, I	Not looked for	More than 50 percent altered to quartz and laumontite.
811 - 201a	do	Pebbly mudstone	Vg, P, Pr, M	Q, C, Ch, S, Ce, Fe, A	Barren	Pumiceous.
811 - 201b	do	Volcanic dike	P, Au, M	Vesicles: L, S+Ch+L, Q; Matrix: Q, Fe, Ch	Not looked for	
811 - 101	do	Silty sandstone	Vg, P, M, Au, Q	Q, Fe, Ce, I-Mu, Y, L, A	Barren	Poorly sorted, pumiceous.
811 - 201	do	Volcanic wacke	VRF, P, Pr, Q	Al, Q, Y, Fe, L, Ch	do	
803 - 101	Southeast of Andrew Lake.	Lithic sandstone	P, Q, B, VRF, Ho, Cr	Ac-T, E, Q, Fe, Ch, V	do	Finger Bay Volcanics, compact.
805 - 101	Gannet Cove	Quartzite and epidosite	Q, P, Cg, F, B	E, C, Q, Mu, Fe, Ch, Pi?	Ghosts of microfossils.	Finger Bay Volcanics, poorly sorted.
803 - 701	Clam Lagoon	Hydrothermal vein	W, Ca, V, Cl, He, St	Not looked for	Not looked for	Vein cuts Finger Bay Volcanics.

volcanic rocks are assigned to the Finger Bay Volcanics. The top of the formation is in the area covered by tundra between outcrop localities 803-300 and 803-400 (figs. 2 and 4).

Fossils (table 2) indicate that the strata of the redefined Andrew Lake Formation were deposited in a marine environment, probably at water depths between 200 and 500 m. Sediments were reworked by bottom currents and by infauna. Lenses containing diatoms or devitrified ash are locally abundant; however, laminated porcelanite, black pyritic shale, and laminated shale from the middle part of the section suggest that the depositional basin was for a time "starved" or cut off from active terrigenous sedimentation. Consequently, mainly biogenic material accumulated, although an active infauna was not present.

Other sedimentary structures and current-direction indicators are rare. They include ripple lamina-

tions and poorly developed graded bedding. Sandstone beds are graded and have flute casts, and sandstone and shale sequences are rhythmically bedded, which suggests deposition by turbidity currents. Rare crossbedding indicates eastward current flow. Deposition of most of the Andrew Lake Formation is ascribed to a combination of biogenic-pelagic, turbidity-current, hemipelagic, and pyroclastic processes.

SECONDARY MINERALS

Most rocks of the Andrew Lake Formation are silicified and in part altered to clay minerals and iron oxides (table 1). In most samples, plagioclase of intermediate anorthite content is partly altered to albite. In the lower part of the section where volcanogenic sedimentary rocks, pyroclastic debris, and volcanic dikes and sills are abundant, quartz and

TABLE 2.—Foraminifers from the Andrew Lake Formation

[Fossils identified by Kristin McDougall, R. Z. Poore, and W. V. Sliter]

Sample No.	Benthic forams	Other microfossils	Age range	Depth of water
802-101	<i>Bathysiphon</i> sp. -----	-----	Indeterminate ---	
803-200	<i>Cyclammina pacifica</i> ? -----	Echinoid spines -----	Late Eocene -----	Upper bathyal.
	<i>Cyclammina</i> sp. -----	Radiolarians -----		
	<i>Dentalina</i> sp. -----			
	<i>Eponides</i> sp. -----			
	<i>Gyroidina soldanii</i> d'Orbigny -----			
	<i>Lenticulina</i> sp. -----			
	<i>Valvulineria</i> sp.? -----			
803-207	<i>Bathysiphon eocenicus</i> -----	Echinoid spines -----	Late Eocene -----	Upper bathyal.
	<i>Bathysiphon</i> sp. -----	Fish debris -----		
	<i>Cyclammina pacifica</i> Beck -----	Radiolarians -----		
	<i>Dentalina</i> sp. -----			
	<i>Eponides</i> sp. -----			
	<i>Gyroidina soldanii</i> d'Orbigny -----			
	<i>Lenticulina</i> sp. -----			
	<i>Melonis umbilicatus</i> (Montague) -----			
803-601	<i>Cyclammina</i> sp. -----	Echinoid spines -----	Intermediate -----	
803-204	<i>Bathysiphon eocenicus</i> ? -----		Cretaceous	
	<i>Rhabdammina eocenica</i> ? -----		through	
			Oligocene.	

laumontite occur as interstitial cement and replace volcanic debris along with vermiculite, chlorite, smectite² and vermiculite-chlorite (randomly inter-layered). Some volcanic rock fragments are almost completely altered to iron oxides and clays. Locally calcite, analcime, clinoptilolite, and stilpnomelane replace volcanic debris.

Three samples (802-202, -201, -204 in fig. 4) from the upper part of this section rich in volcanic detritus contain abundant actinolite, epidote, chlorite, and calcite. These minerals, commonly found in greenschist-facies metamorphic rocks, occur as detrital minerals in these three samples (table 1). Adjacent to dikes and sills, however, secondary prehnite and epidote have formed (for example, prehnite in sample 802-204, table 1).

Because minerologically unstable volcanic debris is less abundant, fewer secondary minerals characterize the chert-porcelanite part of the section. Quartz and minor calcite and pyrite are the most important secondary minerals. Quartz indiscriminately replaces most sediment components and fills all available void space; thus abundant siliceous shale and porcelanite are produced. Calcite replaces quartz and is therefore a relatively late stage mineral.

Ash-fall tuff in the Andrew Lake Formation has altered to smectite and minor clinoptilolite. In places smectite was subsequently converted to vermiculite.

Locally vermiculite, chlorite, hematite, and celadonite replace volcanic detritus (table 1).

Pyroclastic rocks that overlie the Andrew Lake Formation as redefined herein contain unaltered framework grains, but most of the glassy volcanic material is replaced by wairakite and to a lesser extent by clinoptilolite, quartz, and celadonite. Vermiculite, smectite, chlorite, and iron oxides are present; calcite is rare (table 1). Plagioclase is of intermediate composition. Celadonite in this part of the section is blue, whereas lower in the section it is green.

Secondary mineral assemblages or mineral facies in the stratigraphic section can indicate the history of burial metamorphism of the rocks. Accordingly, quartz, vermiculite, vermiculite-chlorite, smectite, chlorite, iron oxides, and celadonite are ubiquitous. Clinoptilolite is present in places but is most common at the top. Stilpnomelane and laumontite are in the lower part; wairakite occurs near the top of the section. Calcite and pyrite are mainly at midsection (table 1).

AGE

The Andrew Lake Formation was assigned a middle or late Eocene age by Scholl and others (1970) on the basis of microfossils and megafossils. Our collections of benthic foraminifers (table 2) indicate that the Andrew Lake Formation was deposited during the late Eocene, virtually identical to the foraminiferal age assigned in Scholl and others

² Smectite is the internationally accepted group name for the clay minerals that include montmorillonite, nontronite, and saponite (Brindley and Pedro, 1975). It is used as a general term.

TABLE 3.—K-Ar data and age for an andesite sill, Andrew Lake Formation

[Potassium measurements by A. Berry; argon measurement and age calculation by A. Berry and E. Sims]

Sample No.	Mineral	Percent K ₂ O	⁴⁰ Ar _{rad} (moles/g)	⁴⁰ Ar _{rad} / ⁴⁰ Ar _{total}	Calculated age (millions of years)
802 - 802	Plagioclase	0.079	1.640×10^{-12}	0.04	14.4 ± 3.5

⁴⁰K decay constants: $\lambda_e = 0.572 \times 10^{-10}/\text{yr.}$, $\lambda_{\beta'} = 8.73 \times 10^{-13}/\text{yr.}$, $\lambda_{\beta} = 4.905 \times 10^{-10}/\text{yr.}$ Abundance ratio ⁴⁰K/K = 1.167×10^{-4} percent atomic.

(1970). According to Berggren (1972), late Eocene represents an absolute age of 37.5 to 43.0 m.y.

A K-Ar date on fresh plagioclase from an andesite sill cutting the Andrew Lake Formation was 14.4 ± 3.5 m.y. (table 3).

We speculate that the pyroclastic rocks that overlie the Andrew Lake Formation as redefined, but included in the formation by Scholl and others (1970), are part of a younger series of volcanic rocks. These strata are structurally concordant with the lower part of the formation, but the unaltered framework grains and only mild alteration of glass shards differ markedly from the relatively high degree of alteration of samples from only slightly lower stratigraphically. Similar mild alteration is typical of other Neogene volcanic rocks on Adak; for example, the sill (802-802) cutting the Andrew Lake Formation dated by the K-Ar method as middle Miocene (table 3). Perhaps these little-altered pyroclastic rocks are associated with the intrusion of Miocene granodiorite plutons and related dikes and pyroclastic deposits (Fraser and Snyder, 1959). However, eruption of the pyroclastic rocks at any time after the Eocene cannot be ruled out.

HYDROCARBON POTENTIAL

Two samples of shaly siltstone were analyzed for TOC (total organic carbon), EOM (chloroform extractable bitumen), and R_o (vitrinite reflectance). These quantities, as well as EOM/TOC, are listed in table 4. Sample 803-204 (fig. 4 and tables 1 and 4) contains 0.41 weight percent of TOC, the highest value recorded for any rocks on Adak Island. This value, however, is still below the 0.50 weight percent quantity generally considered to separate a possible source rock from one with no source-rock potential. The R_o value of 2.1+ indicates that sample 802-804 has been heated well beyond the level of crude oil stability (A. J. Koch, written commun., 1976). A low EOM/TOC ratio can be interpreted as resulting from the "cracking" of organic material; the break-up of organic compounds probably resulted from the

TABLE 4.—Organic geochemistry of Tertiary sedimentary rocks from Adak Island

[Analyses of total organic carbon (TOC) by U. S. Geol. Survey Organic Geochemistry Laboratory, Lakewood, Colo. Analyses of chloroform extractable bitumen (EOM), vitrinite reflectance (R_o), and EOM/TOC by Mobil Oil Corp., Dallas, Tex.]

Sample No.	Location	TOC (weight percent)	EOM (ppm)	R_o	EOM/ TOC (percent)
803 - 204	Andrew Lake	0.41	28.6	2.1+	0.70
803 - 206	--do -----	.04	28.7	*	7.10
810 - 302	Wedge Point	.05	44.3	*	8.90
810 - 402	--do -----	.09	40.2	*	4.50
810 - 502	--do -----	.07	29.3	*	4.20
811 - 302	--do -----	.04	26.4	*	6.60

* Insufficient organic carbon for vitrinite reflectance measurement.

heat produced by nearby intrusions such as the numerous dikes and sills observed in outcrop.

Sample 803-206 has a very low TOC content, but the EOM/TOC ratio indicates that it has not been subjected to excessive heat. A low TOC content means that there probably never was a significant quantity of organic material present. Attempts to recover organic residue for measurement of R_o were unsuccessful.

YAKAK PENINSULA STRATA (WEDGE POINT AREA)

Fraser and Snyder (1959) mapped a section of sedimentary, volcanic, and volcanoclastic strata on the west side of Yakak Peninsula (fig. 3) as part of the Finger Bay Volcanics. On the basis of lithologic composition, degree of alteration and induration, and the types of secondary minerals present (see below), we propose that these strata are temporally equivalent to the Andrew Lake Formation. Study of the mineralogy and petrology of samples from two stratigraphic sections, one immediately south of and one at Wedge Point (fig. 3), complements the reconnaissance work done by Fraser and Snyder.

STRATIGRAPHY AND DEPOSITIONAL ENVIRONMENT

The section south of Wedge Point (figs. 3 and 4) consists predominantly of interbedded sandstone, shale, and pebbly mudstone, with minor ash-flow and ash-fall tuff (including slightly welded tuff); volcanic dikes cut the section. Sandstone beds are primarily lithic arenite but include lithic to feldspathic arenite and wacke. Virtually all lithic grains are volcanic rock fragments, generally subrounded. Plagioclase, pyroxene, and locally quartz are other common framework grains. Poorly sorted rocks abound, but graded, layered, and well-sorted beds occur near the top of the section. Sandstone is com-

monly cemented by laumontite, yugawaralite,³ iron oxides, or clays.

Pebbly mudstone beds contain mostly subangular grains, although a complete range of grain roundness is present. Again, the framework grains are dominantly volcanic rock fragments and, in some samples, are primarily pumiceous. These poorly sorted rocks are texturally like mudflows and are probably lahars. The mudflow units are as much as several tens of meters thick, and they include rock fragments up to 1 m in diameter.

Ash-flow tuff is purplish to gray, commonly with a green mottled surface reflecting replaced volcanic glass globules (replaced collapsed pumice lapilli?). Texturally, it appears massive to weakly flow banded. Sample 810-101 (figs. 3 and 4; table 1) is mostly glass globules and flattened pumice fragments (greater than 3 mm) replaced by yugawaralite. Sample 810-401 has pumice with an elongation ratio of 20:1. Large plagioclase and augite glomerocrysts (Carlisle, 1963, p. 58) are present. The groundmass appears to be collapsed pumice and glass shards replaced by illite or muscovite.

The section includes many porphyritic volcanic dikes altered to zeolites, quartz, and iron oxides. Vesicles and amygdules are filled with zeolites, quartz, and clays. Phenocrysts are mostly plagioclase, partly or wholly altered to albite, and pyroxene that is locally fresh.

The section at Wedge Point (figs. 3 and 4) is similar to the one to the south just described but is capped by 7 m of alternating sandstone (volcanic wacke) and shale; two pebbly sandstone beds occur in this section. Wacke makes up 93 percent of this 7-m section and consists of beds 3 to 130 cm thick (average 47 cm), whereas the 7 percent of shale consists of beds 2 to 12 cm thick (average 5.4 cm). In general, beds increase in thickness up section. Framework grains are mostly volcanic fragments, plagioclase, pyroxene, and altered volcanic glass. Samples rich in relict volcanic glass also contain abundant zeolites. The matrix is made up mostly of clays, iron oxides, and fine-grained counterparts of framework grains.

Relative to the section south of Wedge Point, intrusive bodies at Wedge Point are more highly altered. From 50 to 75 percent of the host volcanic rock may be altered to zeolites, quartz, and clays.

The presence of ash-flow tuff and boulder lahars and the apparent absence of microfossils suggest

that the rocks at Wedge Point were deposited in a subaerial to shallow marine environment and that volcanism was active near the site of deposition. Fiske (1963) and Fiske and Matsuda (1964) have demonstrated that submarine ash-flow tuff is not welded. Rocks at Wedge Point must therefore be, in part, subaerial deposits. Further, the presence of graded lithic arenite and sequences of alternating lithic wacke and shale suggest turbidity-current deposition; if so, Wedge Point rocks are in part subaqueous deposits (probably shallow marine). No freshwater fossils or lacustrine deposits were found at Wedge Point.

SECONDARY MINERALS

Porphyritic basaltic and andesitic rock fragments are altered to iron oxides (mostly hematite) and clay minerals (dominantly chlorite and illite). Plagioclase is altered to albite that has approximately parallel extinction and little or no relict zoning. In contrast, clinopyroxene is commonly unaltered. Much pumice is replaced by vermiculite and chlorite. Other glassy volcanic fragments are replaced dominantly by zeolites such as yugawaralite, analcime, and laumontite, and to a lesser extent by quartz, illite, chlorite, celadonite, hematite, vermiculite, and smectite. The rare zeolite, yugawaralite, is the most common zeolite in these rocks on Yakak Peninsula.

Sandstone is cemented by analcime, yugawaralite, laumontite, chlorite, illite, and hematite. Thin (0.005-0.1 millimeter) clay films coat all grains in some beds of arenite. The framework grains are compact and penetrate adjacent grains, and the remaining pore spaces (commonly very small, maximum 0.4 mm² in cross section between grains) are filled with a zeolite such as analcime in sample 810-403 (figs. 3 and 4; table 1). These observations mean that the grains acquired their clay rim after deposition and were subsequently compacted (probably by deep burial) before cementation by zeolite. The zeolite cement is a relatively late occurrence. Galloway (1974) suggested that these diagenetic changes could occur after 300 to 1200 m of burial. He showed that the surface coatings of authigenic clay were the result of mobilization of silica and aluminum from the volcanic debris.

The groundmass of dikes and sills is replaced by quartz, laumontite, analcime, stilpnomelane, albite, iron oxides, chlorite, illite, and calcite; calcite is the latest mineral. Minerals found in vesicles and amygdules suggest the following paragenetic sequence: quartz (occasionally replaced by laumontite), granular material (unidentifiable), analcime, phyl-

³ Yugawaralite, a rare calcium zeolite, has been reported from only one other locality in North America, near Fairbanks, Alaska (Eberlein and others, 1971). It has also been reported from Heinabergsjökull, Iceland (Barrer and Marshall, 1965) and from Japan (Sakurai and Hayashi, 1952; Seki and Okumura, 1968; Sameshima, 1969; Seki and others, 1969).

losilicates (stilpnomelane, chloride, celadonite, rarely vermiculite or hematite), laumontite, phyllosilicates again (minor), and rarely quartz, calcite, pyrite, or epidote. The filling of an amygdale may begin any place in this sequence, and four or five different minerals may occur in one amygdale. The granular material listed above is a very fine grained, high-relief, highly birefringent mineral that may be calcite or epidote. It occurs as a thin and at places discontinuous band separating the first and second minerals formed in the vesicles. Laumontite and terminated quartz crystals more than 2 cm long suggest that these minerals formed from hydrothermal solutions.

AGE

No fossils were recovered from the strata on Yakak Peninsula. From the lithologic composition, and degree of alteration and induration, we infer that these strata are probably temporal equivalents of the Andrew Lake Formation.

HYDROCARBON POTENTIAL

Four samples from the Wedge Point area (table 4) show consistently low values of total organic carbon and are not considered to be potential source rocks for petroleum. No organic residue for determination of vitrinite reflectance was removed from any of these samples.

FINGER BAY VOLCANICS

Coats (1956) and Fraser and Snyder (1959) described the Finger Bay Volcanics as pervasively altered to chlorite, albite, epidote, and silica. We examined two samples (803-101 and 805-101) of sandstone from the Finger Bay Volcanics (fig. 2; fig. 3, inset) for comparison with sedimentary rocks of the Andrew Lake Formation and of Yakak Peninsula.

Sample 803-101, collected from a quarry southeast of Andrew Lake, is a compact, poorly sorted feldspathic arenite. The main framework grain is plagioclase with accessory quartz, biotite, volcanic rock fragments, and chert. Silica and less abundant clays cement the rock. Abundant epidote, quartz, and actinolite-tremolite replace pyroxene(?) and feldspar grains and fill veins (table 1). Plagioclase is altered to albite. Chlorite, vermiculite, and hematite are less abundant secondary minerals.

Quartz sandstone, quartzite, and minor epidosite are found at Gannet Cove on the west coast of Adak Island (sample 805-101, fig. 3, inset). Quartz, epidote, and muscovite are secondary minerals that now

compose the bulk of the rocks. Piemontite, calcite, chlorite, iron oxides, and illite are minor secondary minerals. Granular quartz and deeply corroded and replaced plagioclase are probably the only primary grains remaining. Faint structures are reminiscent of glass shards, collapsed pumice, and microfossils. Rare chlorite spherulites occur. Although the Finger Bay Volcanics is highly altered, it is not penetratively deformed. Open folds with dips generally less than 40° occur (Fraser and Snyder, 1959).

METAMORPHISM

Secondary mineral assemblages (Fraser and Snyder, 1959) suggest that the Finger Bay Volcanics was subjected to regional greenschist-facies metamorphism. The diagnostic mineral assemblages range from actinolite- or tremolite-epidote-chlorite-albite-quartz to epidote-quartz-muscovite-chlorite-albite (table 1). Prehnite and pumpellyite mineral assemblages, indicative of lower temperature grades than actinolite-greenschist facies (Coombs, 1953; Seki, 1969, Coombs and others, 1970), appear in the Finger Bay Volcanics (Fraser and Snyder, 1959), although the reconnaissance nature of the work by Fraser and Snyder precludes delineation of a coherent regional pattern of metamorphic facies. Certainly, the actinolite and epidote greenschist assemblages appear to be dominant on Adak Island.

It is not clear whether emplacement of granodiorite plutons contributed significantly to metamorphism (contact metamorphism) of the Finger Bay Volcanics or whether metamorphism was dominated by a regional thermal event. Fraser and Snyder (1959) described only a thin zone of contact-metamorphic hornfels adjacent to the plutons. It is worth noting, however, that although some outcrops of the Finger Bay Volcanics and the Andrew Lake Formation are equidistant from exposed plutonic rocks, these formations show significant differences in metamorphic mineral assemblages. More fieldwork is needed to fully distinguish regional patterns from contact metamorphism.

In contrast to the Finger Bay Volcanics, sedimentary and pyroclastic rocks on Yakak Peninsula and the Andrew Lake Formation at Andrew Lake have not been subjected to greenschist- or even zeolite-facies regional metamorphism. These rocks have been moderately altered by low-temperature supergene and hydrothermal processes of the zeolite facies and nowhere show greenschist-facies metamorphism. Thermal metamorphism associated with emplacement of dikes and sills, together with the supergene

and hypogene mineralization, has created a complex milieu of secondary minerals.

AGE

Except for sedimentary rocks of the Andrew Lake Formation, Paleogene rocks of Adak Island are apparently devoid of fossils. Fossil findings indicate that the Andrew Lake Formation accumulated during the late Eocene (37.5–43 m.y. ago; Scholl and others, 1970; table 2). The Finger Bay Volcanics is estimated to be as old as the initial formation of the Aleutian ridge and no younger than the overlying Andrew Lake Formation. The Finger Bay Volcanics therefore formed sometime before the late Eocene (before about 40 m.y. ago) but probably after latest Cretaceous (about 65 m.y. ago) (Marlow and others, 1973; Scholl and others, 1975). The Finger Bay Volcanics and associated sedimentary rocks evolved through a sequence of deposition, burial, regional greenschist-facies metamorphism, uplift, and erosion before the Andrew Lake Formation was deposited. We therefore favor an age representative of the older part of this (40–65 m.y.) timespan, perhaps late Paleocene or early Eocene (about 50 m.y. ago), but rocks may be as old as early Paleocene (60 m.y.). Certainly the episode of regional metamorphism must have ended at least 45 m.y. ago. Unfortunately, it may not be possible to obtain reliable radiometric dates from the Finger Bay Volcanics because of the thermal effects associated with the intrusion of plutonic rocks. The granodiorite on adjacent Kagalaska Island is Miocene (dated as 13.2 and 13.7 m.y.; Marlow and others, 1973; DeLong and others, 1978), approximately the same age as an andesite sill (table 3) cutting the Andrew Lake Formation, and is probably the same age as plutons on Adak.

Available published data (Fraser and Barnett, 1959; Powers and others, 1960; Lewis and others, 1960; Carr and others, 1970 and 1971; Gates and others, 1971) suggest that the oldest exposed rocks on the western Aleutian Islands (Attu, Agattu, Shemya, Amchitka, Rat, Amatignak, Ulak, Tanaga, Kanaga) have undergone variable but mild alteration. Variability of alteration, presence of fresh calcic plagioclase, only weakly altered volcanic glass, and the occurrence of a variety of temperature-sensitive zeolites argue against regional greenschist-facies metamorphisms of the exposed rocks on these islands. Accordingly, the Finger Bay Volcanics on Adak Island appears to be unique among the rocks that crop out on the western Aleutian Islands and may represent the oldest rocks described to date

from these areas. Alternatively, the basement rocks of other Aleutian islands may be the same age as, but were not as deeply buried as the Finger Bay Volcanics on Adak Island.

DISCUSSION

PALEOGENE SEDIMENTATION

Fraser and Snyder (1959) estimated that the exposed section of the Finger Bay Volcanics includes about 70 percent pyroclastic, 20 percent flow, and 10 percent sedimentary rocks and that most of this 2400-m-thick section was deposited in a marine environment. We infer that this occurred in the late Paleocene or early Eocene. Coats (1956) provided evidence for a minimum thickness of about 600 m and speculated that the maximum is 4600 m. These observations suggest that the Finger Bay Volcanics is part of the initial series rocks, the Aleutian ridge basement complex (See Jake and White, 1969; Mitchell and Bell, 1973; Marlow and others, 1973.)

SOURCE OF SEDIMENT

The Finger Bay Volcanics was deposited and metamorphosed before deposition of the next recognizably younger strata, the Andrew Lake Formation. Probably by middle Eocene time, the growing Aleutian ridge had nearly reached sea level, and subaerial volcanoes contributed debris to surrounding basins. At times, the Finger Bay Volcanics may have contributed sediment to the Andrew Lake Formation, as clasts in some samples (samples 802–201, 802–202, table 1) are lithologically similar, but the overall amount of sediment derived from the Finger Bay Volcanics appears to be relatively small. The main source of Andrew Lake detritus was most likely contemporaneous volcanism. The host volcanic centers were eventually deeply eroded and perhaps in part covered by younger debris.

Because hydrothermal silicification of the Andrew Lake Formation was intense, it is difficult to identify the origin of the silica in the chert beds. It is not clear whether the silica in the chert-porcelanite section of the Andrew Lake Formation is released by the dissolution of siliceous biogenic debris, deposition from hydrothermal solutions, or both. Diatoms and minor radiolarians from the quartz chert occur in all states of preservation, from ghosts to specimens that retain frustule ornamentation. This suggests that at least part of the silica was derived from dissolution of siliceous microfossils. The calcite in this section is probably redeposited carbonate

released when foraminifers were replaced by quartz.

DEPOSITIONAL BASIN

The dimensions of the depositional basin of the Andrew Lake Formation are not known. Scholl and others (1970) speculated that the Andrew Lake strata accumulated in a fairly deep (500 m) basin along an early Tertiary Aleutian ridge. If the Yakak Peninsula strata (Wedge Point) are temporally equivalent to the Andrew Lake Formation, then they possibly represent the subaerial and shallow-marine facies of the deeper water Andrew Lake strata. The basin seems to have been no deeper than 500 m (fossils suggest 200–500 m), a situation very much like the present Aleutian Islands and the adjacent 200-m-deep Aleutian ridge platform. We infer that these rocks were deposited on the subaerial flanks of a volcanic complex and in adjacent offshore shelf and slope environments. The presence of a small enclosed basin, one isolated from turbidity-current deposition, is evident in the laminated chert and porcelanite of the Andrew Lake Formation.

ALTERATION OF SEDIMENTARY ROCKS

Burial diagenesis, local thermal metamorphism by dikes and sills, and hydrothermal activity contributed to the alteration of Eocene rocks. Burial diagenesis was an important process in the early stages of alteration of these rocks, primarily because they contain a large fraction of unstable mafic to intermediate volcanic rock fragments. Burial caused the transformation of the glassy parts of volcanic rock fragments to clays. These structurally weak rock fragments, upon further burial, decomposed to form a sedimentary rock consisting of framework grains of plagioclase, pyroxene, and rock fragments in a clay matrix. All the original glass shards and glass globules were altered or replaced during burial.

After uplift and some erosion, two additional stages of alteration strongly affected the character of the sedimentary rocks:

1. Numerous late Tertiary dikes and sills intruded and thermally metamorphosed adjacent wall-rock. Sedimentary rocks adjacent to dikes were baked, and locally epidote and prehnite formed. More commonly chlorite, hematite, quartz, and vermiculite mixed-layer clay phases formed next to dikes.
2. A more significant episode of alteration occurred in conjunction with the intrusion of Miocene plutonic rocks, when extensive formation of zeolites occurred.

Many observations favor hydrothermal fluids rather than zeolite-grade regional or burial metamorphism as the mechanism of alteration of the Andrew Lake and the Yakak Peninsula rocks:

1. At Andrew Lake, wairakite, the highest temperature zeolite, stratigraphically overlies laumontite and clinoptilolite, minerals characteristic of a relatively lower temperature metamorphic facies (Coombs, 1961; Harada, 1969; Seki and others, 1969).
2. Nonequilibrium mineral assemblages are common; for example, smectite is associated with laumontite. Low-temperature zeolites occur in close association with higher-temperature forms; for example, laumontite, clinoptilolite, and wairakite at Andrew Lake and laumontite, analcime, and yugawaralite at Wedge Point. (See Coombs and others, 1959; Seki, 1969; Kossovskaya, 1975.)
3. There is no apparent stratigraphic or spatial variation in the metamorphic grade of zeolites. The distribution of zeolites does not show zonal relations.
4. A wide variety of secondary minerals is associated with the zeolites.
5. Calcium zeolites (yugawaralite, laumontite, and wairakite) greatly predominate over sodium varieties (analcime; Kossovskaya, 1975).
6. Some crystals of quartz and laumontite are more than 2 cm long.

Less diagnostic but supporting evidence is that (1) ubiquitous quartz silicification suggests deposition from circulating hydrothermal fluids (Fournier, 1973; Coombs, and others, 1959), (2) mixed-layer clays, for example vermiculite-smectite-chlorite in our samples, commonly form in hydrothermal deposits (Bundy and Murray, 1959; Lovering and Shepard, 1960; Heystek, 1963; Steiner, 1968), (3) secondary mineral assemblages (except in the biogenic chert-porcelanite section) are independent of original rock type (Sigvaldason and White, 1961), and (4) reported occurrences of yugawaralite (and at most locations, wairakite) are from geothermal areas (Sakurai and Hayashi, 1952; Barrer and Marshall, 1965; Harada and others, 1969).

Hydrothermal solutions associated with emplacement of plutons and with the contemporaneous volcanic activity apparently permeated the Paleocene rocks and sealed any available pore space by deposition of secondary minerals. Rocks close to the main thoroughfares of circulating fluids were 50–75 percent replaced. Deposition of secondary minerals in

vesicles probably resulted from several different passes of hydrothermal solutions during which time the temperature decreased and the chemistry of fluids changed. Analysis for iron yielded 3.8, 5.6, and 6.8 weight percent Fe for samples 810-201, 810-301, and 811-201b, respectively, values that are similar to those found for mafic and intermediate volcanic rocks (Turner and Verhoogen, 1960). Circulating fluids apparently did not add much iron to the system; rather, the iron in the volcanic rocks was mobilized to form iron oxides and hydroxides, chlorite, celadonite, and stilpnomelane. Alteration of plagioclase and ferromagnesian minerals and ions from the circulating hydrothermal solutions provided abundant calcium for formation of laumontite, yugawaralite, wairakite, and minor calcite. Solutions were silica saturated with respect to quartz. Eberlein and others (1971) stated that the conditions for yugawaralite formation include low fluid pressure, 200-300°C, and alkaline solutions with silica saturated with respect to quartz.

REGIONAL TECTONICS

In recent years, there has been much speculation about what effect the subduction of an active oceanic ridge (spreading center) has on an island-arc complex (for example, Atwater, 1970; Grow and Atwater, 1970; Uyeda and Miyashiro, 1974; DeLong and Fox, 1977; DeLong and others, 1978). It has been proposed by some workers (Atwater, 1970; Hayes and Pitman, 1970; Marlow and others, 1973; among others) that subduction of a ridge will terminate ridge spreading. Uyeda and Miyashiro (1974) believed that spreading can continue long after subduction of the spreading center. They also suggested that widespread volcanism accompanies subduction of ridges. Grow and Atwater (1970) equated middle and late Tertiary orogeny in the Aleutian Islands and Alaska to subduction of the Kula ridge beneath the Aleutian-Alaskan part of the North American plate. DeLong and others (1978) speculated that regional greenschist-facies metamorphism in the Aleutian Islands resulted from subduction of the Kula ridge beneath the Aleutian island arc.

By the interpretation of Grow and Atwater (1970) and DeLong and others (1978), the Kula ridge entered the Aleutian trench between 20 and 35 m.y. ago (favored age is 30 m.y.). Our results, however, suggest that the 30-m.y. K-Ar ages on which DeLong and McDowell (1975) and DeLong and others (1978) base their conclusions are initial cooling ages of Aleutian island volcanic rocks and

not metamorphic ages. If ridge subduction produces an episode of regional lowgrade metamorphism, as DeLong and others speculate, then because the Andrew Lake and probably correlative sedimentary rocks on Adak Island are not regionally metamorphosed, subduction of the Kula ridge must have occurred before the late Eocene, about 50 m.y. ago. Models for North Pacific plate motion allow subduction of the Kula ridge at 50 m.y. or 35 m.y. ago depending on whether relative motions have been discontinuous or continuous, respectively (Cooper and others, 1976, fig. 4). Although the plate models are approximations, there is increasing evidence of discontinuous motion with faster rates of convergence in early Cenozoic time and slower rates during the middle and late Cenozoic; this evidence, then, favors subduction of the Kula ridge 50 m.y. ago (Hayes and Pitman, 1970; Hein, 1973; Hamilton, 1973; Scholl and others, 1977; also, see Francheteau and others, 1970; Larson and Pitman, 1972). Therefore, evidence for the timing and the effects of ridge subduction as proposed by DeLong and others (1978) can be interpreted variously. More likely, early Tertiary (Paleocene or Eocene) metamorphism resulted from the depositional burial and tectonic uplift of more than 4000 m of volcanic and sedimentary rocks. Emplacement of plutonic rocks at depth during early development of the arc complex may have contributed to the observed metamorphism.

CONCLUDING REMARKS

We suggest that sedimentary and volcanogenic rocks in the Wedge Point area are temporally equivalent to the upper Eocene, Andrew Lake Formation. However, despite the similarity in lithologic composition, degree of alteration, and induration, age-diagnostic fossils must be found in rocks in the Wedge Point area to justify including them as part of the Andrew Lake Formation. These rocks accumulated approximately 40 m.y. ago on the flanks of an active volcanic complex. Subaerial and marine (maximum 200-500 m deep) rocks are represented. Deposits underwent burial diagenesis that significantly reduced porosity and produced authigenic clay minerals, iron oxides, and possibly quartz. Additional alteration occurred in conjunction with intrusion of sills, dikes, and especially granodiorite plutons. Secondary minerals formed during these late-stage thermal and hydrothermal events are primarily zeolites (yugawaralite, laumontite, analcime, wairakite), clays, iron oxides, and quartz. Most pore spaces that remained after burial diagenesis were filled during this episode, essentially

eliminating any reservoir potential these strata may have had. Organic matter was either initially very low in these rocks, or if present was in places subsequently "cooked" by the heat of igneous intrusions. Consequently, these strata are unlikely sources of hydrocarbons.

The Finger Bay Volcanics was regionally metamorphosed to the greenschist facies some time before the late Eocene (possibly 50–55 m.y. ago). These rocks represent the oldest rocks exposed in the western Aleutian Islands. DeLong and McDowell (1975) and DeLong and others (1978) inferred from K-Ar ages that subduction of the Kula ridge spreading center resulted in a regional greenschist metamorphic event along the Aleutian arc about 35 m.y. ago (Oligocene). The absence of regional metamorphism in the Andrew Lake Formation suggests other interpretations. If Adak is typical of other Aleutian islands, either the Kula ridge was subducted about 50 m.y. ago or greenschist metamorphism need not accompany subduction of a spreading center.

REFERENCES CITED

- Atwater, Tanya, 1970, Implications of plate tectonics for the Cenozoic tectonic evolution of western North America: *Geol. Soc. America Bull.*, v. 81, p. 3513–3536.
- Barrer, R. M., and Marshall, D. J., 1965, Synthetic zeolites related to ferrierite and yugawaralite: *Am. Mineralogist*, v. 50, p. 484–489.
- Berggren, W. A., 1972, A Cenozoic time scale—Some implications for regional geology and paleobiogeography: *Lethaia*, v. 5, p. 195–215.
- Brindley, G. W., and Pedro, G., 1975, Meeting of the Nomenclature Committee of A.I.P.E.A.: *Clays and Clay Minerals*, v. 23, p. 413–414.
- Bundy, W. M., and Murray, H. H., 1959, Argillization in the Cochise Mining District, New Mexico: *Clays and Clay Minerals*, v. 6, p. 342–368.
- Carlisle, Donald, 1963, Pillow breccias and their aquagene tuffs, Quadra Island, British Columbia: *Jour. Geology*, v. 71, p. 48–71.
- Carr, W. J., Gard, L. M., Bath, G. D., and Healey, D. L., 1971, Earth-science studies of a nuclear test area in the western Aleutian Islands, Alaska: An interim summation of results: *Geol. Soc. America Bull.*, v. 82, p. 699–706.
- Carr, W. J., Quinlivan, W. D., and Gard, L. M., 1970, Age and stratigraphic relations of Amchitka, Banjo Point, and Chitka Point Formations, Amchitka Island, Aleutian Islands, Alaska: *U.S. Geol. Survey Bull.* 1324-A, p. A16–A22.
- Coats, R. R., 1947, Geology of northern Adak Island: *U.S. Geol. Survey Alaskan Volcano Inv. Rept.* 2, pt. 5, p. 71–85.
- , 1956, Geology of northern Adak Island, Alaska: *U.S. Geol. Survey Bull.* 1028-C, p. C45–C67.
- Coombs, D. S., 1953, The pumpellyite mineral series: *Mineralog. Mag.*, v. 30, p. 113–135.
- , 1961, Some recent work on the lower grades of metamorphism: *Australian Jour. Sci.*, v. 24, p. 203–215.
- Coombs, D. S., Ellis, A. J., Fyfe, W. S., and Taylor, A. M., 1959, The zeolite facies, with comments on the interpretations of hydrothermal synthesis: *Geochim. et Cosmochim. Acta*, v. 17, p. 53–107.
- Coombs, D. S., Horodyski, R. J., and Naylor, R. S., 1970, Occurrence of prehnite-pumpellyite facies metamorphism in northern Maine: *Am. Jour. Sci.*, v. 268, p. 142–156.
- Cooper, A. K., Scholl, D. W., and Marlow, M. S., 1976, Plate tectonic model for the evolution of the eastern Bering Sea Basin: *Geol. Soc. America Bull.*, v. 87, p. 1119–1126.
- DeLong, S. E., and Fox, P. J., 1977, Geological consequences of ridge subduction: *Am. Geophys. Union Ewing Symposium*, v. 1, p. 221–228.
- DeLong, S. E., Fox, P. J., and McDowell, F. W., 1978, Subduction of the Kula Ridge at the Aleutian Trench: *Geol. Soc. America Bull.*, v. 89, p. 83–95.
- DeLong, S. E., and McDowell, F. W., 1975, K-Ar ages from the Near Islands, western Aleutian Islands, Alaska: Indication of a mid-Oligocene thermal event: *Geology*, v. 3, p. 691–694.
- Eberlein, G. D., Erd, R. C., Weber, F. R., and Beatty, L. B., 1971, New occurrence of yugawaralite from the Chena Hot Springs Area, Alaska: *Am. Mineralogist*, v. 56, p. 1699–1717.
- Fiske, R. S., 1963, Subaqueous pyroclastic flows in the Ohanapecosh Formation, Washington: *Geol. Soc. America Bull.*, v. 74, p. 391–406.
- Fiske, R. S., and Matsuda, Tokihiko, 1964, Submarine equivalents of ash-flows in the Tokiwa Formation, Japan: *Am. Jour. Sci.*, v. 262, p. 76–106.
- Fournier, R. O., 1973, Silica in thermal waters: Laboratory and field investigations, in *Proceedings of symposium on hydrogeochemistry and biogeochemistry*, Tokyo, 1970: Washington, D.C., The Clarke Co., p. 122–139.
- Francheteau, Jean, Harrison, C. G. A., Sclater, J. G., and Richards, M. L., 1970, Magnetization of Pacific seamounts: A preliminary polar curve for the northeastern Pacific: *Jour. Geophys. Research*, v. 75, p. 2035–2061.
- Fraser, G. D., and Barnett, H. F., 1959, Geology of the Delarof and westernmost Andreanof Island, Aleutian Islands, Alaska: *U.S. Geol. Survey Bull.* 1028-I, p. 211–248.
- Fraser, G. D., and Snyder, G. L., 1959, Geology of southern Adak Island and Kagalaska Island, Alaska: *U.S. Geol. Survey Bull.* 1028-M, p. 371–408.
- Galloway, W. E., 1974, Deposition and diagenetic alteration of sandstone in northeast Pacific arc-related basins: Implications for graywacke genesis: *Geol. Soc. America Bull.*, v. 85, p. 370–390.
- Gates, Olcott, Powers, H. A., and Wilcox, R. E., 1971, Geology of the Near Islands, Alaska: *U.S. Geol. Survey Bull.* 1028-U, p. 709–822.
- Grow, J. A., and Atwater, Tanya, 1970, Mid-Tertiary tectonic transition in the Aleutian Arc: *Geol. Soc. America Bull.*, v. 81, p. 3715–3722.
- Hamilton, E. L., 1973, Marine geology of the Aleutian Abyssal Plain: *Marine Geology*, v. 14, p. 295–325.
- Harada, Kazuo, 1969, Further data on the natural association of Ca-zeolites: *Geol. Soc. Japan Jour.*, v. 75, p. 629–630.
- Harada, Kazuo, Nagashima, Kozo, and Sakurai, Kin-Ichi, 1969, Chemical composition and optical properties of

- yugawaralite from the type locality: *Am. Mineralogist*, v. 54, p. 306-309.
- Hayes, D. E., and Pitman, W. C., 1970, Magnetic lineations in the North Pacific: *Geol. Soc. America Mem.* 126, p. 291-314.
- Hein, J. R., 1973, Increasing rate of movement with time between California and the Pacific plate: From Delgada submarine fan source areas: *Jour. Geophys. Research*, v. 78, p. 7752-7762.
- Heystek, Hendrik, 1963, Hydrothermal rhyolitic alteration in the Castle Mountains, California: *Clays and Clay Minerals*, v. 11, p. 158-168.
- Jakeš, P., and White, A. J. R., 1969, Structure of the Melanesian arcs and correlation with distribution of magma types: *Tectonophysics*, v. 8, p. 223-236.
- Kossovskaia, A. G., 1975, Genetic types of zeolites in stratified rocks: *Litologia i Poleznye Iskopayemye*, no. 2, p. 162-178.
- Larson, R. L., and Pitman, W. C., 1972, World-wide correlation of Mesozoic magnetic anomalies and its implications: *Geol. Soc. America Bull.*, v. 83, p. 3645-3662.
- Lewis, R. Q., Nelson, W. H., and Powers, H. A., 1960, Geology of Rat Island, Aleutian Islands, Alaska: *U.S. Geol. Survey Bull.* 1028-Q, p. 555-562.
- Lovering, T. S., and Shepard, A. O., 1960, Hydrothermal argillic alteration on the Helen claim, East Tintic District, Utah: *Clays and Clay Minerals*, v. 8, p. 193-202.
- Marlow, M. S., Scholl, D. W., Buffington, E. C., and Alpha, T. R., 1973, Tectonic history of the central Aleutian Arc: *Geol. Soc. America Bull.*, v. 84, p. 1555-1574.
- Mitchell, A. H., and Bell, J. D., 1973, Island-arc evolution and related mineral deposits: *Jour. Geology*, v. 81, p. 381-405.
- Powers, H. A., Coats, R. R., and Nelson, W. H., 1960, Geology and submarine physiography of Amchitka Island, Alaska: *U.S. Geol. Survey Bull.* 1028-P, p. 521-554.
- Sakurai, Kin-Ichi, and Hayashi, A., 1952, "Yugawaralite," a new zeolite: *Yokohama Natl. Univ., Sci. Rept.*, sec. II, no. 1, p. 69-77.
- Sameshima, T., 1969, Yugawaralite from Shinoda, Shizuoka Pref. Central Japan: *Earth Sci. (Jour. Japanese Assoc. Amateur Mineralogists)*, v. 20, p. 70-78.
- Scholl, D. W., Buffington, E. C., and Marlow, M. S., 1975, Plate tectonics and the structural evolution of the Aleutian-Bering Sea region: *Geol. Soc. America Spec. Paper* 151, p. 1-31.
- Scholl, D. W., Greene, H. G., and Marlow, M. S., 1970, Eocene age of the Adak 'Paleozoic(?)' rocks, Aleutian Islands, Alaska: *Geol. Soc. America Bull.*, v. 81, p. 3583-3592.
- Scholl, D. W., Hein, J. R., Marlow, M. S., and Buffington, E. C., 1977, Meiji sediment tongue: North Pacific evidence for limited movement between the Pacific and North American plates: *Geol. Soc. America Bull.*, v. 88, p. 1567-1576.
- Seki, Yotaro, 1969, Facies series in low-grade metamorphism: *Geol. Soc. Japan Jour.*, v. 75, p. 255-266.
- Seki, Yotaro, Oki, Yasue, Matsuda, Tokihiko, Mikami, Keizo, and Okumura, Kimio, 1969, Metamorphism in the Tanya-wa Mountains Central Japan (II): *Japanese Assoc. Mineralogists, Petrologists, and Econ. Geologists Jour.*, v. 61, p. 50-75.
- Seki, Yotaro, and Okumura, Kimio, 1968, Yugawaralite from Onikobe active geothermal area, northeast Japan: *Japanese Assoc. Mineralogists, Petrologists, and Econ. Geologists Jour.*, v. 60, p. 27-33.
- Sigvaldason, G. E., and White, D. E., 1961, Hydrothermal alteration of rocks in two drill holes at Steamboat Springs, Washoe County, Nevada: *U.S. Geol. Survey Prof. Paper* 424-D, p. 116-122.
- Steiner, A., 1968, Clay minerals in hydrothermally altered rocks at Wairakei, New Zealand: *Clays and Clay Minerals*, v. 16, p. 193-213.
- Turner, F. J., and Verhoogen, John, 1960, *Igneous and metamorphic petrology*: New York, McGraw-Hill, 694 p.
- Uyeda, Seiya, and Miyashiro, Akiho, 1974, Plate tectonics and the Japanese Islands: A synthesis: *Geol. Soc. America Bull.*, v. 85, p. 1159-1170.

The Livengood Dome Chert, a New Ordovician Formation in Central Alaska, and Its Relevance to Displacement on the Tintina Fault

By ROBERT M. CHAPMAN, FLORENCE R. WEBER, MICHAEL CHURKIN, JR.,
and CLAIRE CARTER

SHORTER CONTRIBUTIONS TO STRATIGRAPHY AND
STRUCTURAL GEOLOGY, 1979

GEOLOGICAL SURVEY PROFESSIONAL PAPER 1126-F

*A newly defined formation provides a key to the
correlation of lower Paleozoic formations
and right-lateral movement on the
Tintina fault in east-central Alaska*



CONTENTS

	Page
Abstract	F1
Introduction	1
Acknowledgments	1
Original description of the Livengood Chert	2
The Livengood Dome Chert	2
Areal distribution	2
Lithology and structure	6
Reference section in the Lost Creek borrow pit	8
Paleontology	9
Regional correlation of rocks in the Livengood and Charley River quadrangles ..	11
Tectonic significance	12
References cited	12

ILLUSTRATIONS

	Page
FIGURE 1. Generalized bedrock geologic map of the central part of the Livengood quadrangle, showing the Livengood Dome Chert and other major rock units	F3
2. Reference section of the Livengood Dome Chert in the Lost Creek borrow pit	4
3. Map showing the location of the Lost Creek borrow pit and cross section A-A'	6
4. Geologic cross section A-A' through the Lost Creek borrow pit, showing the structural interpretation ...	8
5. Photograph of graptolite-bearing shale beds in the Livengood Dome Chert at the Lost Creek borrow pit	9
6. Drawings of graptolites from the Livengood Dome Chert	10

THE LIVENGOD DOME CHERT, A NEW ORDOVICIAN FORMATION IN CENTRAL ALASKA, AND ITS RELEVANCE TO DISPLACEMENT ON THE TINTINA FAULT

By ROBERT M. CHAPMAN, FLORENCE R. WEBER, MICHAEL CHURKIN, JR.,
and CLAIRE CARTER

ABSTRACT

The discovery of Late Ordovician graptolites in the Livengood Chert plus new data from field mapping and other paleontologic studies in the Livengood quadrangle necessitate major revisions in the Paleozoic stratigraphy in central Alaska. The term "Livengood Chert," pertaining to a formation consisting of chert, limestone, dolomite, shale, and argillite and originally assigned a Mississippian age, is abandoned. A predominantly chert formation, the Livengood Dome Chert, is herein newly defined and is dated by the graptolites as Late Ordovician. It is exposed in an east-northeast-trending belt about 91 km long in the Livengood quadrangle, and the type area is near Livengood Dome. Its structure is complex, and well-exposed thick sections are scarce; therefore the estimated thickness of 300–600 m is uncertain. The Livengood Dome Chert is overlain by an unnamed formation, composed largely of dolomite and limestone, that is provisionally assigned a Middle Silurian to Early Devonian age; the chert is underlain by Cambrian and Precambrian (?) argillite, slate, quartzite, siltstone, limestone, and chert. Extensive chert units similar to the Livengood Dome Chert in lithology and stratigraphic and structural position but paleontologically undated are present in the Tanana, Kantishna River, and Fairbanks quadrangles to the west and southwest. A chert unit that may be correlative with the Livengood Dome Chert crops out in the Circle quadrangle to the east. A correlation is suggested between the Livengood Dome Chert and the Ordovician part of the Road River Formation that lies farther east in the Charley River quadrangle. A correlation between the chert and other rock units of similar ages and lithologies in the Livengood and Charley River areas is significant to understanding the tectonics of the region because these areas are respectively south and north of the Tintina fault zone. The correlation implies about 300 km of right-lateral offset along this major fault system.

INTRODUCTION

Recent advances in the stratigraphic and paleontologic knowledge of Paleozoic rocks in central Alaska have provided data to allow revision of sev-

eral major rock units and their ages and to support significant new regional correlations and tectonic interpretations. A predominantly chert formation, the Livengood Dome Chert, is newly described in this report, and its age is identified as Late Ordovician on the basis of graptolites that were discovered in it in 1971. A formation consisting mainly of dolomite and limestone that immediately overlies the Livengood Dome Chert is also described but is not named. These formations formerly constituted the Livengood Chert that was described and assigned a Mississippian age by Mertie (1937, p. 105–111), and in this paper the term "Livengood Chert" is abandoned.

ACKNOWLEDGMENTS

The information presented here is largely the result of geologic mapping and studies in the Livengood quadrangle by several geologists between 1960 and 1971 (Chapman, Weber, and Taber, 1971). The discovery of graptolites by Donald M. Triplehorn, of the University of Alaska, Michael Churkin, Jr., and Claire Carter was a major contribution to this study (U.S. Geological Survey, 1972, p. A51–A52). Regional correlations and tectonic interpretations are based also on geologic work in the Charley River quadrangle (Brabb and Churkin, 1969) and the Tanana and Kantishna River quadrangles (Chapman, Yeend, Brosgé, and Reiser, 1975; Chapman, Yeend, and Patton, 1975).

We have benefited also from the geologic investigations in the Livengood area and the description of several chert thin sections by Robert L. Foster, from paleontologic and stratigraphic studies in the Livengood and White Mountains areas by J. Thomas

Dutro, Jr., and from geologic mapping by Donald Grybeck, who worked in the eastern part of Livengood quadrangle with Chapman and Weber in 1968. The geologic report on the Yukon-Tanana region, by Mertie (1937), who defined the major rock units and many of the geologic problems, was a most helpful base for the more recent work in the Livengood quadrangle.

ORIGINAL DESCRIPTION OF THE LIVENGOOD CHERT

The name Livengood Chert was first used in 1926 but without definition (Mertie, 1926, p. 79). However, Mertie had previously mapped and described this rock unit near Livengood, referring to it as "a stratigraphic series consisting dominantly of chert," and stated that the valley of Livengood Creek may be considered as its type locality (Mertie, 1918, p. 239-244). In 1937 the Livengood Chert was first defined, and it was described as extending "from a point north of the Sawtooth Mountains to the valley of Beaver Creek, north of the White Mountains, a distance of about 65 miles. The maximum width of this belt, in the vicinity of Livengood, is 8½ miles" (Mertie, 1937, p. 105). This belt is within the Livengood quadrangle. Mertie (1937, p. 105-111) identified an eastward extension of this formation in the hills "between the lower valleys of Beaver and Preacher Creeks" (Circle quadrangle) and "in a narrow belt crossing Woodchopper and Coal Creeks a short distance south of the Yukon River" (Charley River quadrangle). He also described westward extensions that occur as isolated beds in the vicinity of Sawtooth Mountain and as "metamorphosed equivalents of these rocks" in the Rampart district (Tanana quadrangle).

The lithology is dominantly chert, ranging in color from light smoky gray to black, and interbedded minor amounts of limestone, shale, and argillite (Mertie, 1937, p. 105-109). The limestone is commonly white to cream, crystalline, and in various stages of silicification and is less commonly dark gray, noncrystalline, thin bedded, and mostly unsilicified. Another rock type is chert conglomerate "composed essentially of chert pebbles in a matrix of chert" that "appears to lie at or near the base of the Livengood chert. Numerous small bodies of basaltic or diabasic greenstone are also found with the sedimentary rocks, but these igneous members are believed to be largely intrusive and therefore of later origin."

The rocks, according to Mertie, are closely folded, generally strike N. 60° E., and dip steeply south, forming a sequence overturned from south to north in which the same beds are probably repeated several times. Owing to the complex structure, no measurement of true thickness is possible, but "a considerable thickness of beds, perhaps several thousand feet," is estimated.

The Mississippian age determination was based on one fossil collection, 18AOF8 (Mertie, 1937, p. 110), from a limestone bed on a tributary of Lost Creek that contained crinoid stems *Batostomella* sp. and *Athyris* sp. This collection was accepted, with certain reservations, as of Carboniferous, probably Late Mississippian, age, although it lacked the more diagnostic Late Mississippian fossils that were found in collections of the undifferentiated Carboniferous rocks farther north in this region. Mertie states that "it is doubtful if this collection alone, considered without reference to others, even justifies a definite assignment to the Carboniferous," and "* * * the best estimate of the geologic age of the Livengood chert * * * is that it probably represents the base of the Carboniferous sequence in this region, and it is therefore classified as Mississippian."

THE LIVENGOOD DOME CHERT

In recent geologic mapping prior to discovery of the Ordovician graptolites, Mertie's Livengood Chert was divided into two unnamed units, provisionally assigned an Ordovician to Devonian age: a lower unit that is predominantly chert and minor amounts of interbedded shale and some other rocks and an upper unit of predominantly limestone, dolomite, and minor amounts of chert and shale (Chapman, Weber, and Taber, 1971).

The lower, predominantly chert unit in the Livengood quadrangle that is now dated by the Ordovician graptolites is here named the Livengood Dome Chert. The upper, predominantly carbonate unit is here differentiated as a separate but unnamed formation. The term "Livengood Chert" as defined by Mertie is therefore abandoned.

AREAL DISTRIBUTION

The Livengood Dome Chert crops out in an east-northeast-trending belt (fig. 1) between the Mud Fork and the headwaters of Victoria Creek, a distance of about 91 km. The width of this belt generally is about 5 km but ranges from 1.6 to 9.6 km. Minor amounts of some other rocks, either unrecognized or too small to be shown at the map scale,

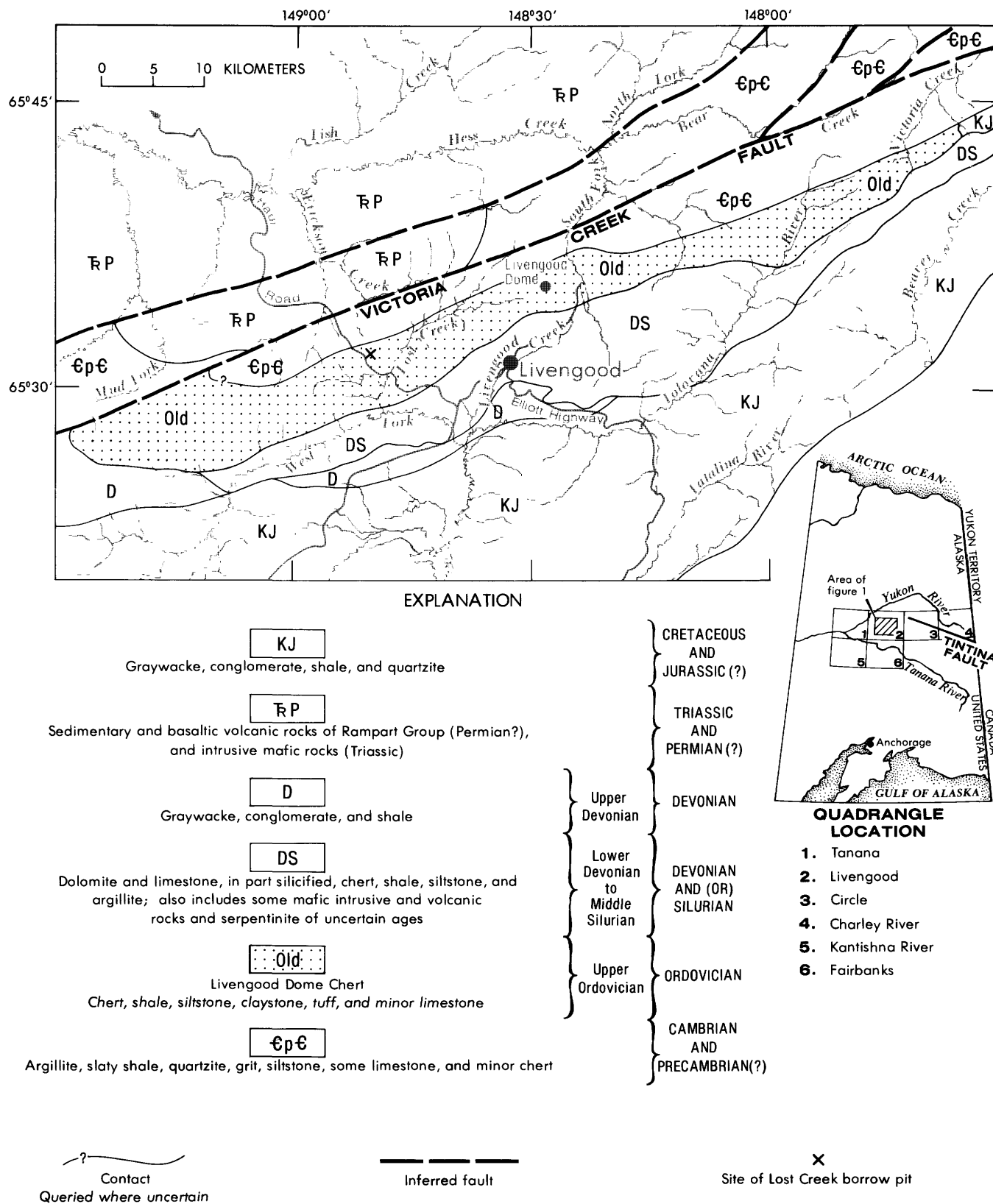


FIGURE 1.—Generalized bedrock geologic map of the central part of the Livengood quadrangle, showing the Livengood Dome Chert and other major rock units. Base from U.S. Geological Survey quadrangle, scale 1:250,000 (1956).

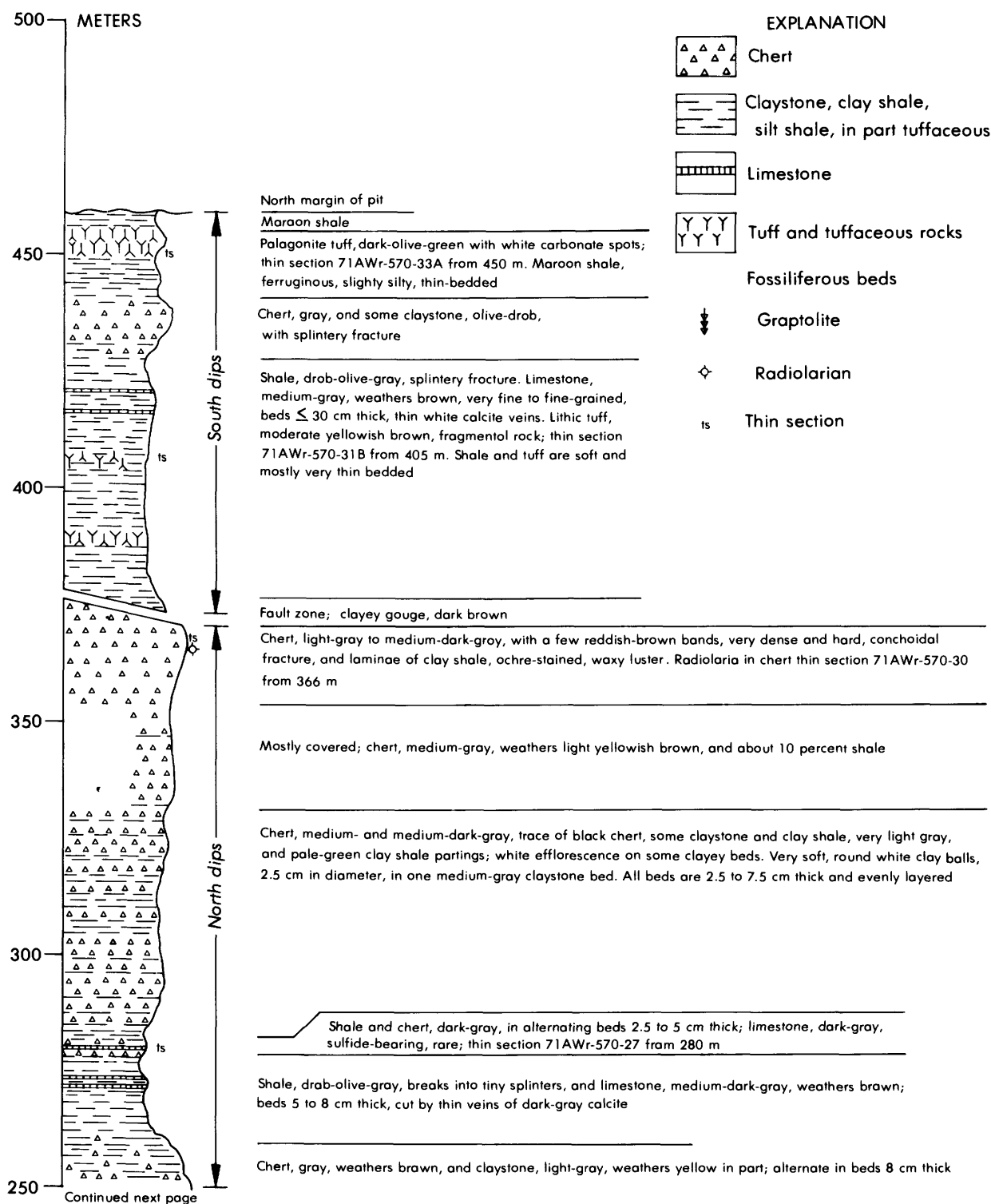
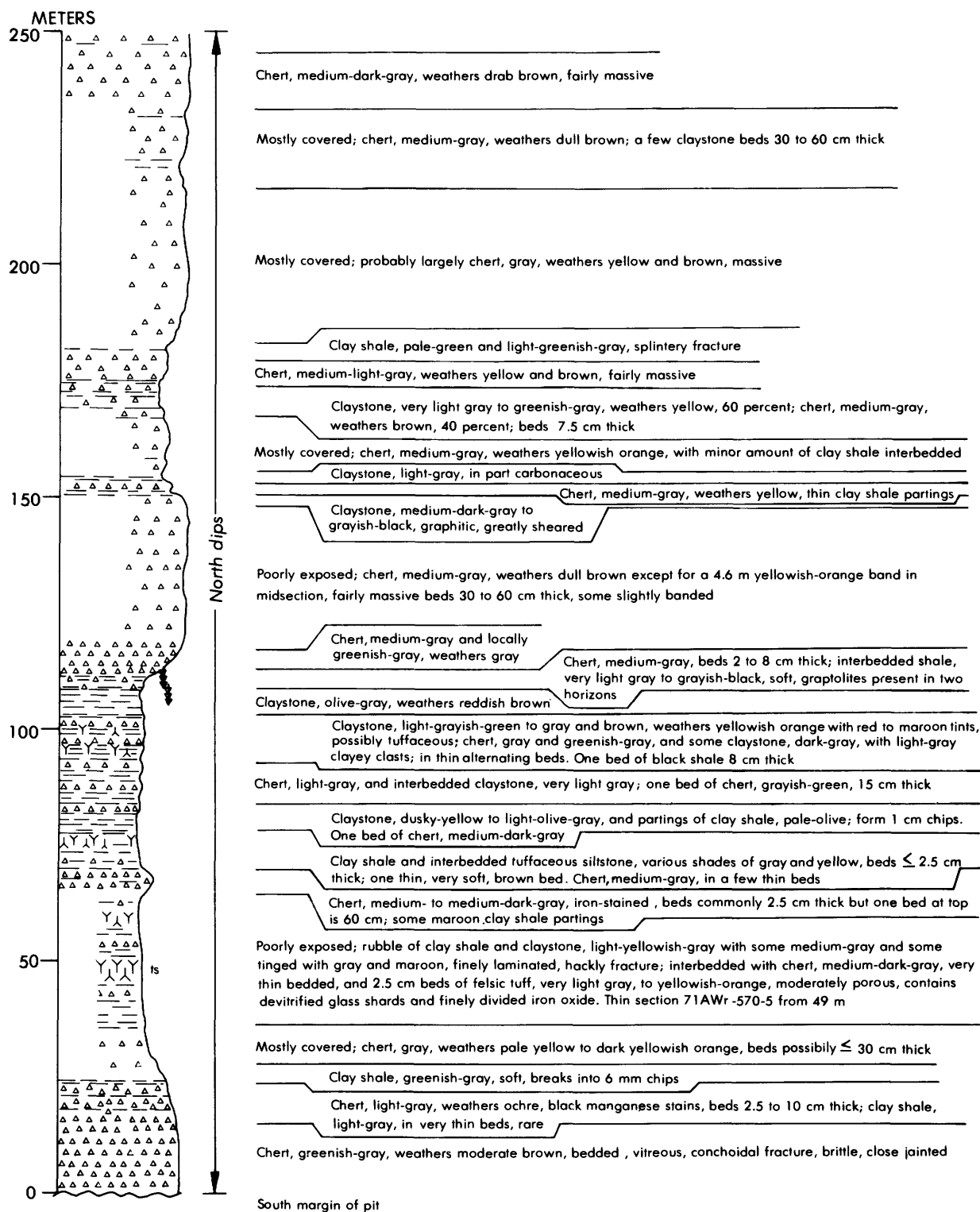


FIGURE 2.—Reference section of the Livengood Dome Chert in the Lost Creek borrow pit (see fig. 3 for location). The stratigraphic section is shown. The amount and direction of movement on the fault are unknown,

are included. The exposures are such that a complete section and the exact lower contact could not be found, and the upper contact was seen at only

one place. Within this belt the Livengood Dome Chert is best exposed in the area between the valleys of Lost Creek and the South Fork of Hess Creek,



graphic orientation and continuity of this section are uncertain because tops and bottoms of beds rarely could be determined and some beds may be repeated owing to undetected isoclinal folding.

which is herein designated its type area. The formation name is taken from Livengood Dome, which is underlain largely by this chert and is the most

prominent topographic feature in the type area. The thickest section, a reference section (fig. 2), was uncovered during 1970-71 in a large highway bor-

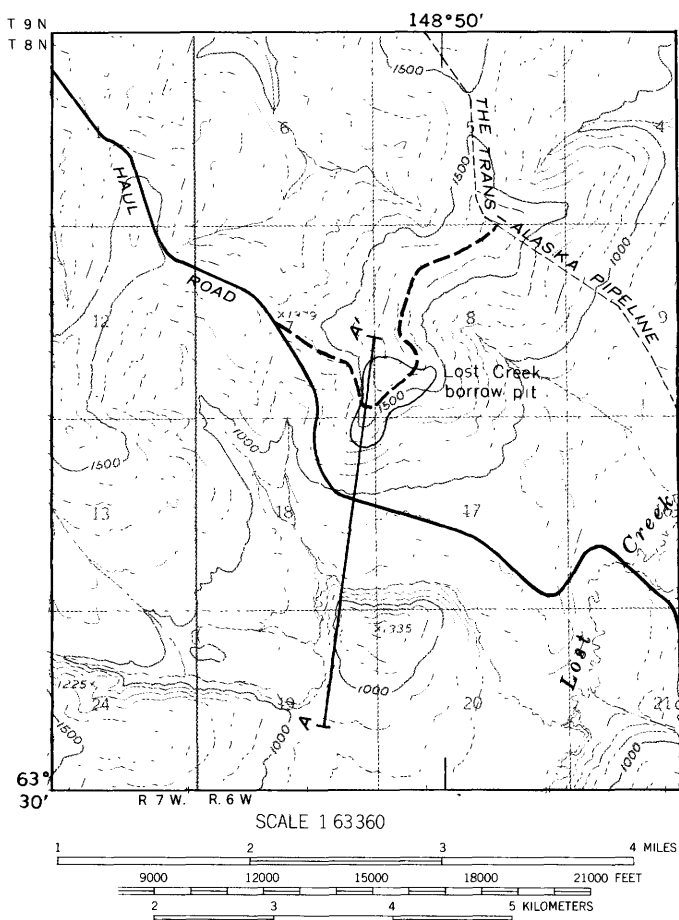


FIGURE 3.—Location of the Lost Creek borrow pit and cross section A-A' (fig. 4). Base from U.S. Geological Survey Livengood C-4 quadrangle, 1951.

row pit 13.6 km west of the town of Livengood and about 2.4 km west of Lost Creek in the SW $\frac{1}{4}$ sec. 8, T. 8 N., R. 6 W. (fig. 3).

West of the Mud Fork a belt of chert and meta-chert, apparently correlative with the Livengood Dome Chert, is present in the Tanana quadrangle (fig. 1) and extends over a distance of about 73.6 km between Hoosier Creek and Point Tilman on the Yukon River (Chapman, Yeend, Brosgé, and Reiser, 1975). An extensive, predominantly chert unit has been mapped in the northeastern and south-central part of the Kantishna River quadrangle (Chapman, Yeend, Brosgé, and Reiser, 1975; Chapman, Yeend, and Patton, 1975) and in the northwest corner of the Fairbanks quadrangle (Péwé and others, 1966). These cherts outside the Livengood quadrangle are tentatively correlated with the Livengood Dome Chert on the basis of lithologic similarities and stratigraphic and structural position. There is no definitive paleontologic evidence that these cherts

are all the same age. However, the recent discovery of radiolarians of probable early Paleozoic age in samples from both the Livengood Dome Chert and the chert in the south-central part of the Kantishna River quadrangle (D. L. Jones, oral commun., 1978) supports a general correlation of these two chert units.

To the east of Victoria Creek in the Circle quadrangle, the belt of chert mapped by Mertie (1937, pl. 1) between Beaver and Preacher Creeks was examined briefly by Churkin in 1968; no definitive age information was obtained here or in the immediately adjacent areas. Farther east, in the Charley River quadrangle, the Livengood Chert as mapped by Mertie in the Woodchopper and Coal Creeks area, on the north side of the Tintina fault, has been reinterpreted by Brabb and Churkin (1969) as two units: an argillite and chert unit of late Paleozoic age and the Step Conglomerate of Permian age. However, the Road River Formation (Churkin and Brabb, 1967; Brabb and Churkin, 1969) in the southeastern part of the Charley River quadrangle and also on the north side of the Tintina fault has, in part at least, the same age and lithology as the Livengood Dome Chert.

LITHOLOGY AND STRUCTURE

The Livengood Dome Chert in the type area consists of more than 50 percent chert that commonly ranges from light gray to grayish black, weathers to light and very light shades of gray, green, yellow, reddish brown, and red, and commonly has iron and manganiferous stains and thin coatings. Bedding, which in many outcrops is obscure, ranges from thick and massive (as much as 100 cm) to thin (2–8 cm) and includes some ribbon chert units; in part of the unit, banding accentuated by slight color differences is present. The chert and associated rocks are commonly jointed, irregularly fractured, and in places brecciated; thin to hairline white quartz veins are common along fractures and in places form a reticulated boxwork pattern.

Very thin layers and partings (a few millimeters to several centimeters thick) of clay shale, argillite, siliceous slaty shale, and siltstone are interbedded with chert, and there are uncommon thin units of tuff, tuffaceous siltstone, limestone, and possibly some graywacke. All these rocks, which form less than 50 percent of any chert section, range from light gray and olive gray to dark gray; included also are a few shaly beds that are grayish red to dark red and reddish brown and some pale-yellow to

yellowish-orange lithic tuffs. Because these rocks are thinner bedded and less resistant to weathering than the chert, they are poorly exposed or absent in natural outcrops and rubble patches, and our observations of them have been made chiefly in manmade cuts. A distinctive thin unit of small-pebble conglomerate, consisting of chert pebbles in a siliceous or chert cement, is present at several places near Livengood and Lost Creek. This chert pebble conglomerate apparently is in the lower part of the formation, but owing to complex structure and discontinuous outcrops, its stratigraphic position is uncertain.

In thin section the chert is cryptocrystalline but includes some microcrystalline quartz. In part it contains altered remnants of radiolarians (71AWr-570-30); some sponge spicules are also visible in hand specimens. Minor amounts of sericite and argillaceous grains are present. Hairline fractures filled with quartz, iron oxides, and mica are abundant. One section shows evidence of at least three sets of fractures and a granular quartz that has been invaded by silica. The deformation, fracturing, and rehealing of fractures are indicative of incipient or very low grade metamorphism.

A thin section of grayish-black siliceous siltstone, which is interbedded with chert in a borrow pit 6.4 km southwest of Livengood, shows the siltstone to be a moderately sheared and altered volcanoclastic rock containing quartz, much altered albitic plagioclase, colorless mica, chlorite, a zeolite (probably laumontite), and a large amount of what appears to be altered glass. The veinlets are largely quartz or zeolite plus quartz (J. W. Hawkins, written commun., 1966).

Tuff is interbedded with the chert in the Lost Creek borrow pit (fig. 2). A very light gray to pale yellowish-orange tuff (71AWr-570-5) in thin section shows cryptocrystalline to microcrystalline chert, probable devitrified glass shards, and some yellow, red, and brown earthy iron oxides and microcrystalline white mica; the tuff has a relict clastic or pyroclastic texture, and could be a water-laid sediment. Two other moderate yellowish-brown to dark-olive-green tuffaceous rocks (thin sections 71AWr-570-31B and -33A) are crystal to vitric tuff and vesicular palagonite tuff, which are generally less extensive and derived probably from basaltic or andesitic rocks.

Several medium-dark-gray limestones, in beds 5-8 cm in thickness and interbedded with shale and chert in the Lost Creek borrow pit, are calcarenites. A thin section (71AWr-570-27) shows about 85

percent interlocking sand-size carbonate grains that have been recrystallized and 15 percent iron oxides and sulfide that occur as tiny grains and fracture fillings.

Well-consolidated medium- to dark-gray and greenish-gray polymictic small-pebble conglomerates and conglomeratic volcanic graywackes noted in the area between Lost Creek and the headwaters of Erickson Creek are apparently interbedded in the Livengood Dome Chert. In thin sections, angular chert pebbles and grains are abundant, and angular pebbles and grains of quartz, feldspar, pyrite, shale, and mafic volcanic rock are common in a very fine grained graywacke matrix.

The structure throughout the type area of the Livengood Dome Chert is complex; tight, isoclinal, and overturned folds, joints, irregular fractures, and faults of indeterminate magnitude are common. The regional strike is generally N. 60-70° E.; both south and north dips generally exceed 45°. The rocks throughout this area have been subjected to some degree of low-grade metamorphism, and the metamorphism appears to be controlled by the structural setting and relative competence of the rock type. Foliation is crudely formed in some of the weaker rocks.

An accurate thickness for this formation cannot be determined because of the structural complexity, absence of continuous exposures, and concealed upper and lower contacts. The reference section in the Lost Creek borrow pit has an apparent thickness of about 459 m, but because this section is cut by a fault of unknown displacement and includes dip reversals, it has a smaller and unknown true stratigraphic thickness. An estimated thickness of 300-600 m for the Livengood Dome Chert would be compatible with its relatively broad outcrop belt in the Livengood quadrangle and with similar size belts of probably correlative chert units in adjacent quadrangles.

The position of the upper contact of the Livengood Dome Chert can be mapped within narrow limits at many places in the outcrop belt, but the contact zone has been seen at only one site, on the north side of a hill 1.2 km south of the Lost Creek borrow pit (fig. 4). Here the section of rocks, all dipping 55°-65° S., consists of at least 9 m of greenish-gray to black, banded and thin-bedded chert overlain by about 60 m of medium-dark-gray thin-bedded chert wacke and interbedded silty shale, in which graded bedding indicates that this unit is in upright position. These rocks are in turn overlain by about 15 m of massive fine- to medium-grained sparsely fos-

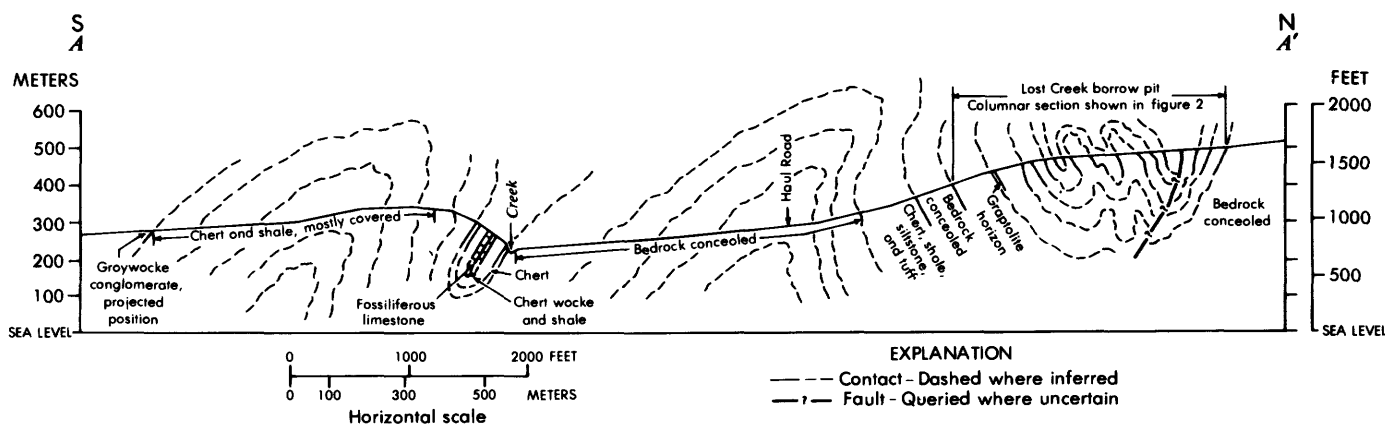


FIGURE 4.—Geologic cross section A-A' through the Lost Creek borrow pit, showing the structural interpretation. See figure 3 for location.

siliferous light-gray limestone, the basal 61 cm of which has thin lenticular beds containing some dark-gray rounded chert pebbles. The upper contact of the Livengood Dome Chert is placed immediately below the base of the limestone.

Where more fully represented in the Livengood quadrangle, the unnamed formation that overlies the Livengood Dome Chert is composed predominantly of very light gray to light-gray dolomite and limestone, is commonly slightly to nearly completely silicified, includes a minor amount of medium-dark-gray to black chert occurring as thin beds, lenses, and nodules and contains some thin beds of slaty shale, siliceous siltstone, and argillite. The uniformly dark color of this chert contrasts with the various shades of gray and other light colors that are characteristic of the chert in the Livengood Dome Chert. The other noncarbonate rocks in both formations are generally similar.

The exact age of this dominantly carbonate rock formation, shown as "dolomite and limestone" on figure 1, is uncertain. Based on exhaustive studies of the several small collections of fragmentary conodonts, corals, and brachiopods made in recent years and of collection 18AOF8 (Mertie, 1937, p. 110), the maximum age range of the fauna in the apparently basal unit is Middle Ordovician through Middle Devonian (Givetian). The conodont elements have a long range of Middle Ordovician to Middle Devonian (A. G. Epstein, written commun., 1976). The corals have a range of Silurian through Middle Devonian (W. A. Oliver, Jr., written commun., 1963). The brachiopods have a possible range of Middle Silurian through Early Devonian, but a Middle Silurian age is considered most reasonable by J. T. Dutro, Jr., (written commun., 1976). Therefore, an

age range of Middle Silurian to Early Devonian is provisionally assigned to this unnamed formation. Some mafic intrusive and volcanic rocks and serpentine are, for convenience in mapping, included with this formation. They are closely associated with the carbonate rocks and are considered to be of Silurian and (or) Devonian age; however, their exact ages and relations to the carbonate rocks are uncertain, and a discussion of these rocks is beyond the scope of this paper.

The lower contact of the Livengood Dome Chert has not been seen in the outcrop belt. It is, however, closely approximated within a zone of discontinuous outcrops and rubble patches along the northern margin of the outcrop belt. Older lower Paleozoic and Precambrian(?) rocks, including maroon and green argillite and slate, quartzite, siltstone, chert, and some limestone, lie immediately north of this contact zone but were not found in direct contact with identifiable Livengood Dome Chert. Near this contact zone, chert conglomerate and some chert breccia of uncertain origin occur in the Livengood Dome Chert. The nature of the contact is not clear, but we believe that it is unconformable and probably in part a fault contact.

REFERENCE SECTION IN THE LOST CREEK BORROW PIT

The thickest continuously exposed section of the Livengood Dome Chert known in the type area was examined in 1970 and 1971 in the Lost Creek borrow pit (figs. 2 and 3), which was opened in 1969–70 as a source of rock for construction of the Alyeska pipeline haul road north from Livengood. Subsequently this pit has been smoothed by bulldozing; in

1976 most of the bedrock section was not well exposed, and the graptolite beds were covered.

A section having an apparent stratigraphic thickness of about 459 m was measured across the floor of the pit from the lower, south edge to the north edge near the top of the hill. About 60 percent of the section is chert, and 40 percent includes thin beds of shale, claystone, siltstone, tuff, and tuffaceous rocks and a few thin beds of limestone. The beds strike about N. 70° E., dip 50°–70° N. in the southern part of the section, and dip about 70° S. in the north part of the section. Graded beds in one outcrop within the north-dipping part of the section suggest that these beds are overturned. Possibly all of the north-dipping section is overturned, but other evidence for this and for the orientation of the beds in the south-dipping part of the section was not found. A fault of unknown displacement, marked by a dark-brown clayey gouge zone, separates the north- and south-dipping parts of the section.

A detailed description of this section, including the positions of the graptolite horizon and thin-section specimens, is given in figure 2. A diagrammatic

cross section through the pit and continuing to the south to include a part of the unnamed limestone formation is shown in figure 4.

The true stratigraphic thickness represented in this section is not known because the bed orientation, dip reversals, and movement on the fault could not be accurately evaluated and because the section may be repeated by undetected isoclinal folding. Neither the chert conglomerate, which is probably characteristic of the lowest part of the Livengood Dome Chert, nor rocks of other formations above and below the Livengood Dome Chert were found in the pit. Therefore, this section is presumably representative of a part of the formation and does not include either of its contact zones.

PALEONTOLOGY

Graptolites were discovered in and collected (collection 71ACn-391) from thin shale beds interbedded with chert (fig. 5) in the Lost Creek borrow pit by D. M. Triplehorn, Claire Carter, and Michael Churkin, Jr., in 1971. Subsequently, an additional collection (71ACh-287, about 1.5 m above 71ACn-



FIGURE 5.—Graptolite-bearing shale beds, indicated under the hammer, in the Livengood Dome Chert at the Lost Creek borrow pit.

391) was made from this site by others. Both collections of graptolites present problems in identification and age determination. The only genera present are of the biserial scandent type, a group that ranges in age from Middle Ordovician to Early Silurian. The usual variety of distinctively shaped genera that characterize most graptolite assemblages is unfortunately not found here.

Climacograptus aff. *C. longispinus supernus* Elles and Wood (fig. 6A) resembles *Climacograptus bicornis tridentatus* Lapworth in its three-spined proximal end, but it is narrower and differs also in the arrangement of its proximal thecae and spines. It resembles *C. l. supernus* in the arrangement of proximal thecae and lateral spines, but it has a much larger rhabdosome and also has an elongated virgella (middle spine), which *C. l. supernus* lacks. It is more than 57 mm long and 0.7–1.8 mm wide. *C. l. supernus* is an Upper Ordovician species from Great Britain (Elles and Wood, 1901–18, p. 196–197; Toghil, 1970, p. 22; Riva, 1974a, p. 120–125).

Climacograptus cf. *C. miserabilis* Elles and Wood (fig. 6D) is a small species measuring about 15 mm long and about 1 mm wide, having 14–10 thecae per centimeter. The thecal apertures are nearly opposite each other. The Alaskan form differs from *C. miserabilis* s.s. in the spacing of its thecae: *C. miserabilis* s.s. has 10–11 thecae per centimeter. *C. miserabilis* is found in Upper Ordovician and Lower Silurian rocks of Great Britain (Elles and Wood, 1901–18, p. 186–187). It also occurs in Upper Ordovician and Lower Silurian rocks of the Kolyma Basin in the northeastern U.S.S.R. (Koren' and Sobolevskaya, 1977).

Amplexograptus? pacificus pacificus (Ruedemann) (fig. 6H) is characterized by a short rhabdosome and double genicular spines (Riva, 1974b). The Alaskan specimen is about 19 mm long and 1.0–2.1 mm wide; it has 8 thecae in the proximal 5 mm and 13 thecae per centimeter distally. The genicular spines are about 0.5 mm long and occur in pairs on only a few thecae, perhaps owing to imperfect preservation. Most of the thecae are of the amplexograptid type, which has distinctly everted apertures and outwardly inclined supragenicular walls. T. N. Koren' (written commun., 1976) has found the Alaskan form to be no different from her specimens of *A.? p. pacificus* from the Kolyma region of the northeastern U.S.S.R. *A.? p. pacificus* is found in Upper Ordovician rocks in Idaho (Ruedemann, 1947, p. 429; Ross and Berry, 1963, p. 125; Riva, 1974b, p. 1457) and in the *Climacograptus supernus* Zone (= *Dicellograptus ornatus* Zone) of

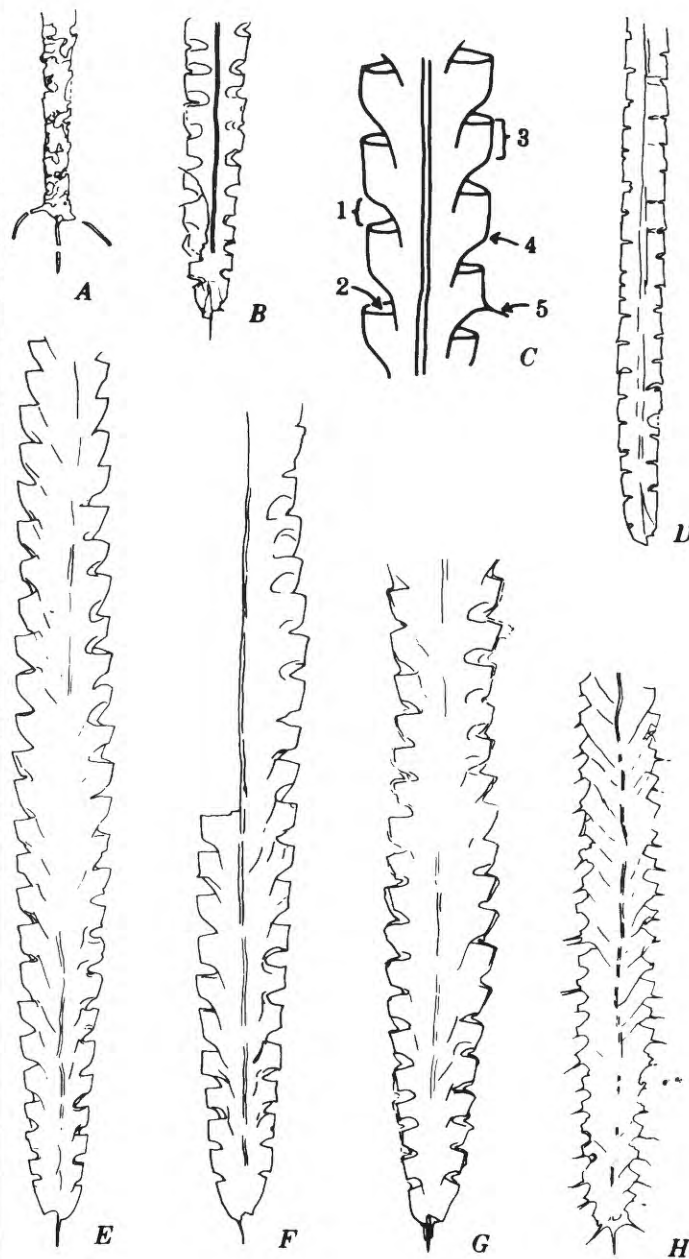


FIGURE 6.—Graptolites from the Livengood Dome Chert (all $\times 5$). A, *Climacograptus* aff. *C. longispinus supernus* Elles and Wood, USNM241051, collection 71ACh-287. B, *Climacograptus* sp., USNM241052, collection 71ACn-391. C, Diagram illustrating parts of thecae, as discussed in text: 1, apertural excavation, 2, thecal aperture, 3, supragenicular wall, 4, geniculum, 5, genicular spine. D, *Climacograptus* cf. *C. miserabilis* Elles and Wood, USNM241053, collection 71ACn-391. E, *Climacograptus* sp., USNM241054, collection 71ACn-391. F, *Climacograptus* sp., USNM241055, collection 71ACn-391. G, *Amplexograptus?* sp., USNM241056, collection 71ACn-391. H, *Amplexograptus? pacificus pacificus* (Ruedemann), USNM241057, collection 71ACh-287.

the Kolyma Basin and Kazakhstan, U.S.S.R. (Koren' and Soboleyskaya, 1977).

The specimen illustrated in figure 6G is questionably referred to the genus *Amplexograptus*. It is larger than other species of *Amplexograptus* (32 mm long, 1.3–3.0 mm wide, 12–10 thecae per centimeter) and differs in the details of the proximal end, but it possesses the outwardly inclined supragenicular walls characteristic of the genus.

A few small climacograptids with genicular spines similar to those of *A.?* *p. pacificus* occur in collection 71ACh–287. The remainder of both collections consists of numerous large- and medium-size climacograptids (figs. 6B, E, and F). Some of these may be transitional forms between previously described species, or they may be new species, but they lack any distinguishing features other than rhabdosome dimensions by which to identify them. Specimen F in figure 6 shows greatly retarded growth of one series of thecae. Only one other specimen having similar biserial-uniserial development was found, but it is a much wider form that has different thecal characteristics from the illustrated specimen. It is possible that this biserial-uniserial development may be due to injury, or it may be a prelude to the uniserial forms, such as *Monograptus*.

This fauna is Late Ordovician, even though it lacks the dicellograptids and distinctively spined species of *Climacograptus* that are characteristic of most Late Ordovician faunas of the Cordillera. This age assignment has been confirmed by John Riva (written commun., 1972) and W. B. N. Berry (oral commun., 1972). On the basis of our illustrations (fig. 6), Koren' (written commun., 1976) has correlated the Livengood Dome Chert fauna with faunas from the upper part of the Late Ordovician Zone of *C. supernus* (= *Dicellograptus ornatus* Zone) of the Kolyma Basin (Lukav beds) and Kazakhstan (Tchokpar horizon).

Nondiagnostic radiolarians and sponge spicules are the only other fossils that were known in the Livengood Dome Chert until early in 1978. Pending final determinations, radiolarians of probable early Paleozoic age have been identified by Brian Holdsworth and D. L. Jones in chert from the Lost Creek borrow pit and from the chert and slate unit of probable Ordovician age (Chapman, Yeend, and Patton, 1975) in the south-central part of the Kantishna River quadrangle (D. L. Jones, oral commun., 1978). Conodonts were looked for but not found in the shale interbedded with chert in and near the Lost Creek borrow pit.

REGIONAL CORRELATION OF ROCKS IN THE LIVENGOD AND CHARLEY RIVER QUADRANGLES

The graptolites discovered in the Livengood Dome Chert indicate that it is coeval with part of the Road River Formation, a similar, but not identical unit that occurs much farther east in the Charley River quadrangle (Churkin and Brabb, 1965) and is widespread still farther east in Yukon Territory (Jackson and Lenz, 1962; Green, 1972). Much of the Livengood Dome Chert is pure chert that contains only minor shaly partings. The Road River, in contrast, is mainly graptolitic shale that has only a minor amount of siliceous shale and chert. The Livengood Dome Chert has some green tuff beds not found in the Road River Formation, and the Road River has a few conglomerate beds containing limestone and dolomite fragments that have not been recognized in the Livengood Dome Chert. The Road River in the Charley River area unconformably overlies a thick section of mainly limestone (Brabb, 1967) that in its upper part is rich in Cambrian trilobites (Palmer, 1968). The Road River underlies the McCann Hill Chert, a thin-bedded chert and siliceous shale unit that has a basal limestone unit rich in shelly fossils of Early Devonian age (Churkin and Brabb, 1965; Churkin and Brabb, 1967).

The fossiliferous Cambrian limestone and distinctive carbonate-rich formations of the Tindir Group of Precambrian age that occur below the Road River Formation are apparently absent in the Livengood quadrangle. Instead, the rocks structurally or stratigraphically below the Livengood Dome Chert along the north side of its outcrop belt are mainly siliceous. However, the presence of a thin fossiliferous limestone immediately overlying the chert, chert wacke, and silty shale of the Livengood Dome Chert suggests a correlation of this limestone with the basal limestone and shale member of the McCann Hill Chert. Certain other younger formations in the Livengood quadrangle also appear to have close relatives in the Charley River area. For example, the coarse clastic rocks of Late Devonian age near Livengood may be a facies equivalent of the Nation River Formation; the volcanic and clastic rocks of the Rampart Group of probable Permian age may be related to the Circle Volcanics and associated clastic rocks of late Paleozoic age in the Charley River area; finally, the Lower Cretaceous Kandik Group of the Charley River area appears to have its counterpart in the Jurassic (?) and Cretaceous graywacke formations exposed in the Livengood and

Tanana quadrangles. Quartzites, unique to these Mesozoic sections in both the Livengood and Charley River areas, contain *Buchia*, which further strengthens this correlation.

TECTONIC SIGNIFICANCE

The tectonic significance of these stratigraphic correlations between the Livengood and Charley River areas is that the two areas of relatively unmetamorphosed Paleozoic strata occur on opposite sides of the Tintina fault zone. The Tintina fault in Alaska, where it crosses the Alaska-Yukon Territory boundary, separates greenschist, quartzite, phyllite, and greenstone of Paleozoic age on the south from essentially unmetamorphosed Precambrian, Paleozoic, and younger strata on its north side. This contrast in geology across the fault zone can be traced as far west as the western boundary of the Circle quadrangle, where the Tintina apparently splays into the several faults that are mapped in the northeastern part of the Livengood quadrangle (Chapman and others, 1971). On the south side of these faults near the eastern boundary of the Livengood quadrangle, unmetamorphosed rock sequences like those on the north side of the fault zone in the Charley River area first appear.

This geologic correlation strongly suggests a major right-lateral displacement along the Tintina fault system. The distance is about 300 km between the west end of the Road River Formation exposures near Nation in the Charley River quadrangle and the east end of the Livengood Dome Chert exposures near the head of Victoria Creek. Mainly on the basis of data from the Canadian part of the fault, Roddick (1967) estimated a 352- to 416-km displacement on the Tintina-Rocky Mountain trench system, and more recently, Tempelman-Kluit, Gordey, and Read (1976) suggested a displacement of 450 km.

A possible explanation for the differences in the calculated amounts of displacement is that the Tintina fault has splayed into several faults, and the total offset of an originally widespread unit, such as the Livengood Dome Chert, may be disguised by partial offset of detached, fault-bounded blocks of the unit within the fault system, for example: the Crazy Mountains, Little Crazy Mountains, and the hills between Preacher and Beaver Creeks, which are along the north boundary of the Tintina fault system in the northern part of the Circle quadrangle. Some of the more widespread rock units noted in this area in a brief reconnaissance by Churkin in

1968 are chert (probably part of the Livengood Dome Chert), chert-pebble conglomerate, basaltic rocks interlayered with chert (probably part of the Rampart Group), and interbedded quartzite, phyllite, and siltstone that in part contains *Oldhamia*, a fan-shaped trace fossil of either Cambrian or late Precambrian age. The structurally complex sequences of various rock types, apparently including both lower and upper Paleozoic units, that form these hills are tentatively interpreted, on the basis of limited field data and aeromagnetic data (U.S. Geological Survey, 1974), as parts of detached, fault-bounded blocks, or a block, within the Tintina fault system.

REFERENCES CITED

- Brabb, E. E., 1967, Stratigraphy of the Cambrian and Ordovician rocks of east-central Alaska: U.S. Geological Survey Professional Paper 559-A, 30 p.
- Brabb, E. E., and Churkin, Michael, Jr., 1969, Geologic map of the Charley River quadrangle, east-central Alaska: U.S. Geological Survey Miscellaneous Geologic Investigations Map I-573, scale 1:250,000.
- Chapman, R. M., Weber, F. R., and Taber, Bond, 1971, Preliminary geologic map of the Livengood quadrangle, Alaska: U.S. Geological Survey open-file report, scale 1:250,000.
- Chapman, R. M., Yeend, W. E., Brosgé, W. P., and Reiser, H. N., 1975, Preliminary geologic map of the Tanana and northeast part of the Kantishna River quadrangles, Alaska: U.S. Geological Survey Open-File Report 75-337, scale 1:250,000.
- Chapman, R. M., Yeend, W. E., and Patton, W. W., Jr., 1975, Preliminary reconnaissance geologic map of the western half of the Kantishna River quadrangle, Alaska: U.S. Geological Survey Open-File Report 75-351, scale 1:250,000.
- Churkin, Michael, Jr., and Brabb, E. E., 1965, Ordovician, Silurian, and Devonian biostratigraphy of east-central Alaska: American Association of Petroleum Geologists Bulletin, v. 49, no. 2, p. 172-185.
- , 1967, Devonian rocks of the Yukon-Porcupine Rivers area and their tectonic relation to other Devonian sequences in Alaska, in Oswald, D. H., ed., International Symposium on the Devonian System, Calgary, 1967: Calgary, Alberta Society of Petroleum Geologists, v. 2, p. 227-258.
- Elles, G. L., and Wood, E. M. R., 1901-18, A monograph of British graptolites: London, Paleontographical Society, 526 p., 52 pls.
- Green, L. H., 1972, Geology of Nash Creek, Larsen Creek, and Dawson map-areas, Yukon Territory: Geological Survey of Canada Memoir 364, 157 p.
- Jackson, D. E., and Lenz, A. C., 1962, Zonation of Ordovician and Silurian graptolites of northern Yukon, Canada: American Association of Petroleum Geologists Bulletin, v. 46, no. 1, p. 30-45.
- Koren', T. N., and Sobolevskaya, R. R., 1977, Noviy etalon postedovatel' nosti kompleksov graptolitov na rubezhe

- Ordovika-Silura (Severo-Vostok S.S.S.R.): *Doklady Akademii Nauk S.S.S.R.*, Tom 236, no. 4, p. 950-953.
- Mertie, J. B., Jr., 1918, The gold placers of the Tolovana district: U.S. Geological Survey Bulletin 662, p. 239-244.
- 1926, The Paleozoic geology of interior Alaska [abs.]: *Washington Academy of Sciences Journal*, v. 16, p. 78-79.
- 1937, The Yukon-Tanana region, Alaska: U.S. Geological Survey Bulletin 872, 276 p.
- Palmer, A. R., 1968, Cambrian trilobites of east-central Alaska: U.S. Geological Survey Professional Paper 559-B, 115 p.
- Péwé, T. L., Wahrhaftig, Clyde, and Weber, F. R., 1966, Geologic map of the Fairbanks quadrangle, Alaska: U.S. Geological Survey Miscellaneous Geologic Investigations Map I-455, scale 1:250,000.
- Riva, John, 1974a, Late Ordovician spinose climacograptids from the Pacific and Atlantic faunal provinces, in Rickards, R. B., Jackson, D. E., and Hughes, C. P., eds., *Graptolite studies in honour of O. M. B. Bulman: Paleontology Special Paper* 13, p. 107-126, pl. 7.
- 1974b, Graptolites with multiple genicular spines from the Upper Ordovician of western North America: *Canadian Journal of Earth Sciences*, v. 11, no. 10, p. 1455-1460.
- Roddick, J. A., 1967, Tintina trench: *Journal of Geology*, v. 75, no. 1, p. 23-32.
- Ross, R. J., and Berry, W. B. N., 1963, Ordovician graptolites of the Basin Ranges in California, Nevada, Utah, and Idaho: U.S. Geological Survey Bulletin 1134, 177 p., 13 pls.
- Ruedemann, Rudolf, 1947, Graptolites of North America: *Geological Society of America Memoir* 19, 652 p., 92 pls.
- Tempelman-Kluit, D. J., Gordey, S. P., and Read, B. C. 1976, Stratigraphy and structural studies in the Pelly Mountains, Yukon Territory, in *Report of activities, Part A: Canadian Geological Survey Paper* 76-1A, p. 97-106.
- Toghill, Peter, 1970, Highest Ordovician (Hartfell Shales) graptolite faunas from the Moffat area, south Scotland: *British Museum (Natural History) Bulletin, Geology*, v. 19, no. 1, p. 1-26, 16 pls.
- U.S. Geological Survey, 1972, Geological Survey research 1972: U.S. Geological Survey Professional Paper 800-A, p. A51-A52.
- 1974, Aeromagnetic map of the Circle quadrangle, northeastern Alaska: U.S. Geological Survey Open-File Report 74-101, scale 1:250,000, 1 sheet.

Intertonguing between the Star Point Sandstone and the Coal-Bearing Blackhawk Formation Requires Revision of some Coal-Bed Correlations in the Southern Wasatch Plateau, Utah

By ROMEO M. FLORES, PHILIP T. HAYES, WALTER E. MARLEY III,
and JOSEPH D. SANCHEZ

SHORTER CONTRIBUTIONS TO STRATIGRAPHY AND
STRUCTURAL GEOLOGY, 1979

GEOLOGICAL SURVEY PROFESSIONAL PAPER 1126-G

*Stratigraphic boundary relationship of the
Star Point Sandstone and Blackhawk Formation
and its bearing to coal correlations*



CONTENTS

	Page
Abstract	G1
Introduction	1
Description of the intertonguing and correlation of coal beds	1
References cited	3

ILLUSTRATIONS

	Page
FIGURE 1. Map of Muddy Canyon-Emery area, Utah, showing the position of contact and the zone of intertonguing between the Star Point Sandstone and the Blackhawk Formation, the location of the panoramic photograph, and the location of the diagrammatic sections	G2
2. Composite panoramic photograph and diagrams of the north wall of Muddy Canyon in E½ sec. 36, T. 20 S., R. 5 E., and W½ sec. 6, T. 21 S., R. 6 E., showing intertonguing relations between the Star Point Sandstone and the Blackhawk Formation and showing Blackhawk coal-bed correlations of Spieker and revised coal-bed correlations proposed in this paper	4
3. Diagrammatic section along the Wasatch Plateau front, showing relations among the Star Point Sandstone, the Blackhawk Formation, and tongues of the Star Point and the Blackhawk	6
4. Diagrammatic section along a downfaulted block near Emery, Utah, showing relations among the Star Point Sandstone, the Blackhawk Formation, and tongues of the Star Point and the Blackhawk ----	6

INTERTONGUING BETWEEN THE STAR POINT SANDSTONE AND THE COAL-BEARING BLACKHAWK FORMATION REQUIRES REVISION OF SOME COAL-BED CORRELATIONS IN THE SOUTHERN WASATCH PLATEAU, UTAH

By ROMEO M. FLORES, PHILIP T. HAYES, WALTER E. MARLEY III,
and JOSEPH D. SANCHEZ

ABSTRACT

Geologic mapping and detailed measurement and description of closely spaced stratigraphic sections across the contact between the Upper Cretaceous Blackhawk Formation and the Star Point Sandstone of the Wasatch Plateau, Utah have established the presence of a southeast-trending zone of intertonguing between these rock units. The contact between the formations drops stratigraphically about 20 m within about 1 km as a result of the intertonguing. This relationship requires a revision of correlations of lower Blackhawk coal beds between the two sides of the zone of intertonguing. The Hiawatha coal bed of the east side of the zone is apparently correlative with the Muddy No. 2 coal bed of the west side of the zone and possibly with the Upper Ivie bed of the Convulsion Canyon area. Beds referred to as the Hiawatha, Upper Hiawatha, and Muddy No. 1 on the west side of the zone of intertonguing pinch out eastward toward the Star Point Sandstone.

INTRODUCTION

As described by Spieker (1931), the thickest coal beds of the southern part of the Wasatch Plateau near Emery, Utah, (fig. 1) occur in the lower 30 m of the Upper Cretaceous Blackhawk Formation. According to him, there are two major coal groups in the lower part of the Blackhawk: a lower group consisting of the Hiawatha and Upper Hiawatha coal beds and an upper group consisting of the Muddy No. 1 and Muddy No. 2 coal beds. The Hiawatha coal bed was recognized as immediately overlying the Star Point Sandstone, which was mapped as a continuous, ledge-forming unit. The discontinuous Upper Hiawatha coal bed was considered to be separated from the Hiawatha coal bed by about 6 m of interbedded sandstone, siltstone, shale, and carbonaceous shale. The Muddy No. 1 coal bed was considered to lie 9 to 12 m above the

Upper Hiawatha and 8 to 12 m below the Muddy No. 2.

During recent geologic mapping (Hayes and Sanchez, 1977; Sanchez and Hayes, 1977) and detailed measurement and description of closely spaced stratigraphic sections of the upper part of the Star Point Sandstone and lower part of the Blackhawk Formation (Marley and Flores, 1977), a zone of intertonguing between the two formations was observed at several localities within a 10-km-long and 1-km-wide belt extending south-southeastward from the north wall of Muddy Canyon to a downfaulted block near the town of Emery (fig. 1). As a result of this intertonguing, the contact between the two formations is stratigraphically about 20 m higher to the east than it is to the west. The coal-bed correlations of Spieker (1931) are correspondingly in error.

DESCRIPTION OF THE INTERTONGUING AND CORRELATION OF COAL BEDS

Figure 2 consists of a composite panoramic photograph showing the intertonguing on the north wall of Muddy Canyon and of diagrams of the same area showing the coal-bed correlations of Spieker (1931) and our revised correlations. As shown on the figure, the base of the Blackhawk Formation drops about 20 m westward between Spieker's sections 463 and 464, owing to the pinching out of the tongue of the Star Point Sandstone. Because Spieker did not recognize the intertonguing and considered the top of the Star Point to be a uniform stratigraphic horizon, he correlated the coal beds immediately overlying the Star Point at the two localities, referring to them

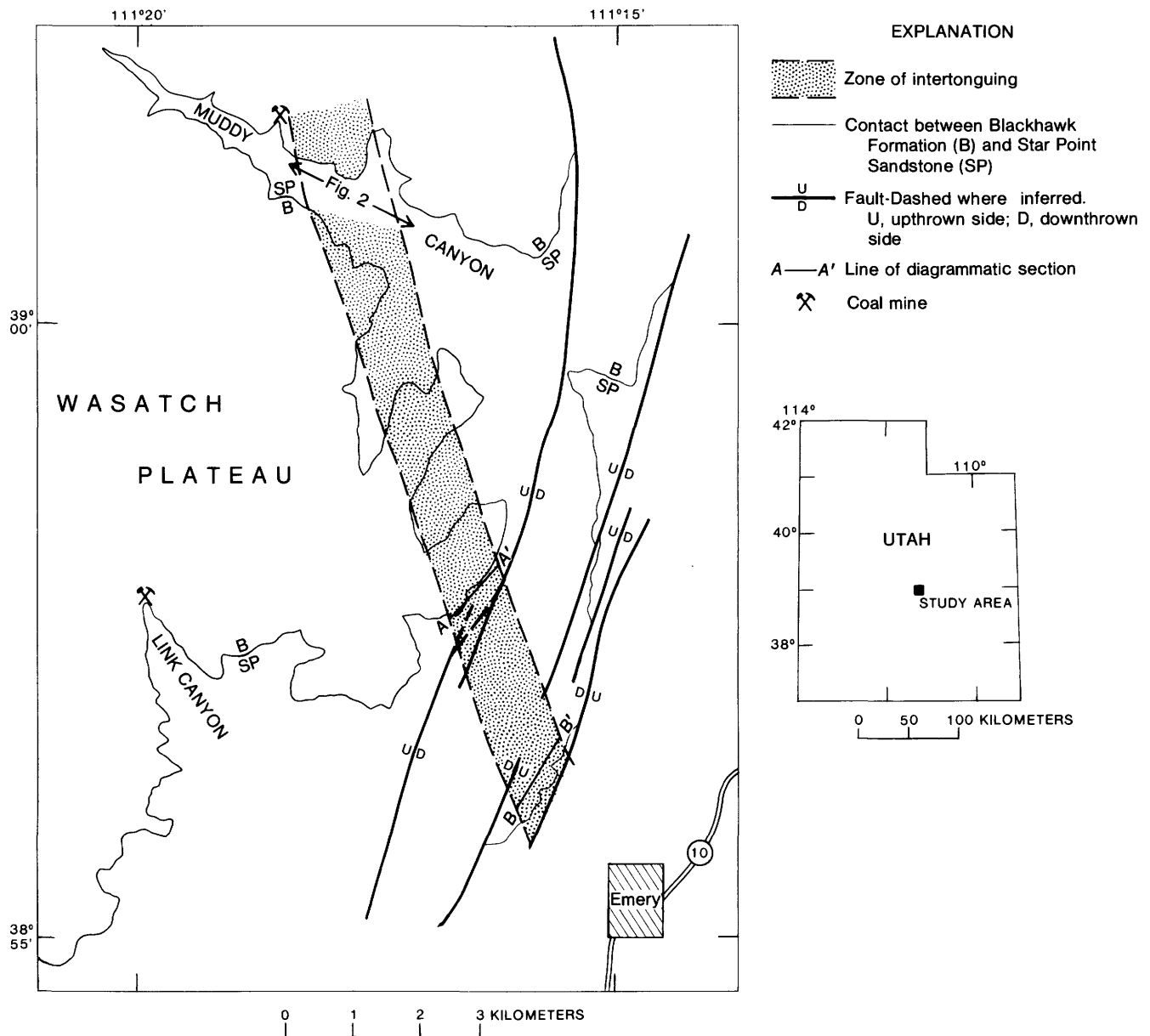


FIGURE 1.—Map of Muddy Canyon-Emery area showing position of contact and zone of intertonguing between Star Point Sandstone and Blackhawk Formation, location of panoramic photograph fig. 2, and diagrammatic sections (figs. 3 and 4). Geology modified from Spieker (1931).

both as the Hiawatha. In the revised correlations, the Hiawatha coal bed at section 464 occurs within a sequence of rocks in the Blackhawk Formation that pinches out eastward between lower and upper sandstone ledges of the Star Point. The Muddy No. 1 coal bed of section 464 appears to be at the horizon of the tongue of the Star Point Sandstone but is probably cut out by a channel sandstone of the Blackhawk Formation between sections 464 and 463. The Muddy No. 2 coal bed of section 464 is cor-

related with the Hiawatha coal bed of sections 461 and 463.

Figure 3 and 4 are diagrammatic sections constructed from closely spaced stratigraphic sections that were measured along the Wasatch Plateau front (A-A', fig. 1) and in a downdropped fault block near Emery (B-B', fig. 1). Although different in some details, the lower coal beds in both areas are exposed to the southwest to the pinch out within the Blackhawk Formation or are truncated to the east

by a tongue of the Star Point Sandstone. The coal bed immediately overlying the Star Point in areas to the northeast is generally traceable southwestward into beds that crop out well above the Star Point Sandstone. As a result of the intertonguing, the Star Point-Blackhawk contact drops about 21 m southwest in the exposure along the Wasatch Plateau front and about 16 m in the exposure along the fault block.

Although Spieker and Reeside (1925) were aware of intertonguing among various Cretaceous units exposed in the Wasatch Plateau, Spieker (1931), in his excellent bulletin on the Wasatch Plateau coal field, commented on the remarkable "evenness and persistency" of the contact between the Star Point Sandstone and the Blackhawk Formation and apparently was unaware of intertonguing between the two rock units within the coal field. Spieker's concept of a very regular contact probably holds true for most localities, but our findings suggest that other examples of intertonguing between the Star Point Sandstone and the Blackhawk Formation may be found within the Wasatch Plateau as more detailed geologic work is done.

On the basis of our present knowledge, it is necessary to revise the terminology in areas to the south and west of the zone of intertonguing described here. For example, the upper coal bed mined in the abandoned mine in Muddy Canyon (fig. 1), referred to as the Muddy No. 2 coal bed by Spieker (1931), is apparently the Hiawatha coal bed of areas to the northeast of the zone of intertonguing, and a thick (2.5-5 m) coal bed found 12 to 19 m above the Star Point Sandstone in several holes drilled in the Emery West quadrangle west of the zone of intertonguing (Blanchard and others, 1977) may also be the Hiawatha of areas to the northeast. The coal bed mined in the abandoned Link Canyon mine (fig. 1), identified by Doelling (1972) as the Upper Hiawatha coal bed, is replaced to the east by the Star Point Sandstone tongue and is about 20 m below the stratigraphic position of the Upper Hiawatha coal bed to the east of the zone of intertonguing. Correlations of coal beds in our study area with those of the Southern Utah Fuel Co. mine in Convulsion Canyon, 14 km to the southwest, are still uncertain, but it may be pertinent to note that the thick bed presently being mined there crops out about 20 m above the top of the Star Point Sandstone and may be equiv-

alent to the Hiawatha coal bed of the revised correlation. According to Doelling (1972), the coal bed mined in Convulsion Canyon is the Upper Ivie coal bed.

The intertonguing noted here, along with data gathered by Marley and Flores (1977), have significant paleogeographic and paleoenvironmental implications that are beyond the scope of this report. Some of these implications are presented in preliminary form by Marley, Flores, and Cavaroc (1978) and in more detail by Flores (1979) and Marley, Flores, and Cavaroc (1979).

REFERENCES CITED

- Blanchard, L. F., Ellis, E. G., and Roberts, J. V., 1977, Lithologic and geophysical logs of holes drilled in the Wasatch Plateau Known Recoverable Coal Resource Area, Carbon, Emery, and Sevier Counties, Utah: U.S. Geological Survey Open-File Report 77-133, 324 p.
- Doelling, H. H., 1972, Central Utah coal fields; Sevier-Sanpete, Wasatch Plateau, Book Cliffs and Emery: Utah Geological and Mineralogical Survey Monograph Series No. 3, p. 1-496.
- Flores, R. M., 1979, Coal depositional models in some Tertiary and Cretaceous coal fields in the U.S. Western Interior: International Association of Sedimentology, Organic Geochemistry volume (in press).
- Hayes, P. T., and Sanchez, J. D., 1977, Preliminary geologic map of the Emery West quadrangle, Emery and Sevier Counties, Utah: U.S. Geological Survey Open-File Report 77-822.
- Marley, W. E., III, and Flores, R. M., 1977, Descriptions of stratigraphic sections, Upper Cretaceous Blackhawk Formation and Star Point Sandstone in the Emery West and Flagstaff Peak quadrangles, Utah: U.S. Geological Survey Open-File Report 77-833, 257 p.
- Marley, W. E., III, Flores, R. M., and Cavaroc, V. V., 1978, Lithogenetic variations of the Upper Cretaceous Blackhawk Formation and Star Point Sandstone in the Wasatch Plateau, Utah: Geological Society of America Abstracts with Programs, v. 10, no. 5, p. 233.
- , 1979, Coal accumulation in Upper Cretaceous marginal deltaic environments of the Blackhawk Formation and Star Point Sandstone, Emery, Utah: Utah Geology (in press).
- Sanchez, J. D., and Hayes, P. T., 1977, Preliminary geologic map of the Flagstaff Peak quadrangle, Emery, Sanpete, and Sevier Counties, Utah: U.S. Geological Survey Open-File Report 77-823, scale 1:24,000.
- Spieker, E. M., 1931, The Wasatch Plateau coal field, Utah: U.S. Geological Survey Bulletin 819, 210 p.
- Spieker, E. M., and Reeside, J. B., Jr., 1925, Cretaceous and Tertiary formations of the Wasatch Plateau, Utah: Geological Society of America Bulletin, v. 36, p. 435-454.

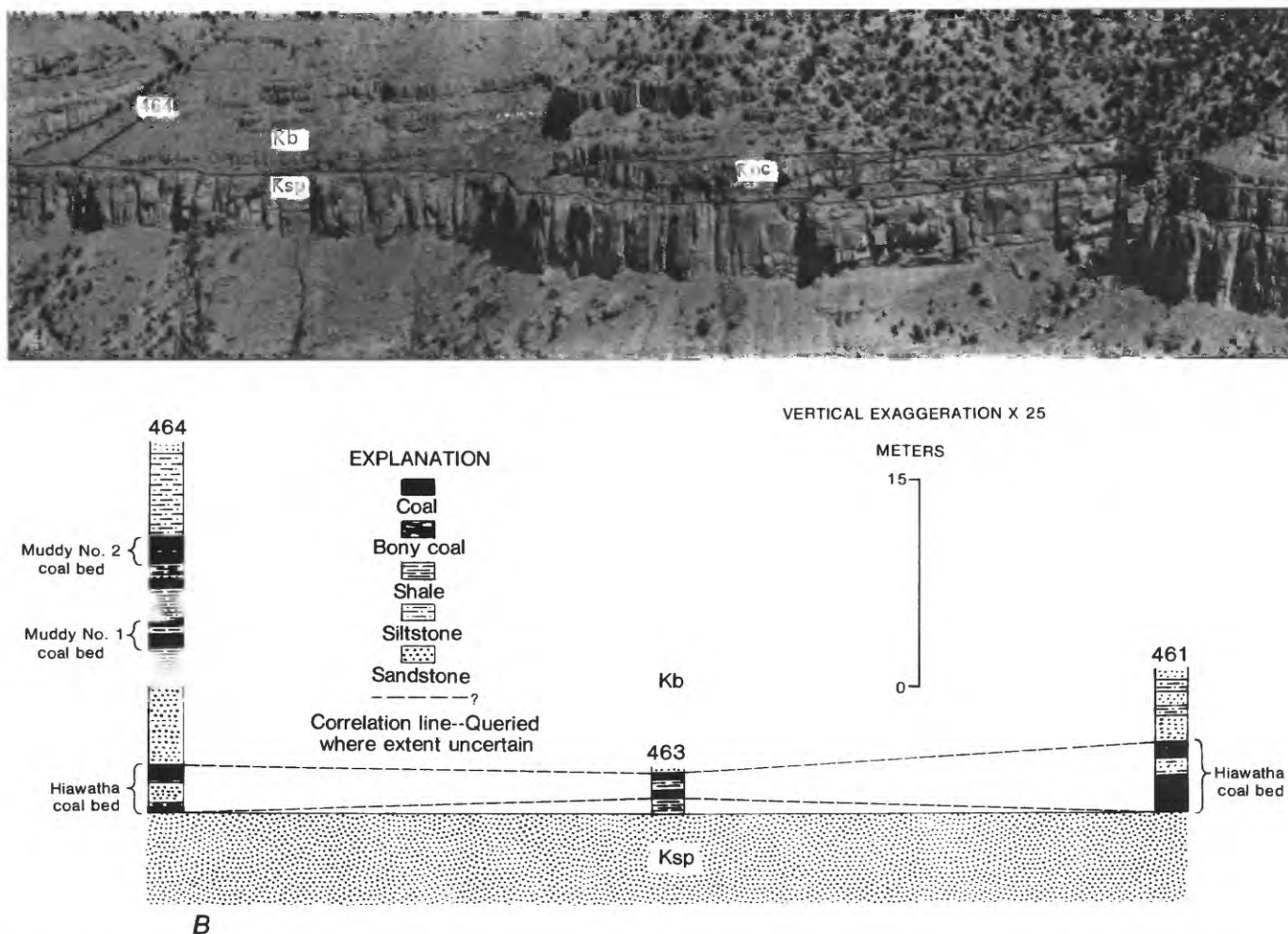
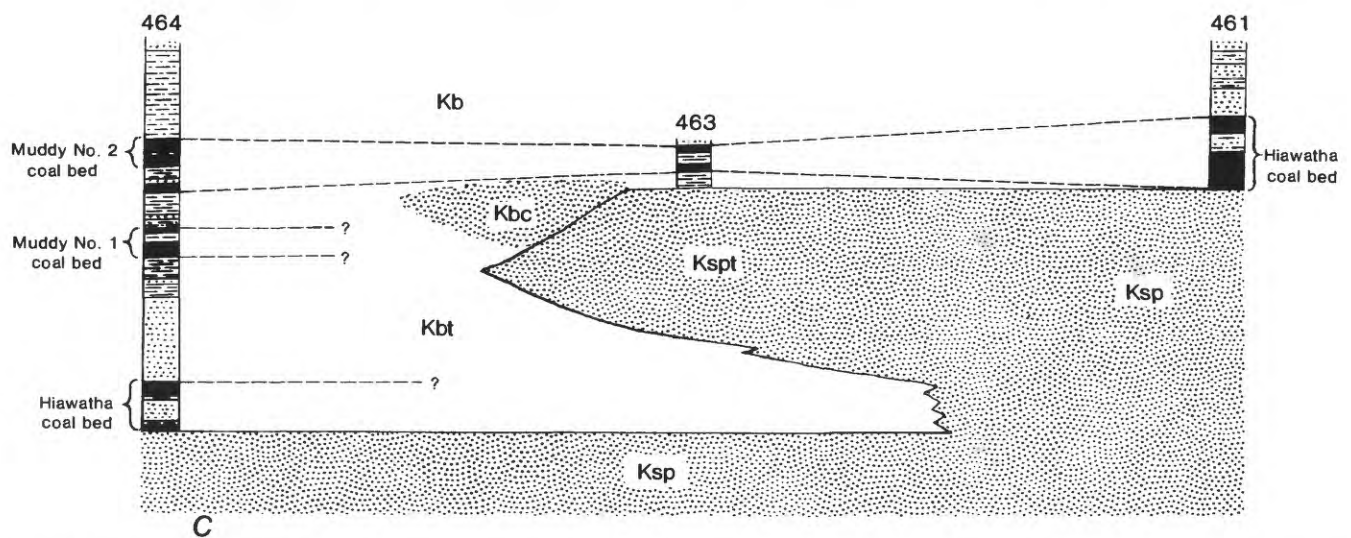


FIGURE 2.—A, Composite panoramic photograph of the north wall of Muddy Canyon in E $\frac{1}{2}$ sec. 36, T. 20 S., R. 5 E., and W $\frac{1}{2}$ sec. 6, T. 21 S., R. 6 E. Intertonguing relations between Star Point Sandstone (Ksp) and Blackhawk Formation (Kb) are shown. The westward projecting tongue of Star Point (Kspt) overlies the eastward projecting tongue of Blackhawk (Kbt); they have a combined thickness of about 20 m. Channel sandstone (Kbc) in Blackhawk and approxi-



mate locations of Spieker's (1931) coal sections 461, 463, and also shown. Outcrop is about 2 km in length and location is indicated on figure 1. *B*, Blackhawk coal-bed correlations of Spieker (1931). *C*, Revised coal-bed correlations proposed in this paper. (Coal-bed names are those of Spieker.)

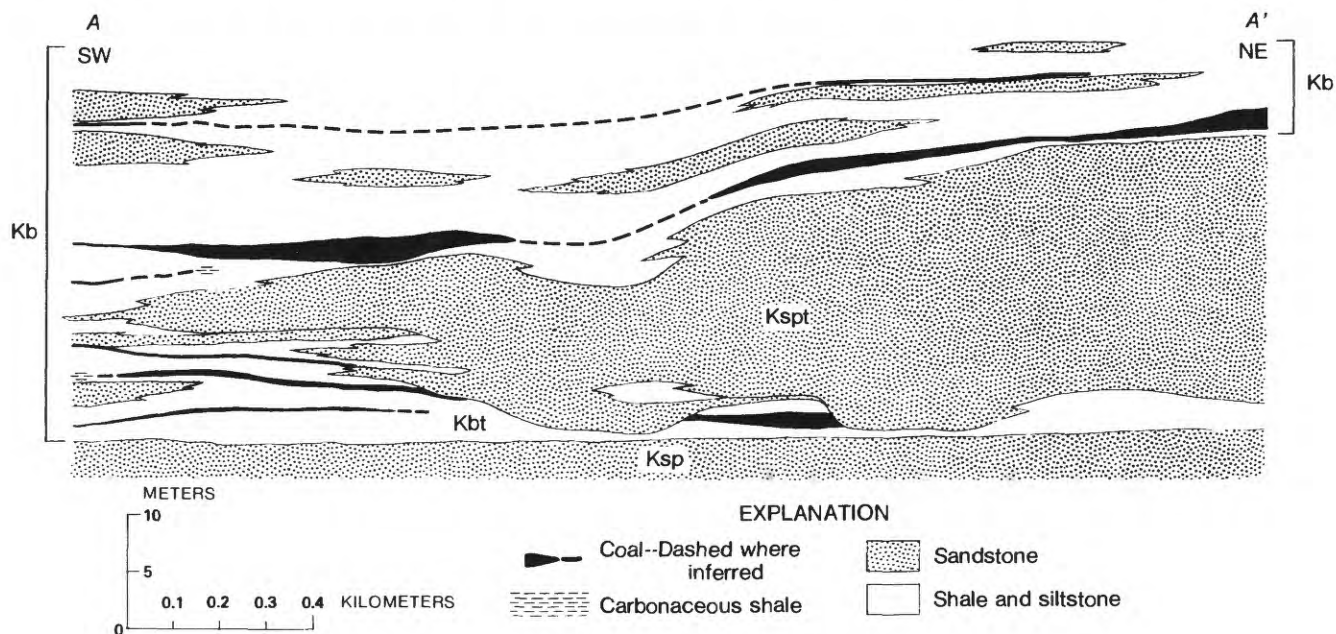


FIGURE 3.—Diagrammatic section A-A' (southwest to northeast) along Wasatch Plateau front (see fig. 1) showing relations among Star Point Sandstone (Ksp), Blackhawk Formation (Kb), and tongues of Star Point (Kspt) and Blackhawk (Kbt). Section is based on tracing of key beds among 13 detailed stratigraphic sections.

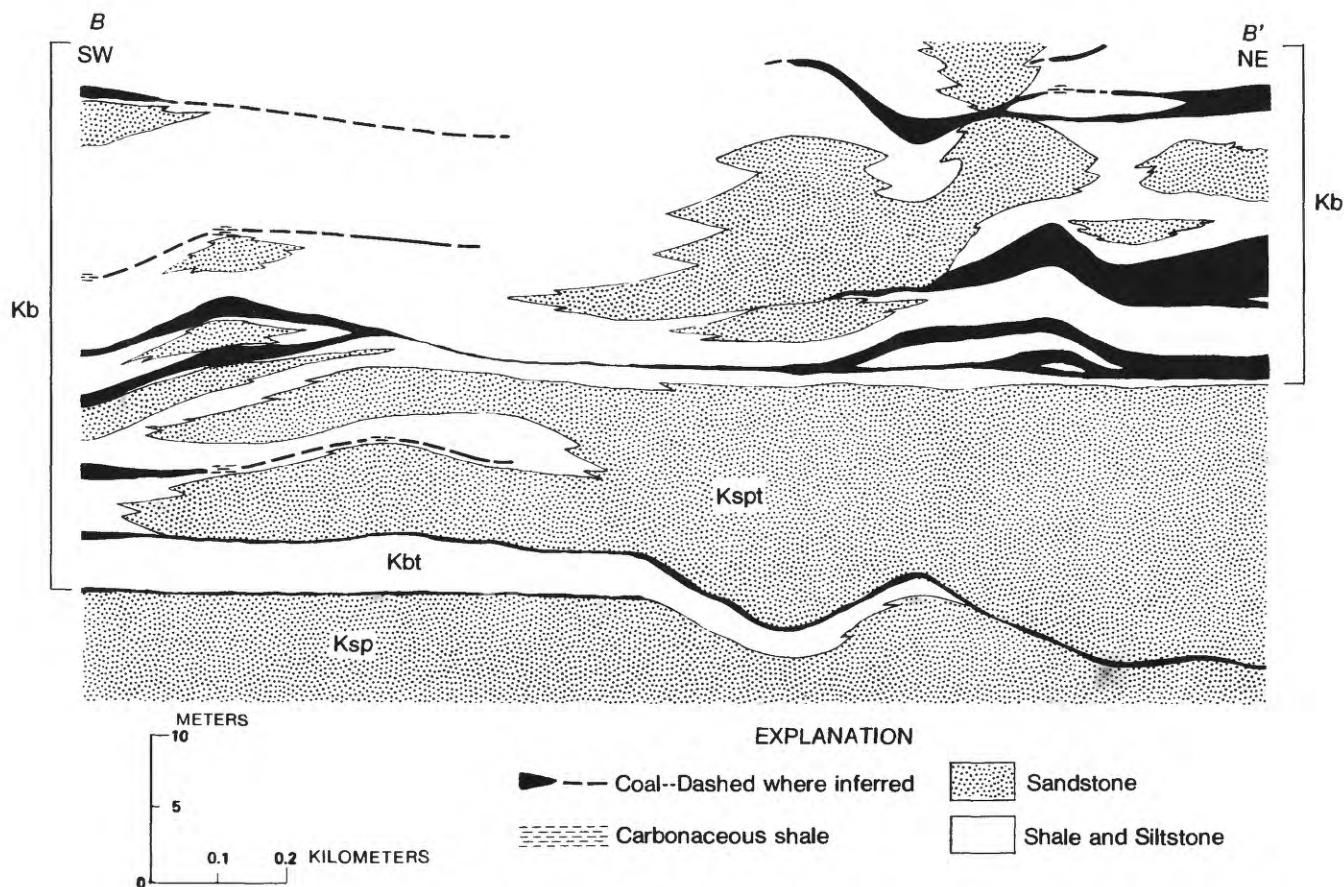


FIGURE 4.—Diagrammatic section B-B' (southwest to northeast) along downfaulted block near Emery (see fig. 1) showing relations among Star Point Sandstone (Ksp), Blackhawk Formation (Kb), and tongues of Star Point (Kspt) and Blackhawk (Kbt). Section is based on tracing of key beds among 12 detailed stratigraphic sections.

New Evidence Supporting Nebraskan Age for Origin of Ohio River in North-Central Kentucky

By W C SWADLEY

SHORTER CONTRIBUTIONS TO STRATIGRAPHY AND
STRUCTURAL GEOLOGY, 1979

GEOLOGICAL SURVEY PROFESSIONAL PAPER 1126-H

*Prepared in cooperation with
the Kentucky Geological Survey*



CONTENTS

	Page
Abstract	H1
Introduction	1
Regional setting	1
Glacial deposits	3
Discussion	5
References cited	6

ILLUSTRATIONS

	Page
FIGURE 1. Map showing the preglacial drainage of the northern Kentucky region and the southern limit of glaciation	H2
2. Map showing location of glacial deposits described in this study	4

NEW EVIDENCE SUPPORTING NEBRASKAN AGE FOR ORIGIN OF OHIO RIVER IN NORTH-CENTRAL KENTUCKY

By W C SWADLEY

ABSTRACT

Glacial deposits at four localities in north-central Kentucky support a Nebraskan age for the origin of the Ohio River drainage system. These deposits, including till and outwash, are deeply weathered and must be as old as Kansan. They occur in valleys that deeply dissect the pre-Pleistocene Madison divide and that were carved by the Ohio River and its tributaries during a long period of erosion. Thus the glacial diversion that disrupted the Pliocene drainage and created the Ohio River substantially preceded the Kansan Glaciation and must have occurred during the Nebraskan Glaciation.

INTRODUCTION

Our understanding of the glacial history of northern Kentucky and of the glaciated portion of the Ohio River has undergone considerable change in recent years. Prior to about 1950, the glacial deposits of northern Kentucky were generally considered to be of Illinoian age. In 1956 Rich determined that the upland till in southwestern Ohio and northern Kentucky was pre-Illinoian, and in 1957 Ray described deposits of deeply weathered till along the Ohio valley in northern Kentucky, to which he assigned a Kansan age. In 1965 Leighton and Ray reported two deeply weathered tills separated by a paleosol on the uplands of northern Kentucky a few miles southwest of Cincinnati. On the basis of the degree of weathering and topographic position of the deposits, they identified the lower till as being of Nebraskan age and the upper as being of Kansan age. In describing the glacial history of the area they attributed the disruption of the preglacial drainage and the formation of the Ohio River to the Nebraskan Glaciation. Swadley (1971) traced the valley of the preglacial Kentucky River northeastward from the area of Carrollton, Ky., and discussed its relation to the development of the Ohio River. In the most comprehensive recent study of the gla-

cial history of the region, Ray (1974) described in more detail the evolution of the glaciated Ohio River and again attributed the development of the Ohio drainage system to Nebraskan Glaciation. Ray's study, based largely on reconnaissance work, has been substantiated by detailed mapping of the joint mapping program recently completed by the U.S. and Kentucky Geological Surveys.

Mapping in north-central Kentucky west of Carrollton has revealed three small deposits of deeply weathered till and outwash that occur at low topographic levels. The low topographic position and deep weathering of these deposits, and their distribution along a major preglacial divide lend further support to a Nebraskan age for the initiation of the present Ohio River.

REGIONAL SETTING

The preglacial drainage system of northern Kentucky consisted of three principal streams; the Kentucky, Licking, and Manchester Rivers (Ray, 1974, p. 15). These streams flowed northward across the central lowland of Kentucky (fig. 1). This lowland, underlain largely by Ordovician limestones and shales, is bordered on the east and the west by outward-dipping escarpments capped by more resistant limestones and dolomites of Silurian age. The preglacial Kentucky River headed in southeastern Kentucky and flowed northwestward essentially along its present course to the area of Carrollton, Ky. Near Carrollton the course of the preglacial Kentucky is marked by an abandoned high-level valley that trends northeast then north from Carrollton to the area of the mouth of the Great Miami River, about 24 km west of Cincinnati. The river flowed through a broad meander belt that lies largely south and east of the present Ohio River (Swadley,

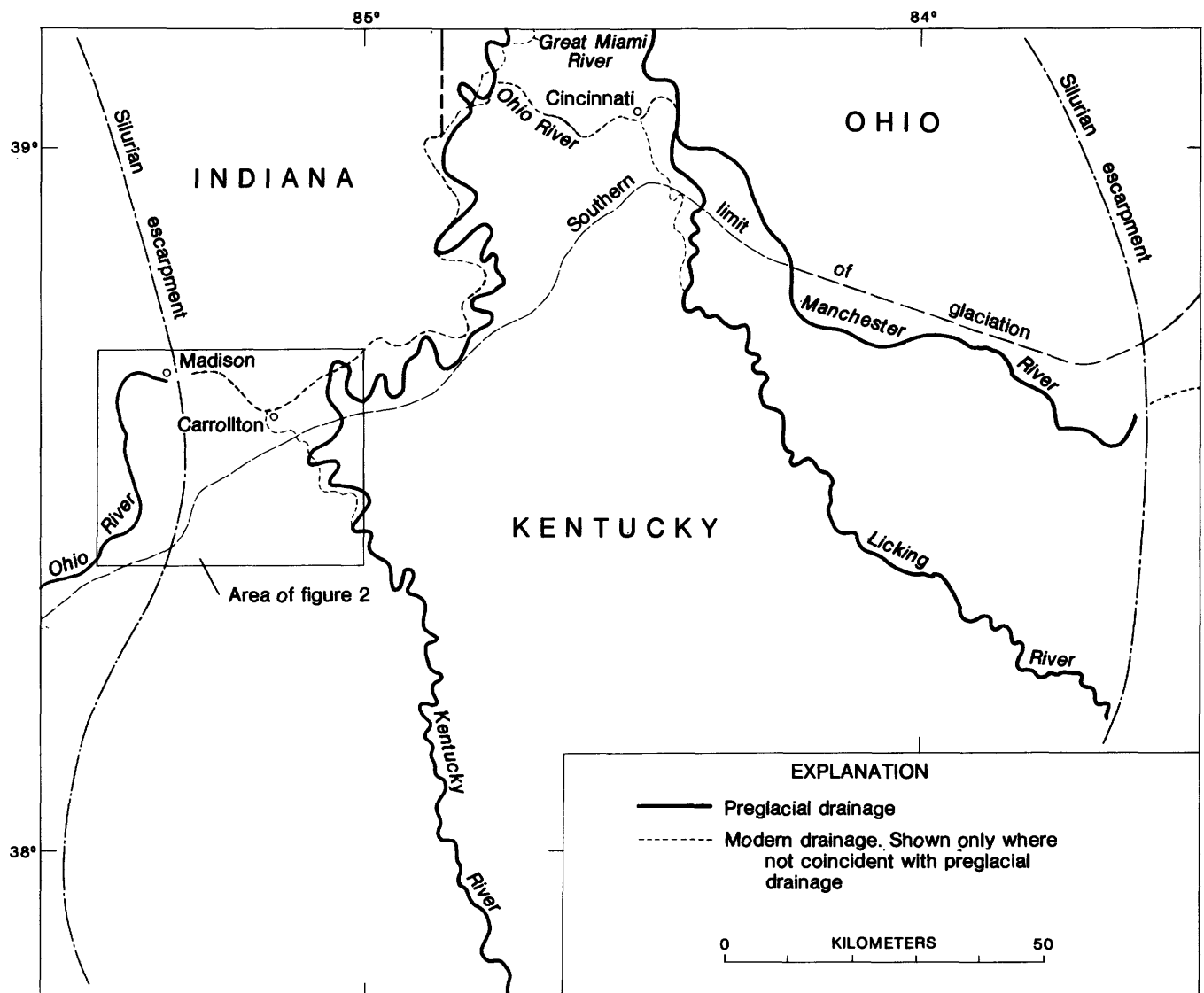


FIGURE 1.—Map showing the preglacial drainage of the northern Kentucky region and the southern limit of glacialiation. Modified from Swadley (1971) and Ray (1974).

1971). West of Cincinnati it turned northeast again, flowing generally along the valley of the modern southwest-flowing Great Miami River. The Kentucky continued northeastward into central Ohio, where it joined the preglacial master stream of the north-central states, the Teays-Mahomet River.

The preglacial Licking River headed in east-central Kentucky and flowed essentially along its present course. South of Cincinnati it flowed east of its modern valley, passed to the east of Cincinnati, and continued northward to join the Kentucky near Hamilton, Ohio, about 32 km to the north. The preglacial Manchester River headed along the eastern Silurian escarpment and flowed northwest to join the Licking River near Cincinnati.

The glacial history of northern Kentucky, as described by Ray (1974), began with ponding of the north-flowing streams by Nebraskan ice moving into Ohio. As the Teays-Mahomet River became dammed by ice, the drainage was diverted to the southwest across the Madison divide. With the advance of ice into northern Kentucky, the valley of the Kentucky River below Carrollton became largely filled with drift, and the drainage over the Madison divide was forced farther to the south (Swadley, 1971). Drift was deposited on the northern Kentucky uplands and in many of the existing stream valleys. After the ice front had retreated from its maximum advance (fig. 1), the developing Ohio River established its new valley. The Ohio entered

the valley of the Manchester River through a break in the eastern Silurian escarpment and then followed that valley to a point north of Cincinnati. North of Cincinnati the Ohio turned southwest along what is now the valley of the Great Miami River, thus reversing the direction of flow of the preglacial Kentucky. From the mouth of the Great Miami it cut a new valley along the edge of the Kentucky River meander belt to the Carrollton area, then flowed westward, probably reversing an east-flowing tributary of the Kentucky, across the Madison divide into the valley of the preglacial Ohio.

The Aftonian Interglaciation, following the Nebraskan Glaciation, was a time of weathering and erosion in northern Kentucky. The Nebraskan Drift was subjected to intense weathering. In the Madison area, dissection by the Ohio River and its tributaries cut more than 90 m below the drift-filled preglacial valleys on the uplands of the divide (Ray, 1974, p. 34).

The Kansan Glaciation seems to have been less extensive than the Nebraskan in northern Kentucky. The limit of the Kansan Drift is vague, because the two tills cannot be distinguished except at a few localities, such as those where two tills are found in superposition. The Kansan ice probably blocked the Ohio River drainage temporarily, but no significant drainage changes have been recognized.

The second interglacial period (Yarmouth) was also a time of weathering and active stream erosion. The Ohio River system eroded to its greatest depth, the so-called "Deep Stage" (Durrell, 1961, p. 52). Most of the Kansan Drift was removed from the Ohio River valley, except for small areas in protected localities. The high-level Nebraskan Drift and its partial covering of Kansan deposits were subjected to further weathering and erosion that destroyed any distinctive topographic expression.

The advance of the Illinoian Glaciation into Kentucky was very limited. Southeast of Cincinnati the ice occupied the Ohio valley and only a small upland area. To the southwest it was confined to the Ohio valley and the lower reaches of a few tributary streams. The only Illinoian Drift recognized in Kentucky within the study area is one deposit at Carrollton and a smaller deposit 4 miles to the west (Swadley, 1976). Permanent drainage modifications affecting northern Kentucky were limited to the Cincinnati area, where the northern loop of the Ohio around Cincinnati was abandoned and the river shifted to its present position on the south side of the city.

The Sangamon Interglaciation, following the Illinoian Glaciation, was another period of erosion and weathering. Tributaries of the Ohio were probably deepened and extended headward, but erosion along the major stream was limited largely to removal of Illinoian Drift and valley train deposits.

Ice of the Wisconsin Glaciation, the last of the four glaciations, failed to reach Kentucky. The most pronounced result of the Wisconsin Glaciation on northern Kentucky was extensive alluviation of the Ohio by glaciofluvial deposits and the accompanying ponding of tributary streams.

GLACIAL DEPOSITS

The glacial deposits of this study lie along the Silurian escarpment at the western edge of the central Kentucky lowland. The escarpment is an area of sharply dissected flat-topped ridges capped by resistant, cliff-forming dolomites and limestones of Silurian age. These formations dip gently westward and form a well-defined cuesta above less resistant limestones and shales of the underlying Ordovician formations. The area (fig. 2) is bordered on the north and west by the Ohio River and on the east by the valley of the Kentucky River. The elevations of the higher ridges range from 260 to 275 m. The area is cut by a number of short, steep streams that flow generally southwestward into the Ohio River at an elevation of 128 m. Streams heading on the east side of the divide flow into the Little Kentucky River, a tributary of the Ohio. Where the Ohio River cuts through the escarpment at Madison, the valley is very narrow with nearly vertical walls.

The glacial deposits of the study area (fig. 2) consist of till and lesser amounts of outwash. Most are deeply weathered. A high-level till forms thin, discontinuous caps on many of the flat-topped ridges but exhibits no distinctive topographic expression. The deposits are generally poorly exposed, but where mapped in the Bedford area (Swadley, 1977a, 1977b) they occur at elevations above 245 m. The till consists of reddish-orange to reddish-brown clayey silt that contains common to locally abundant gravel and sand. Limonite pellets and nodules are generally abundant. The till is as much as 10 m thick locally, but most ridgetop caps are probably only 3–5 m thick. The gravel portion of the till consists largely of angular fragments of weathered chert of the type produced by weathering of the Silurian dolomites of the area. Other clasts found in the gravel are rounded pebbles, cobbles, and boulders of quartz, quartzite, basalt, granite, gneiss, and schist.

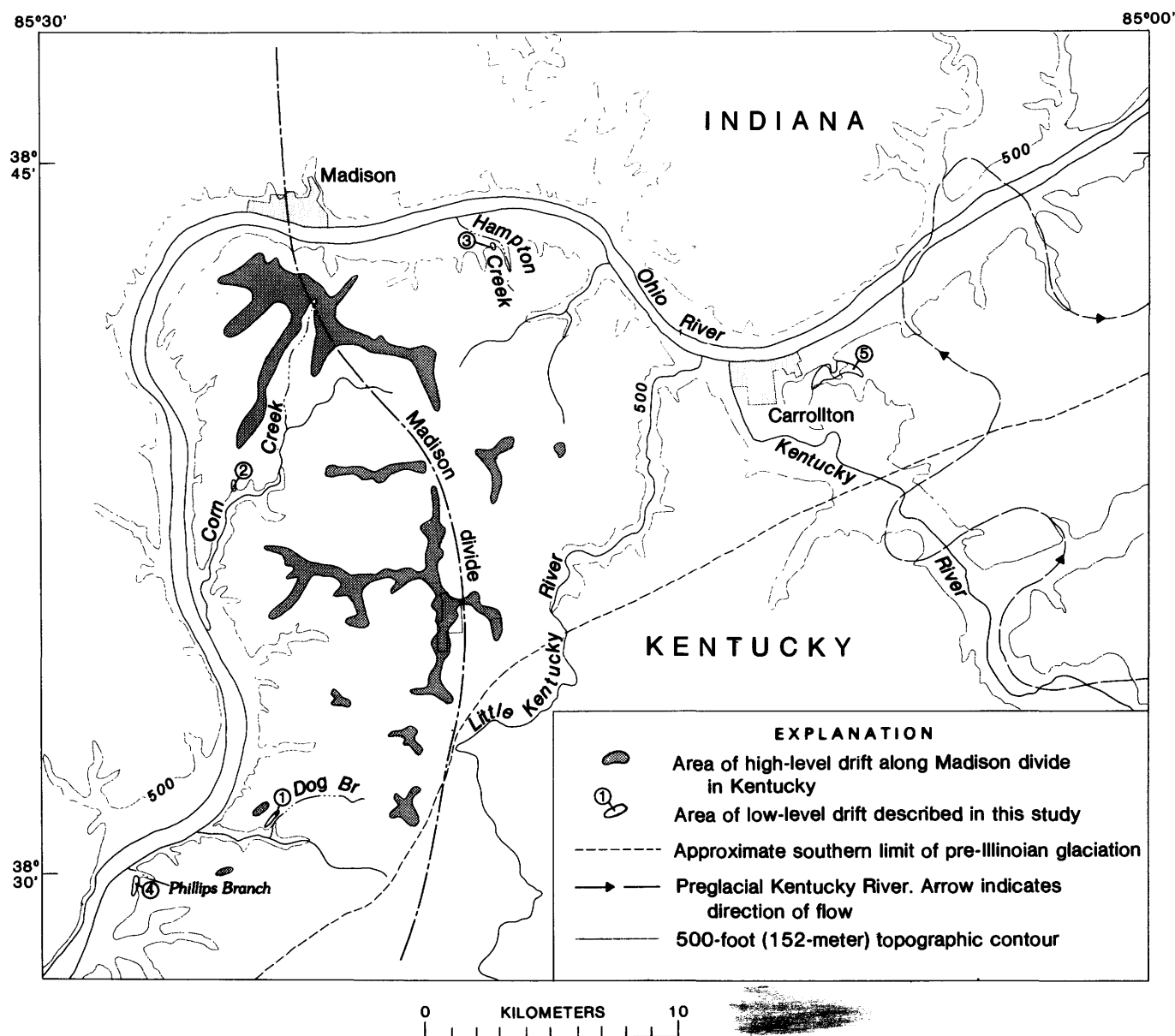


FIGURE 2.—Map showing location of glacial deposits described in this study

Many igneous rock fragments are thoroughly weathered and crumble easily. In all exposures studied, the drift was completely leached of carbonate minerals. Locally the drift drapes down along valley sides in what appear to be deposits that filled preglacial valleys at elevations as low as 245 m.

Low-level drift occurs at four localities in the study area. Three of these were unreported prior to the Kentucky mapping program. The fourth occurrence was reported by Ray (1957). At the first locality (fig. 2, locality 1), outwash and till occur on low ridges on both sides of Dog Branch in the southern part of the Bethlehem quadrangle (Swadley, 1977b).

The ridge along the north side of Dog Branch is capped by a narrow band of drift for a distance of 1.3 km. The base of the drift descends from an elevation of 230 m at the north end to 170 m at the south. The drift is poorly exposed but seems to consist largely of weathered sand and gravel that contains no calcareous minerals. The drift includes chert, quartz, quartzite, and igneous and metamorphic rocks similar to those in the high-level drift. The composition and configuration indicate the deposit is glacial outwash that filled a small, steep valley. Subsequent erosion has cut new valleys on either side, producing a topographic reversal. Dog

Branch now flows at approximately 152 m elevation in this area. The ridge along the southeast side of Dog Branch is capped for about 0.3 km by two small areas of drift (not shown in fig. 2) at an elevation of about 230 m. The drift consists of weathered, noncalcareous silty clay till similar to the high-level till but less oxidized. Boulders, including some basalt and calcitic dolomite, are common and generally less weathered than those of the higher till. The till is 3 to 5 m thick.

The second low-level drift exposure (fig. 2, locality 2) is in the Madison West quadrangle (Swadley, 1978), in the valley of Corn Creek 3.4 km upstream from where it joins the Ohio River valley. Here drift caps a small ridge along the north side of Corn Creek valley at an elevation of 208 m and extends downward along the nose of the ridge to 152 m. Most of the deposit appears to be gravelly sand outwash. Near the base, an abandoned borrow pit exposes 5 m of reddish-brown, limonite-stained sand and clayey sand containing common to abundant siliceous gravel. This is underlain by 2.4 m of light-brown sandy clay till with scattered chert, quartz, and igneous clasts. The till, which is leached of calcareous minerals and includes igneous boulders that crumble easily, rests on ledges of Ordovician limestone.

The third occurrence is about 6.4 km upstream from Madison, Ind., at the base of the south wall of the Ohio River valley (fig. 2, locality 3). This deposit, at an elevation of 152 m, lies 0.3 km west of the point where Hampton Creek debouches into the Ohio River valley (Madison East quadrangle, Gibbons, 1978). Here drift and loess form a low spur about 12 m high that juts northward from the main valley wall. Drift is exposed along the nose and east side of the spur in natural exposures as well as along a drainage ditch that cuts across the north end of the spur. A steep face at the end of the spur exposes 5.2 m of medium-brown sandy silt-clay till overlain by 4.6 m of reddish-brown loess. Abundant gravel in the till consists largely of angular fragments of weathered chert but also includes well-rounded quartz and chert pebbles and cobbles of weathered granite, basalt, and gneiss. The till matrix is leached of carbonate minerals and includes no limestone gravel. Along the east side of the deposit an excavation for a pond spillway exposes 2.1 m of till resting on limestone. The till is pale-yellowish-brown noncalcareous silty clay streaked with limonite stains.

A fourth occurrence of low-level drift in the study area was known prior to the recent mapping. At the mouth of Phillips Branch on the west side of the

Madison divide (fig. 2, locality 4), drift forms a number of steep, sharply dissected ridges as much as 30 m high. Ray (1957) described the drift in fresh roadcut exposures and assigned a Kansan age based on the weathering profile. Mapping of the Bethlehem quadrangle (Swadley, 1977b) indicates that the deposit includes both till and outwash. Till capping the ridges is reddish-brown clayey silt containing scattered to abundant chert, quartz, and igneous and metamorphic pebbles and cobbles. Most of the drift body is crossbedded limonite-stained sand and coarse, poorly sorted gravel that includes abundant limestone clasts and local calcite cement. The basal calcareous till described by Ray is now slumped and covered. The drift rests on a bedrock bench at an elevation of 137 to 143 m.

In marked contrast to the deeply weathered drift are the deposits of drift of Illinoian age in the study area. About 22 km east of Madison, at Carrollton (fig. 2, locality 5), is a body of drift that has long been recognized as being Illinoian in age (Ray, 1974, p. 48). The deposit occurs in an abandoned meander of the Kentucky River valley at a point where the valley wall separating the Kentucky and Ohio Rivers had been breached by lateral erosion of the two rivers, allowing Illinoian ice moving down the Ohio to push into the Kentucky valley. The till deposited was largely protected from later erosion that removed most of the Illinoian glacial deposits from the Ohio valley in the area. The deposit consists of medium-gray calcareous clay till that contains abundant limestone clasts and common to scattered pebbles and cobbles of quartz, chert, and igneous and metamorphic rocks. The elevation of the deposit ranges from 150 to 160 m; the base is not exposed. During the mapping of the Carrollton area (Swadley, 1976) good exposures of till were noted in roadcuts and in a small borrow pit at the north edge of the deposit.

DISCUSSION

Field evidence in the study area indicates the presence of two tills along the Madison divide. The high-level till is the more deeply weathered and older of the two and occurs at elevations of 245 m and above. Before the Silurian escarpment had been breached, the area was drained by the north-flowing preglacial Kentucky River on the east and by local consequent streams to the west. Near Carrollton the Kentucky flowed at an elevation of 204 m (Swadley, 1971). The Madison divide, 30 km to the west, was part of a broad upland that stood well above the

valley of the Kentucky. The maximum preglacial dissection along the divide is indicated by remnants of shallow valleys occupied by the high-level till at about 245 m. The deep dissection of the divide by the Ohio River had not begun at the time the high-level till was deposited, as indicated by the following evidence.

West of the Madison divide the modern Ohio River follows the valley of the preglacial Ohio (fig. 1). Upstream from Cincinnati it largely coincides with the preglacial Manchester River, but in the area between Carrollton and the mouth of the Great Miami River, the Ohio does not follow the preglacial drainage. As the Madison divide was cut and the ponded waters began draining to the southwest, the Ohio created a new valley, which closely paralleled the preglacial Kentucky River valley and intersected it at several points (fig. 1) but did not occupy it. In order for this to occur some mechanism would have been required to make the preglacial Kentucky unavailable to the developing Ohio.

In a description of the preglacial Kentucky River between Carrollton and the mouth of the Great Miami, Swadley (1971) reported field evidence in northern Kentucky that indicates the glacial lake ponded against the Madison divide was still intact when the first glacier entered Kentucky. That report suggests that the major breaching of the Madison divide and the initiation of the Ohio occurred after the first glacier had withdrawn from its maximum advance and after the preglacial Kentucky valley northeast of Carrollton had been filled with drift. The Ohio developed, probably as an ice-margin stream, along the edge of the preglacial Kentucky River meander belt but did not occupy the existing valley because it had been filled with drift. Remnants of this drift still occur along the course of the old Kentucky at many points. Therefore, drift deposition by the first glacier occurred south of the Ohio in the study area prior to the cutting of the Ohio valley and at elevations equal to or above the preglacial drainage. Thus, the elevations would have been about 200 meters within the old Kentucky valley and well above that along the Madison divide.

The low-level drift at the Dog Branch, Corn Creek, and Hampton Creek localities was deposited by a later glacial advance. These deposits occur at elevations as low as 150 m, well below the level of the main drainage (204 m at Carrollton) at the start of glacial activity in the region. Therefore, they must have been deposited much later than the high-level till, after a lengthy period of active stream erosion during which the Ohio and its small trib-

utaries were entrenched as much as 100 m below the preglacial surface. These exposures, although less weathered than the high-level till, are completely lacking in limestone gravel and appear to be much more extensively leached than either the calcareous Illinoian Till at Carrollton (locality 5) or similar bodies of limestone-rich Illinoian Till further upstream along the Ohio valley (Swadley, 1973).

The Hampton Creek locality, in the Ohio valley 16 km downstream from Carrollton, is considered to be pre-Illinoian only on the basis of the degree of weathering described above. The Dog Branch and Corn Creek localities are considered to be pre-Illinoian because of both the degree of weathering and their topographic position. They occur in sharply incised valleys about 3.2 km upstream from where these valleys join the Ohio. These locations, well back from the Ohio in areas where no indications of Illinoian Glaciation have been recognized on the surrounding uplands, make it very unlikely that they are Illinoian. Deposition by a tongue of Illinoian ice moving down the Ohio valley, as was postulated for the origin of the till at Carrollton (Ray, 1974, p. 48), would require a minor tongue to have split off at an obtuse angle and have moved more than 3.2 km up a narrow creek valley from the Ohio. Such an explanation seems untenable. On the basis of their topographic position and the degree of weathering, the deposits are here assigned a Kansan age.

Thus, the presence of drift of Kansan age at low topographic levels within the Ohio River drainage system indicates that the Ohio predates the Kansan Glaciation and, therefore, that the glacial disruption of the Pliocene drainage and the initiation of the Ohio River occurred during the Nebraskan Glaciation.

REFERENCES CITED

- Durrell, R. H., 1961, The Pleistocene geology of the Cincinnati area, in *Guidebook for field trips, Cincinnati meeting, 1961*: New York, Geological Society of America, p. 47-57.
- Gibbons, A. B., 1978, Geologic map of part of the Madison East quadrangle, Trimble and Carroll Counties, Kentucky: U.S. Geological Survey Geologic Quadrangle Map GQ-1471, scale 1:24,000.
- Leighton, M. M., and Ray, L. L., 1965, Glacial deposits of Nebraskan and Kansan age in northern Kentucky, in *Geological Survey research 1965*: U.S. Geological Survey Professional Paper 525-B, p. B126-B131.
- Ray, L. L., 1957, Two significant new exposures of Pleistocene deposits along the Ohio River valley in Kentucky: *Journal of Geology*, v. 65, no. 5, p. 542-545.
- , 1974, *Geomorphology and Quaternary geology of the glaciated Ohio River Valley—a reconnaissance study*: U.S. Geological Survey Professional Paper 826, 77 p.

- Rich, J. L., 1956, Pre-Illinoian age of upland till in southeastern Indiana, southwestern Ohio, and adjacent parts of Kentucky [abs.]: Geological Society of America Bulletin, v. 67, no. 12, pt. 2, p. 1756.
- Swadley, W C, 1971, The preglacial Kentucky River of northern Kentucky, in Geological Survey research 1971: U.S. Geological Survey Professional Paper 750-D, p. D127-D131.
- 1973, Geologic map of parts of the Vevay South and Vevay North quadrangles, north-central Kentucky: U.S. Geological Survey Geologic Quadrangle Map GQ-1123, scale 1:24,000.
- 1976, Geologic map of part of the Carrollton quadrangle, Carroll and Trimble Counties, Kentucky: U.S. Geological Survey Geologic Quadrangle Map GQ-1281, scale 1:24,000.
- 1977a, Geologic map of the Bedford quadrangle, north-central Kentucky: U.S. Geological Survey Geologic Quadrangle Map GQ-1409.
- 1977b, Geologic map of part of the Bethlehem quadrangle, Trimble and Oldham Counties, Kentucky: U.S. Geological Survey Geologic Quadrangle Map GQ-1436, scale 1:24,000.
- 1978, Geologic map of part of the Madison West quadrangle, Trimble County, Kentucky: U.S. Geological Survey Geologic Quadrangle Map GQ-1469, scale 1:24,000.

Reconnaissance Geologic Study of the Vazante Zinc District Minas Gerais, Brazil

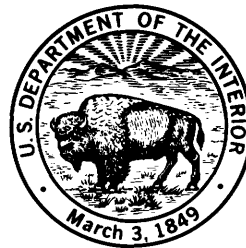
By CHARLES H. THORMAN, U.S. GEOLOGICAL SURVEY, *and*
SAMIR NAHASS, MINISTERIO DAS MINAS E ENERGIA, BRAZIL

SHORTER CONTRIBUTIONS TO STRATIGRAPHY AND
STRUCTURAL GEOLOGY, 1979

GEOLOGICAL SURVEY PROFESSIONAL PAPER 1126-I

*Prepared in cooperation with the
Ministerio das Minas e Energia, Brazil*

*The geology and the structural control of
the Vazante Zinc deposits in the
Paraopeba Formation were determined
primarily from aerial photographs*



CONTENTS

	Page
Abstract	II
Introduction	1
Acknowledgments	2
Regional setting	2
Description of geologic units	3
Paraopeba Formation	3
Unit A	3
Unit B	3
Unit C	7
Structure	8
Folds	8
Lineations	8
Faults	8
Mineralization and reserves	10
Summary	11
References cited	11

ILLUSTRATIONS

	Page
FIGURE 1. Index map of Brazil and the Vazante region	I2
2. Geologic map and cross sections of the Vazante zinc district, Minas Gerais, Brazil	4
3. Diagrammatic stratigraphic sections of the late Precambrian Bambuí Group (1,000–600 m.y.) for the western side of the Bambuí basin and of the Paraopeba Formation in the Vazante district	6
4. Photograph of thin-bedded, folded phyllite of unit A	7
5. Panoramic view of Serra do Poço Verde, viewed from the south	7
6. Diagrammatic examples of ways in which breccia zones may form along step-bedding faults	10
7. Photograph of resistant ridge of mineralized breccia (primarily hemimorphite, hydrozincite, willemite) on the north end of Serra do Poço Verde	11

RECONNAISSANCE GEOLOGIC STUDY OF THE VAZANTE ZINC DISTRICT, MINAS GERAIS, BRAZIL

By CHARLES H. THORMAN and SAMIR NAHASS¹

ABSTRACT

The Vazante district, Minas Gerais, 130 km south of Paracatu, produces most of Brazil's zinc metal. The district is in the western part of the late Precambrian Bambuí basin along the eastern and leading edge of the north-trending Brazilian orogenic belt (ca. 600–500 m.y.). Bedding and low-angle thrust faulting, folding, and low-grade metamorphism dominated the structural development. Trends within the district are northeast, and dips are 20°–45° NW. Three sets of folds developed during the main period of eastward thrusting of older Precambrian rocks over the west margin of the Bambuí basin. A fourth fold set is transverse to the regional trend. Rocks in the district are tentatively assigned to the Paraopeba Formation of the Bambuí Group and are designated units A through C in ascending order. The contacts between units A, B, and C are interpreted to be low-angle or bedding faults; their original stratigraphic positions with respect to each other are unknown.

The Vazante deposit is epigenetic. Zinc silicate minerals (hemimorphite and willemite) occur in a folded breccia zone in the lower part of unit B of the Paraopeba Formation. The breccia zone is interpreted to be tectonic in origin, having formed along the step of a step-bedding-plane fault during Brazilian time. The source of the zinc is probably syngenetic in the Paraopeba Formation. Broad uplift and deep weathering of the region and concurrent supergene enrichment took place during late Mesozoic and Cenozoic time. Approximately 110,000 metric tons of zinc metal were produced from 1965 to 1974; reserves may be as much as 3 million metric tons.

INTRODUCTION

The Vazante zinc district, the largest zinc-producing area in Brazil, is about 130 km south of Paracatu and 120 km northwest of Patos de Minas in the western part of the State of Minas Gerais (fig. 1). Companhia Mineira de Metais at Serra do Poço Verde and Companhia Mercantil Industrial Ingá at Serra do Ouro Podre (fig. 2), the only companies operating in the district, produced approximately 110,000

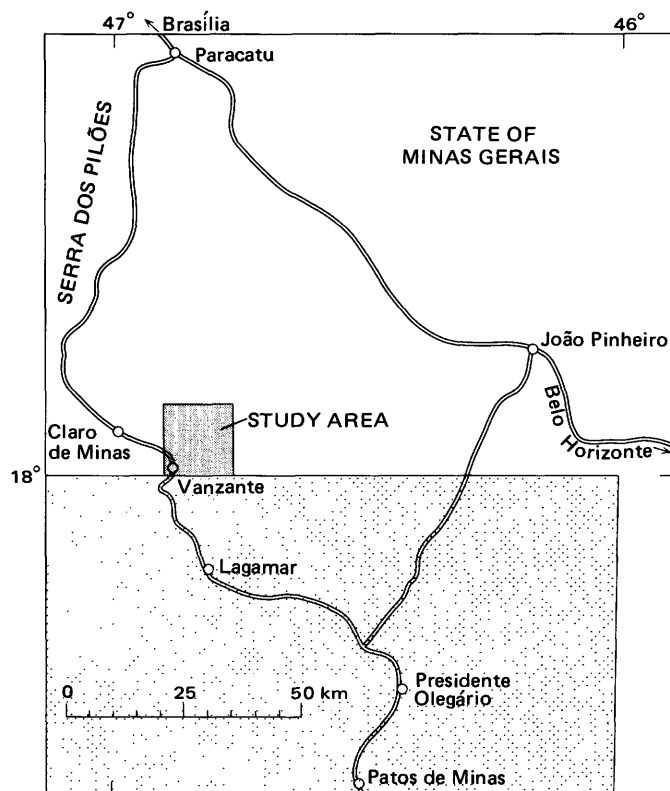
metric tons of zinc metal from 1965 to 1974 (White and Nagell, 1975; Bohomoletz, 1975, p. 176).

The purpose of our investigation was twofold: First, a geologic map of the Vazante region was needed to serve as a base for a pilot geochemical study of the Vazante district. This pilot study was the initial phase of Projeto Bambuí, a reconnaissance geochemical exploration program of the Bambuí basin undertaken by the CPRM (Companhia de Pesquisa de Recursos Minerais) for the DNPM (Departamento Nacional de Produção Mineral). Second, a better understanding of the structural setting of the district was needed to evaluate the feasibility of looking for additional Vazante-type deposits. This report was prepared as part of the cooperative program of the Ministério das Minas e Energia (MME) and the U.S. Geological Survey (USGS), sponsored by the Government of Brazil and the U.S. Agency for International Development (USAID), of the U.S. Department of State.

Luciana Jacques de Moraes (unpublished data, 1955) presented the first study of Vazante, and Moore (1956), of the USGS, studied the Serra do Poço Verde. Subsequently, Carvalho, Dequech, and Guimarães (1962), Branco (1962), Guimarães (1962), and Cassedanne (1968a,b) reported on the Vazante deposit. These studies were restricted primarily to the deposit and to the narrow cuesta along which mineralization occurs. Amaral (1968) was the first to map the surrounding terrain. Companhia Mercantil e Industrial Ingá began production in 1965, and Companhia Mineira de Metais, in 1970.

This investigation was of a reconnaissance nature. Approximately three weeks were spent preparing a photogeologic map from 1:25,000-scale aerial photographs (fig. 2). Five days in March and April 1974 were spent field checking the photogeologic interpretations.

¹ Companhia de Pesquisa de Recursos Minerais, Ministério das Minas e Energia, Rio de Janeiro, Brazil.



Several local names for individual parts of the main cuesta near the base of unit B (subunit B-3) along which mineralization took place are shown on the geologic map. We are not aware of any single name that applies to the entire cuesta. For ease of reference we have adopted the informal term "mineralized cuesta" to refer to the entire feature.

ACKNOWLEDGMENTS

We wish to acknowledge the many fruitful discussions with Dr. Oscar P. G. Braun, CPRM, that helped us develop our thoughts and ideas on the geology of the region. The aid and support of Dr. Benedito P. Alves, late Chief of the CPRM Agency in Belo Horizonte, was especially appreciated. Drs. Carlos Alberto Heineck and Hugo Peter Steiner, CPRM, took part in our field work, and their assistance is gratefully acknowledged. Dr. Percio Branco, CPRM made several pertinent, helpful suggestions during the final preparation of the manuscript. We especially acknowledge the support of Dr. João Batista de Vasconcelos Dias, CPRM who was Director and Coordinator of the MME-USAID agreement during our investigation.

REGIONAL SETTING

The study area is in a deformed belt (fig. 1) along the western margin of the Bambuí basin, a late Precambrian basin (1,000–600 m.y.) filled with siltstone, marl, conglomerate, sandstone, limestone, and dolomite of the Bambuí Group. The clastic and pelitic rocks were derived from a highland west of the deformed belt. Older Precambrian rocks were thrust eastward over the western edge of the basin during the Brazilian orogeny (ca. 600–500 m.y.); the orogeny formed a major north-trending deformed belt about 1,000 km long, characterized by low-angle thrust faults, bedding-plane faults, large folds, and widespread low-grade metamorphism. Allochthonous rocks in the belt include the following Precambrian units, in ascending order (Barbosa and others, 1970): granite-gneiss complex; mica schist, quartzite, and amphibolite of the Araxá Group; quartzite and phyllite of the Canastra Group; and calc-schist of the Ibiá Formation, a basal unit of the Canastra. The Vazante area is about 30 km east of the Serra dos Pilões, in which the easternmost major thrust brings Canastra over the Bambuí (fig. 1). Smaller scale thrusting and broad folding of the deformed belt extend to about 100 km east of Vazante. Only the Bambuí Group is present in the study area.

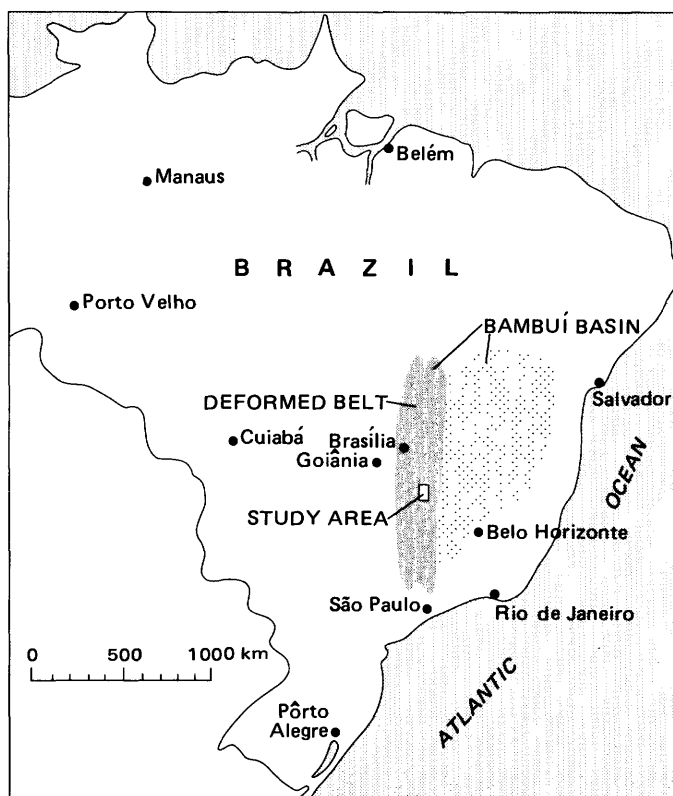


FIGURE 1.—Index map of Brazil and the Vazante region. Triângulo Mineira area (patterned) south of Vazante, studied by Barbosa and others (1970).

Previous workers interpreted the structural setting at Vazante as one of normal faulting or tensional tectonics. A plausible alternative presented here involves compressional tectonics associated with essentially no normal faulting but with thrust, bedding, and step-bedding faulting and related structural complications consistent with the structural environment of the deformed belt within which the Vazante district is located. Barbosa and others (1970) mapped these types of structures in the Triângulo Mineira immediately to the south of Vazante (fig. 1).

DESCRIPTION OF GEOLOGIC UNITS

Braun (1968; and oral commun., 1974) assigns all the rocks in the Vazante region, herein mapped, to the Paraopeba Formation of the Bambuí Group; Amaral (1968) considered the eastern two-thirds of the Vazante region to be underlain by the Sete Lagoa Formation of the Bambuí Group and the western one-third, by the Canastra Group. This report follows the work of Braun. We divided the Paraopeba Formation into three informal units (A, B, and C, in ascending order). Figures 3A and 3B are diagrammatic stratigraphic sections of the Bambuí Group of the western side of the Bambuí basin and of the Paraopeba Formation in the study area. It is possible that unit A includes some Paranoa Formation and unit C some Tres Marias Formation.

The relative stratigraphic positions of units A, B, and C are not clear at this time. The contact between units A and B—the Santa Catarina fault—is based on the marked contrast between the pronounced, pervasive, penetrative deformation and low-grade metamorphism of unit A and the generally local and much weaker low-grade metamorphism of unit B. Beds on opposite sides of the Santa Catarina fault are more or less concordant. The nature of the contact between unit B and C—the Vazante fault—is less clear. Along the southern half of the fault's exposure, beds are commonly discordant on a small scale across the contact, whereas beds are concordant across the contact to the north. Sandstone is more abundant than limestone in unit C, whereas limestone is more abundant than sandstone in unit B.

The Vazante fault, between units B and C, is here interpreted as a bedding fault that locally has brought about discordant stratigraphic relationships, thus implying that unit B is older than and grades upward into unit C. In contrast, the Santa Catarina fault appears to be a larger structure, and

the stratigraphic relationship between unit A and units B and C is open to question.

PARAOPEBA FORMATION

UNIT A

Unit A is dominantly a silty micaceous phyllite with thin lenses of quartzite. The phyllite varies in color from tan to brown to reddish yellow: the quartzite beds are cream colored and have dark red-brown iron-oxide coatings on weathered surfaces. The rocks are commonly laminated (fig. 4). A moderate to well-developed foliation at 20°–90° to the bedding is typical and has often been misidentified as bedding. Fracture and crenulation cleavage and incipient foliation at 20°–40° to the bedding are common in the quartzite lenses. Lineations and small-scale folds are common. Thickness of the unit is unknown, but it probably exceeds 500 m.

UNIT B

Unit B forms a sinuous northeast-trending belt that ranges in width from 5 km in the southwest to 2 km in the northeast. The dominant lithology is massive to medium-bedded, cream-colored to light-gray, aphanitic to fine-grained dolomitic limestone. *Collenia*, an algal stromatolite, occurs in some beds (Cassadanne, 1968a), and siliceous layers are locally present. A few thin beds of medium-grained, well-sorted, light-colored quartzite were noted near the crest of Serra do Poço Verde. Interbedded with the limestone are thin-bedded, in part laminated marl, shale, and siltstone that vary in color from red to buff to brown to green.

The massive to thick-bedded limestone underlies cuestas and isolated hills that alternate with elongate and irregularly shaped valleys underlain by marl, shale, siltstone, and, in some places, limestone. This topography is typical of unit B. A major characteristic of the Paraopeba Formation is the rapid lateral and vertical facies change from carbonate to argillaceous rocks (Braun, 1968). A major problem in understanding the geology of the Vazante area is deciphering the relationship of the limestone hills to the shale and marl valleys that are on strike with the hills. At several localities a 50- to 80-m section of limestone will change along strike to a comparable thickness of shale within less than 20 m. In a small pit about 2 km south of the Ingá mining operation, approximately 10 m of thick-bedded limestone containing thin argillaceous partings grades laterally into shale and thin-bedded limestone in a distance of about 20 m.

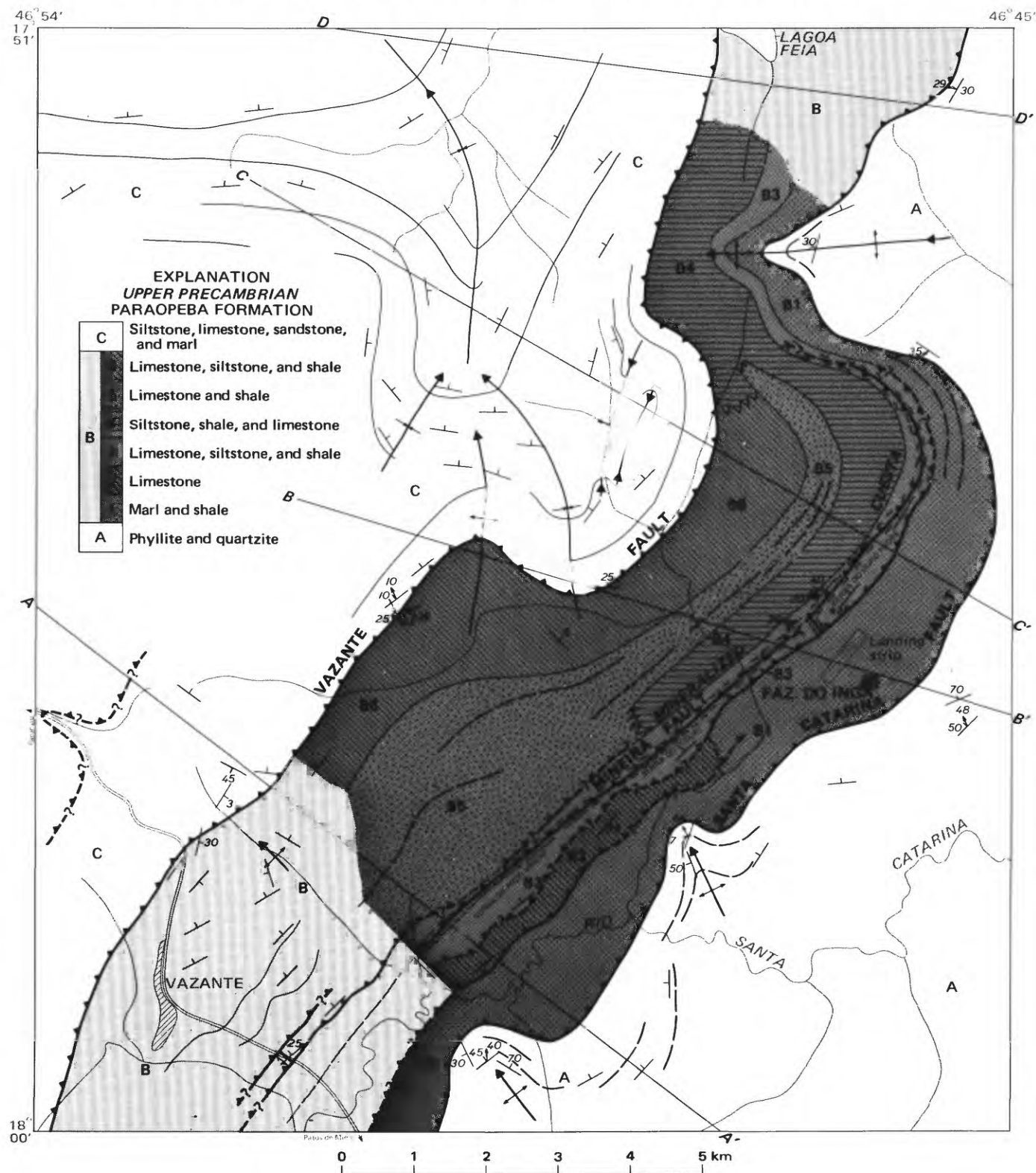
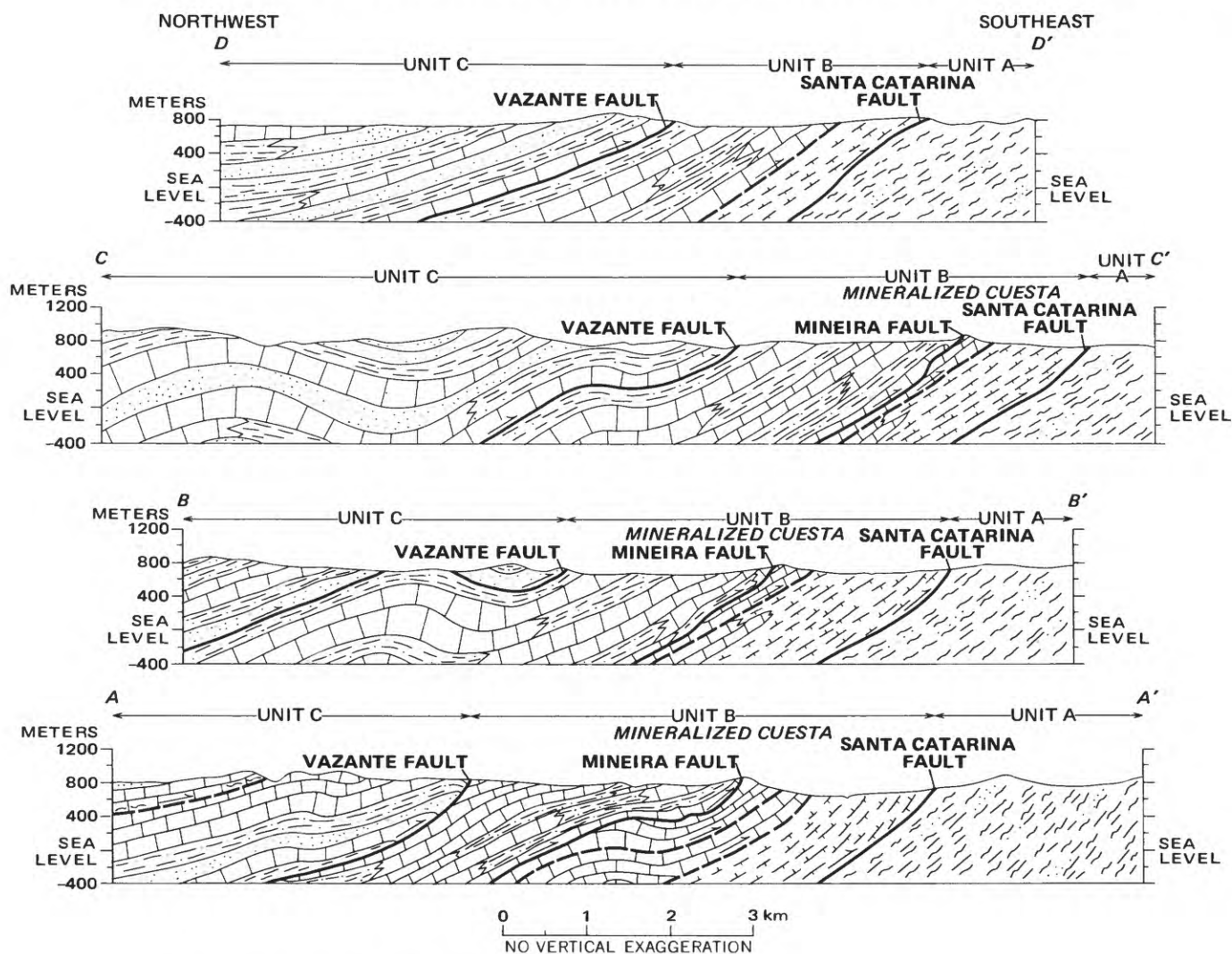
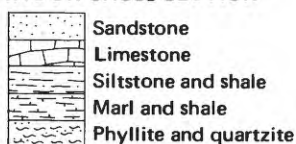


FIGURE 2.—Geologic map and cross sections of the Vazante district, Minas Gerais, Brazil.



LITHOLOGIC UNITS ON CROSS SECTION



Thrust fault—Arrows show direction of relative movement. Dashed where inferred

MAP AND CROSS SECTION EXPLANATION

- Trace of marker bed from aerial photographs
- Trend or lineament from aerial photographs
- Contact—Dashed where approximate
- Possible facies change—Photogeologic interpretation
- Thrust fault—Dashed where inferred. Teeth on upper plate. Arrows show direction of relative movement

- Possible thrust fault along bedding plane
- Tear fault bounded by thrust fault or bedding fault
- ATTITUDES OF BEDS
- Strike and dip
- Strike and dip showing plunge of lineation
- Interpreted from aerial photographs

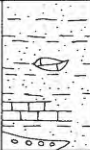
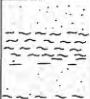

LARGE-SCALE FOLDS—Showing crestline and direction of plunge

- Anticline
- Syncline

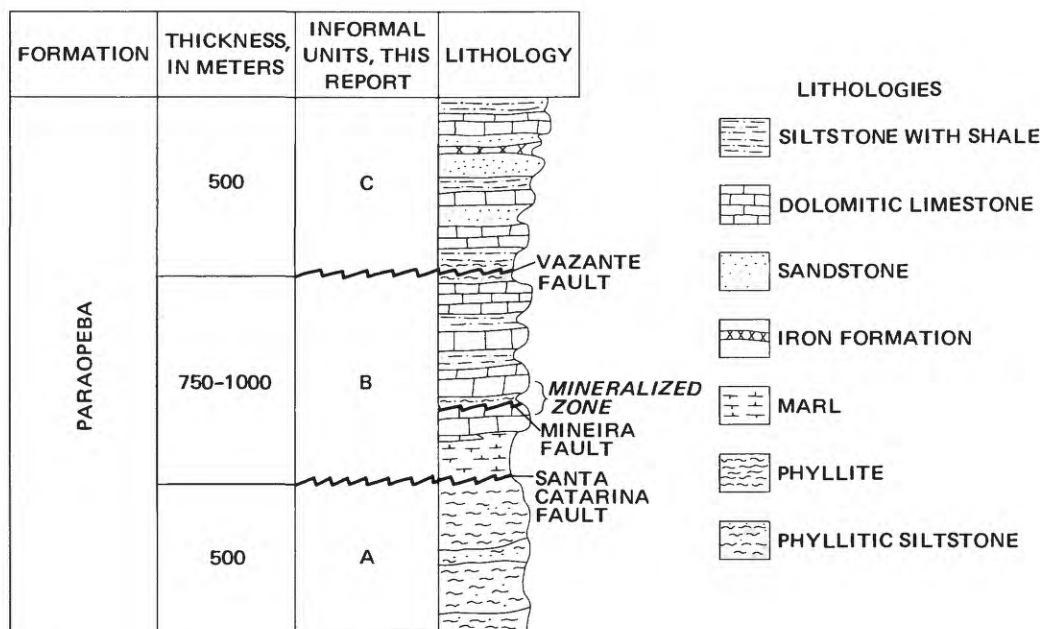
SMALL-SCALE FOLDS—Showing plunge

- Mineralized breccia zone
- Road
- Stream

FIGURE 2.—Continued.

GROUP	FORMATION	LITHOLOGY		THICKNESS IN METERS
BAMBUÍ	TRES MARIAS	Arkose, micaceous siltstone, graywacke, arkosic sandstone, argillaceous limestone lenses		20-400
	PARAOPEBA (Fig. 3B)	LAGUNAR CONGLOMERATE	→	1000-1400
		SAMBURA CONGLOMERATE	→	
		Pelitic and carbonate rocks including facies named "Sete Lagoas," "Lagoa Jacaré," "Serra de Santa Helena". Sandstone, siltstone, argillite, marl, limestone		
	PARANOÁ	CARRANCAS CONGLOMERATE	→	100-3800
Quartzites with interbedded phyllite and metasiltstone				
CANASTRA GROUP		SÃO MIGUEL CONGLOMERATE	→	

A



B

FIGURE 3.—Diagrammatic stratigraphic sections. A, Stratigraphic section of the late Precambrian Bambuí Group (1,000-600 m.y.) for the western side of the Bambuí basin (Braun, 1968). B, Stratigraphic section of the Paraopeba Formation in the Vazante district. Unit A may include some Paranoá Formation and unit C some Tres Marias Formation

Unit B has a minimum thickness of approximately 300 m; it is subdivided into six subunits, numbered B-1 at the base to B-6 at the top (fig. 2), primarily on the basis of photointerpretation of geologic and geomorphic features. Some of the subunits are shown intertonguing with others (fig. 2), a reflection of the abrupt facies changes in the Paraopeba Formation. Subunit B-1 consists of marl and shale

and forms a lowland occupied in part by the Rio Santa Catarina (fig. 5). Subunit B-2 consists of limestone, which forms a narrow zone of subdued parallel ridges; the limestone appears to grade into the marl and shale of B-1 to the northeast. Subunit B-3, which contains the Vazante ore bodies, forms the prominent "mineralized cuesta" and is limestone along most of its length; shale and siltstone con-



FIGURE 4.—Thin-bedded, folded phyllite of unit A. These are f_1 folds. Note the crenulation cleavage along axial planes. Camera lens cap is 6 cm wide.

stitute a major portion of the subunit at the south end of Serra de Ouro Podre. Subunit B-4 is characterized by very low relief and probably is composed largely of fine-grained clastic and argillaceous rocks interlayered with some thin-bedded limestone; a few isolated hills are underlain by thin- to medium-bedded limestone. Subunit B-5 is characterized by numerous low cuestas and hills of moderately dipping thin-bedded to massive limestone; several hills are traceable on aerial photographs for 3 to 6 km. Subunit B-6 is distinguished by low, isolated hills

of gently dipping to horizontal, thick-bedded to massive limestone beds that are discontinuous; the intervening areas are flat pasture land underlain by thin- to medium-bedded limestone, siltstone, shale, and marl.

Subunits B-1, B-3, and B-4 were not separated in the northern part of the area, because B-3 becomes subdued and unrecognizable. B-2 and B-3 terminate to the southwest against a tear fault. The rocks on the southwest side of the tear fault are mapped as unit B. Subunits B-5 and B-6 are not distinguishable immediately northeast of Vazante because of folding and possibly because of stratigraphic complications. The basal contact of subunit B-5, however, appears to merge with the Mineira fault or to become a bedding fault to the southwest of the tear fault.

UNIT C

Unit C underlies a terrain of undulating hills and cuestas in the western part of the area. It consists of interbedded siltstone, marl, sandstone, and dolomitic limestone. These rocks are lithologically similar to those in unit B, but they have a much higher ratio of siltstone and marl to limestone. Limestone underlies most of the prominent, sharp-crested cuestas, whereas sandstone generally underlies rounded, more subdued cuestas. The thickness of unit C probably exceeds 500 m; the top of the unit is not exposed in the map area.



FIGURE 5.—Panoramic view of Serra do Poço Verde, viewed from the south. The valley to the right (northeast) is underlain by shale and marl of subunit B-1. The ridge is Serra do Poço Verde, at the southwest end of the mineralized cuesta; the Companhia Mineira de Metais mine is on the opposite side of the ridge. Low hill in the foreground is unit A; hills in the background are unit C.

STRUCTURE

The Vazante district displays many structures typical of a deformed belt. During the Brazilian orogeny (ca. 600–500 m.y.), older Precambrian rocks were thrust eastward over the western margin of the Bambuí basin along a front approximately 1,000 km long. Large-scale thrusting died out west of Vazante; the easternmost major thrust is in the Serra dos Pilões, about 30 km to the west of Vazante (fig. 1).

The effects of the orogeny are widespread at Vazante, and at least two phases of tectonism can be documented. First, low-angle, bedding, and step-bedding thrust faults developed, as did some related folding. Low-grade metamorphism and penetrative deformation either preceded or was coeval with the thrusting. Second, broad cross folds deformed all previous structures. Interpretation of the types of structures is based on their characteristics as seen in the field and as interpreted on aerial photographs, as well as on the geological history of the surrounding region.

FOLDS

Four sets of folds (f_1 through f_4) are recognized. Set f_1 consists of folds that trend N. 20°–50° W. and range in size from microfolds less than 1 mm to some having wavelengths of 2–5 cm and amplitudes of 1–3 cm (fig. 4). This fold set is best developed in unit A, is well developed along the contact between units B and C, and is also present in units B and C, where it was observed only in pelitic rocks interbedded with massive limestone and sandstone beds.

Set f_2 consists of two north-northwest-plunging anticlines, in unit A and in the lower part of unit B. The folds die out upward in the basal marl-shale member of unit B; the overlying cuesta-forming mineralized member is not affected by the f_2 folds. A west-plunging anticline, 2.5 km south of Lagoa Feia, is also interpreted as belonging to set f_2 . This fold is a complex anticline that underwent possibly two stages of folding. A tightly folded axial zone is interpreted to be an f_2 fold that was refolded about a larger, more open f_4 fold. The f_2 folds have wavelengths and amplitudes of about 0.5 km and are at least 2 km in length. The sets of f_1 and f_2 folds are parallel.

The third fold set, f_3 , consists of large-scale structures that trend N. 10° W. to N. 40° E., parallel to regional structural trends. All units and f_1 and f_2 folds are folded about f_3 axes. The folds are broad,

open, and slightly asymmetrical. They are overturned to the southeast; wavelengths are 0.5 to 2 km, and amplitudes are 0.1 to 1.5 km. Set f_3 folds are more abundant and more pronounced in units B and C than in unit A. Most of the folds are doubly plunging and discontinuous. Disharmonic folding is dominant, with the more intense folding having occurred in resistant limestone and sandstone beds.

Set f_4 folds are large west-northwest-plunging folds transverse to the regional trend. All structures in the northern part of the area are folded about f_4 axes.

Set f_1 folds, the oldest, formed early in the Brazilian orogeny during the major period of widespread dynamic metamorphism. Lineations in all units are interpreted as being of this same age. Set f_2 folds postdate the Santa Catarina fault, which is folded about f_2 axes, but appear to predate the Vazante fault and most structures in the lower part of unit B. Both f_1 and f_2 axes are more or less normal to the direction of Brazilian thrust faulting. Set f_3 folds are interpreted as being related to the major period of Brazilian folding and thrust faulting. Transverse folding of all structures by f_4 folds is the youngest event, postdating all thrust faulting.

LINEATIONS

Three types of mutually parallel lineations were noted: streaks of fine-grained sericite, f_1 fold axes, and traces of fractures that intersect parting and bedding planes. The streaking and smearing out of sericite appears to be the most widespread form of lineation. The fractures were noted only where f_1 folds were present and are parallel to f_1 axial planes. Quartz-filled fractures are common. The lineations occur throughout unit A and in most of the thin argillaceous beds in units B and C. In units B and C, lineation is strongest at and near the contacts between argillaceous beds and sandstone and carbonate beds. The thinner the argillaceous bed between massive competent beds the better developed the lineation.

FAULTS

Low-angle and bedding faults and related tear faults are believed to be the dominant style of faulting. The mineralized breccia zone on the mineralized cuesta may be related to this faulting. The upper and lower contacts of unit B are herein considered to be thrust faults throughout most of the map area. This faulting predates f_3 folding. High-angle normal faulting is probably relatively insignificant.

The Santa Catarina fault, which separates units A and B, marks a major contrast between the pronounced and pervasive penetrative deformation and low-grade metamorphism of unit A rocks and the generally locally developed and much weaker low-grade metamorphism of unit B rocks. Beds on opposite sides of the fault are generally more or less concordant; however, minor but important discordances do occur. In the basal member of unit B, several marker horizons traceable on aerial photographs are truncated toward the north at a low angle against the fault. The thickness of this basal member is also reduced by at least one half from the southern edge of the map to the point where the marker beds are truncated.

The contact between unit B and unit C is thought to be a low-angle thrust and bedding fault, herein named the Vazante fault. We consider the contact to be one continuous fault that is a low-angle thrust southwest of the north-plunging anticline about which it is folded; the thrust climbs up the stratigraphic section to the northeast or east and becomes a bedding fault east and northeast of the anticline. Structures in unit B, south of the anticline, consist of a series of broad, open folds that apparently involve the same beds, indicating that the dip of unit B is very low in this area. In this same area, unit C dips uniformly and more steeply than unit B and is not folded, thus indicating a structurally discordant relationship across the contact. Strata along both sides of the fault in this interval are discordant and irregular, probably indicating drag folding and related faulting. East and northeast of the anticline, beds in both units are more or less parallel to each other. The contact is a folded surface as evidenced by the general continuity of strata in both units.

Transverse high-angle normal faults have been used by previous workers to explain minor offsets or suspected offsets of strata in unit B. However, on aerial photographs numerous marker horizons can be seen to be continuous both above and below some of these offsets. Thus, the faulting that is responsible must be confined by these marker beds. We suspect that multiple bedding faults and step-bedding faults formed, and differential movement of the intervening beds created tear faults that terminated at the bounding bedding faults. In this fashion, an uptilted sequence of rocks would have tear faults that offset only a few beds in a limited stratigraphic interval; these tear faults would have all the characteristics of high-angle normal faults but would terminate abruptly at overlying and underlying layers.

Two examples of this type of tear-fault relationship will illustrate the point. About 2 km southeast of Vazante along the road to Patos de Minas, a low ridge, on the north side of the road, is underlain by at least 20 m of northwest-dipping limestone. This limestone is not present in the drainage ditch alongside the road, a distance of about 10 m from limestone outcrops. Instead, only folded shale is present in the ditch and the roadbed. A second example can be seen in the streambed that crosses the mineralized cuesta about 0.75 km west of the airstrip at Fazenda do Ingá. Northeast of the streambed, the cuesta is underlain by 50–80 m of massive to thick-bedded limestone, whereas in the streambed and to the southwest along the cuesta moderately folded siltstone and shale are present. The change from limestone to siltstone is limited to an interval of about 10 m. In both areas, bounding strata are not offset. Thus, tear faulting bounded by bedding-thrust faults best explains the relationships. Facies changes may have been the dominant factor in controlling the location of such tear faults.

The mineralized cuesta has been interpreted as a northwestward tilted fault block by previous workers (Branco, 1962; Carvalho and others, 1962; Amaral, 1968). If their interpretation is correct, the prominent limestone beds underlying the cuesta might be expected to crop out between the cuesta and the Santa Catarina fault, which they do not. An alternative explanation, the one favored in this report, is of a poly-folded and thrust-faulted sequence of interbedded resistant and less resistant strata, which have eroded to ridge-and-valley-type topography.

The mineralized breccia zone, on the dip slope of the mineralized cuesta, has also been considered by previous workers (Moore, 1956; Branco, 1962; Carvalho and others, 1962; Guimarães, 1962; Amaral, 1968) as being due to normal faulting. The breccia zone ranges from less than 1 m to 200 m in width; the bounding faults are very steep, dipping both to the northwest and southeast. There are several possible explanations for the formation of the breccia zone. The one favored here is that the breccia formed along the step of a step-bedding fault, herein named the Mineira fault, that originated during the major period of Brazilian tectonism. Both the breccia zone and the regional dip, which is 30° to 45° southwest, are folded about f_4 fold axes. Removal of the regional dip and f_4 folding would change the breccia zone from a curved and near vertical structure to a linear, moderately steeply southwest-dipping structure like that of a step-bedding fault (fig.

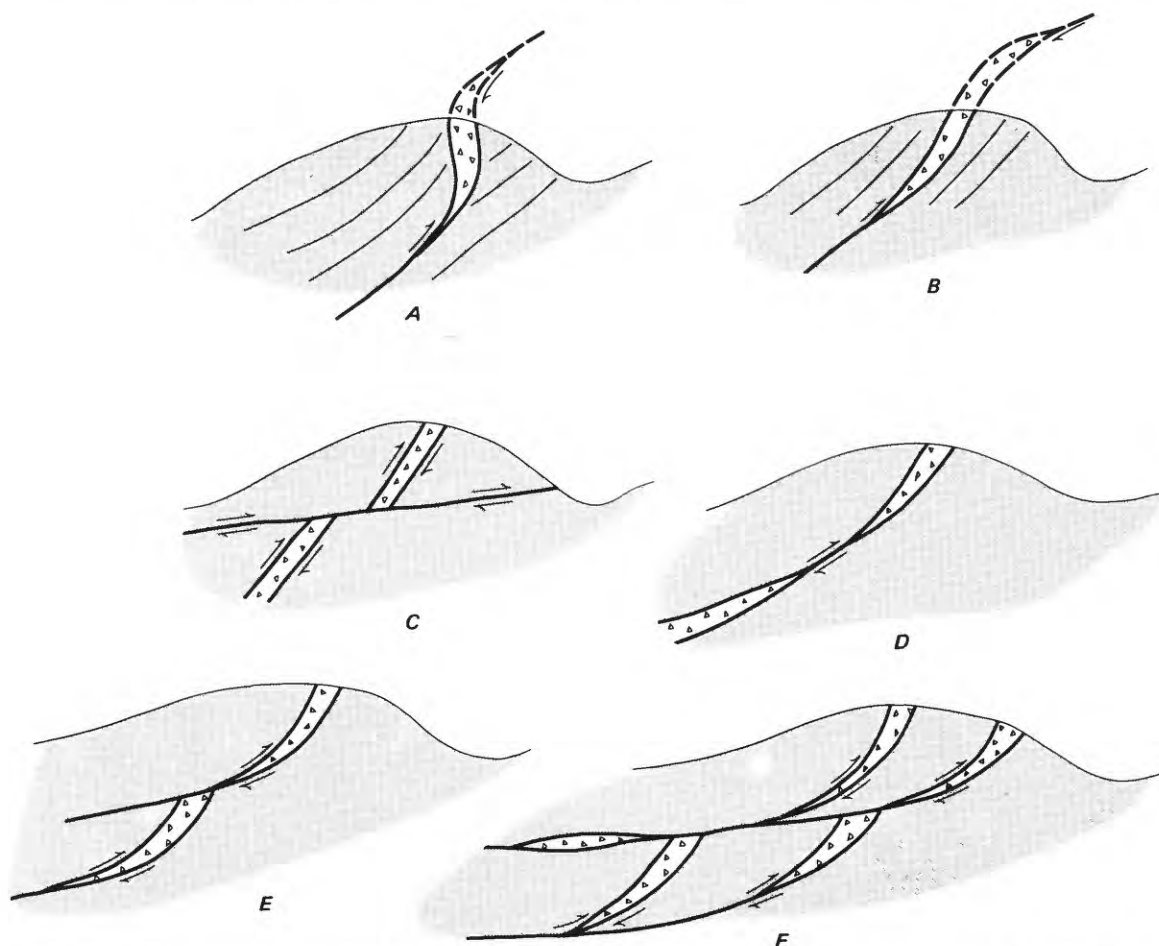


FIGURE 6.—Diagrammatic examples of ways in which breccia zones may form along step-bedding faults. A, Tilted, steep step-bedding fault resembling a normal fault. B, Tilted, low-angle step-bedding fault. C, Breccia zone cut by younger low-angle fault. D, Multiple breccia zone along a single fault. E, Two breccia-zone step-bedding faults, one cutting the other. F, Several stages of faulting and brecciation.

6A). This structure would have developed prior to or coeval with f_1 , f_2 , and (or) f_3 folding but definitely before f_4 folding. Some variations in the possible forming of a step-bedding-plane breccia zone are shown in figure 6. Multiple steps could form. Or, one or a series of steps might be cut by a low-angle fault, thus planing off and moving the upper portion of the breccia zone some distance from the lower portion, which in turn would be overlain by unbrecciated "upper plate" rocks. Other interpretations for the origin of the breccia include: a high-angle fault, as proposed by previous workers; a fault-zone vein that predated f_4 folding but was postthrusting, and perhaps was of a rebound tensional nature; a faulted and metamorphosed Mississippi-valley type or similar type of "stratabound" deposit; a faulted and metamorphosed massive sulfide syngenetic deposit.

MINERALIZATION AND RESERVES

The zinc deposits occur in breccia zones along the Mineira fault, primarily along the dip slope of the mineralized cuetsa (fig. 7). These breccia zones are variable in width and depth; they range from 1 to 200 m in width and are at least 80 m deep. A wide variety of minerals are present and are listed in decreasing order of abundance: hemimorphite (referred to as calamine in Brazilian reports of the district), willemite, hydrozincite, cerussite, smithsonite, chalcocite, brochantite, pyromorphite, covellite, zincite, cuprite, native copper, malachite, linarite, aurichalcite, acanthite, and native silver (Amaral, 1968). The main ore minerals are hemimorphite, willemite, and hydrozincite. Secondary zinc silicate minerals extend downward to at least 80 m. Sulfide minerals are recognized at greater



FIGURE 7.—Resistant ridge of mineralized breccia (primarily hemimorphite, hydrozincite, willemite) on the north end of Serra do Poço Verde. Trees do not grow over the mineralized zone.

depth, but their limits are poorly defined, and they apparently occur in irregular small bodies.

Proven reserves on the Companhia Mineira de Metais concession are about 6,200,000 metric tons of 16-percent zinc ore (largely hemimorphite ore) and an additional 800,000 metric tons of 40-percent zinc ore (largely willemite ore), or about 1,312,000 metric tons of zinc metal (White and Nagell, 1975). Reserve data are not available for the Ingá deposit but probably are of a similar size. Probable and possible reserves half again as large as proven reserves seem to indicate that total zinc metal reserves could be as much as 3 million metric tons.

SUMMARY

The Vazante district, which occurs along the leading edge of a deformed belt, has been subjected to considerable compression, and the rocks have responded accordingly. Low-grade dynamic metamorphism of argillaceous rocks, broad folding, and low-angle and bedding faulting and associated tear faulting dominate the structural history. Almost all the structures in the Vazante district were formed probably during the Brazilian orogeny (ca. 600–500 m.y.).

The breccia zone along the mineralized cuesta is only a very small part of the area, but is economically important. The breccia probably formed in response to step-bedding-plane faulting along the base of the carbonate rocks underlying the mineralized cuesta. Localization of the step-bedding faulting may have been controlled by earlier structures, such

as high-angle faults or collapse-breccia zones. The step-bedding-plane faulting resulted in the brecciation of carbonate and argillaceous rocks. The amount of stratigraphic separation is unknown but it probably was not large.

The Vazante deposit is considered to be epigenetic. The source of the mineralization is incompletely understood. We favor a source from syngenetic minerals in host-rock dolomitic limestone of the Paraopeba Formation. Cassedanne (1968b) arrived at such a conclusion for at least part of the mineralization, pointing out that *Collenia*-bearing dolomite in the district has an abnormally high zinc and lead content. Amaral and Kawashita (1967, 1968) dated shales at Vazante from the Sete Lagoas Formation (which we refer to as the Paraopeba Formation) as 600 ± 22 m.y. old. Amaral (1968) reported an age of 600 ± 30 m.y. for galena at Vazante. The presence of abnormally high amounts of zinc and lead in certain carbonate facies coinciding with the similar ages for shale and galena in the district strongly supports a syngenetic interpretation for the source of the zinc and lead. Subsequent concentration of the deposit into its present form as an epigenetic deposit probably was made possible because Brazilian orogenic events formed breccias that provided the “plumbing” system for the later migration of ore-bearing fluids. Redeposition in the breccia zone along the mineralized cuesta formed a deposit that was subsequently oxidized by surface or near-surface waters. During the redeposition and oxidation phases, possibly during late Mesozoic or early Cenozoic time, the breccia was so altered that whether its origin is tectonic or solution cannot be determined. Solution and collapse features are common in the breccia zone, but they reflect probably only the latest history of the zone.

This interpretation suggests that future exploration for Vazante-type deposits should be concentrated along the deformed belt where folded carbonate rocks are interbedded with argillaceous rocks. This coincidence of structural and stratigraphic situations is favorable for disharmonic folding, which, in turn, leads to bedding and step-bedding faulting. The end result of these events may have been the formation of breccia zones that were potential depositional sites for ore-bearing fluids.

REFERENCES CITED

- Amaral, Gilberto, 1968, Contribuição ao conhecimento dos depósitos de Zn-Pb-Cu-Ag da Serra do Poço Verde, Vazante, Estado de Minas Gerais: Sociedade Brasileira

- Geologia Congresso, 22d, Belo Horizonte, 1968, Anais, p.13-31.
- Amaral, Gilberto, and Kawashita, Koji, 1967, Idade do grupo Bambuí: [abs.]. Parananaense Geociências Bol. 26, p. 39-40.
- 1968, Idade do grupo Bambuí por determinações Rb-Sr em folhelhos: Sociedade Brasileira Geologia Congresso, 21st, Curitiba, 1967, Anais, p. 214.
- Barbosa, Octavio, Braun, Oscar P. G., Dyer R. C., Cunha, Carlos, and Rodrigues, A. B., 1970, Geologia da região do Triângulo Mineiro: Brazil Divisão Fomento Produção Mineral, Bol. 136, 140 p.
- Bohomoletz, M. L., 1975, Brazil's metallurgical industry—after a slow start it now learns how to run: Engineering and Mining Journal, v. 176, no. 11, p. 176 to 176-D1.
- Branco, Jose Jaime R., 1962, Principais ocorrências de zinco em Minas Gerais: Sociedade Intercâmbio Cultural e Estudos Geologia, Ouro Preto, pub. 2, p. 151-184.
- Braun, Oscar P. G., 1968, Contribuição à estratigrafia do grupo Bambuí: Sociedade Brasileira Geologia Congresso, 22d, Belo Horizonte, 1968, Anais, p. 155-166.
- Carvalho, P., Dequech, D., and Guimarães, D., 1962, Jazida plumbo-zincífera do Município de Vazante, Minas Gerais: Brazil Divisão Fomento Produção Mineral Bol. 110, 119 p.
- Cassedanne, Jacques, 1968a, Description du biostrome à Colenias de la mine de Vazante (Minas Gerais): Academia Brasileira Ciências Anais, v. 40, no. 2, p. 215-225.
- 1968b, Nota sobre o ambiente de sedimentação das rochas encaixando a mineralização de Vazante (MG): Sociedade Brasileira Geologia Congresso, 22d, Belo Horizonte, 1968, Anais, p. 33-40.
- Guimarães, Djalma, 1962, Gênese do minério de zinco de Vazante, Minas Gerais: Sociedade Intercâmbio Cultural e Estudos Geologia, Ouro Preto, pub. 2, p. 101-147.
- Moore, Samuel L., 1956, Zinc and copper deposits of the Vazante area, Minas Gerais, Brazil: U.S. Geological Survey open-file report, 16 p.
- White, M. G., and Nagell, R. H., 1975, Lead and zinc resources of Brazil: U.S. Geological Survey Open-File Report 75-49, 49 p.

Constraints on the Latest Movements On the Melones Fault Zone, Sierra Nevada Foothills, California

By J. ALAN BARTOW

SHORTER CONTRIBUTIONS TO STRATIGRAPHY AND
STRUCTURAL GEOLOGY, 1979

GEOLOGICAL SURVEY PROFESSIONAL PAPER 1126-J

*Potassium-argon dates for
late Tertiary intrusions
provide age control for
the latest movements on
the Melones fault zone in
the Sierra Nevada foothills*



CONTENTS

	Page
Abstract	J1
Introduction	1
Acknowledgments	1
Age of the Mehrten Formation	1
Age of dacite intrusions	3
Discussion	4
References cited	4

ILLUSTRATIONS

	Page
FIGURE 1. Geologic map of the area southwest of Mokelumne Hill, Calaveras County, Calif.	J2
2. Diagram showing the correlation of some Tertiary stratigraphic units in the western Sierra Nevada, showing age control from K-Ar dating of volcanic rocks	3

TABLES

	Page
TABLE 1. Chemical data on late Tertiary intrusions	J3
2. Analytical data for K-Ar age determinations	4

CONSTRAINTS ON THE LATEST MOVEMENTS ON THE MELONES FAULT ZONE, SIERRA NEVADA FOOTHILLS, CALIFORNIA

By J. ALAN BARTOW

ABSTRACT

K-Ar dates of 4.12 million years (m.y.) and 4.03 m.y. for two small dacite and rhyodacite intrusive bodies near Mokelumne Hill, Calif., provide important age control for the late Tertiary Mehrten Formation in this area because the Mehrten both is intruded by the dacite and rhyodacite and depositionally overlies the dacite of one intrusion. These dates also establish a maximum age for the latest movement on the Mother Lode fault, a part of the Melones fault zone, because the Mehrten Formation is displaced by this fault and because younger colluvium containing clasts from one of the intrusive bodies is in fault contact with the Mehrten.

INTRODUCTION

Four small dacitic to rhyodacitic intrusive bodies near Mokelumne Hill, Calaveras County, Calif., (fig. 1) are closely associated with the Mehrten Formation, a late Tertiary volcanoclastic unit. Inasmuch as the dacite and rhyodacite bodies intrude the Mehrten and are locally overlain by it, dating the intrusions would give an age within the Mehrten Formation in this area. This age has added significance because recent work in the Sierra Nevada foothills belt by Woodward-Clyde Consultants for the Pacific Gas and Electric Co. has revealed that the Mehrten Formation is displaced by the Mother Lode fault (fig. 1) near the intrusive bodies. The base of the Mehrten is offset by as much as 30 m (down to the northeast) (J. R. McCleary, oral commun., 1976), and a trench excavated across the Mother Lode fault adjacent to Hamby dome (visited by the author) shows that the highest exposed Mehrten on the ridge crest is juxtaposed with younger colluvium containing clasts of rhyodacite apparently identical with the rhyodacite of the Hamby dome intrusion. The minimum offset on the colluvium-Mehrten contact is about 5 m (T. A. Grant, oral commun., 1977).

ACKNOWLEDGMENTS

R. L. Blum, of the Pacific Gas and Electric Co., and J. R. McCleary and T. A. Grant, of Woodward-Clyde Consultants, have kindly shared information resulting from their investigations in the Sierra Nevada foothills fault zones. Dennis Sorg prepared mineral separates, and Marvin Lanphere and J. C. Von Essen were helpful in obtaining the K-Ar dates. The manuscript has benefited from the comments of T. A. Grant.

AGE OF THE MEHRTEN FORMATION

The Mehrten Formation, a widespread and easily recognized stratigraphic unit in the western Sierra Nevada, is composed principally of andesitic clastic and pyroclastic material. The formation was originally described by Piper, Gale, Thomas, and Robinson (1939) in the lower Sierra Nevada foothills, west of the area of this report, where the formation is composed mostly of sandstone and minor amounts of conglomerate, mudstone, and breccia. In the Mokelumne Hill area, the formation consists mainly of coarse andesitic conglomerate and minor interbedded sandstone (Rose, 1959). The Mehrten unconformably overlies either rhyolitic tuff and conglomerate of the Valley Springs Formation (late Oligocene and early Miocene) or pre-Tertiary bedrock consisting of deformed metasedimentary rocks, metavolcanic rocks, and plutonic igneous rocks.

Piper, Gale, Thomas, and Robinson (1939) considered the age of the Mehrten Formation, on the basis of sparse fossil evidence, to be late (?) Miocene and Pliocene (?). More recent work has established that the Mehrten contains a vertebrate fauna of early Clarendonian age below the latite flow of Table

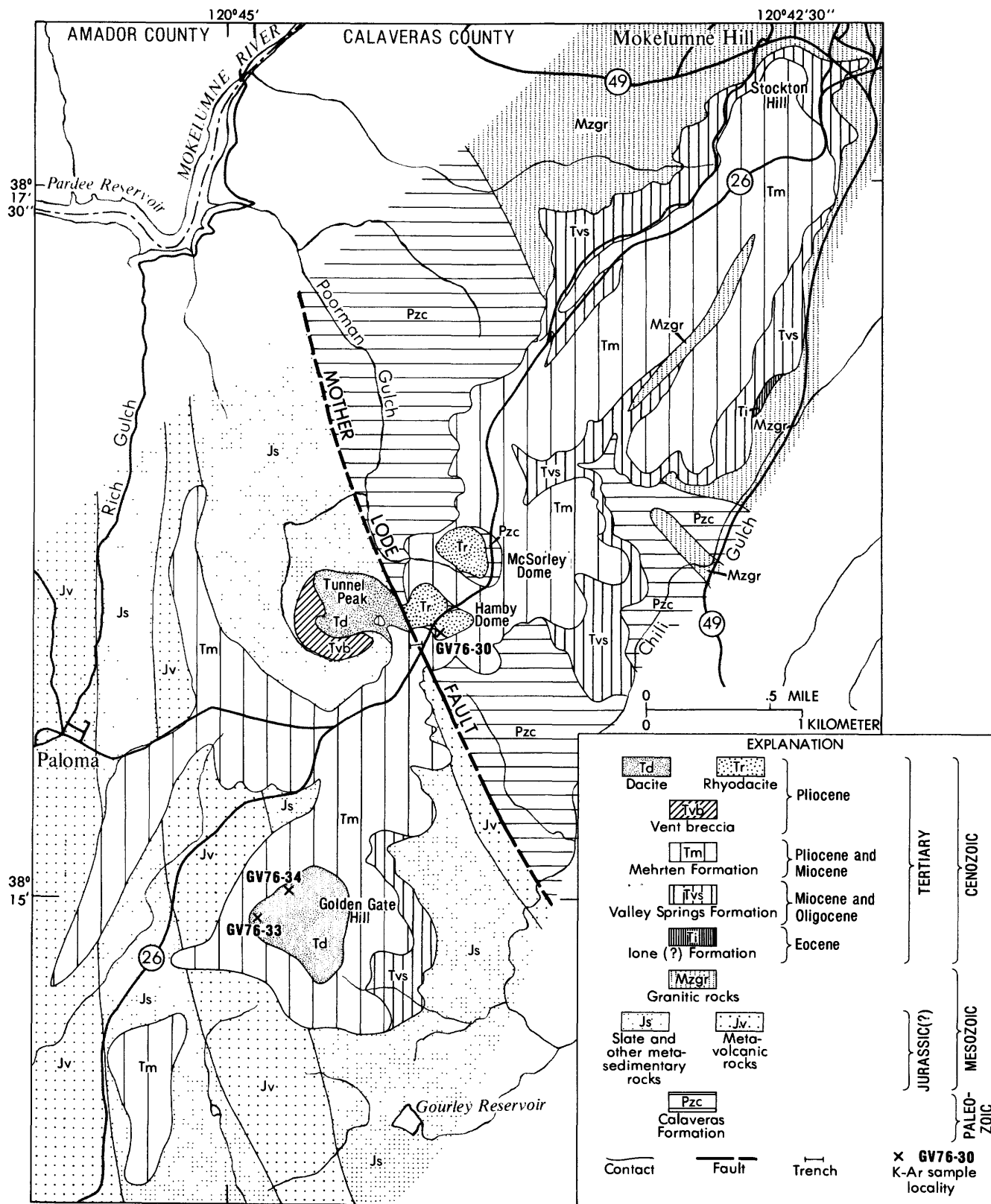


FIGURE 1.—Geologic map of the area southwest of Mokelumne Hill, Calaveras County, Calif. Geology modified from Rose (1959) and Goldman (1964). Base from U.S. Geological Survey, Jackson, Mokelumne Hill, San Andreas, and Valley Springs 7.5 minute quadrangle.

Mountain, about 15 km southeast of the map area (Stirton and Goeriz, 1942), and one of late Hemphillian age above the latite (Stirton and Goeriz, 1942, Wagner, 1976) indicating that the Mehrten is Miocene and Pliocene. Correlation of K-Ar dates with the North American mammalian chronology by Evernden, Savage, Curtis, and James (1964) indicates that the lower part of the Mehrten is at least 11 to 12 m.y. (million years) old and that the top must be as young as 4 to 6 m.y. K-Ar dating of Cenozoic volcanic rocks in the Sierra Nevada (Dalrymple, 1963, 1964) provides further control on the age of the Mehrten Formation (fig. 2). The date of 9.0 m.y. for the latite of Table Mountain, which occurs as a tongue in the Mehrten Formation, is in good agreement with the vertebrate ages.

AGE OF DACITE INTRUSIONS

The petrology of the intrusive bodies has been described by Rose (1959) and is not repeated here. Rose classified the larger bodies of Golden Gate Hill and Tunnel Peak (fig. 1) as hornblende-biotite dacite and hornblende dacite, respectively. The smaller two

TABLE 1.—Chemical data on late Tertiary intrusions

[X-ray spectrographic analyses by L. F. Espos and G. M. Kawakita. Chemical analyses (*) by M.J. Cremer. Cr, Ni, Ba, Rb, Sr, V, Sc, and Y in parts per million; others in weight percent.]

	Hamby dome GV76-30	Golden Gate Hill GV76-33
SiO ₂ -----	67.92	59.97
Al ₂ O ₃ -----	16.10	15.63
Fe ₂ O ₃ -----	1.24	5.00
FeO*-----	.52	< .1
MgO-----	.90	4.46
CaO-----	2.24	5.07
Na ₂ O-----	6.09	4.24
K ₂ O-----	2.97	.78
TiO ₂ -----	.33	.81
P ₂ O ₅ -----	.10	.27
MnO-----	.032	.076
H ₂ O+*-----	.89	1.05
H ₂ O-*-----	.21	.25
CO ₂ *-----	.03	.02
S ₂ (total)-----	.001	.006
Cr-----	55	155
Ni-----	26	113
Ba-----	960	1250
Rb-----	83	64
Sr-----	1600	1650
V-----	27	116
Sc-----	5	15
Y-----	<5	6

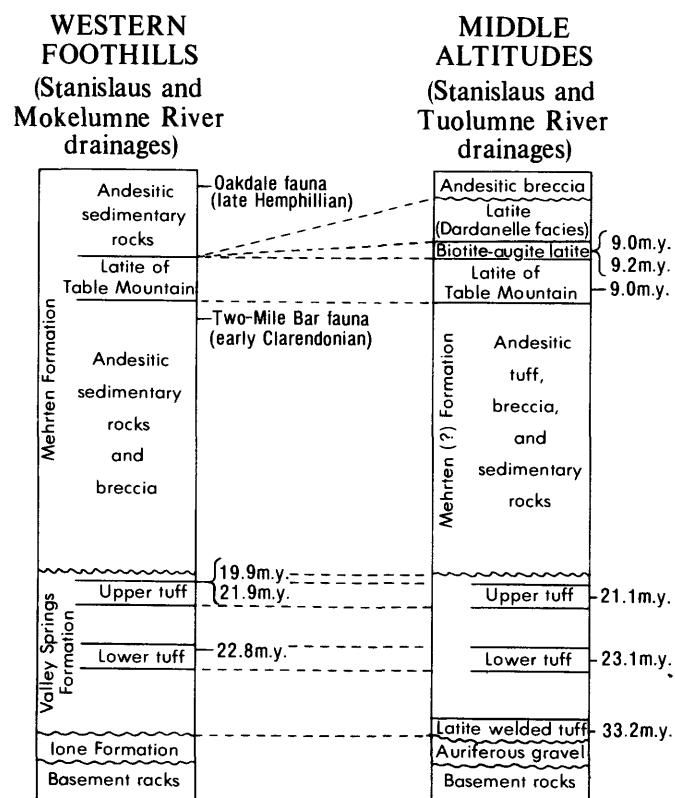


FIGURE 2.—Correlation of some Tertiary stratigraphic units in the western Sierra Nevada, showing age control from K-Ar dating of volcanic rocks (from Dalrymple, 1964).

intrusive bodies, referred to as Hamby dome and McSorley dome, were classified as hornblende rhyodacite. New chemical analyses (table 1) indicate that the Hamby dome intrusion is rhyodacite and the Golden Gate Hill intrusion is dark rhyodacite in Rittmann's (1952) classification.

According to Rose's (1959) interpretation of the structural relations, the dacite of Tunnel Peak and the two small rhyodacite bodies are clearly intrusive into and therefore younger than the Mehrten Formation. At McSorley and Hamby domes, the Calaveras Formation has been dragged up between the rhyodacite and the surrounding Mehrten Formation, and the Mehrten has been deformed adjacent to the intrusive bodies. The dacite of Tunnel Peak is surrounded by a tuff breccia, interpreted by Rose (1959) as a vent breccia, that contains Mehrten andesite pebbles. More recent mapping in the area by Woodward-Clyde Consultants has shown that although the Mehrten has been intruded by the dacite of Tunnel Peak, the uppermost part of the Mehrten depositionally overlies part of the dacite (T. A. Grant, written commun., 1977).

Rose (1959) believed that the dacite of Golden Gate Hill, unlike the other small intrusions in the

TABLE 2.—Analytical data for K-Ar age determinations

[GV76-30 - Rhyodacite of Hamby dome; GV76-34 - Dacite of Golden Gate Hill. Potassium measurements: J. H. Tillman. Argon measurements and age calculation: E. Sims. ^{40}K decay constants: $\lambda_e = 0.572 \times 10^{-10} \text{ yr}^{-1}$, $\lambda_\beta = 8.78 \times 10^{-13} \text{ yr}^{-1}$, $\lambda_g = 4.962 \times 10^{-10} \text{ yr}^{-1}$. Abundance ratio: $^{40}\text{K}/\text{K} = 1.167 \times 10^{-4}$ atom percent.]

Field No.	Mineral	Percent K_2O	$^{40}\text{Ar}_{\text{rad}}$ (moles/g)	$^{40}\text{Ar}_{\text{rad}}/^{39}\text{Ar}_{\text{total}}$	Calculated age (10^6 years)
GV76-30	Hornblende	1.061 1.057	6.283×10^{-12}	0.20	4.12 ± 0.11
GV76-34	Hornblende	1.186	6.900×10^{-12}	0.33	4.03 ± 0.26

area, was older than the Mehrten Formation or equivalent to the oldest part of the Mehrten in the area. As evidence, he cited the large angular blocks of dacite "identical to that which forms Golden Gate Hill" (Rose, 1959, p. 14), that were found in the basal part of the Mehrten Formation just southeast of the hill.

A sample of dacite from Golden Gate Hill that was presumed to be older than the Mehrten Formation and one of rhyodacite from Hamby dome that was presumed to be younger than the Mehrten were selected for K-Ar dating. The results, summarized in table 2, indicate that both intrusions are only a little more than 4 m.y. old and that the ages are analytically indistinguishable.

DISCUSSION

The age of 4.12 m.y. for the rhyodacite of Hamby dome, together with the structural relations described by Rose (1959) for Hamby and McSorley domes, suggests that the Mehrten Formation in this area is older than 4 m.y. If all the intrusions are approximately the same age, however, the structural relations at Tunnel Peak indicate that the date must fall within the Mehrten, probably within the upper part. This age for the Mehrten Formation is in fair agreement with the upper limit of 4 to 6 m.y. inferred from the vertebrate ages.

The dacite of Golden Gate Hill (4.03 m.y.) may be considered to be the same age as the rhyodacite of Hamby dome and must also be approximately equivalent in age to the upper part of the Mehrten Formation. The talus blocks of dacite that Rose (1959)

interpreted as being within the basal part of the Mehrten might be better interpreted as landslide debris or younger colluvium incorporating dacite talus with debris from the Mehrten Formation.

A more important conclusion to be drawn from the data presented here is that the latest movement on the Mother Lode fault, one of several faults making up the Melones fault zone of the Sierra Nevada foothills metamorphic belt, was more recent than the youngest part of the Mehrten Formation, which is about 4 to 6 m.y. old. Because colluvium containing blocks of rhyodacite from Hamby dome is involved in the faulting, the latest movement must be more recent than 4 m.y., but no other time constraints can be placed on the movement at this site.

REFERENCES CITED

- Dalrymple, G. B., 1963, Potassium-argon dates of some Cenozoic volcanic rocks of the Sierra Nevada, California: Geological Society of America Bulletin, v. 74, p. 379-390.
- , 1964, Cenozoic chronology of the Sierra Nevada, California; California University Publications in Geological Sciences, v. 47, 41 p.
- Evernden, J. F., Savage, D. E., Curtis, G. H., and James, G. T., 1964, Potassium-argon dates and the Cenozoic mammalian chronology of North America: American Journal of Science, v. 262, p. 145-198.
- Goldman, H. B., 1964, Tertiary fluvial deposits in the vicinity of Mokelumne Hill, Calaveras County, California: Los Angeles, California University M.A. thesis, 56 p.
- Piper, A. M., Gale, H. S., Thomas, H. E., and Robinson, T. W., 1939, Geology and ground-water hydrology of the Mokelumne area, California: U.S. Geological Survey Water-Supply Paper 780, 230 p.
- Rittmann, A., 1952, Nomenclature of volcanic rocks proposed for the use in the catalogue of volcanoes, and key-tables for the determination of volcanic rocks: Bulletin of Volcanology, ser. 2, v. 12, p. 75-102.
- Rose, R. L., 1959, Tertiary volcanic domes near Jackson, California: California Division of Mines and Geology Special Report 60, 21 p.
- Stirton, R. A., and Goeriz, H. F., 1942, Fossil vertebrates from the superjacent deposits near Knights Ferry, California: California University Publications in Geological Science, v. 26, no. 5, p. 447-472.
- Wagner, Hugh, 1976, A new species of *Pliotaxidea* (Mustelidae: Carnivora) from California: Journal of Paleontology, v. 50, p. 107-127.